

**The Preparation of Aryl-Carboranes and Re-Metallo-carboranes as
Anti-Estrogens**

**The Preparation of Aryl-Carboranes and Re-Metallocarboranes as
Anti-Estrogens**

By

Raymond Chankalal, B.Sc.

A Thesis

Submitted to the School of Graduate Studies

In Partial Fulfilment of the Requirements

For the Degree

Master of Science

McMaster University

© Copyright by Raymond G. Chankalal, February 2005.

MASTER OF SCIENCE (2005)
(Chemistry)

McMASTER UNIVERSITY
Hamilton, Ontario

TITLE: The Preparation of Aryl-Carboranes and Re-Metallocarboranes
as Anti-Estrogens

Author: Raymond Chankalal, B.Sc. (University of Toronto)

Supervisor: Professor John F. Valliant

Number of Pages: xvi, 179

Abstract

The estrogen receptor (ER) plays an integral role in the proliferation of hormone dependent breast cancer. Recently a number of organometallic compounds and *closo*-carboranes, which demonstrate affinity for the estrogen receptor, were prepared as novel types of anti-estrogens. This thesis describes the synthesis and characterization of a new class of inorganic anti-estrogens derived from Re-metallocarboranes.

Chapter 2 describes the first series of targets which include three monoarylated Re-metallocarboranes. Two different synthetic routes were used to complex the $[\text{Re}(\text{CO})_3]^+$ core to carborane ligands, one of which involves microwave irradiation of a one pot mixture that produces the desired complexes in almost complete conversion ratios. One compound, **2.10**, contains a single phenol substituents, which is predicted to show ER binding affinity based on previous reports of the *closo*-carborane analogue.

Chapter 3 describes the synthesis and characterization of diarylated Re-metallocarboranes. Two of the compounds, **3.7** and **3.8**, are expected to show high binding affinity for the ER because they are inorganic analogues of the well known anti-estrogen Tamoxifen.

Acknowledgements

I must first thank my supervisor Dr. John Valliant for allowing me to be a member of his research group. Dr. Valliant has maintained a high level of intensity towards sound research methods and his charisma for organic synthesis is unparalleled in my experience. In particular I must express my appreciation for the efforts made by Dr. Valliant to help this thesis come to be.

I would like to thank my committee members, Drs. Alex Adronov and Gillian Goward for taking interest into my work and for finding the time to handle the project during a very trying period. I could not for a moment expect to have gotten this far without the help of my labmates, past and present. I must recognize Dr. Paul Schaffer for his X-ray crystallography expertise and Arienne King for her help in conducting the 2-D NMR experiments. I would like to thank Andrew Green for his development of the microwave complexation reactions. Conversation often generated new ideas and always provided clarity for the problems at hand. I would like to mention a few names, in no particular order, Karin, Dr. Jane Forbes, Dr. Pierre Morel, Bola, Amanda, Matt, Anika, Tina, Jay, and Stuart.

I can not forget the tremendous efforts of the administrative staff that helped me along the way: Carol Dada, Josie Petrie, Barbra DeJean, and Tammy Feher. I must also thank the facilities staff in the department: Don Hughes, Brian Sayer, Jim Britten, Kirk Green, Tadek Olech, George Timmins, and Brad Sheller.

Finally it is imperative that I thank my parents and sisters for their continued support and tolerance of my bad example of stress management. My friends, Samir, Arif, Kapil, Saaad, Richard, Stu, and Iram for their friendship and reliability, in times when I could not keep my head up you gave me reason and hope to carry on.

Table of Contents

	Page
Chapter 1: Introduction	
1.1 The Estrogen Receptor and Breast Cancer	1
1.2 ER Antagonists	3
1.3 Carborane as ER Binding Agents	6
1.4 Polyhedral Boranes	7
1.5 Dicarba- <i>closo</i> -dodecaborane	9
1.6 Isomerization of Carboranes	11
1.7 Characterization of Carboranes	12
1.8 Synthesis of <i>Ortho</i> -Carboranes	13
1.9 Reactivity of <i>Ortho</i> -Carboranes	15
1.10 <i>Nido</i> -Carboranes	16
1.11 The Dicarbollide Dianion	18
1.12 Metallocarboranes	19
1.13 The Medicinal Chemistry of Carboranes	20
1.14 Re and ^{99m} Tc/ ⁹⁹ Tc-Metallocarboranes and Radiopharmaceuticals	21
1.15 Carboranes as Pharmacophores	24
1.16 Scope and Summary of Research	26
1.17 References	26
Chapter 2: Monoarylated Re-Metallocarboranes	
2.1 Overview	32
2.2 Introduction	32

2.3 Rationale	34
2.4 Synthetic Strategy and Targets	35
2.5 Synthesis of Phenyl Re-Metallocarborane (2.8)	36
2.6 Synthesis of 4-Methoxyphenyl Re-Metallocarboranes (2.9)	46
2.7 Synthesis of 4-Hydroxyphenyl Re-Metallocarboranes (2.10)	54
2.8 Conclusions	61
2.9 Experimental Section	62
2.10 References	67
Chapter 3: Diarylated Re-Metallocarboranes	
3.1 Overview	69
3.2 Introduction	69
3.3 Rationale	71
3.4 Synthetic Strategy and Targets	72
3.5 Synthesis of 1-(4-Methoxyphenyl)-2-Phenyl Re-Metallocarboranes (3.6)	73
3.6 Synthesis of 1-(4-Hydroxyphenyl)-2-Phenyl	81
3.7 Synthesis of 1,2-bis(4-Hydroxyphenyl) Re-Metallocarborane (3.8)	89
3.8 Synthesis of 1-(4-(N,N-Dimethylamino)ethoxyphenyl) -2-Phenyl Re-Metallocarborane (3.9)	96
3.9 Conclusion	101
3.10 Experimental	102
3.11 References	112

Summary and Future Work	113
Appendix: Supplementary Data	114

List of Figures and Schemes

	Page
List of Figures	
Chapter 1: Introduction	
Figure 1.1: 17β -estradiol (1.1), Raloxifen (1.2), Tamoxifen (1.3), 4-Hydroxytamoxifen (1.4).	2
Figure 1.2: Binding of 17β -estradiol to the key residues in the ligand binding domain (LBD) of ER.	2
Figure 1.3: 2-Benzyl-1-phenyl-[4-(dimethylaminoethoxy)phenyl]-but-1-ene (1.5), Iodoxifen (1.6), MER-25 (1.7), Diethylstilbesterol (1.8).	4
Figure 1.4: Cyclofenil (1.9), 9-[bis(4-hydroxyphenyl)methylene] bicyclo[3.3.1]nonane (1.10), 2-[bis(4-methoxyphenyl)methylene]-1,3,3-trimethylbicyclo[2,2,1]heptane (1.11), 3-ethyl-1,2,4-tri-(4-hydroxyphenyl)cyclopentadienyl tricarbonyl rhenium (1.12), and Ferrocifen (1.13).	5
Figure 1.5: Carborane estrogen agonists developed by Endo <i>et al.</i>	6
Figure 1.6: Carborane antiestrogens developed by Endo and coworkers.	7
Figure 1.7: BH_3 (1.18), B_2H_6 (diborane) (1.19).	8
Figure 1.8: The icosahedron (1.20), B_6H_{10} (1.21), and $B_{10}H_{14}$ (1.22).	9
Figure 1.9: $1,2-C_2B_3H_5$ (1.23), $1,2-C_2B_4H_6$ (1.24), and $1,2-C_2B_{10}H_{12}$ (1.25).	10
Figure 1.10: Equilibrium between deprotonated forms of <i>o</i> -carborane.	15
Figure 1.11: The isolobal nature of the dicarbollide dianion (1.38) and cyclopentadienide (1.39).	18
Figure 1.12: Metal tricarbonyl carborane complexes prepared by Hawthorne <i>et al.</i>	20
Figure 1.13: The Venus Flytrap Complex (VFC) of ^{57}Co (1.43).	23
Figure 1.14: Carborane containing retinoids prepared by Endo and co-workers.	25

Figure 1.15: Protein kinase C targeting carborane derivatives.	25
Chapter 2: Monoarylated Re-Metallocarboranes	
Figure 2.1: The (Z)-isomer of Tamoxifen (2.1), 4-hydroxytamoxifen (2.2), 17 β -estradiol (2.3).	32
Figure 2.2: 1-Hydroxyphenyl-12-hydroxy-1,12-dicarba- <i>closo</i> -dodecaborane (2.4), 1-(4-hydroxyphenyl)-12-(hydroxymethyl)-1,12-dicarba- <i>closo</i> -dodecaborane (2.5).	33
Figure 2.3: 1-(4-Hydroxyphenyl)-2-(N-methyl-N-butyl-dodecylacetamide)-1,2-dicarba- <i>closo</i> -dodecaborane (2.6), and 1-(4-(N,N-dimethylamino)ethoxyphenyl)-2-(4-hydroxyphenyl)-1,2-dicarba- <i>closo</i> -dodecaborane (2.7).	34
Figure 2.4: 1-Phenyl-3,3,3-tricarbonyl-3- η^5 -Re-1,2-dicarba- <i>closo</i> -dodecaborate (2.8), 1-(4-methoxyphenyl)-3,3,3-tricarbonyl-3- η^5 -Re-1,2-dicarba- <i>closo</i> -dodecaborate (2.9), and 1-(4-hydroxyphenyl)-3,3,3-tricarbonyl-3- η^5 -Re-1,2-dicarba- <i>closo</i> -dodecaborate (2.10).	35
Figure 2.5: The retrosynthesis of monoarylated Re-metallocarboranes.	36
Figure 2.6: The negative ion electrospray mass spectrum of 2.8 .	43
Figure 2.7: The FTIR (in CH ₂ Cl ₂) spectrum of complex 2.8 .	43
Figure 2.8: ¹ H NMR spectrum (200 MHz, in CDCl ₃) of tetrabutylammonium 1-phenyl-3,3,3-tricarbonyl-3- η^5 -Re 1,2-dicarba- <i>closo</i> -dodecaborate (2.8).	44
Figure 2.9: The X-ray structure for 1-phenyl-3,3,3-tricarbonyl-3- η^5 -Re-1,2-dicarba- <i>closo</i> -dodecaborate, 2.8 . The tetrabutylammonium cation is omitted for clarity.	45
Figure 2.10: ¹ H NMR spectrum (200 MHz in CDCl ₃) of 1-(4-methoxyphenyl)-1,2-dicarba- <i>closo</i> -dodecaborane (2.15).	47
Figure 2.11: ¹¹ B NMR spectrum (500 MHz in CDCl ₃), of 1-(4-methoxyphenyl)-1,2-dicarba- <i>closo</i> -dodecaborane (2.15).	48
Figure 2.12: ¹³ C NMR (200 MHz in CDCl ₃), of 7-(4-methoxyphenyl)-7,8-dicarba- <i>nido</i> -undecaborate (2.12a).	50

Figure 2.13: HPLC chromatogram of crude reaction mixture for complex 2.9 .	52
Figure 2.14: The negative ion electrospray mass spectrum of 2.10 .	60
Figure 2.15: The FTIR (in KBr) spectrum of complex 2.10 .	60
Figure 2.16: ^1H NMR (200 MHz in MeOH- d_4) of 1-(4-hydroxyphenyl)-3,3,3-tricarbonyl- η^5 -Re-1,2-dicarba- <i>closo</i> -dodecaborate (2.10).	61
 Chapter 3: Diarylated Re-Metallocarboranes	
Figure 3.1: Carborane analogues of Tamoxifen.	69
Figure 3.2: Novel ER binding agents.	70
Figure 3.3: The Re-metallocarborane targets: 1-(4-methoxyphenyl)-2-phenyl-3,3,3-tricarbonyl-3- η^5 -Re-1,2-dicarba- <i>closo</i> -dodecaborate (3.6), 1-(4-hydroxyphenyl)-2-phenyl-3,3,3-tricarbonyl-3- η^5 -Re-1,2-dicarba- <i>closo</i> -dodecaborate (3.7), 1,2-bis(4-hydroxyphenyl)-3,3,3-tricarbonyl-3- η^5 -Re-1,2-dicarba- <i>closo</i> -dodecaborate (3.8), and 1-(4-(N,N-dimethylaminoethoxyphenyl)-2-phenyl-3,3,3-tricarbonyl-3- η^5 -Re-1,2-dicarba- <i>closo</i> -dodecaborate (3.9).	71
Figure 3.4: Retrosynthesis of diarylated metallocarboranes.	73
Figure 3.5: ^1H NMR (200 MHz in CDCl_3), of 1-(4-methoxyphenyl)-1,2-dicarba- <i>closo</i> -dodecaborane (3.14).	76
Figure 3.6: ^{11}B NMR (500 MHz in CDCl_3) of 1-(4-methoxyphenyl)-2-phenyl-1,2-dicarba- <i>closo</i> -dodecaborane (3.14).	77
Figure 3.7: The negative ion electrospray mass spectrum of 3.6 .	80
Figure 3.8: ^1H NMR (200 MHz, in CDCl_3) of tetrabutylammonium 1-(4-methoxyphenyl)-2-phenyl-3,3,3-tricarbonyl-3- η^5 -Re-1,2-dicarba- <i>closo</i> -dodecaborate (3.6).	81
Figure 3.9: ^{11}B NMR (CD_3OD , 500 MHz), for <i>nido</i> -carborane 3.11 .	84
Figure 3.10: ^1H NMR spectrum (600 MHz, in CD_3OD), of sodium 1-(4-hydroxyphenyl)-2-phenyl-3,3,3-tricarbonyl-3- η^5 -Re-1,2-dicarba- <i>closo</i> -dodecaborate (3.7).	86
Figure 3.11: a) ^1H - ^1H COSY spectrum (600 MHz, in CD_3OD), of the aromatic region of (3.7). b) One atropisomer of 3.7 .	87

Figure 3.12: ^{13}C NMR spectrum (600 MHz, in CD_3OD), of sodium 1-(4-hydroxyphenyl)-2-phenyl-3,3,3-tricarbonyl-3- η^5 -Re-1,2-dicarba- <i>closo</i> -dodecaborate (3.7).	88
Figure 3.13: The FTIR (in KBr) of Re-metallocarborane 3.7 .	89
Figure 3.14: $^{11}\text{B}\{\text{H}\}$ NMR (500 MHz in CDCl_3) of compound 3.20 .	91
Figure 3.15: $^{13}\text{C}\{\text{H}\}$ NMR (500 MHz, in CD_3OD) of 1,2-bis(4-hydroxyphenyl)-1,2-dicarba- <i>closo</i> -dodecaborane (3.16).	93
Figure 3.16: Two dimensional NMR data in the aromatic region (600 MHz, in CD_3OD) for complex 3.8 . a) ^1H - ^1H COSY, b) ^1H - ^{13}C HSQC, and c) ^1H - ^{13}C HMBC.	94
Figure 3.17: Two possible conformations for compound 3.8 .	95
Figure 3.18: The negative ion electrospray mass spectrum of 3.8 .	96
Figure 3.19: ^1H NMR (200 MHz, in CDCl_3) of <i>closo</i> -carborane 3.17 .	98
Figure 3.20: The ^{13}C NMR (200 MHz, in CDCl_3) spectrum of 3.17 .	98
Figure 3.21: ^1H NMR (200 MHz, in CD_3OD) spectrum of complex 3.9 .	100
Figure 3.22: The FTIR (in KBr) of complex 3.9 .	101
Figure 3.23: The negative ion mode electrospray mass spectrum of complex 3.9 .	101

List of Schemes

Chapter 1: Introduction

- Scheme 1.1:** The thermal isomerization of 1,2-dicarba-*closo*-dodecaborane to the 1,7- and 1,12-isomers. 12
- Scheme 1.2:** The preparation of *o*-carborane, C₂B₁₀H₁₂ (1,2-dicarba-*closo*-dodecaborane). 14
- Scheme 1.3:** Preparation of *o*-carborane derivatives with functionalized alkynes, using ionic liquids. 14
- Scheme 1.4:** Preparation of mono-lithiocarborane (1.33) and subsequent reaction with CO₂. 15
- Scheme 1.5:** Degradation of *ortho*-carborane to corresponding *nido*-carborane. 17
- Scheme 1.6:** Removal of the bridging hydrogen in 7,8-dicarba-*nido*-undecaborate to yield 2,3-[C₂B₉H₁₁]²⁻, (the dicarbollide dianion). 18
- Scheme 1.7:** Restoration of the *closo* structure from the dicarbollide dianion (1.37) to give 3-phenyl-1,2-dicarba-*closo*-dodecaborane (1.40). 19
- Scheme 1.8:** The decay scheme for ⁹⁹Mo. 22
- Scheme 1.9:** Generation of the rhenium (I) tricarbonyl complexes in water. 23

Chapter 2: Monoarylated Re-Metallocarboranes

- Scheme 2.1:** Two synthetic routes to phenylcarborane; 1) alkyne insertion and 2) Ulmann-type coupling. 37
- Scheme 2.2:** Preparation of tetrabutylammonium (+1) 7-phenyl-7,8-dicarba-*nido*-undecaborate (-1), 2.11. 39
- Scheme 2.3:** Synthesis of 2.8, 1-phenyl-3,3,3-tricarbonyl-3-η⁵-Re-1,2-dicarba-*closo*-dodecaborate. 41
- Scheme 2.4:** Preparation of 1-(4-methoxyphenyl)-1,2-dicarba-*closo*-dodecaborane. 46
- Scheme 2.5:** Synthesis of 7-(4-methoxyphenyl)-7,8-dicarba-*nido*-undecaborate, 2.12a. 49

Scheme 2.6: The preparation of tetrabutylammonium 1-(4-methoxyphenyl)-3,3,3-tricarbonyl-3- η^5 -Re-1,2-dicarba- <i>closo</i> -dodecaborate (2.9).	51
Scheme 2.7: One pot preparation of complex 2.9.	53
Scheme 2.8: The synthesis of 1-(4-hydroxyphenyl)-1,2-dicarba- <i>closo</i> -dodecaborane (2.16).	54
Scheme 2.9: Preparation of compounds 2.13a and 2.13b.	56
Scheme 2.10: One pot synthesis of 2.10 under microwave conditions.	59

Chapter 3: Diarylated Re-Metallocarboranes

Scheme 3.1: Synthesis of 1-(4-methoxyphenyl)-2-phenyl acetylene (3.18).	74
Scheme 3.2: Preparation of 1-(4-methoxyphenyl)-2-phenyl-1,2-dicarba- <i>closo</i> -dodecaborane (3.14).	75
Scheme 3.3: The synthesis of <i>nido</i> -carborane 3.10.	78
Scheme 3.4: Synthesis of Re-metallocarborane 3.6.	80
Scheme 3.5: Preparation of 1-(4-hydroxyphenyl)-2-phenyl- <i>closo</i> -carborane (3.15).	82
Scheme 3.6: Deboration of compound 3.15 to generate compound 3.11.	83
Scheme 3.7: Preparation of complex 3.7.	85
Scheme 3.8: Preparation of diarylalkyne 3.19.	89
Scheme 3.9: Preparation of 1,2-bis(4-methoxyphenyl)-1,2-dicarba- <i>closo</i> -dodecaborane (3.20).	90
Scheme 3.10: Demethylation of compound 3.20.	92
Scheme 3.11: Preparation of 1,2-bis(4-hydroxyphenyl)-3,3,3-tricarbonyl-3- η^5 -Re-1,2-dicarba- <i>closo</i> -dodecaborane, 3.8.	94
Scheme 3.12 Preparation of <i>closo</i> -carborane derivative 3.17.	97
Scheme 3.13 Preparation of complex 3.9 using microwave method.	99

List of Abbreviations and Symbols

3c2e	Three-center two-electron bond
2c2e	Two-center two-electron bond
Å	Angstrom
Asp	Aspartic Acid
¹¹ B NMR	Boron 11 Nuclear Magnetic Resonance Spectroscopy
Bmin	1-Butyl-3-Methylimidazolium
Bn	Benzyl
BNCT	Boron Neutron Capture Therapy
Br	Broad signal
¹³ C NMR	Carbon 13 Nuclear Magnetic Resonance Spectroscopy
CIMS	Chemical Ionization Mass Spectrometry
COSY	Correlated Spectroscopy
cm ⁻¹	Wave numbers
Cp	Cyclopentadienyl
d	Doublet
DCM	Dichloromethane
DES	Diethylstilbesterol
DNA	Deoxyribose Nucleic Acid
EIMS	Electron Impact Mass Spectrometry
Et	Ethyl
EtOAc	Ethyl Acetate
EtOH	Ethanol
ER	Estrogen Receptor
ESMS	Electrospray Mass Spectrometry
FTIR	Fourier Transformed Infrared Spectroscopy
Glu	Glutamic Acid
His	Histine
HMBC	Heteronuclear Multiple Bond Correlation
hr	Hour(s)
¹ H NMR	Proton Nuclear Magnetic Resonance Spectroscopy
HPLC	High Pressure Liquid Chromatography
HSQC	Heteronuclear Single Quantum Coherence
HRMS	High Resolution Mass Spectrometry
Hz	Hertz

IR	Infrared Spectroscopy
LBD	Ligand Binding Domain
LD ₅₀	Lethal Dosage-50
M	Molarity
m	Multiplet
Me	Methyl
MER-25	1-(<i>p</i> -2-diethylaminoethoxyphenyl)-1-Phenyl-2- <i>p</i> -Methoxyphenylethanol
MeLi	Methyl lithium
MeOH	Methanol
MHz	Megahertz
min.	Minute(s)
M.O.	Molecular Orbital
M.P.	Melting Point
MRI	Magnetic Resonance Imaging
MS	Mass Spectrometry
<i>m/z</i>	Mass to Charge ratio
<i>n</i> -BuLi	<i>n</i> -Butyl Lithium
NMR	Nuclear Magnetic Resonance Spectrometry
OEt	Ethoxy
PCC	Pyridinium Chloro Chromate
Pet. Ether	Petroleum Ether
pKa	Log ₁₀ of acid dissociation constant (<i>K_a</i>)
Ph	Phenyl
ppm	Parts Per Million
q	Quartet
RAL	Raloxifen
R _f	Retention Factor
RBA	Relative Binding Affinty
s	Singlet
<i>sec</i> -BuLi	<i>sec</i> -Butyl Lithium
t	Triplet
TAM	Tamoxifen
TBA	Tetrabutylammonium
TBAF	Tetrabutylammonium Fluoride
TEA	Tetraethylammonium
TEAF	Tetraethylammonium Fluoride
THF	Tetrahydrofuran
Thr	Threonine

TLC
TOF

Thin Layer Chromatography
Time of Flight

UV

Ultraviolet

VFC

Venus Flytrap Complex

Chapter 1 – Introduction

1.1 The Estrogen Receptor and Breast Cancer

Estrogen receptor (ER) mediated breast cancer accounts for one third of all diagnosed cases of breast cancer.¹ The ER receptor is over expressed on malignant cells, which rely on the binding of estrogen in order to proliferate. Specifically, the binding of 17β -estradiol, also known as 17β -oestradiol,² (**Figure 1.1**) leads to the dimerization of two adjacent hormone receptor complexes which concurrently internalize and attach to specific DNA sequences.^{3,4} Once the necessary co-factors bind, DNA transcription occurs, which, in the case of cancer cells, allows for unregulated cell growth.

In 1997 Brzozowski *et al.* reported the first crystal structure of the ligand binding domain (LBD) of the ER, complexed with 17β -estradiol.² Two ER subtypes exist, ER α and ER β , which share some commonalities in ligand binding.⁵ In the estradiol-ER complex, the phenolic hydroxy group of the A-ring hydrogen bonds to the glutamic acid residue (Glu³⁵³), arginine (Arg³⁹⁴), and to a molecule of water (**Figure 1.2**). The hydroxy group of the D-ring (17β) makes a single hydrogen bond with a histine residue (His⁵²⁴). The remaining stabilization results from the hydrophobic interactions of the rings and the binding pocket. The size of the binding cavity is 450 \AA^3 , which is almost twice the molecular volume of the natural substrate, 245 \AA^3 .

Brzozowski's group also determined the crystal structure of the ER complex containing a known antagonist, Raloxifene (RAL) (**1.2, Figure 1.1**). RAL was shown to bind in a manner similar 17β -estradiol with a phenolic hydroxyl group participating in hydrogen bonding similar to that of the A-ring in the estradiol. However, in order

for the second hydroxy group in 1.2 to hydrogen bond the bulky side chain of RAL induces a rotation of the residue His⁵²⁴ leading to displacement of helix 12 (H12), which in turn prevents the formation of the transcription competent ER structure.^{2,6} The high binding character of RAL results from the secondary amino group located on the side chain, which is judiciously positioned to participate in hydrogen bonding to an aspartic acid residue (Asp³⁵¹).

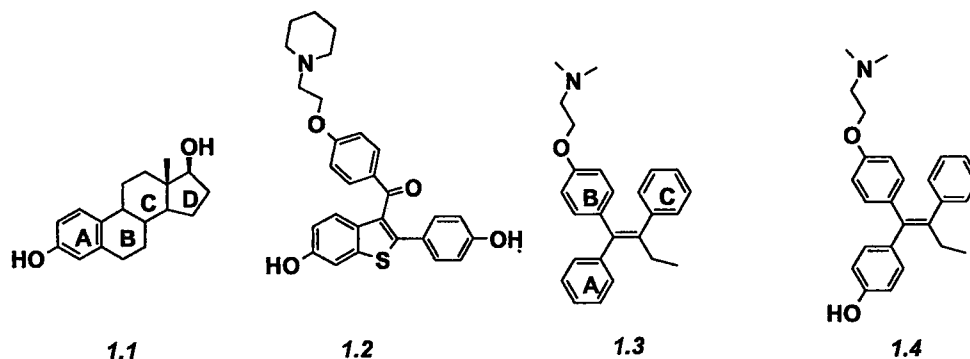


Figure 1.1: 17β-estradiol (1.1), Raloxifen (1.2), Tamoxifen (1.3), 4-Hydroxytamoxifen (1.4).

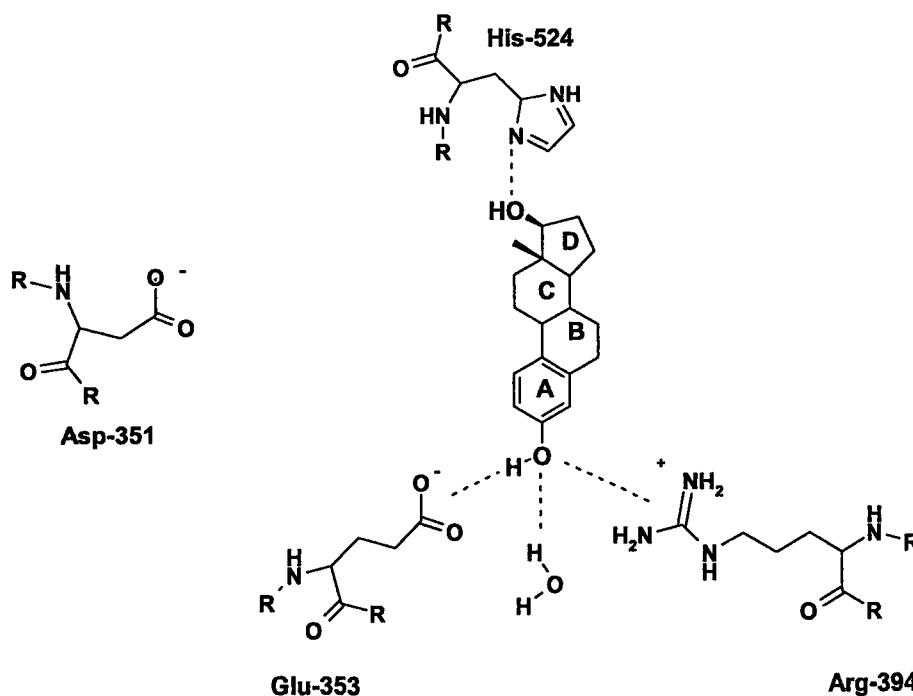


Figure 1.2: Binding of 17β-estradiol to the key residues in the ligand binding domain (LBD) of ER.

1.2 ER Antagonists

The ability of non-steroidal anti-estrogens, like RAL, to inhibit the binding of estrogen, and hence prevent cellular replication was first documented in 1958⁷ when Lerner and co-workers prepared the first non-steroidal anti-estrogen, MER-25 (1.7). These results governed little interest until Tamoxifen (1.3, TAM), (Z)-1[4-(2-dimethylaminoethoxy)phenyl]-1,2-diphenyl-1-butene, was discovered in 1971.⁸

Since its discovery Tamoxifen has been used extensively in the treatment of hormone dependant breast cancer.^{9,10} The pharmacological properties of TAM (Figure 1.1) result from the phenyl rings participation in hydrophobic interactions with the non-polar residues that compose the ER-LBD. The dimethylamino group of Tamoxifen interacts with (Asp³⁵¹) in the receptor binding domain and is a key factor in the compound's anti-estrogenic activity.^{8,11} These intermolecular contacts were evident in the crystal structure of 4-hydroxytamoxifen¹² bound to the ER α -receptor.¹³

Unfortunately, the primary metabolite of TAM, 4-hydroxytamoxifen (1.4) is prone to isomerization of the Z-isomer, which is an antagonist,¹⁴ to the E-isomer, which is a proven estrogen agonist.^{15,16} It is important to note that hydroxylation of the *para*-position of the phenyl ring in 1.3 increases the binding affinity to the ER, compared to TAM itself.⁸

There continues to be active searches for Tamoxifen analogues that display high affinity and antagonist activity which do not undergo the metabolism to toxic by-products. The analogues typically contain the triarylethylene core (Figure 1.3). Zisterer *et al.*¹⁷ for example, prepared a number of Tamoxifen analogues where by each of the phenyl rings were sequentially replaced with benzyl groups.¹⁷ In particular it was observed that insertion of a benzyl group for C-phenyl ring of Tamoxifen was

tolerated so long as there was a secondary amine off the B-Ring (1.5).¹⁷ This work also demonstrated that ER binding was severely affected by substitution off the B-ring.

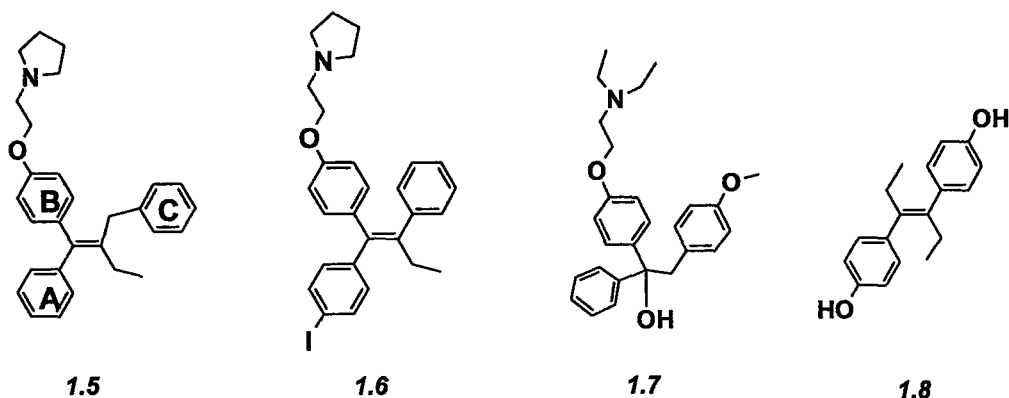


Figure 1.3: 2-Benzyl-1-phenyl-[4-(dimethylaminoethoxy)phenyl]-but-1-ene (1.5), Iodoxifen (1.6),¹⁸ MER-25 (1.7), Diethylstilbesterol (1.8).¹⁹

A greater understanding of the effects of the three dimensional topology of the ER-LBD has resulted in the development of new probes whose 3-D structure, rather than 2-D structure, were used to afford potent agonists.²⁰ To probe the 3-D size, shape and flexibility of the ER-LBD, Katzenellenbogen *et al.* prepared a series of cyclofenil derivatives (Figure 1.4) containing bicyclic and tricyclic moieties off the ethylene unit.²¹ Compound 1.10, for example, exhibited a 500% relative binding affinity (RBA), with 17 β -estradiol showing 100% RBA, while 1.9 was less efficacious with an RBA of 68%.¹⁹ Through the use of computational docking models, the high binding affinity of 1.10 was attributed to site specific hydrogen bonding of the two hydroxyl groups. The first hydroxyl group, analogous to the natural substrate in Figure 1.2, interacts with the two residues Arg³⁹⁴ and Glu³⁵⁴. The second hydroxyl group is well positioned to engage in a hydrogen bond with Asp³⁵¹ and Thr³⁴⁷, generally leading to more effective binding character of the ligand. It was observed that if the correct

spatial orientation of hydrophobic surface was not present in the substrate, a loss in binding affinity occurred. For example, **1.11** displayed RBA of 9% indicating that the ER selectively requires a core that is not excessively over crowded.

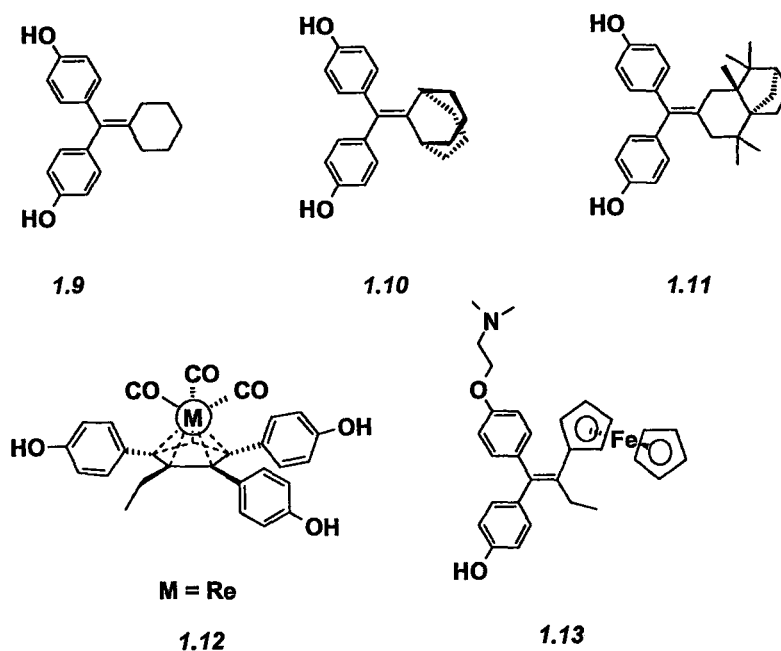


Figure 1.4: Cyclofenil (**1.9**), 9-[bis(4-hydroxyphenyl)methylene]bicyclo[3.3.1]nonane (**1.10**), 2-[bis(4-methoxyphenyl)methylene]-1,3,3-trimethylbicyclo[2.2.1]heptane (**1.11**), 3-ethyl-1,2,4-tri-(4-hydroxyphenyl)cyclopentadienyltricarbonyl rhenium (**1.12**), and Ferrocifen (**1.13**).

In a similar view, Katzenellenbogen and coworkers also used the unique 3-D topology of organometallic compounds derived from cyclopentadienide (**1.12**) to probe the ER as a means of identifying a new class of anti-estrogens (**Figure 1.4**).²² This approach was pioneered by Jaouen and coworkers who developed the use of organometallic compounds as anti-estrogens. For example, Ferrocifen (**1.13**), an organometallic analogue of **1.3** was prepared in which the C-ring of TAM is replaced

with a ferrocene moiety.²³ The first metabolite of 1.13 has been shown to possess anti-cancer properties.²⁴

1.3 Carborane as ER Binding Agents

Using the hydrophobic properties of carboranes, which are clusters of boron, hydrogen and carbon atoms (*vide infra*), a group of potent estrogen receptor (ER) agonists were designed by Endo *et al.*^{25,26} The non-polar carborane was used in place of the C- and D-rings of 17β -estradiol to facilitate enhanced binding interactions through stronger hydrophobic interactions. The compounds were simple aryl-carborane derivatives, where the correct positioning of phenol substituents enhanced relative binding affinity through-site specific hydrogen bonding interactions between the hydroxyl group and the carboxyl group of Glu³⁵³. Screening of a series of carborane derivatives with a Luciferase reporter gene assay²⁷ showed that compounds with phenol groups off the first carbon in the *para*-carborane cage, with the second carbon bearing a hydrogen atom, a hydroxy group, or hydroxy group with one methylene unit spacer, all exhibited greater estrogenic activity than the natural substrate (Figure 1.5).

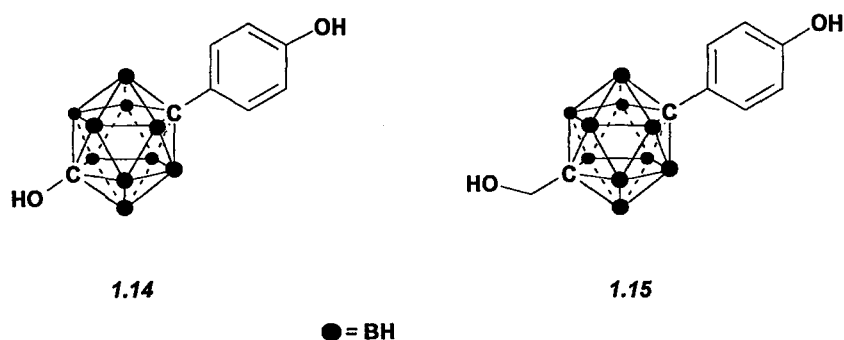


Figure 1.5: Carborane estrogen agonists developed by Endo *et al.*²⁵

The diaryl-*ortho*-carborane (*vide infra*) derivative **1.17**, at concentrations of 10^{-7} M, showed 70% inhibition of the transcriptional response to the natural substrate and at concentrations of 10^{-6} M showed almost complete inhibition (**Figure 1.6**).²⁸ These results are in agreement with the work conducted by Katzenellenbogen *et al.*¹⁹ which showed that large hydrophobic groups can improve estrogen receptor binding if they possess the correct 3-D spatial orientation. The carborane derivatives are attractive not only because of their impact on estrogen receptor binding but because of their potential resistance to catabolism and their potential to be radiolabelled (*vide infra*).²³

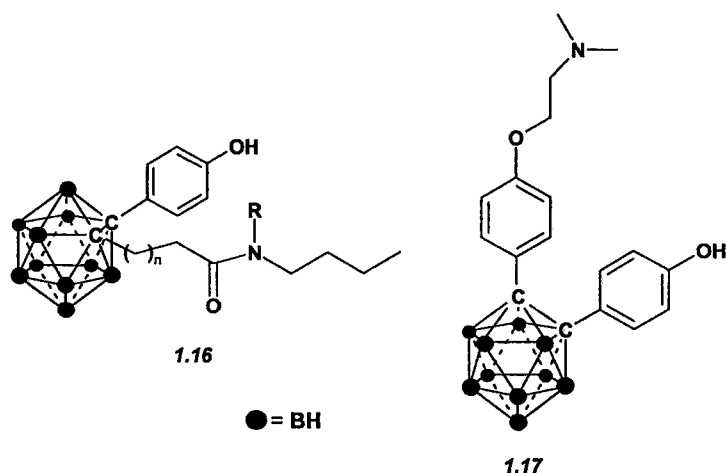


Figure 1.6: Carborane antiestrogens developed by Endo and coworkers.²⁹

1.4 Polyhedral Boranes

Borane hydride clusters were first prepared by Alfred Stock³⁰ in the early 1930's and were later characterized in the 1950's as three dimensional structures made up of an array of three center two electron bonds³⁰ ($3c-2e^-$) as shown by electron³¹ and low temperature X-ray diffraction studies.³⁰ The vertices in polyhedral boranes are composed of boron atoms that are bonded to each other in a $3c-2e^-$ fashion and to at least one *exo*-hydrogeon atom. These hydrogen atoms have a hydride like character

due in part to the formal electron deficiency of the structure and to the electronegativity differences between the boron and hydrogen nuclei.³⁰ Polyhedral boranes are typically electron deficient structures based on conventional two center two electron bonding ($2c-2e^-$) models.

The existence of diborane (**1.18**, **Figure 1.7**) was predicted back in 1921 but it remained until 1943 before the structure was determined unambiguously. The structure consists of a pair of two electron deficient BH_3 units which dimerize via a pair of ($3c-2e^-$) bonds. This simple boron hydride, with a molecular formula of B_2H_6 (**1.19**), is presented as having two bridging hydrogen atoms that are each bonded to two boron centers.^{32,33}

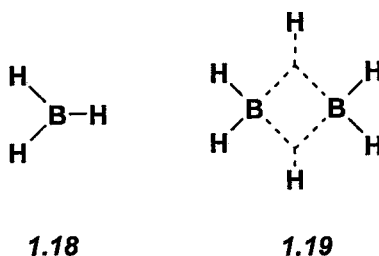


Figure 1.7: **1.18**) BH_3 , **1.19**) B_2H_6 (diborane)

In the 1950's a number of larger neutral boranes including; B_4H_{10} , B_5H_{11} , B_6H_{12} , B_8H_{12} , and B_9H_{15} , were reported and characterized. Neutral boron hydrides are moisture sensitive and are unstable in air. In contrast the borane hydride anions like $[B_{10}H_{10}]^{2-}$ and $[B_{12}H_{12}]^{2-}$, show remarkable stability and are not sensitive to moisture or acid.^{35,34} Researchers first predicted, based on topological models, that the structures of these clusters would resemble distorted fragments of a regular icosahedron, with some exceptions, such as B_5H_9 , that assumes a pyramidal geometry.^{30,35} Only upon later examination of borane clusters of different molecular

formulae did it become evident that the key structural units present in boron polyhedra structures consisted of the most spherical deltahedra, the icosahedron (Figure 1.8).^{35,36,37-41}

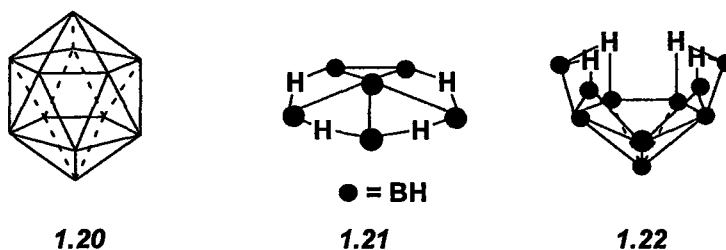


Figure 1.8: The icosahedron (1.20), B_6H_{10} (1.21), and $B_{10}H_{14}$ (1.22).

Borane cages have been evaluated for a number of applications, particularly in the last decade. The applications include doping of semiconductors along with the production of advanced boron-based ceramics.⁴² The high boron content has led to the use of polyhedral borane derivatives as boron delivery vehicles for boron neutron capture therapy (BNCT), which is an experimental modality for cancer therapy.⁴² Other applications include the use of such clusters as catalysts for homogenous hydrogenation, solvent extractions of radionuclides, and the preparation of novel ligands for coordination chemistry and radiopharmaceutical chemistry.⁴²

1.5 Dicarba-*closo*-dodecaborane

Of particular importance to this research was a subset of icosahedral heteroboranes known as dicarba-*closo*-dodecaboranes, which have the general formula $C_2B_{10}H_{12}$ and are commonly referred to as carboranes. These compounds are derived from the $[B_{12}H_{12}]^{2-}$ polyhedron, in which two of the BH vertices are replaced with isolobal CH fragments (Figure 1.9). Carboranes exhibit distinct differences in

chemical and physical properties from their parent binary boranes as a result of the increased electronegativity of the substituted vertices and changes in the overall formal charge.

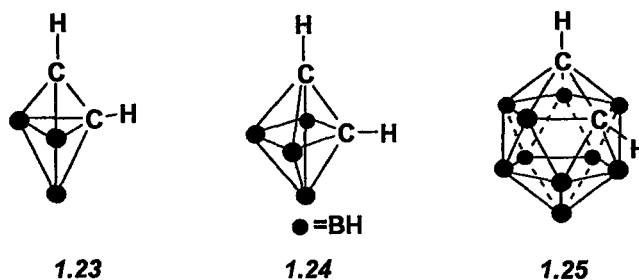


Figure 1.9: $1,2\text{-C}_2\text{B}_3\text{H}_5$ (1.23), $1,2\text{-C}_2\text{B}_4\text{H}_6$ (1.24), and $1,2\text{-C}_2\text{B}_{10}\text{H}_{12}$ (1.25).

The first carboranes to be synthesized were $\text{C}_2\text{B}_3\text{H}_5$ (1.23)^{35,43} and the two isomers of $\text{C}_2\text{B}_4\text{H}_6$ (1.24),^{35,44} while 1,2-dicarbapentaborane, also known as *ortho*-carborane (abbreviated to *o*-carborane), (1.25), was first reported in 1963 by two different groups.^{45,46} At present, polyhedral carboranes from $\text{C}_2\text{B}_3\text{H}_5$ up to $\text{C}_2\text{B}_{10}\text{H}_{12}$ have been successfully isolated in at least one isomeric form.^{47,48}

It is important to point out that both the carbon and boron atoms within the carborane structure are hexacoordinate. The multicenter bonding can be explained through the use of molecular orbital (M.O.) theory. Despite the lack of a sufficient number of electrons needed to satisfy the conventional valence electron count required of stable compounds, the number of bonding orbitals predicted by molecular orbital theory for the point group I_h are, in the case of carboranes, filled. Collectively for icosahedrons there are 12 tangential molecular orbitals and one spherical orbital (a_{1g}) which sum to 13 bonding orbitals, a number that coincides with the number of skeletal electrons predicted by Wade's rules for such a structure.³⁵ Given the molecular formula of *o*-carborane, each boron vertex contributes 2 electrons to the skeletal

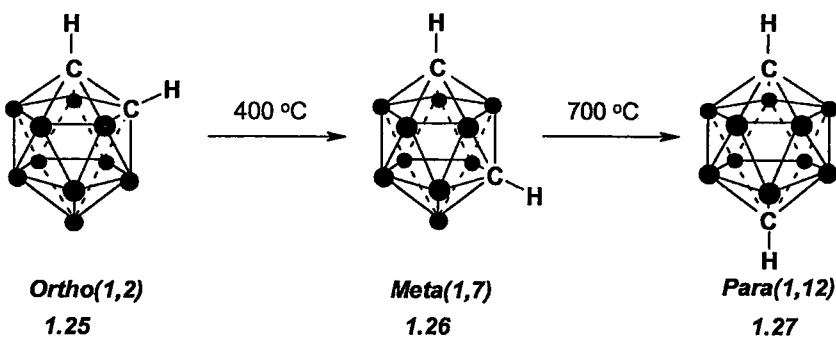
system with the remaining electrons provided by the carbon vertices, together constituting the 26 skeletal bonding electrons. The break down for the electron distribution in the cluster requires two electrons from each vertex along with the two extra electrons arising from the presence of one extra valence electron naturally occurring on the two carbon atoms, with respect to that of boron. The remaining number of electrons from each vertex offers a full complement of electrons required to constitute the bonding of the terminal hydrogen atoms.³⁵

1.6 Isomerization of Carboranes

In 1963 it was reported that attempts to dimerize or possibly polymerize *o*-carborane via thermal dehydrogenation led not to the desired species but instead to two isomeric products.⁴⁷ Under inert atmosphere and temperatures of 465-500 °C, (Scheme 1.1) 1,2-dicarba-*closo*-dodecaborane isomerized to the 1,7-isomer of carborane (1.26).^{35,49-52} This 1,7-dicarba-*closo*-dodecaborane, also known as *neo*- or *meta*-carborane, abbreviated *m*-carborane, closely resembled *o*-carborane in melting points (*meta*- 263 to 265 °C, *ortho*- 287 to 288 °C), odour, appearance, and solubility. 1,7-dicarba-*closo*-dodecaborane was also shown to further thermally isomerize at temperatures near 620 °C, to the 1,12-dicarba-*closo*-dodecaborane, which is referred to as *para*- or *p*-carborane (1.27).^{35,48,53}

There are a number of differences between the isomers in terms of chemical and physical properties. These differences are often attributed to the change in overall polarity associated with the different positioning of the more electronegative carbon vertices within the icosahedral frameworks. The impact of the carbon atom positions within the cluster was demonstrated in a pKa study of three analogous C-substituted

carboxylic acids.⁴⁷ The *ortho*-derivative was appreciably more acidic with a pKa of 22.0 followed by *meta*-carborane and *para*-carborane with pKa values of 25.6 and 26.8 respectively.^{54,55} The increased electronegativity of the two proximal carbon atoms in *ortho*-carborane render this cage more polar than *meta*- and *para*-carborane, which has the smallest dipole of the three isomers.



Scheme 1.1: The thermal isomerization of 1,2-dicarba-closo-dodecaborane to the 1,7- and 1,12-isomers.

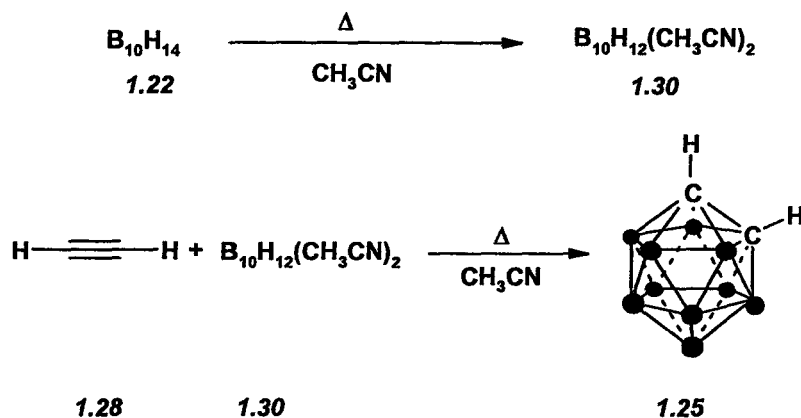
1.7 Characterization of Carboranes

Carboranes can be readily characterized by a number of techniques. The infrared spectrum, for example, of dicarba-*closo*-dodecaboranes exhibits a significant B-H stretch around 2600 cm^{-1} ; a region that generally does not contain signals for organic compounds. The signal is a broad peak reflecting an averaged stretching mode for all B-H bonds of the carborane system.⁵⁵ There is also a C-H stretch mode typically observed around 3080 cm^{-1} . There are also some striking differences between *ortho*- and *meta*-carborane in the fingerprint region, for example a bending mode present at 1212 cm^{-1} for *o*-carborane is absent from the IR spectrum for *meta*-isomer. The symmetry point group of the underivatized *o*-carborane is C_{2v} , with a lowering of symmetry occurring upon mono C-substitution.⁵⁵ The proton NMR spectrum for

carboranes typically consists of a very broad, undulating series of signals observed between 3.5 ppm and 0.5 ppm, which arise from the hydrogen atoms bound to the boron vertices of the cluster. There is also a resonance for the hydrogen atom bound to the carbon vertex of the cage which typically occurs around 3.9 ppm. Another key instrumental technique employed in the characterization of carboranes, and novel carborane derivatives, is mass spectrometry whereby the characteristic $^{10}\text{B}/^{11}\text{B}$ isotopic distribution presents itself as a normal distribution about the median value.⁵⁶

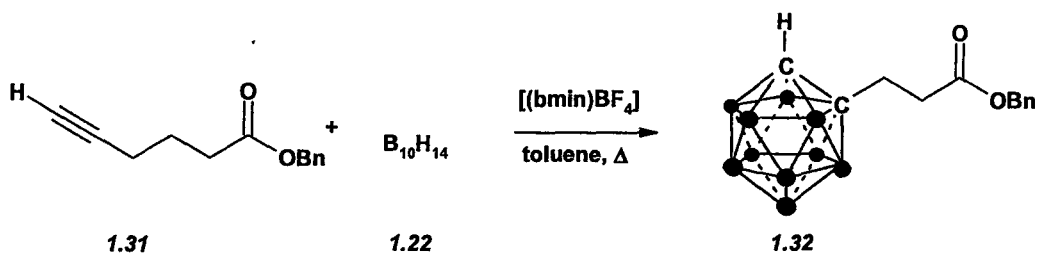
1.8 Synthesis of *Ortho*-Carboranes

Ortho-carboranes prepared by the reaction of an alkyne, acetylene (1.28) being used in the unsubstituted case, with a Lewis base adduct of decaborane, $\text{B}_{10}\text{H}_{14}$ (1.22).^{35,45,46,57,58} The Lewis base adduct is prepared by reacting a weakly coordinating Lewis base such as alkylamines, alkylsulfides, or acetonitrile (1.29) with 1.22 (Scheme 1.2). The alkyne can be added directly to the reaction mixture of the Lewis base adduct generated *in situ*, or the adduct can be isolated and subsequently reacted with the alkyne at a later time. Carbon substituted *ortho*-carborane derivatives can be prepared directly from the corresponding alkyne provided it does not contain a nucleophilic functional group. Alkynes containing alcohols, amines, and carboxylic acids must be protected prior to reaction with decaborane.³⁵ This approach often works well for monosubstituted alkynes but gives poor yields for disubstituted compounds.³⁵



Scheme 1.2: The preparation of *o*-carborane, $\text{C}_2\text{B}_{10}\text{H}_{12}$ (1,2-dicarbonyl-dodecaborane).

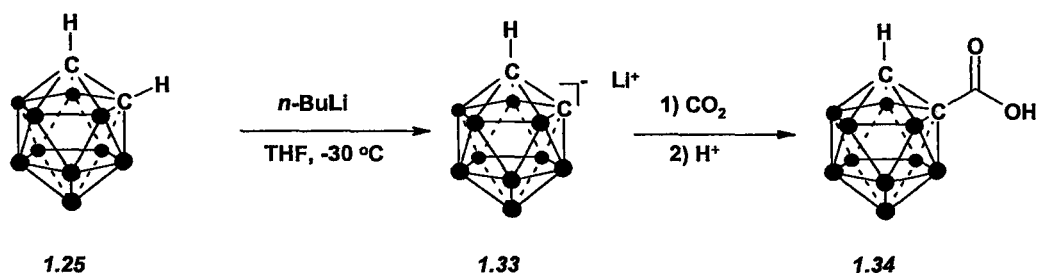
Recently, a new method for the preparation of mono- and di-substituted *ortho*-carboranes has been developed by Sneddon *et al.*,⁵⁹ which improves the overall yields particularly when employing di-substituted alkynes. The method involves reacting the alkyne with decaborane in a mixture of toluene and an ionic liquid such 1-butyl-3-methylimidazolium tetrafluoroborate [(bmin)BF₄]. These conditions typically produce the desired compounds in higher yields and in shorter reaction times than the conventional approach described above (Scheme 1.3).⁵⁹



Scheme 1.3: Preparation of *o*-carborane derivatives with functionalized alkynes, using ionic liquids.

1.9 Reactivity of *Ortho*-Carboranes

The pKa for *ortho*-carborane (22.0) makes it possible to deprotonate the C-H vertex using a stoichiometric amount of strong base (MeLi, *sec*-BuLi, and *n*-BuLi).^{35,60-62} The resulting mono-lithiocarboranes are nucleophilic and react with a range of electrophiles including halogens (X₂), alkyl halides, CO₂, aldehydes, acid chlorides, and epoxides (Scheme 1.4).³⁵



Scheme 1.4: Preparation of mono-lithiocarborane (1.33) and subsequent reaction with CO₂.

It should also be noted that equilibrium between the mono-lithiocarborane (1.33) and di-lithiocarborane (1.35) species is known to exist in solution, with the process favouring the monometallation product when a reaction is run at dilute concentrations (Figure 1.10). The equilibrium constant for formation of the dilithio compound is much smaller for *meta*- and *para*-carborane.⁶³

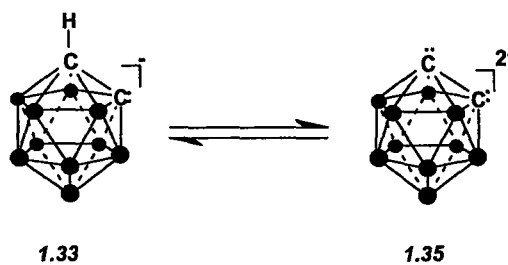


Figure 1.10: Equilibrium between deprotonated forms of *o*-carborane.

Ortho-carboranes are stable to a wide range of reaction conditions, the major exception being the exposure of the carborane cage to strong Brønsted or Lewis bases. As such, it is possible to conduct a diverse number of transformations on carborane derivatives including displacement reactions,⁶⁴⁻⁶⁸ Wittig reactions,⁶⁹ oxidations and reduction reactions.^{68,70} Carborane cages containing phenyl substituents are stable to most electrophilic aromatic substitution conditions allowing for selective substitution of the ring.^{71,72,79} Those carboranes substituted with aliphatic hydroxyl components have been shown to be successfully oxidized by either strong oxidants such as potassium dichromate or milder oxidation methods including Swern oxidation, PCC, and even peracids,^{42,68,73,74} without causing cage degradation. The carboranyl moiety has even been shown to be stable against strong reducing reagents such as lithium aluminium hydride, palladium catalysed hydrogenation, diisobutylaluminum hydride, as well as various borane based reducing agents including $\text{BH}_3 \cdot \text{SMe}_2$.^{62,70,72,75-77}

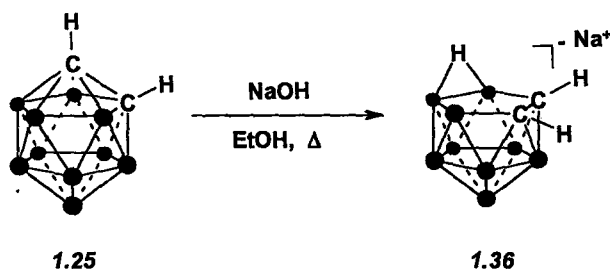
The B-H vertices in carboranes are orthogonal to the C-H vertices in terms of their reactivity, in that the B-H groups react with strong electrophiles.^{35,78} Halogenation of the boron vertices is possible using Lewis acid catalyst, such as AlX_3 , followed by the addition of Cl_2 , Br_2 , I_2 , or mixed halogens such as ICl or IBr .^{79,80}

1.10 *Nido*-Carboranes

In the presence of alkoxide bases and secondary amines both *o*-carborane⁸¹ and *m*-carborane⁸²⁻⁸⁵ and their C-substituted derivatives, are degraded to the respective *nido*-carboranes (Scheme 1.5). The process involves selective loss of one of the two most electrophilic boron vertices, resulting in the formation of an anionic cluster, which is significantly more hydrophilic.^{35,85} In the 1,2-isomer the boron atom removed is either of the B3 or B6 atoms while in the 1,7-isomer the B2 or B3 centers are lost,

yielding 7,8-dicarba-*nido*-undecaborate, $[7,8-C_2B_9H_{12}]^-$, and 7,9-dicarba-*nido*-undecaborate, $[7,9-C_2B_9H_{12}]^-$, respectively. The by-products consist of hydroxyborates and hydrogen gas.⁹⁷ The resulting *nido*-carboranes contain a bridging hydrogen atom, which occupies the vacancy left by the lost boron vertex.⁸⁵ This hydrogen atom has been shown to be fluxional between the 3 boron atoms present on the open face of the structure.⁸⁶ The regioselective nature of the attack was shown convincingly by the stability of *closo*-B3/B6-disubstituted *o*-carboranes towards base.⁸⁷

A wide range of reagents and conditions can be used to prepare both the 7,8- or 7,9- $[C_2B_9H_{12}]^-$ structures including trialkylamines,^{88,89} hydrazine,^{60,90,91,92} ammonia,^{93,95} piperidine,^{85,94} and even fluoride ion.^{95,96} It has also been shown that electron withdrawing substituents located in the α -position to the cage can promote facile degradation to the corresponding *nido*-carborane when such compounds are left in polar protic solvents over extended periods of time.⁹⁷

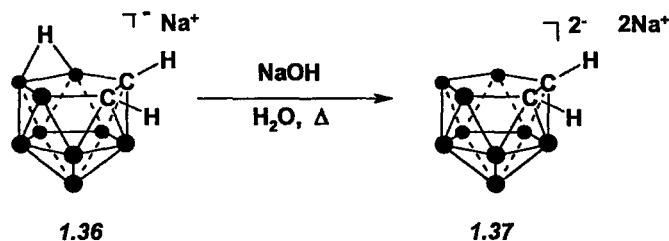


Scheme 1.5: Degradation of *ortho*-carborane to the corresponding *nido*-carborane.

All isomers of dicarba-*closo*-dodecaborane are prone to deboronation by base however *meta*-carborane is generally more resistive to cage degradation than *ortho*-carborane, while *para*-carborane requires harsh conditions of 30% NaOH in propylene glycol heated to 180 °C to afford the corresponding *nido*-carborane.⁹⁸

1.11 The Dicarbollide Dianion

Removal of the bridging hydrogen in *nido*-carborane yields another *nido*-carborane that is referred to as the dicarbollide dianion (1.37). The removal of this hydrogen is accomplished by the addition of stoichiometric amounts of a strong base.⁹⁹⁻¹⁰² The process is reversible particularly when aqueous bases are used (Scheme 1.6).⁹⁹⁻¹⁰¹



Scheme 1.6: Removal of the bridging hydrogen in 7,8-dicarba-*nido*-undecaborate to yield 2,3- $[C_2B_9H_{11}]^{2-}$, (the dicarbollide dianion).

Dicarbollide dianions, which have the molecular formula $[C_2B_9H_{11}]^{2-}$, contain atoms on the open face of the cluster that have sp^3 -like orbitals directed towards the vacant vertex of the icosahedron (1.38).¹⁰³ The number of electrons present within these sp^3 -type orbitals makes the dicarbollide dianion formally isolobal with the cyclopentadienyl anion (Cp) (1.39) (Figure 1.11).¹⁰²

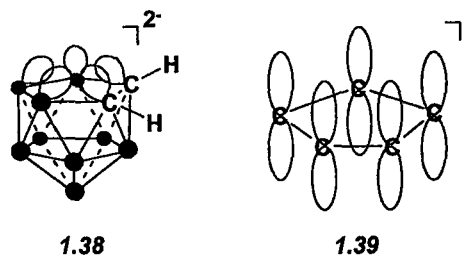
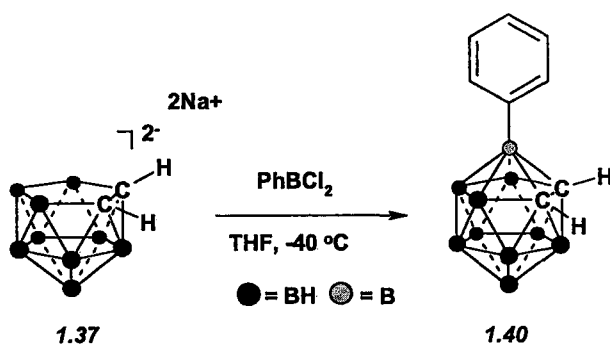


Figure 1.11: The isolobal nature of the dicarbollide dianion (1.38) and cyclopentadienide (1.39).

The arrangement of the orbitals on the open face of the dicarbollide dianion makes it possible to react the *nido*-carborane with capping agents and metal fragments. For example, it has been reported that $[\text{C}_2\text{B}_9\text{H}_{11}]^{2-}$ ions react with monoboron reagents such as aryl- or alkylboron dihalides to form the corresponding *closo*-carborane cage having the aryl or alkyl substituent located off the vertex of the inserted center (Scheme 1.7).^{87,102,104} The dicarbollide dianion has also been shown to react with other main group elements including dimethylberyllium etherate,¹⁰⁵ $(\text{CH}_3)_2\text{Be}(\text{Et}_2\text{O})_2$, aluminium ethyl dichloride,¹⁰⁶ EtAlCl_2 , tin dichloride,¹⁰⁷ SnCl_2 , to produce closed heteropolyhedral structures containing the respective main group elements within the icosahedral framework.



Scheme 1.7: Restoration of the *closo*-structure from the dicarbollide dianion (1.37) to give 3-phenyl-1,2-dicarba-*closo*-dodecaborane (1.40).

1.12 Metallocarboranes

As mentioned earlier, the dicarbollide dianion is isolobal to the cyclopentadienide anion. As such, the dicarbollide dianion has been used as a ligand to prepare a large number of sandwich type complexes. To exemplify the isolobal parallels of the dicarbollide dianion, the carborane analogue of ferrocene, $[(\text{C}_2\text{B}_9\text{H}_{11})_2\text{Fe}]^{101,102}$ and a mixed analogue $(\text{C}_2\text{B}_9\text{H}_{11})\text{Fe}(\text{C}_5\text{H}_5)$ were prepared.¹⁰⁸ The

oxidation state of iron after complexation is +3, but can be lowered to +2 by a reduction reaction with an amalgam of sodium.^{109,110} A substantial number of other metallocene analogues for both *ortho*- and *meta*-isomers have been reported including those of chromium,¹¹¹ cobalt¹⁰² nickel,^{102,112} palladium,^{102,113} as well as copper and gold.^{102,113}

The reaction of *o*- and *m*-dicarbollide dianions (7,8- and 7,9-[C₂B₉H₁₁]²⁻), with hexacarbonyls of chromium, molybdenum, and tungsten under ultraviolet light produced air sensitive dicarbollyl metal tricarbonyl complexes, instead of the bis(dicarbollyl) complexes.^{102,114} For manganese and rhenium, the tripodal complexes of dicarbollide dianion were prepared from *nido*-carborane 1.36, the respective metal bromopentacarbonyls, and a strong base (NaH).^{103,115,116}

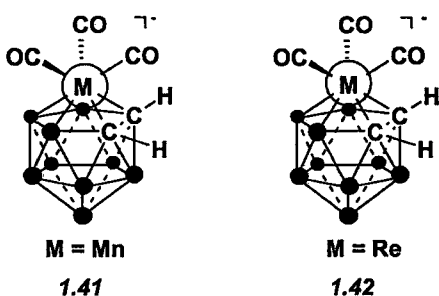


Figure 1.12: Metal tricarbonyl carborane complexes prepared by Hawthorne et al.¹¹⁵

1.13 The Medicinal Chemistry of Carboranes

The original interest in using carboranes for medicinal applications was as a source of boron atoms for boron neutron capture therapy (BNCT). BNCT is a binary cancer therapy regime that was proposed by Locher in 1936.¹¹⁷ The premise of this binary approach to cancer treatment was based on the reaction of neutrons with ¹⁰B isotope, which produces α -particles and lithium ions. The high energy of these ions

can be used to ablate tumours. Carboranes are attractive synthons for BNCT because of their high boron content and because of their versatile synthetic chemistry which allows for unique bioconjugation strategies to be used to facilitate the accumulation of boron at the site of the disease.^{118,119}

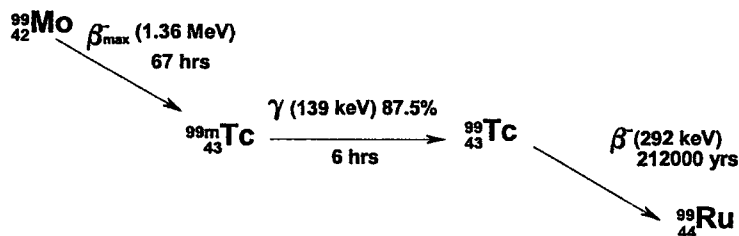
Beyond BNCT, carboranes are attractive synthons for medicinal chemistry because of their resistance to catabolism,⁴² low toxicity ($LD_{50} = 7 \text{ g/kg}$)¹²⁰, and because of their hydrophobic nature. Furthermore, the volume occupied by the carborane cage (5.25 \AA^3) is of similar size to that mapped out by a rotating phenyl ring (4.72 \AA^3).^{46,121} It is therefore possible that for certain classes of compounds carboranes can be used in place of phenyl groups as hydrophobic and/or catabolic resistant pharmacophores or as basic structural elements without significantly affecting the binding to the target receptors.²⁸

The aforementioned properties (high boron content, synthetic flexibility, hydrophobicity, *in vivo* stability) has lead to the preparation of a number of medicinal agents including: carborane nucleoside analogues,^{122,123} carboranyl DNA intercalators,¹²⁴ amino acid analogues,^{125,126} magnetic resonance imaging (MRI) agents,^{127,128} folic acid analogues,¹²⁹ immunoconjugates,^{130,131} liposomes,^{132,133} polyamines,¹³⁴ carbohydrates,^{135,136} estrogen agonists^{28,28} and antagonists,²⁹ and retinoids.^{145,146} The majority of these agents were developed for use as BNCT agents. More recently carboranes have been used as ligands for developing radiotracers.

1.14 Re and ^{99m}Tc/⁹⁹Tc-Metallo-carboranes and Radiopharmaceuticals.

Technetium-99m is the most widely used radionuclide in diagnostic nuclear medicine. This is a result of the ideal nuclear properties of the isotope which includes

emission of a low energy gamma ray (139 keV) and a relatively short half-life (6.02 hrs). ^{99m}Tc is also readily available, at a modest cost, from ^{99}Mo - ^{99m}Tc generators, which takes advantage of the decay of ^{99}Mo to ^{99m}Tc (Scheme 1.8).



Scheme 1.8: The decay scheme for ^{99}Mo .

One approach used to target ^{99m}Tc to specific receptors, is to bind the metal to a biomolecule through a bifunctional ligand. The ligand used to complex the metal must form a stable species, which does degrade *in vivo*. To be of use in a nuclear medicine applications, complexes must be capable of being prepared in water where the concentration of the radionuclide is typically between 10^{-8} M to 10^{-9} M.²²

Carboranes are attractive sythons for preparing radiometal complexes because metallocarboranes can be prepared in water.¹⁴⁰ A number of carborane-metal complexes are very stable and do not undergo spontaneous degradation even in the presence of competing ligands.^{137,138} A further advantage to using carboranes is that they can be easily derivatized with a wide range of groups which creates new ways of targeting the metal complexes to specific receptors.

Hawthorne and collaborators reported the synthesis of pyrazole-bridged bis(dicarbollide dianion) complex of ^{57}Co (1.43).¹³⁸ The ligand is referred to as the Venus flytrap complex (VFC) because it possesses two *nido*-[7,9- $\text{C}_2\text{B}_9\text{H}_{11}$]²⁻ ions hinged together by a bridging pyrazole group. The ligand also contains an ester

functional group, which was later used to append the ligand to a monoclonal antibody (Figure 1.13).¹³⁸ This carborane-radionuclide-antibody conjugate demonstrated specific localization during biological distribution studies.¹³⁹

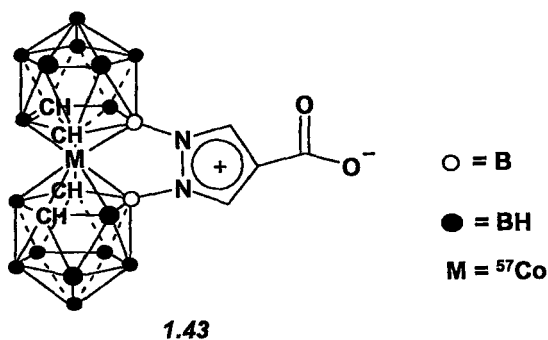
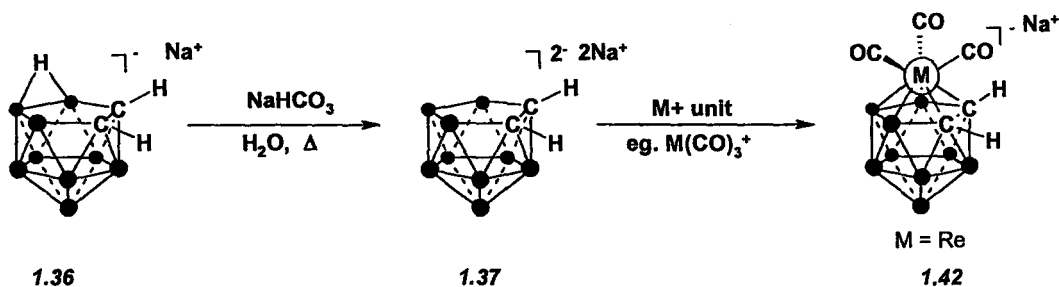


Figure 1.13: The Venus Flytrap Complex (VFC) of ^{57}Co (1.43).

Our group recently reported a new approach for preparing Tc/Re tricarbonyl carborane complexes in both organic and aqueous solutions under conditions suitable for labelling at the tracer level (Scheme 1.9).¹⁴⁰ The procedure involves reacting a *nido*-carborane (1.36) with $[\text{M}(\text{CO})_3\text{Br}_3]^{2-}$ or $[\text{M}(\text{CO})_3(\text{H}_2\text{O})_3]^+$, ($\text{M} = {}^{99}\text{Tc}$ and Re). The latter compound can be prepared at the tracer level using a commercially available kit.²²



Scheme 1.9: Generation of the rhenium (I) tricarbonyl carborane complexes in water.

The stability of the ^{99}Tc -carborane complexes were evaluated by incubating the cluster with an excess of cysteine. No transchelation was observed indicating that the Re/Tc-metallocarboranes are suitable for *in vivo* applications. The ability to form stable complexes of $^{99\text{m}}\text{Tc}$, coupled with the ability to conjugate the clusters to biological targeting agents makes carboranes an interesting synthon from which to design novel radiopharmaceutical and biological probes.

1.15 Carboranes as Pharmacophores

One way of targeting carboranes or metallocarboranes to specific receptor systems is to use the cluster as an integral part of a pharmacophore. For example, Endo and coworkers developed a series of retinobenzoic acid derivatives containing both amide and amine cores having *ortho*-carboranyl groups off either of the 3 or 4 positions of the central aryl group (**Figure 1.14**).¹⁴¹⁻¹⁴³ The carborane analogues were studied because of the finding that the introduction of hydrophobic groups into retinobenzoic acids could generate an antagonistic effect (**Figure 1.14**).¹⁴⁴ It was observed that those retinobenzoic acid derivatized with an amide functionality and an *ortho*-carboranyl unit at the 4-position, at a concentration of 10^{-6} M, were able to inhibit the activity of a potent retinoid, Am80. The presence of an alkyl group off of the carborane cage, in particular a C-substituted methyl group, showed even greater ability for inhibition of cell differentiation triggered by Am80. In comparison, those analogues with the carboranyl unit at the 3-position induced differentiation only when a potent retinoidal synergist was present.¹⁴⁵

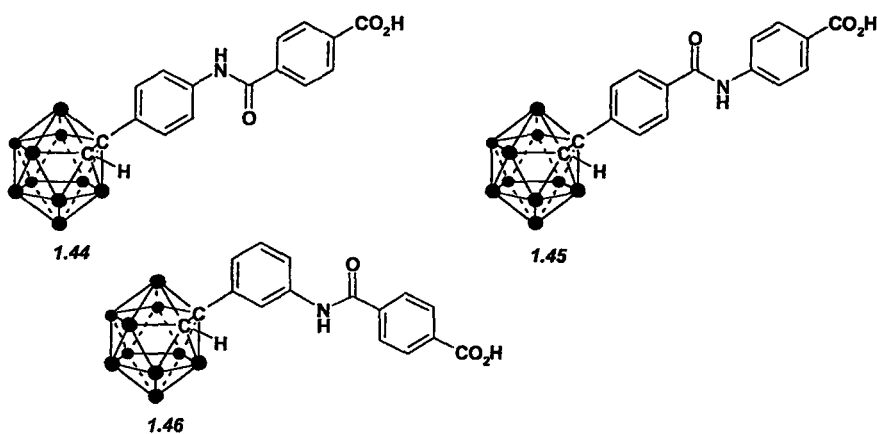


Figure 1.14: Carborane containing retinoids prepared by Endo and co-workers.

Endo and co-workers also used the hydrophobic nature of carboranes to prepare compounds to target protein kinase C.¹⁴⁶ The derivatives (1.47) contained *ortho*-carborane located at the 9-position of a benzolactam core (Figure 1.15). The benzolactam core is a moiety common to a number of compounds known to activate the enzyme. It was observed that both the underivatized carborane benzolactam and those carborane benzolactams that had bulky alkyl groups off the second carbon in the cage were effective at inhibiting tumour growth with the alkylated carboranes showing the highest efficacy.

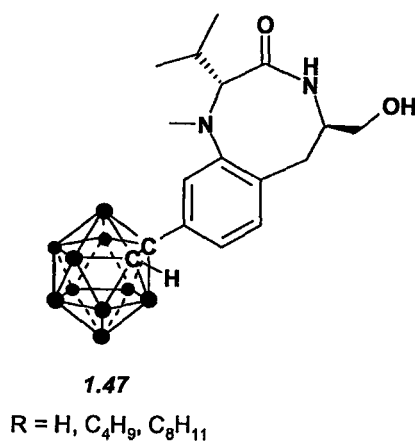


Figure 1.15: Protein kinase C targeting carborane derivatives.

1.16 Scope and Summary of Research

The objective of this thesis was to build on the findings reported by Endo and coworkers and to develop a means to prepare a series of Re-metallocarborane analogues that are capable of binding to the ER. The long-term objective would be to use the methodology to identify metallocarboranes that have high affinity for the ER. These compounds could subsequently be used to prepare novel diagnostic agents ($M=^{99m}\text{Tc}$), radiotherapy agents ($M=^{188}\text{Re}$), and inorganic anti-estrogens ($M=\text{Re}$).

Chapter 2 focuses on the synthesis of monoarylated rhenacarborane derivatives, while Chapter 3 addresses the preparation of diarylated rhenacarborane derivatives. The document is concluded with a discussion of ongoing attempts to synthesize the technetium tricarbonyl carborane derivatives, a discussion of future research including plans to explore the interesting NMR and solid-state structures of congested diarylated rhenacarborane complexes.

1.17 References

- ¹ Theobald, A.J.; *Int. J. Clin. Pract.* **2000**, *54*, 665.
- ² Brzozowski, A.M.; Pike, A.C.W.; Dauter, Z.; Hubbard, R.E.; Bonn, T.; Engstrom, O.; Ohman, L.; Greene, G.L.; Gustafsson, J.; Carlquist, M.; *Nature*. **1997**, *389*, 753.
- ³ Beato, M.; Sanchez-Pacheco, A.; *Endocr. Rev.* **1996**, *17*, 587.
- ⁴ Lerner, L.J.; Jordan, V.C.; *Cancer Res.* **1990**, *50*, 4177.
- ⁵ Kuiper, G.G.J.M.; Carlsson, B.; Grandien, K.; Enmark, D.; Haggblad, J.; Nilsson, S.; Gustafsson, J.S.; *Endocrin.* **1997**, *138*.
- ⁶ Grease, T.A.; *et al. J. Med. Chem.* **1997**, *40*, 146.
- ⁷ Lerner, L.J.; Holthaus, J.F.; Thompson, C.R.; *Endocrin.* **1958**, *63*, 295.
- ⁸ Jordan, V.C.; *J. Steroid Biochem.* **1974**, *5*, 354.
- ⁹ Furr, B.J.A.; Jordan, V.C.; *Pharmacol. Ther.* **1984**, *25*, 127.
- ¹⁰ Lerner, L.J.; Jordan, V.C.; *Cancer Research.* **1990**, *50*, 4177.
- ¹¹ Carter, C.L.; Allen, G.; Henderson, D.E.; *Cancer.* **1989**, *63*, 181.
- ¹² Shiua, A.K.; Barstad, D.; Loria, P.M.; Cheng, L.; Kushner, P.J.; Agard, D.A.; Greene, G.L. *Cell.* **1998**, *95*, 927.

- ¹³ Top, S.; Dauer, B.; Vaissermann, J.; Jaouen, G.; *J. Organomet. Chem.* **1997**, *541*, 355.
- ¹⁴ Harper, M.J.; Walpole, A.; *Nature.* **1966**, *61*, 3890.
- ¹⁵ Shani, J.; Gazit, A.; Livishitz, T.; Biran, S.; *J. Med. Chem.* **1985**, *28*, 1504.
- ¹⁶ MacGregor, J.I.; Jordan, V.C.; *Pharm. Sci.* **1998**, *50*, 151.
- ¹⁷ Meegan, M.J.; Hughes, R.B.; Lloyd, D.G.; Williams, D.C.; Zisterer, D.M.; *J. Med. Chem.* **2001**, *44*, 1072.
- ¹⁸ MaCague, R.; Leclerq, G.; Legros, N.; Goodman, L.; Blackburn, G.M.; Jarman, M.; Foster, A.B.; *J. Med. Chem.* **1989**, *63*, 181.
- ¹⁹ Katzenellenbogen, J.A.; Muthyalal, R. S.; Sheng, S.; Carlson, K. E.; Katzenellenbogen, B. S.; *J. Med. Chem.* **2003**, *46*, 1589.
- ²⁰ Pike, A.C.; Brzozowski, A.M.; Jubbard A.R.E.; Bonn, T.; Thorsell, A.G.; Engstrom, O.; Ljunggren, J.; Gustafsson, J.; Carlquist, M.; *EMBO J.* **1999**, *18*, 4608.
- ²¹ Lunan, C.B.; Klopper, A.; *Clin. Endocrinol. (Oxford)* **1975**, *4*, 551
- ²² Mull, E.S.; Sattigeri, V.J.; Rodriguez, A.L.; Katzenellenbogen, J.A.; *Bioorg. Med. Chem.* **2002**, *10*, 1381.
- ²³ Top, S.; Dauer, B.; Vaissermann, J.; Jaouen, G.; *J. Organomet. Chem.* **1997**, *541*, 355.
- ²⁴ Kopf-Maier, P.; Kopf, H.; *Chem. Rev.* **1987**, *87*, 1137. Houlton, A.; Roberts, R.M.G.; Silver, J.; *J. Organomet. Chem.* **1991**, *418*, 107.
- ²⁵ Endo, Y.; Iijima, T.; Yamakoshi, Y.; Kubo, A.; Itai, A.; *Bioorg. Med. Chem. Lett.* **1999**, *9*, 3313.
- ²⁶ Endo, Y.; Iijima, T.; Yamakoshi, Y.; Fukusawa, H.; Miyaura, C.; Inada, M.; Kubo, A.; Itai, A.; *Chem. Bio.* **2001**, *8*, 341.
- ²⁷ Meyers, Y.; Koop R.; von Angerer, E.; Schonenberger, H.; Holler, E.A.; *J. Cancer Res. Clin. Oncol.* **1994**, *120*, 359.
- ²⁸ Endo, Y.; Yoshimi, T.; Yamakoshi, Y.; *Chem. Pharm. Bull.* **2000**, *48*, 312.
- ²⁹ Endo, Y.; Yoshimi, T.; Iijima, T.; Yamakoshi, Y.; *Bioorg. Med. Chem. Lett.* **1999**, *9*, 3387.
- ³⁰ King, B.R.; *Chem. Rev.* **2001**, *101*, 1119.
- ³¹ Hedberg, K.; Schomaker, V.; *J. Am. Chem. Soc.* **1951**, *73*, 1482.
- ³² Bell, R.P.; Longuet-Higgins, H.C.; *Proc. R. Soc. (London) A* **1945**, *183*, 357.
- ³³ Price, W.C.; *J. Chem. Phys.* **1947**, *15*, 614.; Price, W.C. *J. Chem. Phys.* **1948**, *16*, 894.
- ³⁴ Knoth, W.H.; Miller, H.C.; England, D.C.; Parshall, G.W.; and Muetterties, E.L.; *J. Am. Chem. Soc.* **1968**, *84*, 1056.
- ³⁵ Grimes, R.N.; *Carboranes.* © 1970. Academic Press.
- ³⁶ Williams, R. E.; *Inorg. Chem.* **1971**, *10*, 210.
- ³⁷ Hoffmann, R.; and Lipscomb, W.N.; *J. Chem. Phys.* **1962**, *36*, 2179.
- ³⁸ Hoffmann, R.; and Lipscomb, W.N.; *J. Chem. Phys.* **1962**, *36*, 3489.
- ³⁹ Hoffmann, R.; and Lipscomb, W.N.; *J. Chem. Phys.* **1962**, *37*, 2872.
- ⁴⁰ Lipscomb, W.N.; *Proc. Nat. Acad. Sci. U.S.* **1963**, *47*, 1791.
- ⁴¹ Moore, E. B., Lohr, L.L.; Lipscomb, W.N.; *J. Chem. Phys.* **1961**, *35*, 1329.
- ⁴² Plesek, J.; *Chem. Rev.* **1992**, *92*, 269.
- ⁴³ Shapiro, I.; Good, C.D.; Williams, R. E.; *J. Am. Chem. Soc.* **1962**, *84*, 3837.
- ⁴⁴ Shapiro, I.; Good, C.D.; Williams, R. E.; Keilin, B.; *J. Am. Chem. Soc.* **1963**, *85*, 3167.

- ⁴⁵ Fein, M.M.; Bobinski, H.; Mayes, N.; Schwartz, N.N.; Cohen, M.S.; *Inorg. Chem.* **1963**, *2*, 1111.
- ⁴⁶ Heying, T.L.; Ager, J.W.; Clark, S.L.; Mangold, D.J.; Goldstein, H.L.; Hillman, M.; Polak, R.J.; Szymanski, J.W.; *Inorg. Chem.* **1963**, *2*, 1089.
- ⁴⁷ Grafstein, D.; Dvorak, J.; *Inorg. Chem.* **1963**, *2*, 1128.
- ⁴⁸ Heying, T.L.; Papetti, S.; Obenland, C.O.; *Ind. Eng. Chem. Prod. Develop.* **1965**, *5*, 334.
- ⁵³ Grafstein, D.; Dvorak, J.; *U.S Pat.* **1965**, *3*, 226, 429.
- ⁵⁰ Stanko, V.I.; Klimova, A.I.; *Zh. Obshch. Khim.* **1966**, *36*, 432.
- ⁵¹ Stanko, V.I.; Klimova, A.I.; *Zh. Obshch. Khim.* **1966**, *36*, 2219.
- ⁵² Zakharkin, L.I.; Kalinin, V.N.; *Zh. Obshch. Khim.* **1965**, *36*, 362.
- ⁵³ Heying, T.L.; Papetti, S.; *J. Am. Chem. Soc.* **1964**, *86*, 2295.
- ⁵⁴ Kashin, A.M.; Butin, K.P.; Stanko, V.I.; Beletskaya, I.P.; *Izv. Akad. Nauk. SSSR. Ser. Khim.* **1969**, *9*, 1917.
- ⁵⁵ Lietes, L.A.; *Chem. Rev.* **1992**, *92*, 279.
- ⁵⁶ Hermanek, S.; *Chem. Rev.* **1992**, *92*, 325.
- ⁵⁷ Zakharkin, L.I.; Stanko, V.I.; Brattsev, V.A.; Chapovskii, Y. A.; Okhlobystin, O. Y.; *Izv. Akad. Nauk. SSSR. Ser. Khim.* **1963**, 2238.
- ⁵⁸ Zakharkin, L.I.; Stanko, V.I.; Brattsev, V.A.; Chapovskii, Y.A.; Struchkov, Y.T.; *Izv. Akad. Nauk. SSSR, Ser. Khim.* **1963**, 2069.
- ⁵⁹ Kusari, U.; Li, Y.; Bradley, M.G.; Sneddon, L.G.; *J. Am. Chem. Soc.* **2004**, *28*, 8662.
- ⁶⁰ Grafstein, D.; Bobinski, J.; Dvorak, J.; Smith, H.F.; Schwartz, N.N.; Cohen, M.S.; Fein, M.M.; *Inorg. Chem.* **1963**, *2*, 1120.
- ⁶¹ Heying, T.L.; Ager, J.W.; Clark, S.L., Alexander, R.P.; Papetti, S. Reid, J.A.; Trotz, S. I.; *Inorg. Chem.* **1963**, *2*, 1097.
- ⁶² Zakharkin, L.I.; Stanko, V.I.; Klimova, A.I.; Chapovskii, Y.A.; *Izv. Akad. Nauk. SSSR. Ser. Khim.* **1963**, 2236.
- ⁶³ Zakharkin, L.I.; Grebennikov, A.V.; Kazantsev, A.V.; *Izv. Akad. Nauk SSSR. Ser. Khim.* **1967**, *9*, 2077.
- ⁶⁴ Ujvary, I.; Nachman, R.J.; *Tet. Lett.* **1999**, *40*, 5147.
- ⁶⁵ Teixidor, F.; Rius, J.; Romerosa, A.M.; Miravittles, C.; Escriche, L.; Sanchez, E.; Vinas, C.; Casabo, J.; *Inorg. Chim. Acta*, **1990**, *176*, 287.
- ⁶⁶ Ghaneolhosseini, H.; Tjarks, W.; Sjoberg, S.; *Tetrahedron.* **1998**, *54*, 3877.
- ⁶⁷ Herzog, A.; Knobler, C.B.; Hawthorne, M.F.; *Angew. Chem. Int. Ed.* **1998**, *37*, 1552.
- ⁶⁸ Valliant, J.F.; Schaffer, P.; *Inorg. Biochem.* **2001**, *85*, 43.
- ⁶⁹ Teplyakov, M.M.; Khotina, I.A.; Sakharova, A.A.; Mel'nik, O.A.; Papkov, V.S.; Kvachev, J.P.; *Makromol. Chem.* **1992**, *193*, 351.
- ⁷⁰ Songkram, C.; Tanatani, A.; Yamasaki, R.; Yamaguchi, K.; Kagechika, H.; Endo, Y.; *Tet. Lett.* **2000**, *41*, 7065.
- ⁷¹ Brown, D.A.; Colquhoun, H.M.; Daniels, J.A.; Macbride, J.A.H.; Stephenson, I.R.; Wade, K.; *J. Mater. Chem.* **1992**, *2*, 793.
- ⁷² Iijima, T.; Endo, Y.; Tsuji, M.; Kawachi, E.; Kagechika, H.; Shudo, K.; *Chem. Pharm. Bull.* **1999**, *47*, 398.
- ⁷³ Kabalka, G.W.; Hondrogiannis, G.; *J. Organomet. Chem.* **1997**, 536-537, 327.
- ⁷⁴ Feakes, D.A.; Spinler, J.K.; Harris, F.R.; *Tetrahedron.* **1999**, *55*, 11177.

- ⁷⁵ Endo, Y.; Iijima, T.; Yamakoshi, Y.; Yanmaguchi, M.; Fukasawa, H.; Shudo, K.; *J. Med. Chem.* **1999**, *42*, 1501.
- ⁷⁶ Nakamura, H.; Sekido, M.; Yamamoto, Y.; *J. Med. Chem.* **1997**, *40*, 2825.
- ⁷⁷ Maderna, A.; Herzog, A.; Knobler, C.B.; Hawthorne, M.F.; *J. Am. Chem. Soc.* **2001**, *123*, 10423.
- ⁷⁸ Zakharkin, L.I.; Ol'shevskaya, V.A.; *Russ. Chem. Bull.* **1995**, *44*, 1099.
- ⁷⁹ Yamamoto, K.; Endo, Y.; *Bioorg. Med. Chem. Lett.* **2001**, *11*, 2389.
- ⁸⁰ Jiang, W.; Knobler, C.B.; Hawthorne, M.F.; Curtis, C.E.; Mortimer, M.D.; *Inorg. Chem.* **1995**, *34*, 3491.
- ⁸¹ Wiesboeck, R.A.; Hawthorne, M.F.; *J. Am. Chem. Soc.* **1964**, *86*, 1642.
- ⁸² Garrett, P.M.; Tebbe, F.N.; Hawthorne, M.F.; *J. Am. Chem. Soc.* **1964**, *86*, 5016.
- ⁸³ Hawthorne, M.F.; Wegner, P.A.; Stafford, R.C.; *Inorg. Chem.* **1965**, *4*, 1675.
- ⁸⁴ Hawthorne, M.F.; Young, D.C.; Garrett, P.M.; Owen, M.A.; Schwerin, S.G.; Tebbe, F.N.; Wegner, P.A.; *J. Am. Chem. Soc.* **1968**, *90*, 862.
- ⁸⁵ Zakharkin, L.I.; Kalinin, V.N.; *Izv. Akad. Nauk. SSSR. Ser. Khim.* **1967**, 462.
- ⁸⁶ Lee, H.; Onak, T.; Jaballas, J.; Tran, U.; Truong, T. U.; To, H.T.; *Inorg. Chim. Acta.* **1999**, *289*, 11.
- ⁸⁷ Hawthorne, M.F.; Wegner, P.A.; *J. Am. Chem. Soc.* **1968**, *90*, 896.
- ⁸⁸ Yoshizaki, T.; Shiro, M.; Nakagawa, Y.; Watanabe, H.; *Inorg. Chem.* **1969**, *8*, 698.
- ⁸⁹ Zakharkin, L.I.; Kalinin, V.N.; *Dokl. Akad. Nauk. SSSR.* **1965**, *163*, 110.
- ⁹⁰ Stanko, V.I.; Brattsev, A.V.; *Zh. Obshch. Khim.* **1967**, *37*, 515.
- ⁹¹ Stanko, V.I.; Brattsev, A.V.; *Zh. Obshch. Khim.* **1968**, *38*, 662.
- ⁹² Zakharkin, L.I.; Kalinin, V.N.; *Dokl. Akad. Nauk. SSSR.* **1965**, *164*, 577.
- ⁹³ Zakharkin, L.I.; Grebennikov, A.V.; *Izv. Akad. Nauk. SSSR. Ser. Khim.* **1966**, 2019.
- ⁹⁴ Zakharkin, L.I.; Kalinin, V.N.; *Izv. Akad. Nauk. SSSR. Ser. Khim.* **1965**, 579.
- ⁹⁵ Fox, M.A.; MacBride, J.A.; Wade, K.; *Polyhedron.* **1996**, *16*, 2499.
- ⁹⁶ Tomita, H.; Luu, H.; Onak, T.; *Inorg. Chem.* **1991**, *30*, 812.
- ⁹⁷ Schaeck, J.J.; Kahl, S.B.; *Inorg. Chem.* **1999**, *38*, 204.
- ⁹⁸ Plesek, J.; Hermanek, S.; *Chem. Ind. (London)*, **1973**, 381.
- ⁹⁹ Hawthorne, M.F.; Young, D.C.; Wegner, P.A.; Andrews, T.D.; Howe, D.V.; Pilling, R.L.; Pitts, A.D.; Reintjes, M.; Warren, L.F.; *J. Am. Chem. Soc.* **1968**, *90*, 879.
- ¹⁰⁰ Hawthorne, M.F.; Young, D.C.; Wegner, P.A.; *J. Am. Chem. Soc.* **1965**, *87*, 1818.
- ¹⁰¹ Warren, L.F.; Hawthorne, M.F.; *J. Am. Chem. Soc.* **1967**, *89*, 470.
- ¹⁰² Roscoe, J.S.; Kongpricha, S.; Papetti, S.; *Inorg. Chem.* **1970**, *9*, 1561.
- ¹⁰³ Hawthorne, M.F.; Young, D.C.; Andrews, T.D.; Howe, D.V.; Pilling, R.L.; Pitts, A.D.; Reintjes, M.; Warren, L.F.; and Wegner, P.A.; *J. Am. Chem. Soc.* **1968**, *90*, 879.
- ¹⁰⁴ Hawthorne, M.F.; Wegner, P.A.; *J. Am. Chem. Soc.* **1968**, *90*, 896.
- ¹⁰⁵ Popp, G.; and Hawthorne, M.F.; *J. Am. Chem. Soc.* **1968**, *90*, 6553.
- ¹⁰⁶ Mikhailov, B. M.; and Potapova, T.V.; *Izv. Akad. Nauk. SSSR. Ser. Khim.* **1968**, 1153.
- ¹⁰⁷ Voorhees, R.L.; and Rudolph, R. W.; *J. Am. Chem. Soc.* **1969**, *91*, 2173.
- ¹⁰⁸ Hawthorne, M.F.; and Pilling, R.L.; *J. Am. Chem. Soc.* **1959**, *81*, 3987.
- ¹⁰⁹ Herber, R.H.; *Inorg. Chem.* **1969**, *8*, 174.
- ¹¹⁰ Maki, A.H.; Berry, T.E.; *J. Am. Chem. Soc.* **1965**, *87*, 4437.
- ¹¹¹ Ruhle, H.W.; Hawthorne, M.F.; *Inorg. Chem.* **1968**, *7*, 2279.
- ¹¹² Wilson, R.J.; Warren, L.F.; Hawthorne, M.F.; *J. Am. Chem. Soc.* **1969**, *91*, 758.

- ¹¹³ Warren, L.F.; Hawthorne, M.F.; *J. Am. Chem. Soc.* **1968**, *90*, 4823.
- ¹¹⁴ Hawthorne, M.F.; Ruhle, H.W.; *Inorg. Chem.* **1969**, *8*, 176.
- ¹¹⁵ Hawthorne, M.F.; Andrews, T.D.; *J. Am. Chem. Soc.* **1965**, *87*, 2496.
- ¹¹⁶ Zalkin, A.; Hopkins, T.E.; Templeton, D.H.; *Inorg. Chem.* **1966**, *5*, 1189.
- ¹¹⁷ Locher, G.L.; *Am. J. Roentgenol. Radium. Ther.* **1936**, *36*, 1.
- ¹¹⁸ Zahl, P.A.; Cooper, F.S.; Dunning, J.R.; *Proc. Natl. Acad. Sci. USA*, **1940**, *26*, 589.
- ¹¹⁹ Sweet, W.H.; Javid, M.; *Trans. Am. Neurol. Assoc.* **1951**, *76*, 60.
- ¹²⁰ Sweet, W.N.; Soloway, A.H.; Wright, R.L.; *J. Pharmac. Exp. Ther.* **1962**, *137*, 263.
- ¹²¹ Valliant, J.F.; Guenther, K.J.; King, A.S.; Morel, P.; Schaffer, P.; Sogbein, O.O.; Stephenson, K.A.; *Coord. Chem. Rev.* **2002**, *232*, 173.
- ¹²² Tjarks, W.; *J. Organomet. Chem.* **2000**, *37*, 614.
- ¹²³ Lesnikowski, Z.J.; Shi, J.; Schinazi, R.F.; *J. Organomet. Chem.* **1999**, *581*, 156.
- ¹²⁴ Gedda, L.; Ghaneolhosseini, H.; Nilsson, P.; Nyholm, K.; Pattersson, S.; Sjoberg, S.; Carlsson, J.; *Anti Cancer Drug Des.* **2000**, *15*, 277.
- ¹²⁵ Stanko, V.I.; Brattsev, V.A.; *Zh. Obshch. Khim.* **1969**, *39*, 1175.
- ¹²⁶ Radel, P.A.; Khal, S.B.; *J. Org. Chem.* **1996**, *61*, 4582.
- ¹²⁷ Bradshaw, K.M.; Schweizer, M.P.; Glover, G.H.; Hadley, J.R.; Tippets, R.; Tang, P.P.; Davis, W.L.; Heilbrun, M.P.; Johnson, S.; Ghanem, T.; *Mag. Res. Med.* **1995**, *34*, 48.
- ¹²⁸ Tatham, A. T.; Nakamura, H.; Wiener, E.C.; Yamamoto, Y.; *Mag. Res. Med.* **1999**, *42*, 32.
- ¹²⁹ Rho, K.Y.; Cho, Y.J.; Yoon, C.M.; *Tet Lett.* **1999**, *40*, 4821.
- ¹³⁰ Drechsel, K.; Lee, C.S.; Leung, E.W.; Kane, R.R.; Hawthorne, M.F.; *Tet. Lett.* **1994**, *3*, 6217.
- ¹³¹ Nakanishi, A.; Guan, L.; Kane, R.R.; Kasamatsu, H.; Hawthorne, M.F.; *Proc. Natl. Acad. Sci. USA.* **1999**, *96*, 238.
- ¹³² Soloway, A.H.; Tjarks, W.; Barnum, A.; Rong, F.G.; Barth, R.F.; Codogni, I.M.; Wilson, J.G.; *Chem. Rev.* **1998**, *98*, 1515.
- ¹³³ Shelly, K.; Feakes, D.A.; Hawthorne, M.F.; Schmidt, P.G.; Krisch, T.A.; Bauer, W.F.; *Proc. Natl. Acad. Sci. USA.* **1992**, *89*, 9039.
- ¹³⁴ Zhuo, J.C.; Cai, J.; Soloway, A.H.; Barth, R.F.; Adams, D.M.; Ji. W.; Tjarks, W.; *J. Med. Chem.* **1999**, *42*, 1282.
- ¹³⁵ Giovenzana, G.B.; Lay, L.; Monti, D.; Palmisano, G.; Panza, L.; *Tetrahedron.* **1999**, *55*, 14123.
- ¹³⁶ Teitze, L.F.; Bothe, U.; Griesbach, U.; Nakaichi, M.; Hasegawa, T.; Nakamura, H.; Yamamoto, Y.; *Chem. Biol. Chem.* **2001**, *2*, 326.
- ¹³⁷ Moerlein, S.M.; Welch, M.; *J. Int. J. Nucl. Med. Biol.* **1981**, *8*, 277.
- ¹³⁸ Hawthorne, M.F.; Varadarajan, A.; Knobler, C.B.; Chakrabarti, S.; *J. Am. Chem. Soc.* **1990**, *112*, 5365.
- ¹³⁹ Beatty, B.G.; Paxton, R.J.; Hawthorne, M.F.; Williams, L.E.; Richard-Dickson, K.J.; Do, T.; Shively, J.E.; Beatty, J.D.; *J. Nucl. Med.* **1993**, *34*, 1294.
- ¹⁴⁰ Valliant, J.F.; Morel, P.; Schaffer, P.; Kaldis, J.H.; *Inorg. Chem.* **2002**, *41*, 628.
- ¹⁴¹ Iijima, T.; Endo, Y.; Tsuji, M.; Kawachi, E.; Kagechika, H.; Shudo, K.; *Chem. Pharm. Bull.* **1999**, *47*, 398.
- ¹⁴² Collins, S.J.; Ruscetti, F.W.; Gallagher, R.E.; Gallo, R.C.; *J. Exp. Med.* **1979**, *149*, 964.
- ¹⁴³ Bollag, W.; Holdener, E.E.; *Ann. Oncol.* **1992**, *3*, 513.

- ¹⁴⁴ Kaneko, S.; Kagechika, H.; Kawachi, E.; Hashimoto, Y. Shudo, K.; *Med. Chem. Res.* **1991**, *1*, 220.
- ¹⁴⁵ Endo, Y.; Iijima, T.; Kagechika, H. Ohta, K.; Kawachi, E.; Shudo, K.; *Chem. Pharm. Bull.* **1999**, *47*, 585.
- ¹⁴⁶ Endo, Y.; Yoshima, T.; Kimura, K.; Itai, A.; *Bioorg. Med. Chem. Lett.* **1999**, *9*, 2561.

Chapter 2 - Monoarylated Carboranes

2.1 Overview

A series of monoarylated carboranes and Re-metallocarboranes were prepared as models of a new class of organometallic anti-estrogens and radiopharmaceuticals. The synthetic approach used to prepare the metal complexes was done in a manner that could be performed at the tracer level with ^{99m}Tc . This chapter describes the overall synthetic strategy, experimental details, and characterization data.

2.2 Introduction

As mentioned in section 1.1, the estrogen receptor (ER) is over expressed on malignant cells, which rely on the binding of its substrate in order to proliferate. The binding of 17β -estradiol (**Figure 2.1**) ultimately results in DNA transcription that fuels unregulated cell growth in breast cancer cells.^{1,2} Tamoxifen (**Figure 2.1**) currently is the method of choice for the treatment of hormone dependant breast cancer.^{3,4} Unfortunately, the metabolites of Tamoxifen (**2.2**) have been shown to be estrogenic, which can promote tumour growth.⁵

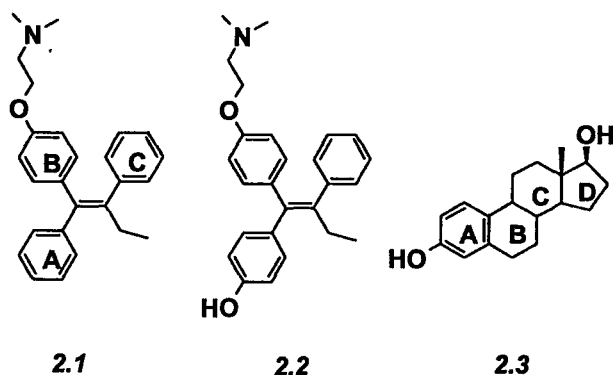


Figure 2.1: The (Z)-isomer of Tamoxifen (2.1), 4-Hydroxytamoxifen (2.2), 17β -estradiol (2.3).

To minimize catabolism and to improve efficacy of the pharmacophore a number of Tamoxifen analogues have been prepared. Endo *et al.*^{6,7} proposed that the hydrophobic carborane core could be used in place of the C and D rings of 17β -estradiol, as a means of preparing a unique class of anti-estrogens. Endo's group successfully showed, with use of the Luciferase binding assay,^{7,9} that a series of substituted carboranes containing phenolic groups (Figure 2.2) possessed binding affinity comparable to that of 17β -estradiol. Compound 2.5 exhibited the highest relative binding affinity (RBA, 155% that of 17β -estradiol).⁹ The estrogen analogue was based on the structure of *p*-carborane substituted with a phenolic group at one carbon vertex and a methyl alcohol on the second. It was also observed that *meta*-substitution of the hydroxy group on the aryl ring resulted in decreased binding affinity.

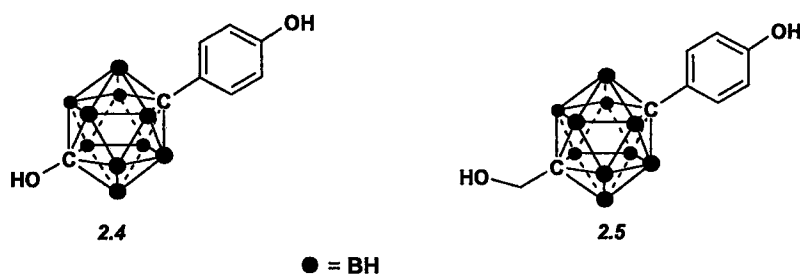


Figure 2.2: 1-(4-Hydroxyphenyl)-12-hydroxy-1,12-dicarba-closo-dodecaborane (2.4), 1-(4-hydroxyphenyl)-12-(hydroxymethyl)-1,12-dicarba-closo-dodecaborane (2.5).

Analogous derivatives of *ortho*- and *meta*-carboranes containing phenolic residues off one carbon vertex and an aliphatic amide or an aromatic ring with an amino chain similar to Tamoxifen (Figure 2.3), off the second carbon atom, demonstrated antagonistic activities.^{8,9} The assay was conducted at various

concentrations of the substituted carboranes in the presence of 17β -estradiol, where the antagonistic character was determined by measuring the ability of the carborane derivatives to prevent the natural substrate from initiating cellular differentiation, as compared to the leading anti-estrogen, Tamoxifen (2.1). At concentrations of 10^{-6} M compound 2.7 inhibited 17β -estradiol binding by 90%, comparable to Tamoxifen at 95% and hydroxytamoxifen at 95%.⁷

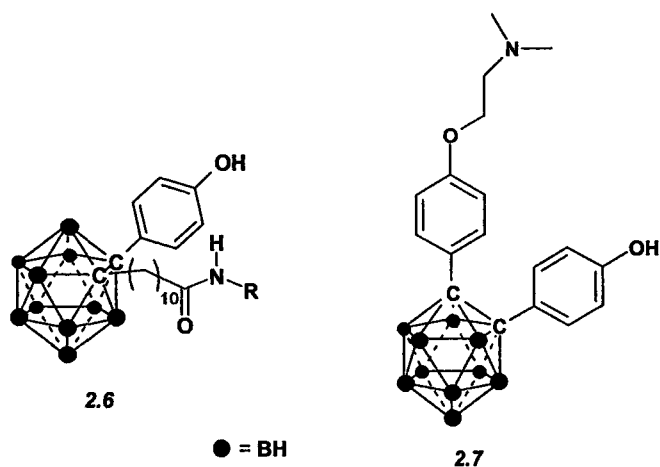


Figure 2.3: 1-(4-Hydroxyphenyl)-2-(N-methyl-N-butyl-dodecylacetamide)-1,2-dicarba-closo-dodecaborane (2.6), and 1-(4-(N,N-dimethylamino)ethoxyphenyl)-2-(4-hydroxyphenyl)-1,2-dicarba-closo-dodecaborane (2.7).

2.3 Rationale

The fact that monoarylated carboranes bind to the ER with affinities greater than the natural substrate, or comparable to that of the leading antiestrogens, it is conceivable that metallocarboranes would also bind to the ER, thereby creating a new type of anti-estrogen. Katzenellenbogen *et al.* showed that the LBD of the ER can accommodate the increased bulk which would be associated with addition of the $M(\text{CO})_3$ fragment (where $M = \text{Re}$) to a carborane.¹⁰ The target compounds serve as

models of the corresponding Tc-compounds which can potentially be used for imaging ER positive tumours.

2.4 Synthetic Strategy and Targets

In light of the relative binding affinities reported by Endo and coworkers, three target compounds were selected (**Figure 2.4**). The first target was a simple phenyl substituted *ortho*-carborane (**2.8**), which was used to develop and optimize the basic synthetic strategy. The second target was a 4-methoxyphenyl substituted *ortho*-carborane (**2.9**), which would determine the effect of the electron donating methoxy-substituent of the phenyl ring on the yield of complexation and the stability of the metal center. This compound is also a precursor to the ultimate target, 4-hydroxyphenyl substituted *ortho*-carborane (**2.10**), which is expected to have high binding affinity for the ER based on the results reported by Endo *et al.*⁹

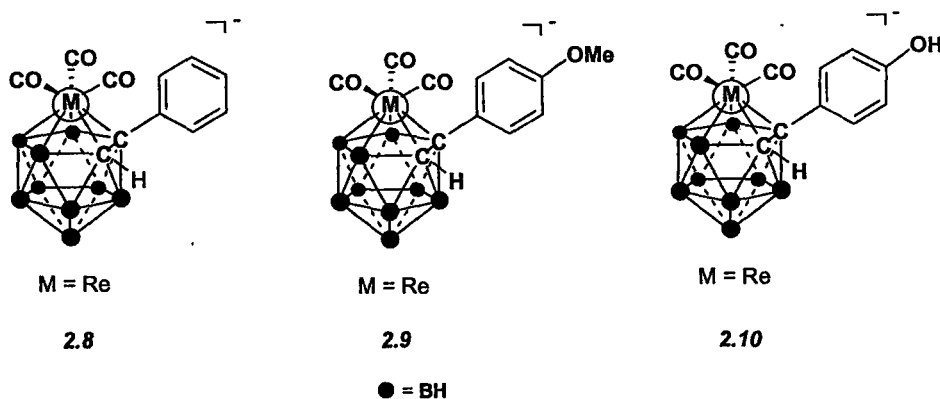


Figure 2.4: 1-Phenyl-3,3,3-tricarbonyl-3- η^5 -Re-1,2-dicarba-closo-dodecaborate (**2.8**), 1-(4-methoxyphenyl)-3,3,3-tricarbonyl-3- η^5 -Re-1,2-dicarba-closo-dodecaborate (**2.9**), and 1-(4-hydroxyphenyl)-3,3,3-tricarbonyl-3- η^5 -Re-1,2-dicarba-closo-dodecaborate (**2.10**).

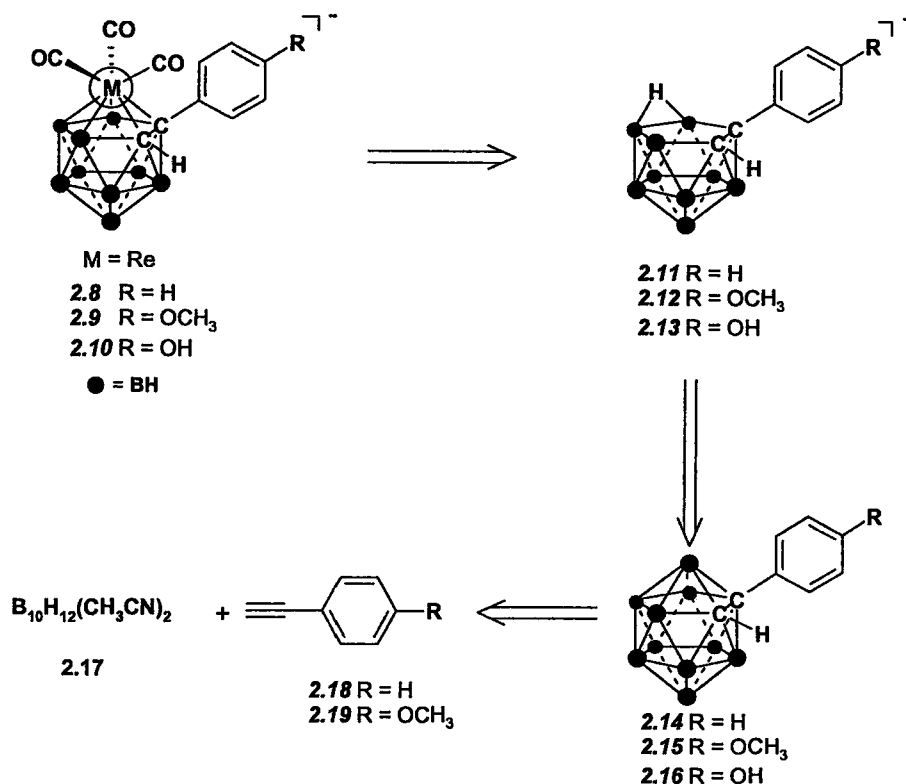


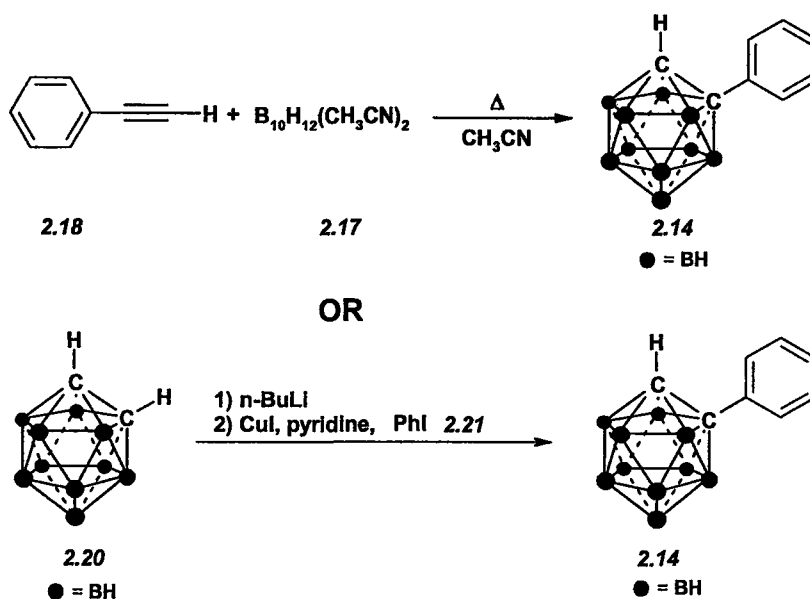
Figure 2.5: The retrosynthesis of monoarylated Re-metallocarboranes.

As shown in the general retrosynthesis (Figure 2.5), the metallocarboranes 2.8-2.10 were prepared from the *nido*-carboranes 2.11-2.13, which were prepared by degradation of the corresponding *closo*-carboranes 2.14-2.16. The *closo*-carboranes were prepared from commercially available phenylacetylene (2.18) and *p*-methoxyethynylbenzene (2.19). This approach was chosen so that if the work is repeated at the tracer level, the radiometal can be added in the final step using a similar strategy.

2.5 Synthesis of Phenyl Re-Metallocarborane (2.8)

The preparation of 1-phenyl-1,2-dicaba-*closo*-dodecarborane, herein referred to as phenyl *closo*-carborane (2.14), can be accomplished by two routes: 1) an alkyne

insertion reaction of phenylacetylene (**2.18**) with the Lewis base adduct of decaborane (**2.17**, $B_{10}H_{12}(CH_3CN)_2$, or **2**) by the copper mediated Ulmann type coupling¹¹ of iodobenzene (**2.21**) and *ortho*-carborane (**2.20**). For reasons that are discussed below, the former approach was employed (Scheme 2.1).



Scheme 2.1: Two synthetic routes to phenylcarborane; 1) alkyne insertion and 2) Ulmann-type coupling.

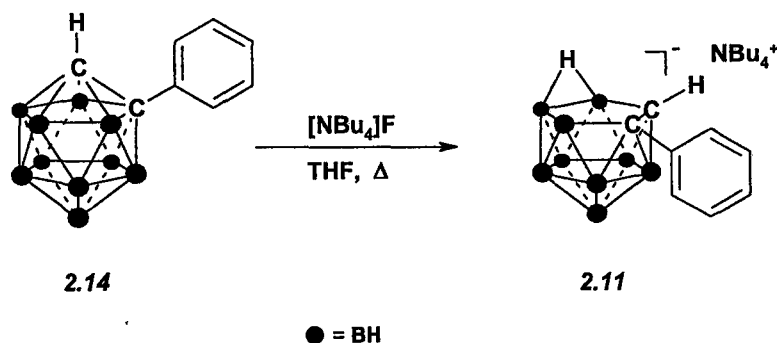
The initial attempts to prepare compound **2.14** was based on a method reported by Giovenzana¹² *et al.* where by 1.1 equivalents of the alkyne was added to one equivalent of **2.17**. The reaction produced the desired product but was complicated by the presence of unreacted alkyne. When the stoichiometry was changed to 0.8 equivalents of the alkyne and the reaction heated to reflux overnight under inert atmosphere,¹³ the existence of the product was shown by TLC (100% petroleum ether) with no remaining alkyne. Compound **2.14** could be visualized through the use of a palladium spray and by illumination using ultraviolet (UV) light. Detection by

palladium involves spraying the TLC plates with a 1.0 M solution of PdCl₂ in hydrochloric acid,¹⁴ which turns black when heated in the presence of boron species.

Compound **2.14** was purified by four successive recrystallizations from low boiling petroleum ether. In the case where residual phenylacetylene remained, a final purification by silica gel column chromatography using 3% ethyl acetate and hexanes as the eluent, was performed. Compound **2.14** was isolated as a white solid in modest yield (30%).

The ¹H NMR spectrum of **2.14** showed a pair of doublets at 7.50 ($J = 4.1$ Hz) and 7.35 ppm along with a multiplet at 7.40 ppm, which is consistent with the literature values for phenylcarborane.¹⁵ A broad singlet was observed at 3.99 ppm for the unsubstituted C-H of the cage. There was also a broad undulating signal along the baseline between 3.89 and 0.89 ppm, characteristic of the hydrogen atoms bonded to the quadrupolar boron nuclei of the carborane cage.¹⁶ The ¹³C NMR spectrum exhibited four distinct aromatic carbon resonances at 133.30, 129.86, 128.79, and 127.43 ppm, and two signals attributed to the carbon vertices of the carborane cage, which appeared at 76.36 and 60.07 ppm. The ¹¹B NMR spectrum contained six signals which appeared at -1.28, -3.60, -8.18, -10.01, -10.54, and -12.02 ppm, which is consistent with the symmetry of a *closo*-monosubstituted *o*-carborane. Infrared analysis of **2.14** exhibited the carborane C-H stretch at 3077 cm⁻¹, along with the B-H stretch at 2600 cm⁻¹.¹⁷ Signals at 1585, 1517, and 1499 cm⁻¹ were also detected and attributed to the C=C bonds of the phenyl group. The molecular ion in the mass spectrum was consistent with the mass of **2.14** and exhibited a characteristic B₁₀ isotopic distribution.

With the phenyl *closo*-carborane in hand, the next step was to prepare the corresponding *nido*-carborane, compound **2.11**. Degradation of the cage can be accomplished using both aqueous and non-aqueous bases.¹⁶ Initial attempts to degrade the cage with KOH in ethanol resulted in poor yields as isolation of the product was laborious. Another reaction, based on a highly efficient method developed by Fox and Wade,¹⁸ involves deboronation of the cage using fluoride (Scheme 2.2). The most commonly employed fluoride reagent for hydrophobic carborane derivatives is tetrabutylammonium fluoride hydrate (TBAF) which along with the parent carborane, dissolved readily into wet tetrahydrofuran (THF). The deboronation was carried out by heating the reaction to reflux. The target (**2.11**) was isolated as a slightly yellow solid in 80% yield following silica gel chromatography using 100% dichloromethane as the mobile phase.



Scheme 2.2: Preparation of tetrabutylammonium 7-phenyl-7,8-dicarba-nido-undecaborate, **2.11**.

The effects of the increased electron density on the carborane cage, in comparison to the *closo*- compounds, resulted in an upfield shift of the signals for the aromatic hydrogen atoms in the ¹H NMR spectrum. The relative order of the aromatic resonances remained unchanged with the doublet at 7.24 ppm arising from the two

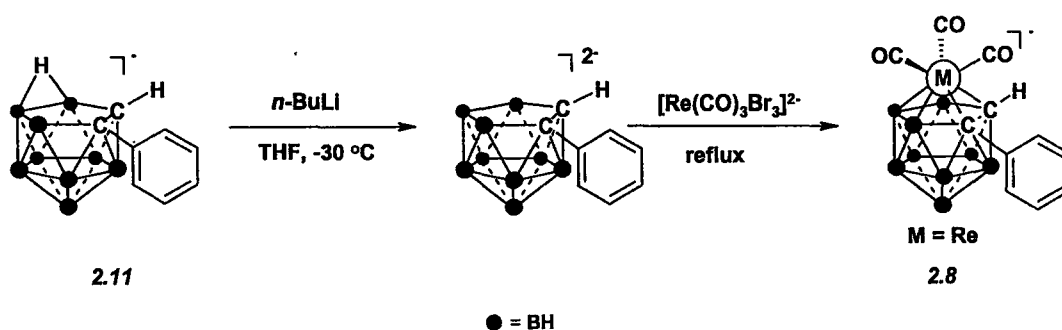
protons closest to the electron withdrawing carborane cage. The broad signal resulting from the B-H components was observed at 3.40-0.55 ppm, and the resonance due to the C-H of the carborane cage was at 2.35 ppm. The counter ion of the *nido*-carborane (**2.11**) was the tetrabutylammonium cation, from the TBAF reagent, which displayed a doublet downfield at 3.05 ppm due to the CH₂ group closest to the nitrogen nuclei, while there were two independent multiplet signals resulting from the two internal methylene groups, at 1.54 ppm and 1.38 ppm. The triplet owing to the methyl group of TBA appeared at 0.97 ppm.

The ¹³C NMR spectra of compound **2.11** showed an upfield shift of the 4 aromatic signals from 133.30, 129.86, 128.79, and 127.43 ppm in compound **2.14**, to 145.37, 127.26, 126.51, and 124.54 ppm in **2.11**. The tetrabutylammonium carbon atoms signals were also present at 58.64, 23.71, 19.45, and 13.46 ppm. The ¹¹B NMR spectra for **2.11** was also shifted upfield to -9.06, -12.97, -18.35, -21.91, -32.38, -35.84, and was more complex than that of compound **2.14** due to the reduction of symmetry, which occurs upon loss of one boron vertex.

The IR spectrum of **2.11** exhibited the characteristic C-H stretch of the cage at 3085 cm⁻¹ and the B-H stretch at 2545 cm⁻¹, which was, as expected, at a lower frequency than the *closo*-analogue **2.14**.¹⁷ This energy difference between the *closo*- and *nido*-carborane is a prominent difference between the two structures. Aromatic C=C stretches were observed at 1596, 1493, and 1480 cm⁻¹. Negative ion mode electrospray mass spectrometry showed the expected molecular ion peak at 209 m/z, with the expected isotopic distribution. Positive mode electrospray mass spectrometry displayed the counter ion peak at 242.1 m/z corresponding to the tetrabutylammonium cation.

The original synthesis of Re-metallocarboranes was reported by Hawthorne *et al.*¹⁹ and involved treating a *nido*-carborane with $\text{Re}(\text{CO})_5\text{Br}$ in the presence of excess NaH. Stone and coworkers²⁰ modifies this method improving the yield to 60%. Our group recently showed that the Re-metallocarboranes could be prepared by reacting *nido*-carboranes in the presence of TIOEt and $[\text{Re}(\text{CO})_3\text{Br}_3]^{2-}$ in THF.²¹ Alternatively the same reaction can be performed using solution of sodium carbonate in place of TIOEt.²¹ This reaction was improved upon in that aqueous fluoride can be used in place of Na_2CO_3 to promote metal complexation.²²

The initial method for preparing **2.8** involved reacting **2.11** with 1.5 equivalents of *n*-butyllithium (*n*-BuLi) at $-30\text{ }^\circ\text{C}$, under N_2 atmosphere, prior to the addition of the bis(tetraethylammonium) tribromotricarbonyl rhenate(I) $[\text{NEt}_4]_2[\text{Re}(\text{Br})_3(\text{CO})_3]$ (**2.22**). After stirring the mixture for thirty minutes, it was necessary to allow the reaction to warm to room temperature for 5-10 minutes, before the addition of an equivalent of the rhenium tricarbonyl precursor **2.22** (Scheme 2.3).²³ It was necessary to heat the reaction mixture to reflux to ensure solubility of the rhenium (I) starting material.



Scheme 2.3: Synthesis of **2.8**, 1-phenyl-3,3,3-tricarbonyl-3- η^5 -Re-1,2-dicarba-closo-dodecaborate.

After allowing the mixture to cool, a small sample of the reaction mixture was submitted for both positive and negative mode electrospray mass spectrometry. The negative ion mode displayed the desired complex **2.8** at 481 m/z along with a signal corresponding to the uncomplexed *nido*-carborane ligand at 211 m/z . TLC of the crude reaction mixture (100% dichloromethane) showed two major components that were both palladium and UV active. This was believed to be the target plus unreacted ligand. The R_f of the target and starting material were very similar ($R_f = 0.28$ and 0.24 , respectively) complicating purification.

In light of the ESMS results and TLC analysis, the mixture was concentrated under reduced pressure to give a yellow solid and the product was isolated by silica gel column chromatography (100% dichloromethane). The metal tricarbonyl complex eluted just ahead of the *nido*-starting material under the given solvent conditions on account of the increased hydrophobicity associated with the rhenium tricarbonyl core. Small fractions exhibiting both palladium and UV activity were analysed by infrared spectroscopy to confirm the presence of the desired Re complex by looking for the B-H stretching mode band ($2600\text{--}2500\text{ cm}^{-1}$), and the two carbonyl stretching bands, $\nu(\text{C}\equiv\text{O})$, which typically appear around 2000 and 1900 cm^{-1} . The two carbonyl stretches result from the local C_{3v} symmetry for rhenium tricarbonyl complexes.²⁴ Fractions containing the expected stretches were then individually submitted for both positive and negative modes of ESMS to identify the nature of the species present in the fractions. Mass spectroscopy revealed that all samples contained some starting material impurity, with the earlier fractions being richer in the desired complex. Samples containing significant amounts of product were recrystallized from dichloromethane and hexanes, yielding pure crystals of compound **2.8**.

Negative ion electrospray spectrometry confirmed that the collected fractions contained the desired product (Figure 2.6). The complex 2.8 had an m/z value of 478.9 m/z , which contained the appropriate boron and rhenium distributions based on an isotopic distribution simulation.

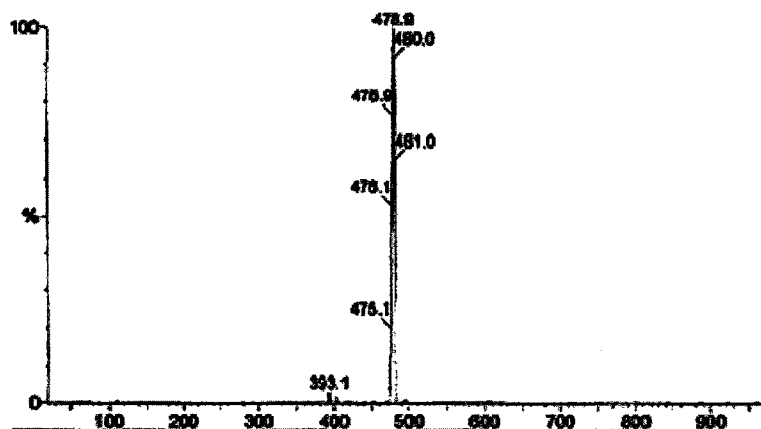


Figure 2.6: The negative ion electrospray mass spectrum of 2.8.

The IR of the purified material showed a B-H stretch at 2560 cm^{-1} , which was higher in energy than the B-H stretch of the ligand (2545 cm^{-1}). The expected carbonyl stretching frequencies with the predicted symmetry were present at 2006 and 1906 cm^{-1} (Figure 2.7).

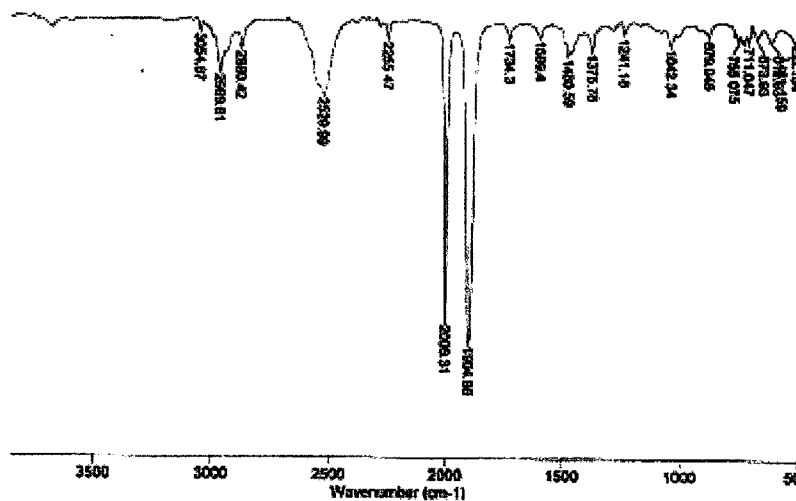


Figure 2.7: The FTIR (in CH_2Cl_2) spectrum of complex 2.8.

The chemical shift of the carborane CH group in the ^1H NMR spectrum of **2.8** (Figure 2.8) exhibits a shift downfield (3.95 ppm) from that of the corresponding *nido*-carborane starting material (**2.11**). This shift suggests that binding of the metal removes electron density from the open face of the carborane cage. Hawthorne *et al.* observed a similar phenomenon in the Re-complex of unsubstituted *o*-carborane.¹⁹

The ^{13}C NMR spectra for **2.8** contains 10 signals. Four of the signals corresponded to the aromatic resonances appearing at 146.13, 127.46, 125.07, and 122.84 ppm. The aliphatic signals of the counter ion were observed at 37.40, 23.94, 19.70, and 13.65 ppm. The M-CO carbon signals appeared at 198.42 ppm while the signal at 58.98 ppm was attributed to the unsubstituted carbon of the cluster. The quaternary carbon atom in the carborane cage was not detected, which is not unexpected based on its long relaxation times.²⁵ ^{11}B NMR spectrum showed broad overlapping signals at -5.23, -10.19, and -22.79 ppm, which is consistent with the underivatized Re-complex reported by Hawthorne *et al.*¹⁹

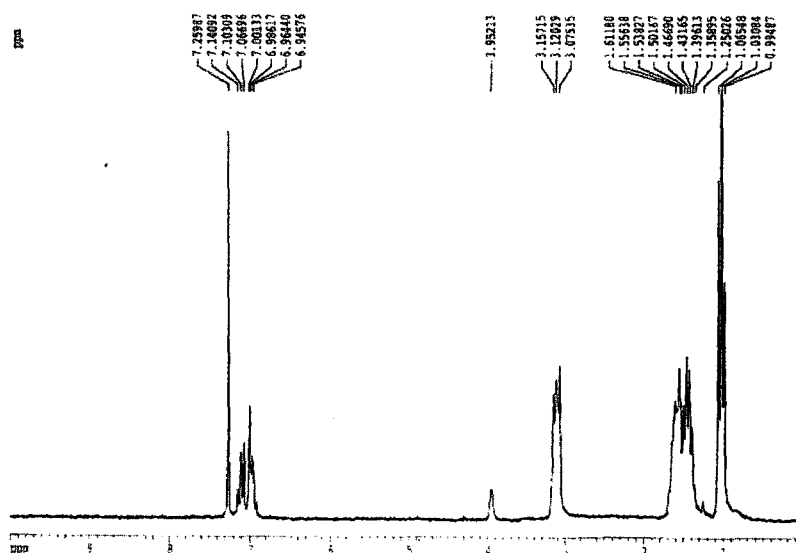


Figure 2.8: ^1H NMR spectrum (200 MHz, in CDCl_3) of tetrabutylammonium 1-phenyl-3,3,3-tricarbonyl- $3-\eta^5$ -Re-1,2-dicarba-closo-dodecaborate (**2.8**).

Crystals of the phenyl substituted rhenium tricarbonyl metallocarborane (**2.8**), were grown from 10% dichloromethane in hexanes at $-10\text{ }^{\circ}\text{C}$ and analysed by X-ray diffraction. The resulting structure (**Figure 2.9**), which was solved in the P-1 space group with two molecules in the unit cell, is similar to the structure reported by Hawthorne *et al.*²⁴ The boron-carbon bond lengths in the carborane cage ranged from 1.708(7) Å to 1.757(6) Å, with the average being 1.731(6) Å, while the boron-boron bond distances ranged from 1.749(8) Å to 1.804(7) Å, with an average of 1.778(8) Å. The carbon-carbon bond length for the carborane cage was 1.650(6) Å, which is slightly larger than the value for the unsubstituted rhenium tricarbonyl carborane. The two bond length for the cage carbon atoms bonded to the rhenium center were 1.897(5) Å and 1.914(5) Å with the average being 1.904(2) Å, which is a little larger than the average observed in the underivatized metallocarborane (1.610 Å).²⁴ The phenyl ring is positioned at an angle of $110.8(3)^{\circ}$ to the carborane cage, and does not seem to have any interaction with any of the carbonyl ligands of the metal center.

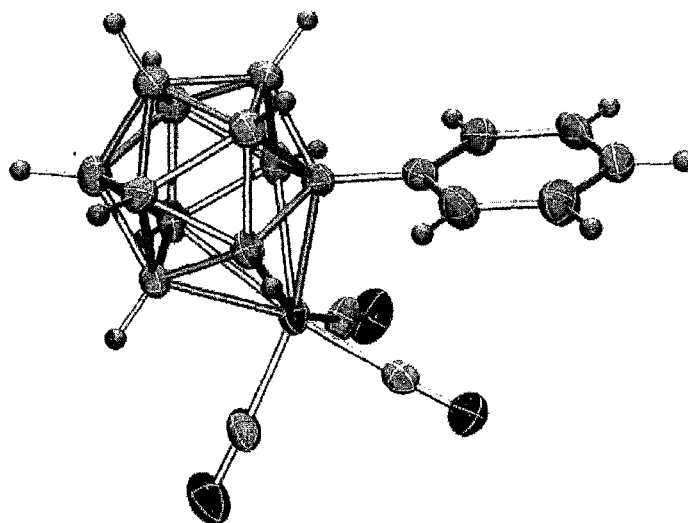
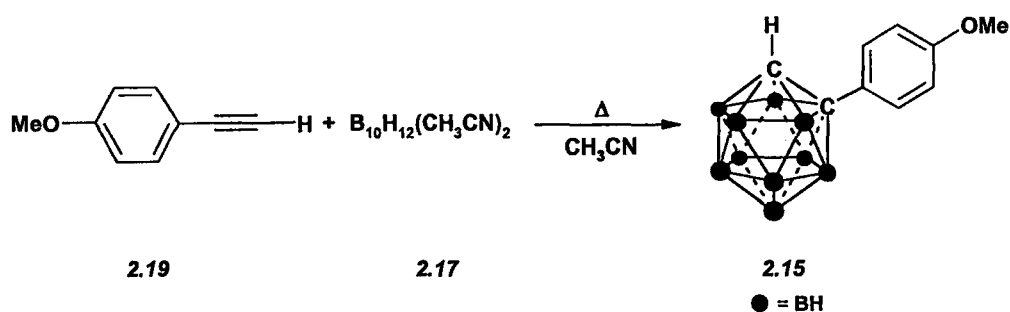


Figure 2.9: The X-ray structure for 1-phenyl-3,3,3-tricarbonyl-3- η^5 -Re-1,2-dicarbocloso-dodecaborate, **2.8**. The tetrabutylammonium cation is omitted for clarity.

2.6 Synthesis of 4-Methoxyphenyl Re-Metallocarboranes (2.9)

The C-(4-methoxyphenyl) substituted *ortho*-carborane (2.15) was reported by Endo *et al.*,⁹ but no characterization data was given. Mingos and coworkers also prepared 2.15 and published the corroborating spectroscopic data.²⁶ Compound 2.15 was prepared following the method of Giovenzana *et al.* by performing the alkyne insertion reaction with 4-methoxy-1-ethynylbenzene (2.19), which is commercially available. Compound 2.19 was added to the Lewis base adduct of decaborane (Scheme 2.4) and the reaction heated to reflux. The reaction, which was originally yellow, changed to an intense red colour, which persisted for the duration of the reaction (48 hrs). The crude reaction mixture was concentrated in vacuo yielding an orange-red solid, which was initially purified by dissolving the crude mixture in ethyl acetate (20 mL) followed by precipitation by the addition of hexanes (100 mL). The precipitate contained an orange/ yellow material, which was removed using multiple precipitations. Purification of the combined supernatant was accomplished by silica gel column chromatography using 3% ethyl acetate and hexanes. The desired product, 1-(4-methoxyphenyl)-1,2-dicarba-*closo*-carborane (2.15), was isolated as a white solid, in 30% yield, which is lower than literature values.²⁶



Scheme 2.4: Preparation of 1-(4-methoxyphenyl)-1,2-dicarba-*closo*-dodecaborane.

The infrared spectra of **2.15** showed the carborane C-H stretch mode at 3075 cm^{-1} and the characteristic B-H stretch for the *closo*-compound at 2602 cm^{-1} . Alkyl stretching frequencies were observed from 3013-2843 cm^{-1} , while the C=C aromatic stretch modes were present from 1611-1464 cm^{-1} . The TOF electron impact mass spectrum of the product (**2.15**) showed a mass to charge ratio of 250.2, which is consistent with the calculated value, having the expected boron isotopic distribution.

^1H NMR spectrum of **2.15** (Figure 2.10) showed two sets of doublets at 7.43 and 6.83 ppm ($J = 4.5$ Hz). The CH group of the carborane cage appeared at 3.89 ppm which is upfield compared to the CH group of phenylcarborane (3.99 ppm). The methoxy-group appears as a singlet at 3.82 ppm, while the B-H signal is apparent between 3.70-1.20 ppm. The observed resonances were in line with reported values.²⁶

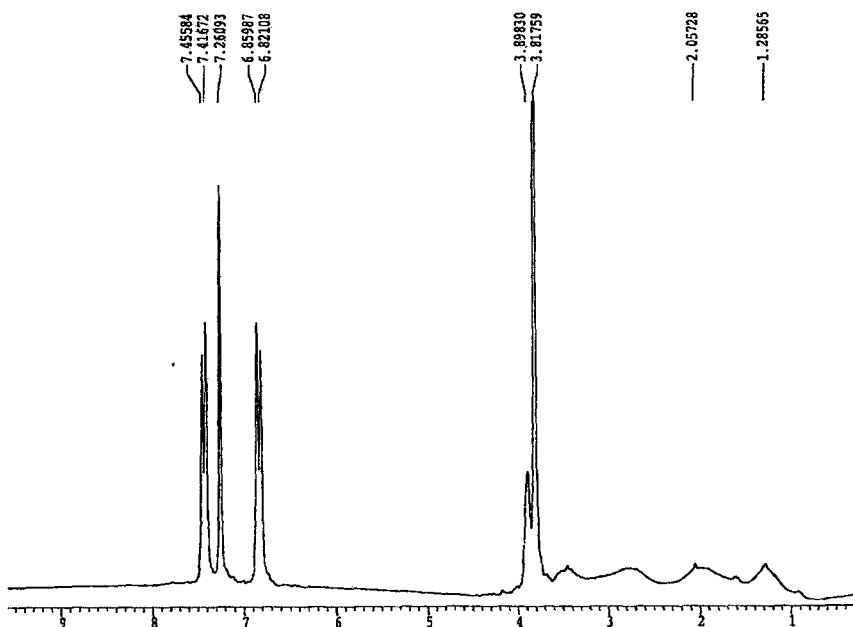


Figure 2.10: ^1H NMR spectrum (200 MHz in CDCl_3) of 1-(4-methoxyphenyl)-1,2-dicarba-*closo*-dodecaborane (**2.15**).

The ^{13}C NMR spectrum of **2.15** showed the ipso carbon atoms of the aromatic ring at 160.70 and 125.39 ppm. The other aromatic signals appeared at 129.20 and 113.96 ppm. The signal corresponding to the substituted carborane carbon atom was observed at 76.80 ppm, while that of the unsubstituted position occurred at 60.96 ppm, compared to 76.36 and 60.07 ppm respectively, for the phenyl substituted carborane (**2.14**). The methoxy-carbon resonance was present at 55.49 ppm. The ^{11}B NMR spectrum of **2.15** displayed the expected number of signals for a monosubstituted *closo*-carborane, which appeared at -1.06, -3.87, -8.25, -9.77, -10.56, and -11.80 ppm (Figure 2.11), which were slightly higher than the values reported previously.

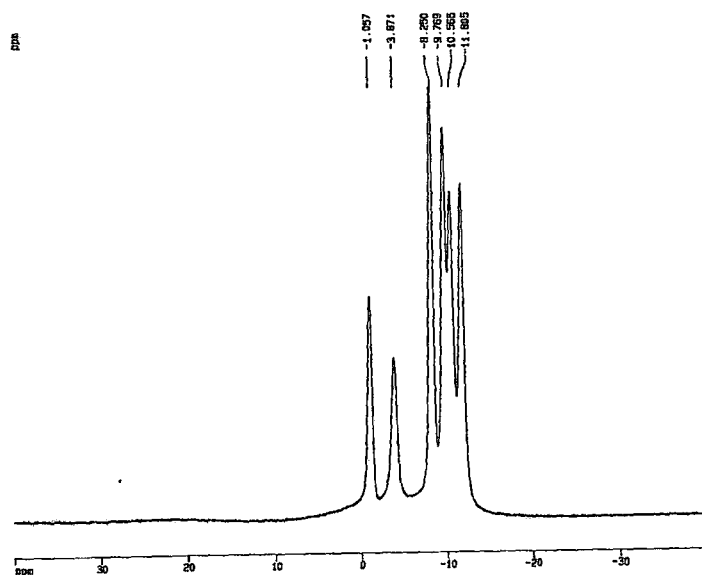
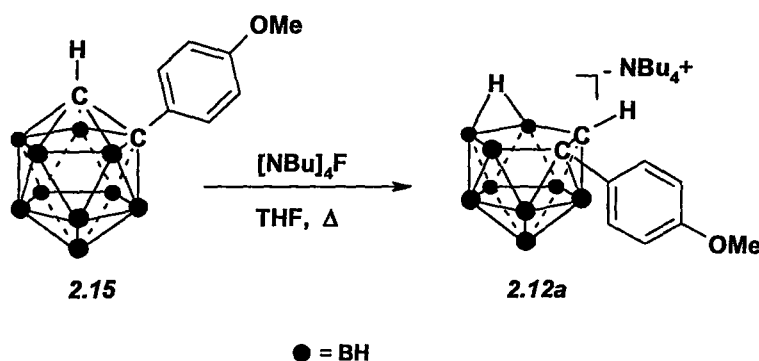


Figure 2.11: ^{11}B NMR spectrum (500 MHz in CDCl_3), of 1-(4-methoxyphenyl)-1,2-dicarba-*closo*-dodecaborane (**2.15**).

In an unsuccessful attempt to improve the yields of **2.15** the procedure reported by Fox and coworkers was attempted.¹¹ The process involved preparing C-lithio-*ortho*carborane at $-10\text{ }^\circ\text{C}$, followed by the addition of pyridine and copper (I) chloride to generate a C-substituted copper carborane. After warming the mixture to

room temperature, the aryl iodide, 4-*para*-iodoanisole (**2.21**), was added and the system heated to reflux for two days. No product was observed therefore this approach was abandoned.

The *nido*-carborane, 7-(4-methoxyphenyl)-7,8-dicarba-*nido*-undecaborate (**2.12a**), was prepared in a manner similar to that used to prepare **2.11**. Five equivalents of TBAF were added to **2.15** and the mixture heated to reflux (Scheme 2.5). The desired *nido*-derivative **2.12a** was purified by silica gel column chromatography using 100% dichloromethane as the eluent. The product, compound **2.12a** was isolated in 70% yield as a colourless solid.



Scheme 2.5: Synthesis of 7-(4-methoxyphenyl)-7,8-dicarba-*nido*-undecaborate, **2.12a**.

The B-H stretch for **2.12a** (2523 cm^{-1}) appeared at lower energy relative to the starting material **2.15**. The C-H stretch of the unsubstituted carbon vertex was observed at 3085 cm^{-1} , while the aliphatic C-H stretches of the cation were observed between $3000\text{-}2840\text{ cm}^{-1}$. The aromatic C=C stretches were observable around 1512 and 1467 cm^{-1} . The negative ion electrospray mass spectrum showed the expected ion mass at 240.0 m/z , with the characteristic isotopic distribution for a B_9 containing species.

The ^1H NMR spectrum of **2.12a**, as the tetrabutylammonium salt, clearly shows that there is an increase of electron density associated with the carborane cage, which caused an upfield shift of the resonance of the hydrogen atom bound to the unsubstituted carbon of the cage. It moved from 3.89 ppm in compound **2.15** to 2.27 ppm in the *nido*-carborane **2.12a**. The doublets from the aromatic CH groups, which appeared at 7.17 and 6.65 ppm ($J = 4.4$ Hz), were also shifted upfield from 7.43 and 6.83 ppm in compound **2.15**. The effects of increased electron density in the cluster is also apparent in the ^{13}C NMR spectrum where the signals from the aromatic carbon atoms, which appeared at 157.01, 137.88, 127.93, and 112.78 ppm, were also shifted upfield compared to compound **2.15** (Figure 2.12). The methoxy- signal was present at 55.22 ppm. The ^{11}B NMR spectrum of **2.12a** showed increased complexity over the *closo*-compound which is expected as a result of the loss of symmetry upon removal of the boron vertex. Eight signals were observed at -8.51, -9.70, -12.88, -15.83, -17.54, -21.70, -31.90, and -36.15 ppm.

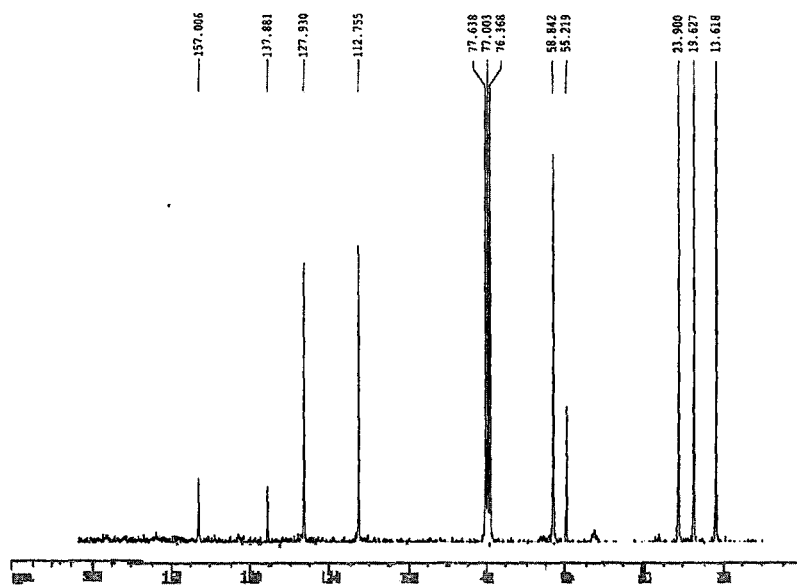
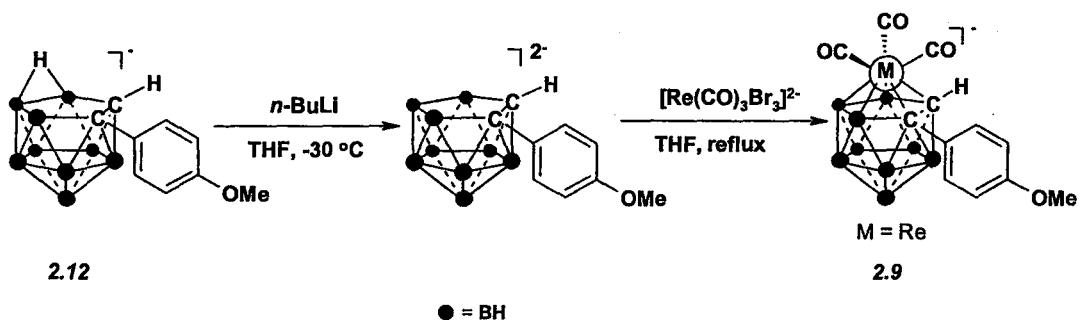


Figure 2.12: ^{13}C NMR (200 MHz in CDCl_3), of 7-(4-methoxyphenyl)-7,8-dicarbanido-undecaborate (**2.12a**).

The rhenium carborane complex **2.9** was generated in a manner similar to that of the phenyl substituted analogue. Removal of the bridging hydrogen from **2.12a** with 1.5 equivalence of *n*-BuLi in freshly distilled THF was performed at $-30\text{ }^{\circ}\text{C}$ giving a slightly yellow heterogeneous solution. After allowing the mixture to warm to room temperature, an equimolar amount of $[\text{NEt}_4]_2[\text{Re}(\text{CO})_3\text{Br}_3]$ was added, which slowly dissolved upon heating the solution to reflux (Scheme 2.6). After cooling, a small sample was submitted for ESMS, which showed **2.9** along with unreacted starting material (**2.12a**).

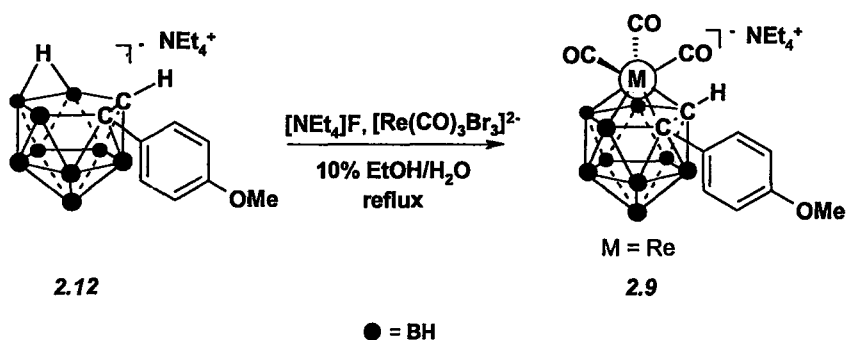


Scheme 2.6: *The preparation of tetrabutylammonium 1-(4-methoxyphenyl)-3,3,3-tricarbonyl-3- η^5 -Re-1,2-dicarba-closo-dodecaborate, (2.9).*

Attempts to purify **2.9** by silica gel chromatography proved futile as the starting material was detected in all fractions. Attempts to purify the target from those fractions containing mostly **2.9**, relative to **2.12a**, via recrystallization from hexanes and dichloromethane failed to yield pure product. Multiple columns run in sequence were unable to remove all impurities consequently semi-preparatory high pressure liquid chromatography (HPLC) was attempted as a means of isolating the desired product.

(TEA) salt of **2.12a**, designated as **2.12b**, was prepared under analogous conditions with the exception of the tetraethylammonium fluoride (TEAF) used in place of TBAF, and 10% EtOH added to help solubilize the fluoride salt. This way, TEAF in water-ethanol mixtures could be used to prepare the desired complex. This approach has the added benefit that it avoids the problem of multiple counterions.

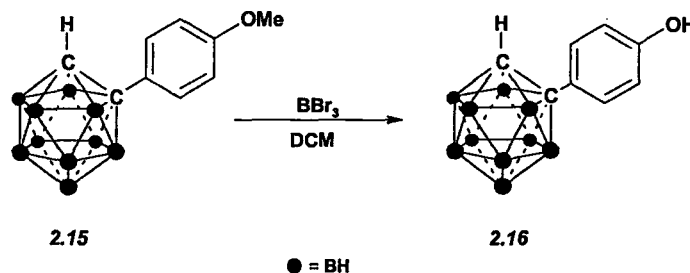
The *nido*-salt **2.12b** and the rhenium starting material (**2.22**) were combined in a 0.1 M 10% ethanol-water solution of TEAF and the reaction heated to reflux. Initially TEAF and **2.12b** was not water soluble but at reflux the mixture became homogenous. After two days, a small sample was submitted for negative ion electrospray mass spectrometry. The majority of the carborane species by ESMS was unreacted *nido*-**2.12b** with only a small peak associated to the desired complex. Addition of a second equivalent of **2.22** and further heating at reflux temperature over two more days produced only minor increases in target complex **2.9** as detected by HPLC and confirmed by ESMS (Scheme 2.7). With the difficulties encountered in complexing the rhenium core to the carborane cage in **2.12b**, attempts to prepare **2.9** were abandoned until better methods (*vide infra*) could be formulated.



Scheme 2.7: One pot preparation of complex **2.9**.

2.7 Synthesis of 4-Hydroxyphenyl Re-Metallocarboranes (2.10)

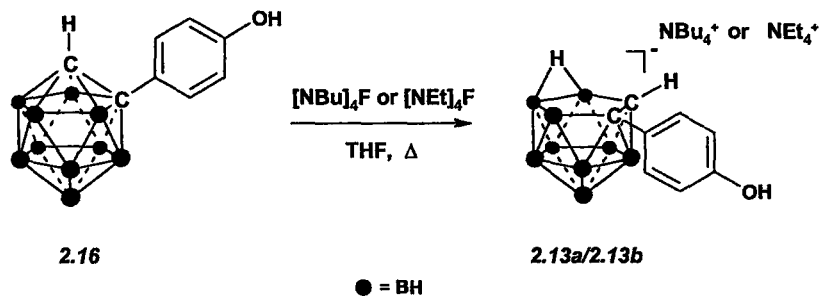
The third target was the metal complexes of hydroxyphenyl substituted *ortho*-carborane (2.10). The *closo*-carborane 2.16 was prepared by deprotecting compound 2.15. A 1.0 M CH₂Cl₂ solution of boron tribromide, BBr₃, was added to compound 2.15 at -30 °C, in freshly distilled dichloromethane under inert atmosphere (Scheme 2.8).²⁷ The reaction was stirred at this temperature for 30 minutes upon which the reaction was allowed to warm to room temperature. At this point the reaction vessel was opened and allowed to slowly evaporate overnight under a stream of N₂ gas. Wet THF was added at -10 °C, and once again the reaction was allowed to slowly evaporate overnight.²⁷ Following the addition of methanol at -10 °C, the crude mixture was concentrated to yield a brown residue from which the desired product was isolated using silica gel column chromatography (10% ethyl acetate in hexanes as the eluent). The target, 1-(4-hydroxyphenyl)-1,2-dicarba-*closo*-dodecaborane (2.16) was isolated as an off-white solid in 90% yield. There was a significant reduction in the R_f value of the hydroxyl species versus the methoxy species, as was to be expected now that the capacity for hydrogen bonding exists between the phenolic group and the silica TLC plate.



Scheme 2.8: The synthesis of 1-(4-hydroxyphenyl)-1,2-dicarba-*closo*-dodecaborane, (2.16).

In the IR spectrum the stretching mode of the C-H bond of the carborane cage was present at 3070 cm^{-1} , while the B-H stretches appeared at 2602 cm^{-1} . There was also a stretch present at 3576 cm^{-1} which was attributed to the O-H bond of the phenol group. The molecular ion was observed in the TOF EIMS, with a mass to charge ratio of 236.2. The existence of the phenolic substituted *closo*-carborane was evident from the ^1H NMR spectrum in which the methoxy signal was no longer present, however there was a signal attributed to the hydroxy proton at 5.14 ppm. The pair of aromatic doublets having chemical shifts of 7.38 and 6.77 ppm were also present ($J= 4.3\text{ Hz}$), while the proton of the unsubstituted carbon vertex of the cage appeared at 3.87 ppm. ^{13}C NMR spectrum of **2.16** exhibited the expected aromatic carbon signals at 156.79, 129.51, 125.79, and 115.48 ppm with the carbon of the carborane cage at 60.96 ppm. The ^{11}B NMR spectrum showed peaks at -1.07, -3.84, -8.24, -9.79, -10.59, and -11.83 ppm, which is similar to the monosubstituted carboranes **2.14** and **2.15**.

Two different methods for the preparations of *nido*-carborane **2.13a** were attempted. The first was analogous to that of the two other monoarylated carboranes, involving heating compound **2.16** with 5 equivalents of TBAF in wet THF (**Scheme 2.9**). After one day of reflux only partial degradation of the cage had occurred with the remaining product being unreacted *closo*-carborane. In an attempt to drive the reaction to completion, an additional 5 equivalents of TBAF was added and the reaction was maintained at reflux for one more day. This approach resulted in complete consumption of the starting material. The target *nido*-compound, tetrabutylammonium 7-(4-hydroxyphenyl)-7,8-dicarba-*nido*-undecaborate, was obtained following purification by silica gel chromatography (5% methanol in dichloromethane) in 50% yield as a white solid.



Scheme 2.9: Preparation of compounds **2.13a** and **2.13b**.

As expected, there was a pronounced upfield shift of signals in the ^1H NMR spectrum due to the increase in electron density in the cage. The doublets associated with the aromatic ring appeared 6.92 and 6.30 ppm, while the signal associated with the carborane C-H group appeared at 1.99 ppm. The hydroxy proton was not observed which is assumed to be a result of exchange with the NMR solvent (deuterated methanol). The aliphatic signals with the expected spin-spin coupling for the tetrabutylammonium cation was also observed at 3.09, 1.54, 1.30, and 0.93 ppm. The ^{13}C NMR spectrum contained four aromatic signals from 155.42, 138.58, 129.04, and 114.93 ppm, which were shifted upfield from those observed in the parent *closo*-carborane **2.16**. The tetrabutylammonium cation signals were observed at 59.57, 24.84, 20.71, and 14.00 ppm. The ^{11}B NMR spectrum of compound **2.13a** revealed a complex array of signals appearing at -7.93, -9.33, -12.33, -15.58, -16.88, -17.87, -21.16, -31.52, and -34.73 ppm. The increased number of signals compared to that of the *closo*-carborane **2.16**, is attributed to the lack of symmetry in the *nido*-compound. In the infrared spectrum of **2.13a** the B-H stretch appeared at 2523 cm^{-1} , a lower energy stretch than that for the *closo*-carborane **2.16**, while the C-H stretch mode of

the cage was observed at 3058 cm^{-1} . The aromatic C=C stretches were observed at 1608 and 1512 cm^{-1} , while the aliphatic sp^3 C-H stretches of the counter ion were present between 2969-2880 cm^{-1} . The O-H stretch was present at 3583 cm^{-1} . The negative ion ESMS showed a parent ion at 225.8 m/z with a B_9 characteristic $^{10}\text{B}/^{11}\text{B}$ isotopic distribution, which are both consistent with the product being **2.13a**.

The second approach to the degradation of **2.16** entailed the use of TEAF (Scheme 2.9). Ten equivalents of TEAF and compound **2.16** were heated to reflux which resulted in rapid conversion of the *closo*-carborane to the respective *nido*-compound (**2.13b**). Compound **2.13b** is more hydrophilic than the TBA salt and was readily isolated in 65% yield by silica gel column chromatography using 10% methanol in dichloromethane as the eluent, in 65% yield. Characterization data for **2.13b** was identical to that of the TBA *nido*-salt, **2.13a**, with the exception of the differences attributed to the two different cations.

With the two salts, **2.13a** and **2.13b**, it was possible to attempt the complexation reaction with the rhenium tricarbonyl core using two different approaches. The first approach involved reacting **2.13a** with 1.5 equivalents of *n*-BuLi in THF at $-30\text{ }^\circ\text{C}$, to generate the dicarbollide dianion *in situ*. This slightly yellow mixture was then allowed to warm to room temperature to ensure the formation of the corresponding dicarbollide dianion. The addition of one equivalent **2.22** resulted in a heterogeneous yellow mixture which, when heated to reflux became homogenous. A small sample from the reaction mixture was submitted for negative ion ESMS which showed the presence of the target mass at 495 m/z . Attempts to isolate the target by silica gel chromatography were unsuccessful as the product fractions were

contaminated with starting material. Preparatory TLC and semi-prep HPLC were equally ineffective in purifying the reaction mixture.

The alternate method entailed replacing *n*-BuLi with a milder base, TEAF. When compound **2.13b** and 10 equivalents of tetraethylammonium fluoride along with 1.0 equivalent of **2.22**, in 10% ethanol-water, were heated to reflux overnight the desired product was produced in small amounts. Increasing the amount of **2.22** in the reaction did not substantially increase the production of **2.10**. Separation of the target from excess ligand was extremely difficult.

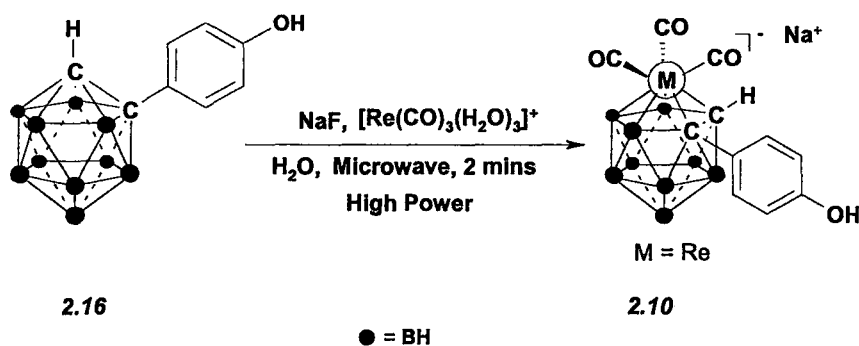
Despite the high yields obtained for other Re(I)-metallocarboranes using the fluoride ion approach it is clear that the aromatic group interferes with the complexation reaction. Preparation of **2.10** is complicated by the fact that to purify the products complete consumption of the *nido*-carborane is required. Clearly an alternative approach was needed which would drive the complexation reactions to completion.

Our group has recently shown that microwave radiation can be used to drive the Re(I)-carborane coupling reactions to completion,²⁸ and that the *closo*-carborane derivatives can be used directly as the ligand when fluoride ion is used.²² For example, an excess of $\text{Re}(\text{CO})_3(\text{H}_2\text{O})_3\text{Br}$ (**2.22a**), which is reported to be more reactive than $[\text{Re}(\text{CO})_3\text{Br}_3]^{2-}$,¹⁰ was combined with glycosylated carboranes and aqueous KF in a Parr microwave vessel for 2 minute at high power. The reaction consumed all of the ligand leaving the desired Re-complex as the major product.²⁸

1-(4-Hydroxyphenyl)-1,2-dicarba-closo-dodecaborane, **2.16**, with 3 equivalents of **2.22a**, in 10 mL of 0.5 M sodium fluoride was irradiated in a Parr microwave vessel at high power for 2 minutes, in two 1-minute intervals. The

reaction was followed by HPLC (UV-vis) which showed the target, **2.10**, as the major product and there was no residual *nido*-carborane starting material (**Scheme 2.10**).

TLC of the crude reaction mixture (20% MeOH/CHCl₃) showed two UV active components but only one was palladium active. The R_f of one of the spots (0.20) was consistent with the desired product. Compound **2.10** was isolated in 48% yield as a brown oil by silica gel chromatography using 15% methanol-chloroform as the mobile phase.



Scheme 2.10: *One pot synthesis of 2.10 under microwave conditions.*

Negative ion electrospray spectrometry confirmed that the collected fractions contained the desired product (**Figure 2.14**). The complex **2.10** had an *m/z* value of 495.2, which contained the appropriate ReB₉ distributions, based on a simulation of the isotope distribution for the formula of the product. The IR of the purified material showed a B-H stretch at 2559 cm⁻¹ which was lower in energy than the B-H stretch of the **2.16** (2602 cm⁻¹). The expected carbonyl stretching frequencies were present at 2001 and 1884 cm⁻¹ (**Figure 2.15**).

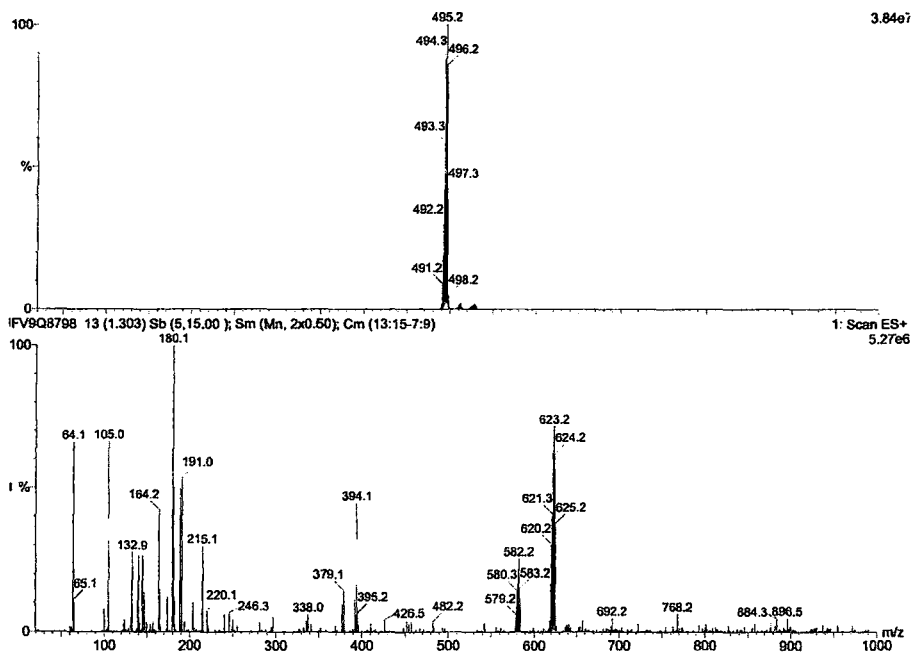


Figure 2.14: The negative ion electrospray mass spectrum of **2.10**.

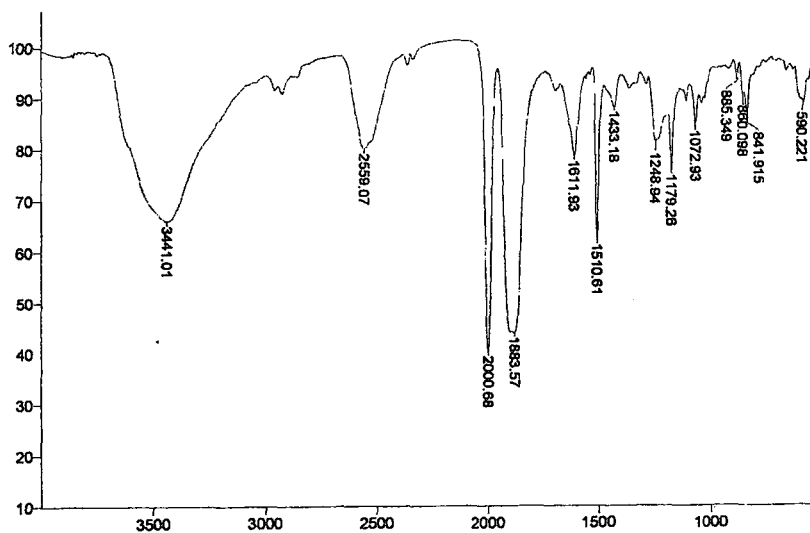


Figure 2.15: The FTIR (in KBr) spectrum of complex **2.10**.

The chemical shift of the carborane CH group in compound **2.10** in the ^1H NMR spectrum (Figure 2.16) possesses a small upfield shift of the aromatic doublets, at 7.25 and 6.50 ppm ($J = 4.3$ Hz), relative to the starting material. However the

unsubstituted C-H group of the carborane cage showed a more pronounced upfield shift to 1.72 ppm. The ^{13}C NMR spectrum, for **2.10** contained 4 aromatic signals at 156.73, 135.48, 130.61, and 114.73 ppm. The carbonyl ligands bonded to rhenium appeared at 200.65 ppm. The two carbon atoms of the carborane occurred at 57.45 and 55.92 ppm. ^{11}B NMR spectrum showed broad signals at -5.21, -9.25, -12.24, -13.63, -16.13, -16.90, -22.61, and -24.16 ppm.

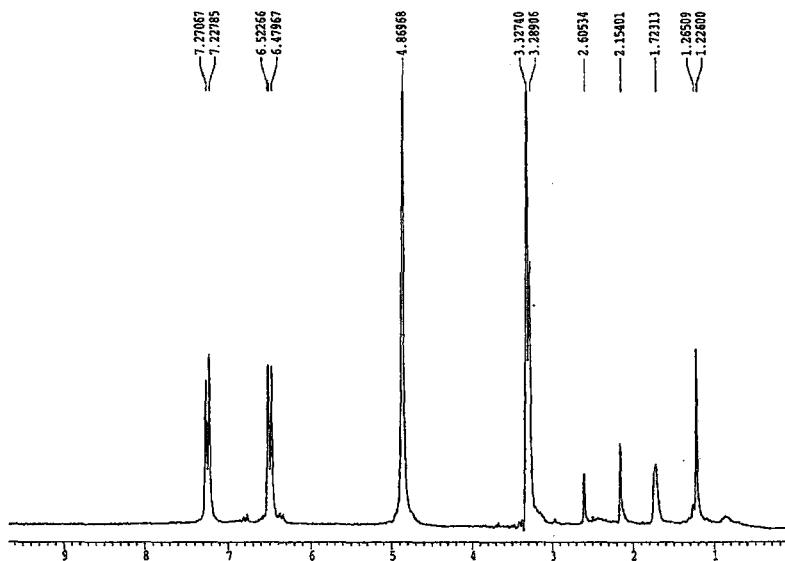


Figure 2.16: ^1H NMR (200 MHz in $\text{MeOH}-d_4$) of 1-(4-hydroxyphenyl)-3,3,3-tricarbonyl- η^5 -Re-1,2-dicarba-closo-dodecaborate, (**2.10**).

2.8 Conclusions

The synthesis and characterization of three novel *nido*-ligands and two monoaryl-carborane complexes of the rhenium (I) tricarbonyl core were completed. Two possible routes for the synthesis of the rhenium complexes were established, the most effective being a microwave method, which drives the complexation reaction to completion.

The monoarylated Re-metallocarboranes are stable and can be produced with sufficient purity to be screened for their biological activity. They were also

synthesized in a manner that can be used to prepare the ^{99m}Tc analogues, which could potentially act as tracers for ER positive tumours.

2.9 Experimental Section

Synthesis of 1-phenyl-1,2-dicarba-*closo*-dodecaborane, 2.14. Acetonitrile (70 mL) was added to decaborane **2.17** (1.30 g, 10.65 mmol) and the mixture stirred at room temperature overnight. Phenylacetylene **2.18** (1.2 mL, 11.72 mmol) was then added and the mixture heated to reflux for 48 h. Upon cooling to room temperature the solvent was removed by rotary evaporation. The product, a white solid, was isolated by recrystallization from ethyl acetate and hexane, giving pure **2.14** (830 mg, 35%). MP.: 60-64 °C. TLC: R_f 0.43 (100% petroleum ether). FTIR (CH_2Cl_2 , cm^{-1}): ν 3077, 2600, 1585, 1517, 1499. ^1H NMR (CDCl_3 , 200 MHz): δ 7.50 (d, $J = 4.1$ Hz, 2H, CH), 7.40 (m, 2H, CH), 7.35 (m, 1H, CH), 3.89-0.85 (br m, BH), 3.99 (br s, CH). $^{13}\text{C}\{^1\text{H}\}$ NMR (CDCl_3 , 500 MHz): δ 133.30, 129.86, 128.79, 127.43, 76.36, 60.07. $^{11}\text{B}\{^1\text{H}\}$ NMR (CDCl_3 , 500 MHz): δ -1.280, -3.607, -8.183, -10.010, -10.545, -12.024. MSCI (TOF, +): found m/z 220.2.

Synthesis of tetrabutylammonium 7-phenyl-7,8-dicarba-*nido*-undecaborate, 2.11. Tetrahydrofuran (100 mL) was added to 1-phenyl-1,2-dicarba-*closo*-dodecaborane **2.14** (670 mg, 3.04 mmol) followed by tetrabutylammonium fluoride hydrate (3.99 g, 15.22 mmol). The mixture was heated to reflux overnight and then the solvent removed by rotary evaporation. The product, a colorless solid, was isolated by silica gel chromatography (100% CH_2Cl_2), giving pure **2.11** (1.10 g, 80%). MP.: 115-118 °C. TLC: R_f 0.30 (100% dichloromethane). FTIR (CH_2Cl_2 ,

cm⁻¹): ν 3085, 3021, 3001, 2963, 2880, 2545, 1596, 1493, 1480. ¹H NMR (CDCl₃, 200 MHz): δ 7.24 (d, J = 3.6 Hz, 2H, CH), 7.08 (m, 3H, CH), 3.40-0.55 (br m, BH), 3.05 (t, J = 4.0 Hz, 2H, NCH₂CH₂CH₂CH₃), 2.35 (br s, 1H, CH), 1.54 (m, 2H, NCH₂CH₂CH₂CH₃), 1.38 (m, 2H, NCH₂CH₂CH₂CH₃), 0.97 (t, J = 3.5 Hz, 3H, NCH₂CH₂CH₂CH₃). ¹³C{¹H} NMR (CDCl₃, 200 MHz): δ 145.37, 127.26, 126.51, 124.54, 58.64, 23.71, 19.45, 13.46. ¹¹B{¹H} NMR (CDCl₃, 500 MHz): δ -9.061, -12.971, -18.351, -21.917, -32.385, -35.844. ESMS (- ion): found m/z 209.2.

Synthesis of tetrabutylammonium 1-phenyl-3,3,3-tricarbonyl-3- η^5 -Re-1,2-dicarba-*closo*-dodecaborate, 2.8. Tetrahydrofuran (10 mL) was added to tetrabutylammonium 7-phenyl-7,8-dicarba-*nido*-undecaborate **2.11** (101 mg, 0.22 mmol) and the subsequent reaction was cooled to -30 °C. Next *n*-Butyllithium (0.14 mL, 0.33 mmol) was added dropwise and stirred at -30 °C for 20 minutes. This was followed by the addition of **2.22** (186 mg, 0.24 mmol), and heating the mixture to reflux overnight. Upon cooling to room temperature, the mixture was diluted with dichloromethane (20 mL), filtered, and the solvent removed by rotary evaporation. The product was isolated by silica gel chromatography (5% hexane/CH₂Cl₂), followed by recrystallization from hexane and dichloromethane to yield pure colourless crystals of **2.8** (73 mg, 46%). MP.: 90-93 °C. TLC: R_f 0.50 (100% dichloromethane). FTIR (CH₂Cl₂, cm⁻¹): ν 3055, 2970, 2880, 2530, 2006, 1905. ¹H NMR (CDCl₃, 200 MHz): δ 7.10 (d, J = 3.7 Hz, 2H, CH), 7.00 (m, 2H, CH), 6.95 (m, 1H, CH), 3.95 (br s, 1H, CH) 3.12 (m, 2H, NCH₂CH₂CH₂CH₃), 1.55 (m, 2H, NCH₂CH₂CH₂CH₃), 1.45 (m, 2H, NCH₂CH₂CH₂CH₃), 1.03 (t, J = 3.6 Hz, 3H, NCH₂CH₂CH₂CH₃). ¹³C{¹H} NMR (CDCl₃, 200 MHz): δ 198.42, 146.13, 127.46, 125.07, 122.84, 58.98, 37.40, 23.94,

19.70,13.65. $^{11}\text{B}\{^1\text{H}\}$ NMR (CDCl_3 , 500 MHz): δ -5.23, -10.19, -22.79. ESMS (- ion): found m/z 478.9. HRMS found m/z 479.1472.

Synthesis of 1-(4-methoxyphenyl)-1,2-dicarba-*closo*-dodecaborane, 2.15.

Acetonitrile (100 mL) was added to decaborane **2.17** (1.030 g, 8.46 mmol) and the mixture stirred at room temperature overnight. 4-Ethynylanisole **2.19** (0.82 mL, 9.3 mmol) was then added and the mixture heated to reflux for 48 h, where an intense red colour developed. Upon cooling to room temperature, the solvent was removed by rotary evaporation, and product **2.15** (120 mg, 8%) isolated by first precipitating out hydrophilic by-products from ethyl acetate and hexane, then by using silica gel column chromatography. MP.: 105-107 °C. TLC: R_f 0.43 (100% petroleum ether). FTIR (CH_2Cl_2 , cm^{-1}): ν 3075, 3013, 2966, 2940, 2914, 2843, 2602, 1611, 1581, 1515, 1464. ^1H NMR (CDCl_3 , 200 MHz): δ 7.43 (d, $J = 4.5$ Hz, 2H, CH), 6.84 (d, 2H, CH), 3.89, (br s, 1H, CH), 3.81 (s, 3H, OCH_3), 3.60-0.81 (br m, BH). $^{13}\text{C}\{^1\text{H}\}$ NMR (CDCl_3 , 200 MHz): δ 160.70, 129.20, 125.39, 113.96, 76.80, 60.96, 55.40. $^{11}\text{B}\{^1\text{H}\}$ NMR (CDCl_3 , 500 MHz): δ -1.06, -3.87, -8.25, -9.77, -10.57, -11.81. MSEI (TOF, +): found m/z 250.2.

Synthesis of tetrabutylammonium 7-(4-methoxyphenyl)-7,8-dicarba-*nido*-undecaborate, 2.12a. Tetrahydrofuran (100 mL) was added to 1-(4-methoxyphenyl)-1,2-dicarba-*closo*-dodecaborane **2.15** (200 mg, 0.8 mmol) and tetrabutylammonium fluoride hydrate (968 mg, 4.0 mmol). The mixture was heated to reflux overnight and then the solvent was removed by rotary evaporation. The product, a colourless solid, was isolated by silica gel chromatography (100% CH_2Cl_2), giving pure **2.12a** (230

mg, 60%). MP.: 101-103 °C. TLC: R_f 0.30 (100% dichloromethane). FTIR (CH_2Cl_2 , cm^{-1}): ν 3085, 2969, 2880, 2840, 2523, 1677, 1608, 1512, 1480. ^1H NMR (CDCl_3 , 200 MHz): δ 7.19 (d, $J = 4.4$ Hz, 2H, CH), 6.67 (d, 2H, CH), 3.73 (s, 3H, OCH_3), 3.10 (t, $J = 3.8$ Hz, 2H, $\text{NCH}_2\text{CH}_2\text{CH}_2\text{CH}_3$), 2.30 (br s, 1H, CH), 1.55 (m, 2H, $\text{NCH}_2\text{CH}_2\text{CH}_2\text{CH}_3$), 1.35 (m, 2H, $\text{NCH}_2\text{CH}_2\text{CH}_2\text{CH}_3$), 0.99 (t, $J = 3.6$ Hz, 3H, $\text{NCH}_2\text{CH}_2\text{CH}_2\text{CH}_3$). $^{13}\text{C}\{^1\text{H}\}$ NMR (CDCl_3 , 200 MHz): δ 157.01, 137.88, 127.93, 112.78, 58.84, 55.22, 23.90, 19.63, 13.62. $^{11}\text{B}\{^1\text{H}\}$ NMR (CDCl_3 , 500 MHz): -8.51, -9.70, -12.88, -15.83, -17.64, -21.70, -31.90, -35.15. ESMS (- ion): found m/z 240.0.

Synthesis of 1-(4-hydroxyphenyl)-1,2-dicarba-*closo*-dodecaborane, 2.16.

Dichloromethane (10 mL) was added to 1-(4-methoxyphenyl)-1,2-dicarba-*closo*-dodecaborane 2.15 (0.45 mg, 0.18 mmol). The temperature was reduced to -30 °C and boron tribromide (0.92 mL, 0.92 mmol) was added dropwise and the mixture was stirred at this temperature for 30 minutes. The mixture was then allowed to warm to room temperature and evaporate overnight. The following morning the temperature was reduced to -10 °C and tetrahydrofuran (10 mL) was added slowly. This was allowed to warm to room temperature and evaporate overnight. The next morning the temperature was dropped to 0 °C and methanol (10 mL) was slowly added. This was stirred for 1 hour before allowing to warm to room temperature. The solvent was then removed under reduced pressures and the product was isolated by silica gel column chromatography (1:10 EtOAc/hexane) to yield a sticky colourless solid, 2.16 (35 mg, 77%). MP.: 104-106 °C. TLC: R_f 0.75 (100% CH_2Cl_2). FTIR (CH_2Cl_2 , cm^{-1}): ν 3586, 3070, 3000, 2602, 1516. ^1H NMR (CDCl_3 , 200 MHz): δ 7.38 (d, $J = 4.3$ Hz, 2H, CH), 6.77 (d, 2H, CH), 5.14 (s, 1H, OH), 3.87 (s, 1H, CH) 3.50-1.0 (br m, BH).

$^{13}\text{C}\{^1\text{H}\}$ NMR (CDCl_3 , 200 MHz): δ 156.79, 129.51, 125.79, 115.48, 60.96. $^{11}\text{B}\{^1\text{H}\}$ NMR (CDCl_3 , 500 MHz): δ -1.06, -3.84, -8.24, -9.79, -10.59, -11.83. MSEI (TOF, +): found m/z 236.2.

Synthesis of tetrabutylammonium 7-(4-hydroxyphenyl) -7,8-dicarba-*nido*-undecaborate 2.13a. Tetrahydrofuran (50 mL) was added to 1-(4-hydroxyphenyl)-1,2-dicarba-*closo*-dodecaborane **2.16** (50 mg, 0.21 mmol) and tetrabutylammonium fluoride hydrate (520 mg, 1.6 mmol), where upon the mixture turned bright orange instantaneously. The mixture was heated to reflux overnight followed by the removal of the solvent rotary evaporation. The product, **2.13a** (60 mg, 61%), a colourless solid, was isolated by silica gel chromatography (1:99 methanol/ CH_2Cl_2). MP.: 72-74 °C. TLC: R_f 0.26 (10% methanol/dichloromethane). FTIR (CH_2Cl_2 , cm^{-1}): ν 3583, 3058, 2969, 2880, 2523, 1608, 1512. ^1H NMR (CDCl_3 , 200 MHz): δ 6.92 (d, $J = 3.8$ Hz, 2H, CH), 6.30 (d, 2H, CH), 3.09 (t, $J = 4.1$ Hz, 2H, $\text{NCH}_2\text{CH}_2\text{CH}_2\text{CH}_3$), 1.99 (s, 1H, CH), 1.54 (m, 2H, $\text{NCH}_2\text{CH}_2\text{CH}_2\text{CH}_3$), 1.30 (m, 2H, $\text{NCH}_2\text{CH}_2\text{CH}_2\text{CH}_3$), 0.93 (t, $J = 3.6$ Hz, 3H, $\text{NCH}_2\text{CH}_2\text{CH}_2\text{CH}_3$). $^{13}\text{C}\{^1\text{H}\}$ NMR (CDCl_3 , 200 MHz): δ 155.42, 138.58, 129.04, 114.93, 59.57, 24.84, 20.71, 14.00. $^{11}\text{B}\{^1\text{H}\}$ NMR (CDCl_3 , 500 MHz): δ -7.93, -9.33, -12.33, -15.58, -16.88, -17.87, -21.15, -31.52, -34.73. ESMS (-ion): found m/z 225.8.

Synthesis of sodium 1-(4-hydroxyphenyl)-3,3,3-tricarbonyl-3- η^5 -Re-1,2-dicarba-*closo*-dodecaborate, 2.10. Aqueous sodium fluoride (0.5 M, 10 mL) was added to **2.16** (50 mg, 0.21 mmol) in a Parr Microwave Digestion Bomb (Model # 4781) along with 3 equivalents of **2.22a** (258 mg, 0.64 mmol) and the mixture

irradiated in a conventional microwave for two 1-minute intervals at high power. After allowing the water to cool (20 min.) the sample was acidified with 5 ml of 10 M HCl. The mixture was diluted with acetonitrile (10 mL) and cooled at $-10\text{ }^{\circ}\text{C}$ until the organic layer separated. The acetonitrile layer was removed by pipet and concentrated under reduced pressures. The product (**2.10**), was isolated by silica gel chromatography (5% methanol/chloroform), (60 mg, 54%). as a dark brown oil. TLC: R_f 0.15 (10% methanol/chloroform). FTIR (KBr, cm^{-1}): ν 3441, 2559, 2001, 1884, 1612, 1511. ^1H NMR (CD_3OD , 200 MHz): δ 7.25 (d, $J = 5.3$ Hz, 2H, CH), 6.05 (m, 2H, CH), 1.72 (br s, 1H, CH). $^{13}\text{C}\{^1\text{H}\}$ NMR (CD_3OD , 200 MHz): 200.66, 156.73, 135.48, 130.61, 114.73, 57.45, 55.92. $^{11}\text{B}\{^1\text{H}\}$ NMR (CD_3OD , 500 MHz): δ -9.25, -12.24, -13.63, -16.13, -16.90, -22.61, -24.16. ESMS (- ion): found m/z 495.2. HRMS found m/z 495.1430.

2.10 References

- ¹ Beato, M.; Sanchez-Pacheco, A.; *Endocr. Rev.* **1996**, *17*, 587.
- ² Lerner, L.J.; Jordan, V.C.; *Cancer Res.* **1990**, *50*, 4177.
- ³ Jordan, V.C.; *J. Steroid Biochem.* **1974**, *5*, 354.
- ⁴ Furr, B.J.A.; Jordan, V.C.; *Pharmacol. Ther.* **1984**, *25*, 127.
- ⁵ Top, S.; Dauer, B.; Vaissermann, J.; Jaouen, G.; *J. Organomet. Chem.* **1997**, *541*, 355.
- ⁶ Endo, Y.; Iijima, T.; Yamakoshi, Y.; Fukusawa, H.; Miyaura, C.; Inada, M.; Kubo, A.; Itai, A.; *Chem. Bio.* **2001**, *8*, 341.
- ⁷ Endo, Y.; Iijima, T.; Yamakoshi, Y.; Kubo, A.; Itai, A.; *Bioorg. Med. Chem. Lett.* **1999**, *9*, 3313.
- ⁸ Endo, Y.; Yoshimi, T.; Yamakoshi, Y.; *Chem. Pharm. Bull.* **2000**, *48*, 312.
- ⁹ Endo, Y.; Iijima, T.; Yamakoshi, Y.; Yamaguchi, M.; Fukasawa, H.; Shudo, K.; *J. Med. Chem.* **1999**, *42*, 1501.
- ¹⁰ Mull, E.S.; Sattigeri, V.J.; Rodriguez, A.L.; Katzenellenbogen, J.A.; *Bioorg. Med. Chem.* **2002**, *10*, 1381.
- ¹¹ Fox, M.A.; MacBride, J.A.H.; Peace, R.J.; Wade, K.; *J. Chem. Soc. Trans.* **1998**, 401
- ¹² Giovenzana, G.B.; Lay, L.; Monti, D.; Palmisano, G.; Panza, L.; *Tetrahedron.* **1999**, *55*, 14123..
- ¹³ Fein, M.M.; Bobinski, H.; Mayes, N.; Schwartz, N.N.; Cohen, M.S.; *Inorg. Chem.* **1963**, *2*, 1111. Heying, T.L.; Ager, J.W.; Clark, S.L.; Mangold, D.J.; Goldstein, H.L.; Hillman, M.; Polak, R.J.; Szymanski, J.W.; *Inorg. Chem.* **1963**, *2*, 1089.

- ¹⁴ PdCl₂ spray is made with 500 mgs of PdCl₂ and 500 mL of 1.0 M HCl.
- ¹⁵ Brain, P.T.; Cowie, J.; Donohoe, D.J.; Hnyk, D.; Rankin, D.W. H.; Reed, D.; Reid, B.D.; Robertson, H.E.; Welch, A.J.; *Inorg. Chem.* **1996**, *35*, 1701.
- ¹⁶ Grimes, R. N.; *Carboranes*, © 1970, *Academic Press*.
- ¹⁷ Lietes, L.A.; *Chem. Rev.* **1992**, *92*, 279.
- ¹⁸ Fox, M.A.; MacBride, J.A.; Wade, K.; *Polyhedron.* **1996**, *16*, 2499.
- ²³ Hawthorne, M.F.; Andrews, T.D.; *J. Am. Chem. Soc.* **1965**, *87*, 2496. Reintjes, M.; Warren, L.F.; *J. Am. Chem. Soc.* **1968**, *90*, 879.
- ²⁰ Ellis, D.D.; Jelliss, P.A.; Stone, F.G.A.; *Organomet.* **1999**, *18*, 4982.
- ²¹ Valliant, J.F.; Morel, P.; Schaffer, P.; Kaldis, J.H.; *Inorg. Chem.* **2002**, *41*, 628.
- ²² Unpublished results conducted by O.O Sogbein, 2003.
- ²³ Alberto, R.; Schibli, R.; Egli, A.; Schubiger, P.A.; *J. Am. Chem. Soc.* **1998**, *120*, 7987. Alberto, R.; Schibli, R.; Egli, A.; Schubiger, P.A.; Herrmann, W.A.; Artus, G.; Abram, T.; Kaden, T.A.; *J. Organomet. Chem.* **1995**, *492*, 217.
- ²⁴ Zalkin, A.; Hopkins, T.E.; Templeton, D.H.; *Inorg. Chem.* **1966**, *5*, 7, 1189.
- ²⁵ Hermanek, S.; *Chem. Rev.* **1992**, *92*, 325.
- ²⁶ Murphy, D.M.; Mingos, M. P.; Forward, J. M.; *J. Mater. Chem.* **1993**, *3*, 67.
- ²⁷ Suarez, A.; *et al. Organomet.* **2002**, *21*, 4611.
- ²⁸ Unpublished results conducted by A. Green, 2004.

Chapter 3 - Diarylated Carboranes

3.1 Overview

Having established a method to prepare rhenium (I) complexes of mono-substituted aryl-carboranes, the next step was to develop a method to prepare diaryl Re-metallocarboranes. To this end, three diaryl substituted metallocarboranes that could potentially serve as organometallic anti-estrogens were prepared. This chapter will discuss the rationale for the choice of the particular di-substituted carboranes along with the practical synthetic details and characterization required to confirm the identity of the target molecules.

3.2 Introduction

As mentioned previously, Endo and co-workers utilized the unique 3-D topology and hydrophobic character of the carborane cage to develop compounds that would interact favourably with the ER.¹ In addition to monoarylated derivatives described in chapter 1, diarylated carborane derivatives were prepared and screened for their ER binding affinities. Three representative examples are the carborane Tamoxifen analogues shown in **Figure 3.1**.

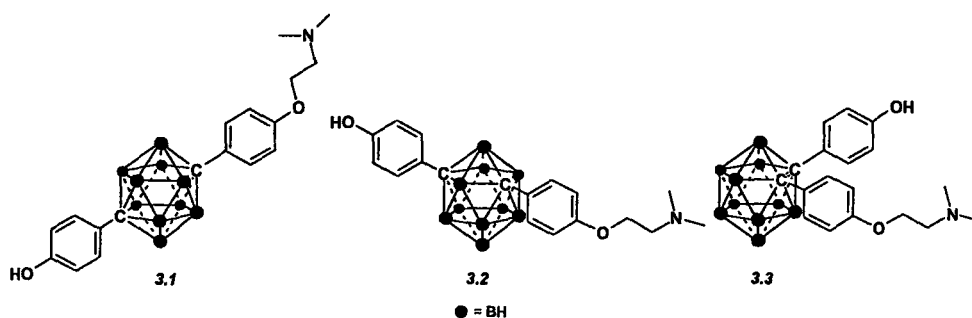


Figure 3.1: Carborane analogues of Tamoxifen.

Endo's group observed the lowest antagonistic character with *para*-derivative, 3.1 (RBA= 8%, relative to hydroxytamoxifen) and attributed this poor result to the diminished degree of hydrogen bonding in the receptor-substrate complex which was due to the incorrect positioning of the phenyl rings. The *meta*-derivative, 3.2, produces better antagonistic effects (RBA = 22%) which is likely due to the hydrogen bonding associated with the change in positioning of the aryl substituents. Compound 3.3, which is derived from *ortho*-carborane, exhibited the best ER binding character (RBA = 53%). This compound can be considered an inorganic analogue of Tamoxifen.

As mentioned previously in Chapter 1, Katzenellenbogen *et al.* investigated the use of substituted Re-cyclopentadienide complexes² and bicyclo- and tricyclo-cyclofenil³ derivatives as ER binding agents (Figure 3.2). The Re-cyclopentadienide derivative which showed the greatest efficacy for the estrogen receptor was 3-ethyl-1,2,4-tri-(4-hydroxyphenyl) cyclopentadienyltricarbonyl rhenium (3.4) with a drop in affinity being observed as the position of the hydroxy substituents was altered and the number of aryl rings decreased.² This finding was strengthened by the work on tricyclo- and bicyclo-derivatives of cyclofenil (Figure 3.2) where the positioning of the hydroxy groups was a critical factor in the observed binding affinity for the ER.³

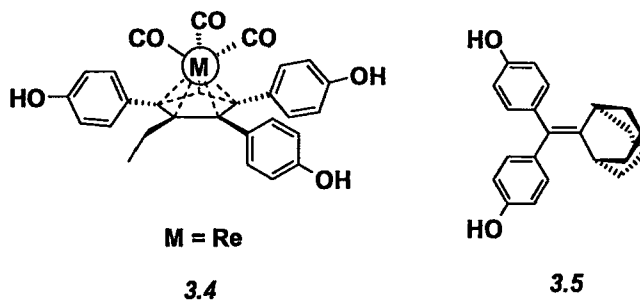


Figure 3.2: Novel ER binding agents.

3.3 Rationale

Considering the anti-estrogenic character displayed by the di-substituted carboranes prepared by Endo *et al.*¹ and the binding affinity observed for the Re-complexes described by Katzenellenbogen *et al.*² a method to prepare diaryl Re-metallocarboranes was developed. The ER-LBD would be expected to accommodate the increase in size associated with substitution of the rhenium tricarbonyl core for a BH vertex. Thus the potential exists to prepare Re and ^{99m}Tc complexes of Endo's compounds without having a detrimental impact on the ER binding affinities.¹ To this end, four diarylated carborane complexes were selected as targets based on the relative binding affinities observed for the parent carboranes. (Figure 3.3)

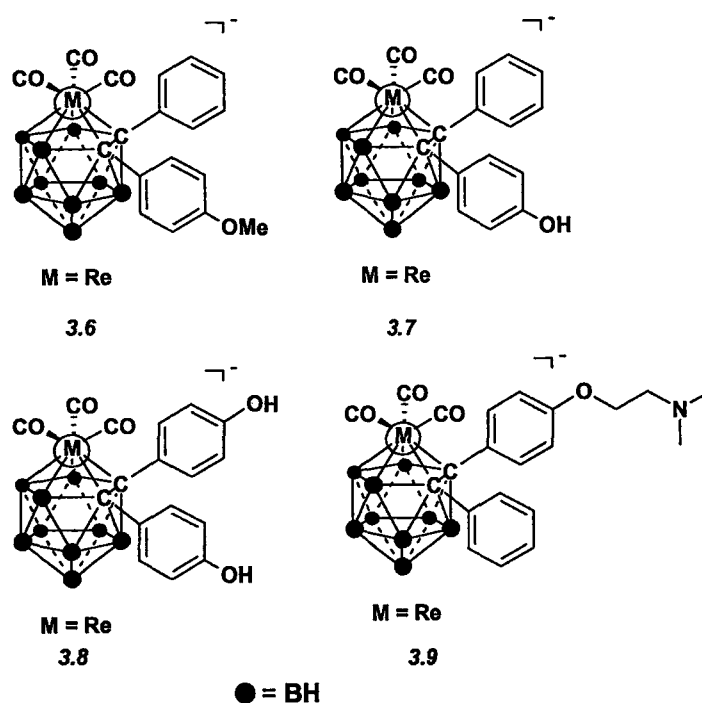


Figure 3.3: The Re-metallocarborane targets: 1-(4-methoxyphenyl)-2-phenyl-3,3,3-tricarbonyl-3- η^5 -Re-1,2-dicarba-closo-dodecaborate (3.6), 1-(4-hydroxyphenyl)-2-phenyl-3,3,3-tricarbonyl-3- η^5 -Re-1,2-dicarba-closo-dodecaborate (3.7), 1,2-bis(4-hydroxyphenyl)-3,3,3-tricarbonyl-3- η^5 -Re-1,2-dicarba-closo-dodecaborate (3.8), and 1-(4-(N,N-dimethylaminoethoxy)phenyl)-2-phenyl-3,3,3-tricarbonyl-3- η^5 -Re-1,2-dicarba-closo-dodecaborate (3.9).

3.4 Synthetic Strategy and Targets

The first target was a diaryl substituted *ortho*-carborane containing one *para*-methoxy phenyl group and a unsubstituted phenyl ring (3.6). This compound, which is the simplest target, was used to develop the overall synthetic strategy and to optimize the reaction conditions used to prepare the other targets. The second target contained a single phenyl ring and a phenol group (3.7). Compound 3.7 is expected to possess high ER binding affinity and it also enabled us to determine if the hydroxy group would impact the yield of the metal complex.

Numerous reports have indicated that increasing the number of hydrogen bond donors, provided the correct spatial distributions are present, can offer increased binding affinities to the ER.³ This observation prompted the synthesis of compound 3.8 whereby two phenolic units with the potential for hydrogen bonding were present as part of the carborane. Along the same line, the final target (3.9) was chosen based on its potential for increased binding affinity. Compound 3.9 is expected to bind the ER at levels comparable to Tamoxifen.

The general synthetic approach taken is presented in **Figure 3.4**. Complex 3.6 was prepared from the *nido*-carborane 3.10, which in turn was generated by the deboronation of the *closo*-carborane 3.14. The preparation of *closo*-carborane 3.14 required the preparation of the 1,2-diaryl alkyne 3.18. Metallocarborane 3.7 was prepared from compound 3.11 in a manner that is analogous to the procedure used to prepare compound 3.6. The *nido*-compound 3.11 was obtained by the degradation of *closo*-compound 3.15, which was prepared from the *closo*-analogue 3.14. Compound 3.8 was obtained by complexation directly from *closo*-carborane 3.16, which was generated by the demethylation of the *closo*-carborane 3.20. Compound 3.20 was in

turn prepared using the alkyne 3.19. Compound 3.9 was generated directly from the *closo*-carborane 3.17, using a textbook strategy discussed herein. The carborane 3.17 was prepared from compound 3.15.

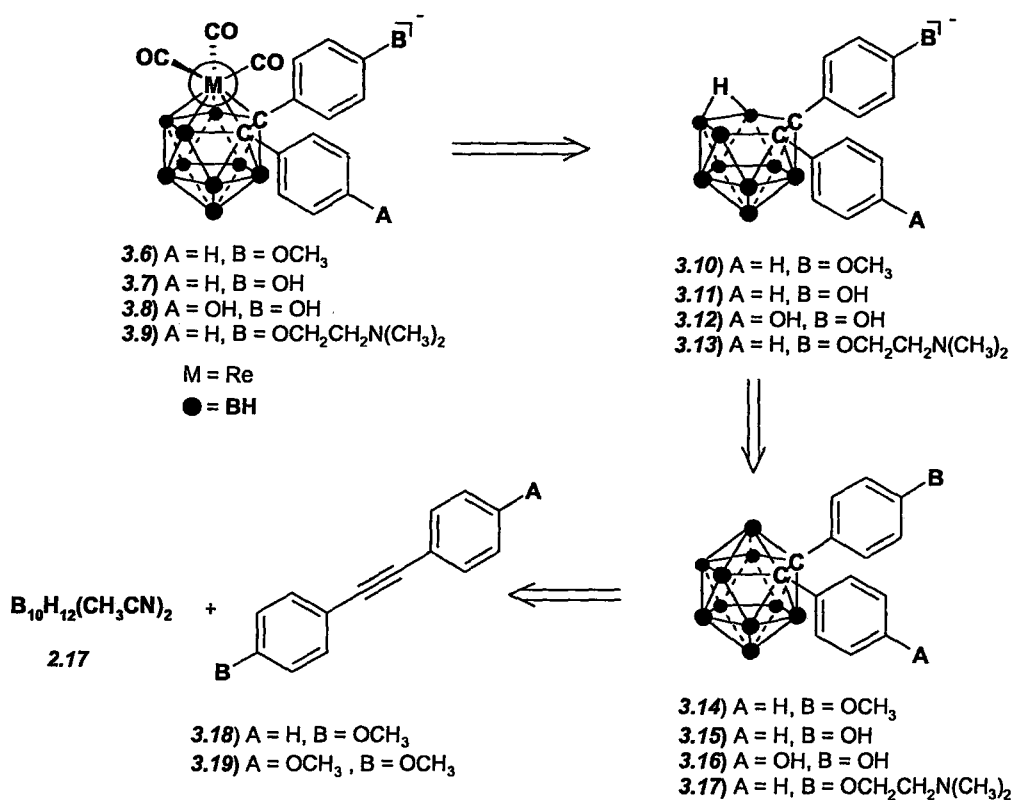
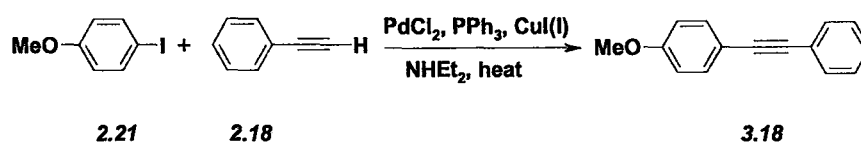


Figure 3.4: Retrosynthesis of diarylated metallocarboranes.

3.5 Synthesis of 1-(4-Methoxyphenyl)-2-Phenyl Re-Metallo-carboranes (3.6)

As a result of the steric bulk associated with aryl substituted carboranes, the synthesis of *ortho*-diaryl carboranes can only be conducted via the alkyne insertion process.^{1,4} In order for the alkyne insertion route to be utilized, the diarylalkyne with appropriate functionalities needed to be prepared. For the purpose of the desired *closo*-carborane, 3.14, it was necessary to synthesize 1-(4-methoxyphenyl)-2-

phenylacetylene (**3.18**). Compound **3.18** was generated using a Sonogashira coupling between phenylacetylene (**2.18**) and *para*-iodoanisole (**2.21**) (Scheme 3.1).⁵ This reaction involves the use of bis(triphenylphosphine) palladium dichloride catalyst (**3.21**) in diethylamine in the presence of a catalytic amount of copper (I) iodide.⁵ Heating the mixture at reflux for 24 hours generated the alkyne **3.18** in 67% yield.



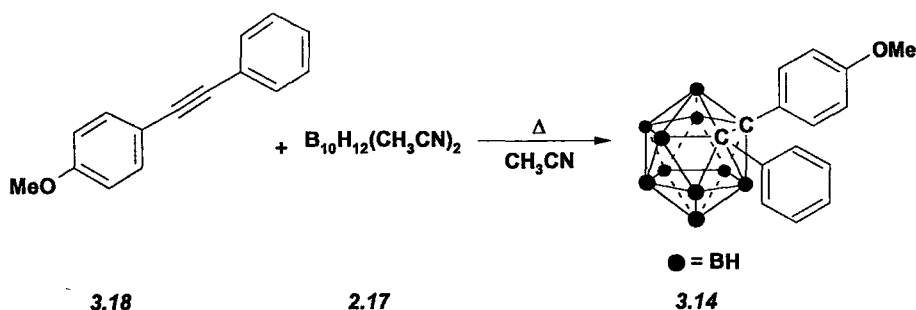
Scheme 3.1: *Synthesis of 1-(4-methoxyphenyl)-2-phenyl acetylene (3.18).*

Compound **3.18**, was visualized by TLC (3% ethyl acetate/hexanes) showing both palladium and UV activity. TLC analysis upon spraying with palladium chloride solution and heating yielded a red spot thus identifying the component of interest. The product was purified by silica gel column chromatography with an eluent consisting of 3% ethyl acetate/hexanes and isolated as a fluffy white solid.

The ¹H NMR spectrum of **3.18** showed aromatic multiplet signals at 7.55, 7.40, and 7.34 ppm and a pair of aromatic doublets at 7.50 ppm (*J* = 4.3 Hz) and 6.89 ppm. The methoxy singlet was observed at 3.83 ppm. The ¹³C NMR spectrum exhibited, as predicted, 8 aromatic signals at; 159.56, 133.99, 131.39, 128.26, 127.88, 123.54, 115.30, 113.94 ppm. The two acetylene carbon atoms were observed at 89.34 and 88.02 ppm, while the methoxy signal occurred at 55.21 ppm. Infrared analysis of **3.18** exhibited the acetylene carbon-carbon triple bond at 2218 cm⁻¹, with the aromatic C=C stretches occurring at 1604, 1599, 1571, and 1511 cm⁻¹. The molecular

ion peak was found at an m/z value of 208.0875 (HRMS). The spectroscopic data is in good agreement with reported values.⁶

Compound **3.14** was prepared by performing an alkyne insertion reaction on **3.18** using the Lewis base adduct of decaborane, **2.17** (Scheme 3.2). Within minutes of heating to reflux, the reaction, which was originally yellow, changed to an intense orange colour, which persisted for the duration of the reaction (48 hrs). The crude reaction mixture was concentrated *in vacuo* yielding an orange-red solid, which was partially purified by the precipitation of unwanted by products using 30% ethyl acetate in hexanes. Isolation of the desired product **3.14** was accomplished in 21% yield by silica gel column chromatography using 5% ethyl acetate and hexanes.



Scheme 3.2: Preparation of 1-(4-methoxyphenyl)-2-phenyl-1,2-dicarba-closo-dodecaborane (**3.14**).

The infrared spectra of **3.14** showed the characteristic B-H stretch for a *closo*-carborane at 2598 cm^{-1} . Alkyl stretching frequencies were observed at 3013 , 2965 , 2939 , 2915 cm^{-1} , while the aromatic C=C stretch modes were present at 1609 , 1515 , and 1464 cm^{-1} . Chemical ionization mass spectroscopy found an m/z value of 326.3, which is consistent with the mass of **3.14**.

^1H NMR spectrum of 3.14 (Figure 3.5) showed three sets of aromatic doublets at 7.44 ppm ($J = 3.5$ Hz), 7.35 ppm ($J = 4.5$ Hz), and 6.63 ppm. The remaining aromatic signals presented as two sets of multiplets at 7.22 and 7.15 ppm. The broad B-H signal is apparent from 3.85-0.80 ppm, while the methoxy-singlet occurs at 3.71 ppm. In the ^{13}C NMR spectrum two quaternary aromatic carbon signals were at 160.76 and 122.87 ppm. The remaining aromatic signals were observed at 132.01, 130.60, 130.10, 128.22, and 113.42 ppm. The carbon atoms of the carborane cage were observed at 85.67 and 85.36 ppm, with the methoxy resonance occurring at 55.21 ppm. The ^{11}B NMR spectra displayed four signals at -1.66, -8.37, -9.81, -10.66, reflecting the nearly symmetric environment imposed on the carborane cage by two similar aromatic rings (Figure 3.6).

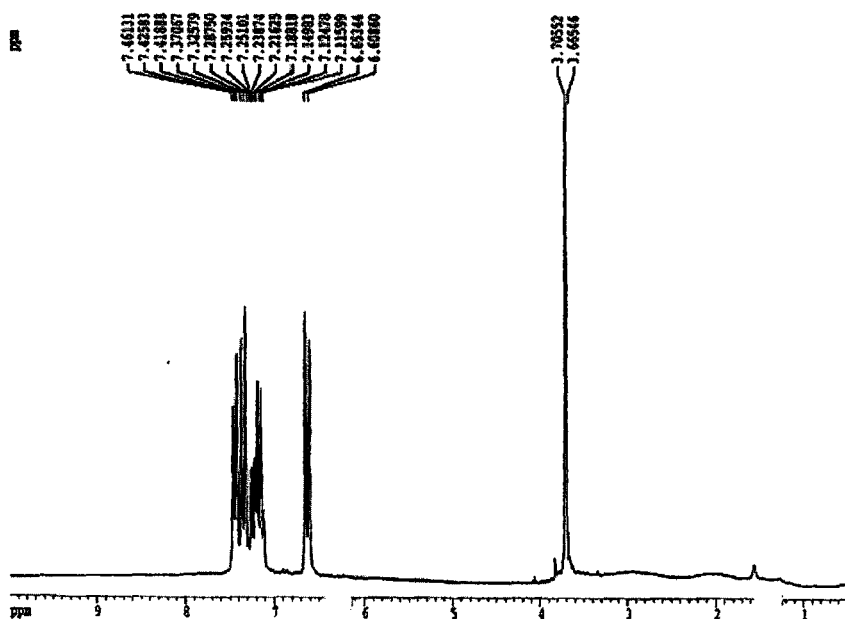


Figure 3.5: ^1H NMR (200 MHz in CDCl_3), of 1-(4-methoxyphenyl)-1,2-dicarba-closo-dodecaborane (3.14).

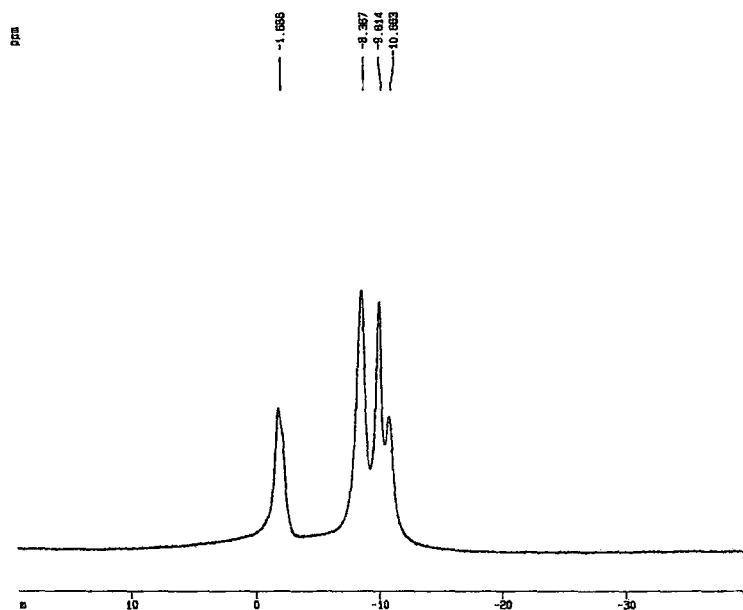
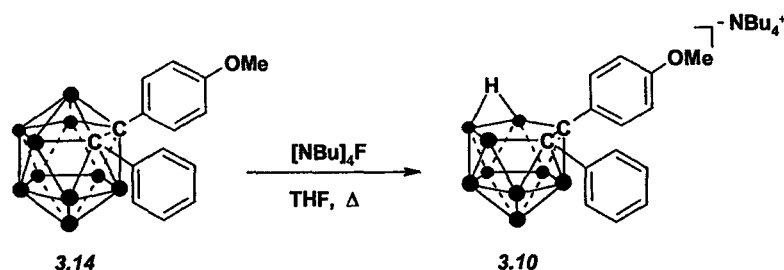


Figure 3.6: ^{11}B NMR (500 MHz in CDCl_3) of 1-(4-methoxyphenyl)-2-phenyl-1,2-dicarba-closo-dodecaborane (3.14).

With the *closo*-carborane 3.14 in hand, the next step was to prepare the corresponding *nido*-carborane, 3.10. Based on the difficulties encountered with purification of the monolarylated *nido*-carboranes (Chapter 2) it was determined that deboronation should be attempted using tetrabutylammonium fluoride (TBAF).⁷ In THF, compound 3.14 and five equivalents of TBAF were heated to reflux (Scheme 3.3). The target (3.10) was identified via TLC (dichloromethane) with a substantially reduced R_f value relative to the 3.14. Compound 3.10 was isolated as an off-white solid in 85% yield following silica gel chromatography using 5% hexanes in dichloromethane as the eluent.



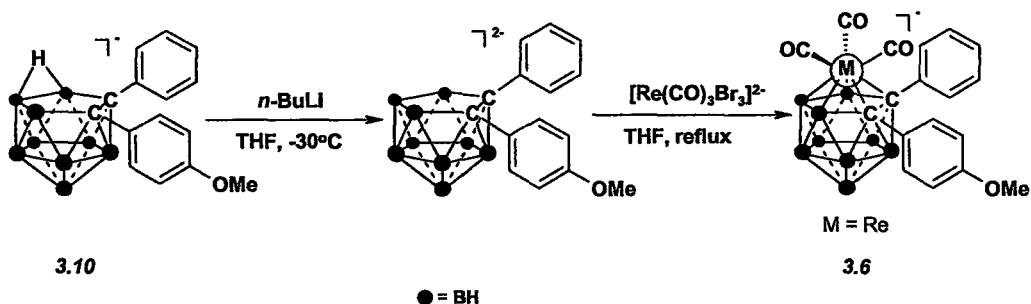
Scheme 3.3: The synthesis of *nido*-carborane **3.10**.

Similar to the monoarylated carboranes in chapter 2, the signals for the aromatic protons in the ^1H NMR spectrum of compound **3.10** exhibited a notable shift upfield, which is a result of the increased electron density on the carborane cage. The order of the aromatic resonances remained unchanged, however the change in electron environment produced increased separation of the signals associated with the phenol ring which appeared at 7.12 and 6.41 ppm ($J = 1.4$ Hz). In addition, a doublet attributed to the *ortho*-protons of the phenyl ring was observed at 7.04 ppm along with two multiplets at 6.87 and 6.83 ppm. The methoxy signal associated with the methoxy protons occurred at 3.60 ppm. The aliphatic signals resulting from the quaternary amine cation were observed at 3.04, 1.51, 1.36, and 0.96 ppm with the expected splitting patterns.

The ^{13}C NMR spectrum of **3.10** displayed an upfield shift of the 8 aromatic signals, which appeared at 157.27, 142.06, 134.36, 132.74, 131.87, 126.65, 125.21, and 112.06 ppm. The methoxy signal was observed at 59.02 ppm. The signals for the counter ion were present at 55.13, 24.18, 19.76, and 13.73 ppm. The ^{11}B NMR spectrum for **3.10**, also shifted upfield, was more complex than that of the starting material which results from the lowering of symmetry upon loss of the BH vertex. The boron signals appeared at -7.60, -13.55, -16.16, -18.04, -32.72, and -35.05 ppm.

The FTIR of *nido*-carborane **3.10** exhibited the characteristic B-H stretch of the cage at 2526 cm^{-1} , which is at a lower energy than that of **3.14**. Aromatic C=C stretches were observed at 1607 and 1511 cm^{-1} . Negative ion mode showed the expected molecular ion peak at 315.2 m/z , with the usual $^{11}\text{B}/^{10}\text{B}$ isotopic distribution. The positive ion mode contained the correct mass to charge ratio for the TBA counterion at 242.1 .

The initial complexation reaction of the carborane **3.10** was done before the microwave reaction described in Chapter 2 was discovered. It involved the removal of the bridging hydrogen in **3.10** with 1.5 equivalents of *n*-BuLi in THF at $-30\text{ }^{\circ}\text{C}$ under inert atmosphere. The reaction was stirred for 30 minutes then it was allowed to warm to room temperature at which point one equivalent of **2.22** was added and the reaction heated to reflux (Scheme 3.4). A small sample of the crude reaction mixture was submitted for ESMS, which showed the mass of the target **3.6** along with a signal corresponding to residual starting material. TLC of the crude reaction mixture (100% dichloromethane) showed that the complex **3.6** ran slightly a head of the ligand **3.10**. Using silica gel chromatography in dichloromethane, palladium and UV active fractions were collected and analyzed by FTIR for the existence of the Re-complex. Those samples which contained **3.6** were identified by the presence of B-H and carbonyl stretches. To determine the extent of contamination by residual starting material, ESMS was employed on each fraction. Fractions containing only compound **3.6** were combined to generate an overall yield of 40%. Attempts to grow crystals of **3.6** using 10% dichloromethane and hexanes were unsuccessful.



Scheme 3.4: Synthesis of Re-metallocarborane 3.6.

Compound 3.6 in the negative ion mode ESMS showed a mass to charge ratio of 585.2, with the expected boron isotopic distribution (Figure 3.7). The infrared spectrum for 3.6 had two carbonyl stretches at 2001 and 1903 cm^{-1} . The B-H stretch occurred at 2560 cm^{-1} which was higher energy than the B-H stretch of the ligand (2535 cm^{-1}).

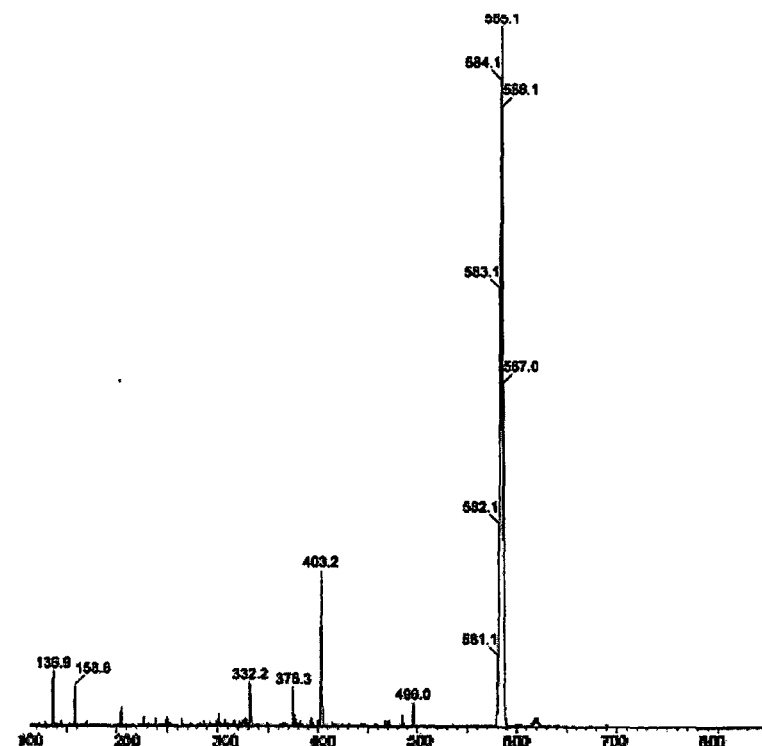


Figure 3.7: The negative ion electrospray mass spectrum of 3.6.

In the ^1H NMR spectrum for **3.6** the aromatic protons occurred as four sets of multiplets at 7.76, 7.15, 7.03, and 6.86 ppm, along with a pair of doublet at 7.55 and 6.71 ppm ($J = 4.4$ Hz). Two signals were observed for the methoxy protons at 3.76 and 3.71 ppm. The presence of two signals is likely the result of the existence of two atropisomers of **3.6** (*vide infra*) (Figure 3.8).^{8,9} The ^{13}C NMR spectrum for **3.6** displayed the carbonyl carbon atoms at 200.12 ppm while there were 10 aromatic signals observed at 129.74, 128.75, 127.51, 126.5, 127.12, 125.40, 124.54, 124.12, 112.71, and 112.55 ppm. The methoxy carbon signal occurred at 59.00 ppm.

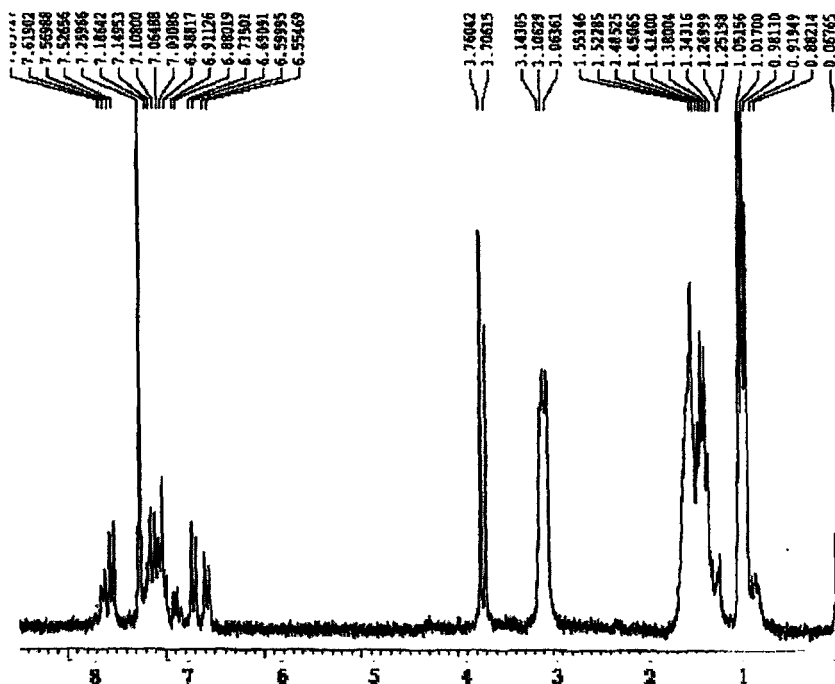
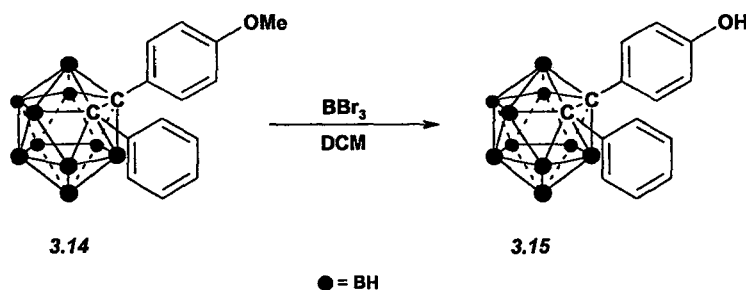


Figure 3.8: ^1H NMR (200 MHz, in CDCl_3) of tetrabutylammonium 1-(4-methoxyphenyl)-2-phenyl-3,3,3-tricarbonyl-3- η^5 -Re-1,2-dicarba-closo-dodecaborate (**3.6**).

3.6 Synthesis of 1-(4-Hydroxyphenyl)-2-Phenyl-Re-Metallocarborane (**3.7**)

To generate 1-(4-hydroxyphenyl)-2-phenyl-1,2-dicarba-closo-dodecaborane (**3.15**), the methyl group in **3.14** was removed. This was accomplished with the use of 5 equivalents boron tribromide in dichloromethane, at -30 °C (Scheme 3.5). After

allowing the reaction mixture to evaporate under a stream of nitrogen gas, methanol was added at 0 °C. TLC of the mixture produced one component which was both palladium and UV active. The TLC spot had an R_f value that was lower than the more hydrophobic starting material. The resulting mixture was concentrated to yield a dark orange-brown residue, which was purified by silica gel chromatography in 5% ethyl acetate in hexanes. The product, **3.15**, was isolated as an off-white solid in 89 % yield.

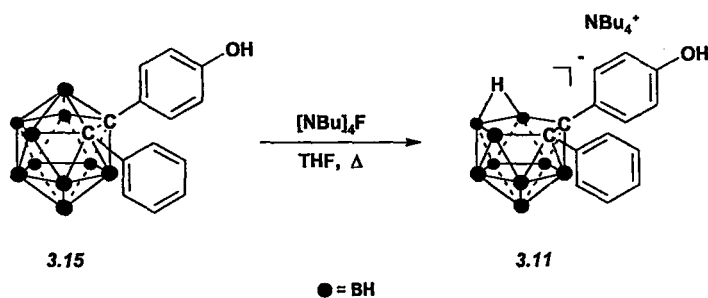


Scheme 3.5: Preparation of 1-(4-hydroxyphenyl)-2-phenyl-ortho-carborane (**3.15**).

The ^1H NMR spectrum of **3.15** displayed a doublet at 7.31 ppm ($J = 3.8$ Hz) and a multiplet at 7.19 ppm associated with the aromatic signals of the unsubstituted phenyl ring, while the 1,4-substituted aromatic ring showed two pairs of doublets occurring at 7.44 and 6.56 ppm ($J = 3.6$ Hz). The hydroxy proton was observed at 5.13 ppm while the B-H undulating signal appeared between 4.00 to 0.90 ppm. The ^{13}C NMR spectrum exhibited seven aromatic peaks at 157.09, 132.27, 130.62, 130.08, 128.23, 123.10, and 115.01 ppm with the signal for the carbon vertex of the cage appearing at 85.34 ppm. In the ^{11}B NMR spectrum of **3.15**, four resonances appeared at -1.60, -8.23, -9.71, and -10.52 ppm. The infrared spectrum of **3.15** contained a hydroxy stretch at 3574 cm^{-1} and the expected B-H stretch centered at 2599 cm^{-1} . The aromatic C=C stretch modes were present at 1612 and 1515 cm^{-1} .

Using electron impact TOF MS, the molecular ion peak was found to be 312.2 m/z, with the characteristic isotope distribution, which is consistent with **3.15**.

Compound **3.15** was subsequently degraded with ten equivalents of TBAF, double the amount used in comparison to the deboronation of **3.14**, to generate the respective *nido*-carborane, **3.11** (Scheme 3.6). The presence of the hydroxyl substituent along with the increased hydrophilic character of the *nido*-carborane relative to **3.15** necessitated the use of more polar solvent systems. The target, **3.11**, was detected on TLC (1:10 methanol/ dichloromethane) with an R_f value of 0.30, with no residual starting material observed. The product was isolated with silica gel chromatography (5% methanol/dichloromethane) as a colourless solid in 52% yield.



Scheme 3.6: Deboronation of compound **3.15** to generate compound **3.11**.

As seen with the deboronation of the methylated analogue **3.10**, the production of the *nido*-carborane **3.11** resulted in a general upfield shift of all signals in the ^1H NMR spectrum relative to the starting material **3.15**. For example two doublets were observed at 6.94 ppm ($J = 3.2$ Hz) and 6.14 ppm ($J = 4.0$ Hz) with a multiplet at 6.73 ppm. The ^{13}C NMR spectrum of compound **3.11** also exhibited the upfield shift relative to the starting material with all eight of the aromatic carbon signals being observed at 155.47, 143.78, 134.86, 133.88, 133.00, 127.30, 125.84, and 114.11

ppm. There were six signals observed in the ^{11}B NMR spectrum at -7.18, -12.95, -15.72, -17.73, -32.23, and -34.52 ppm (Figure 3.9).

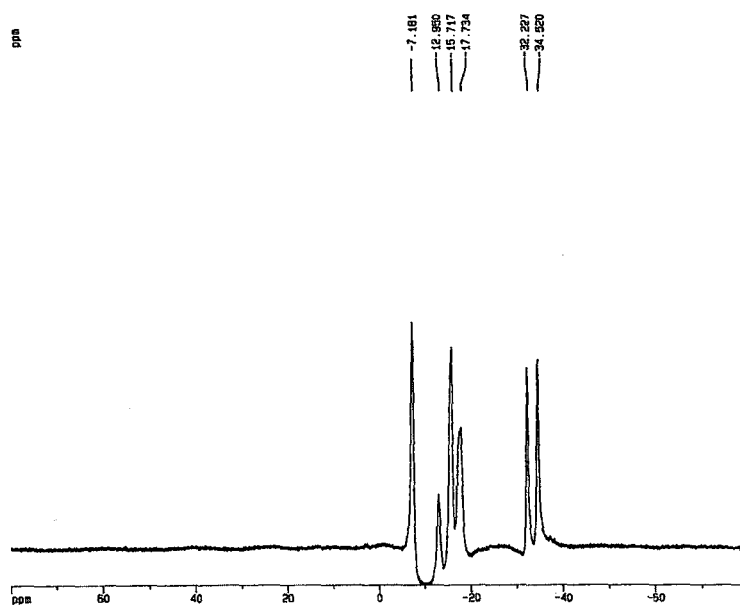


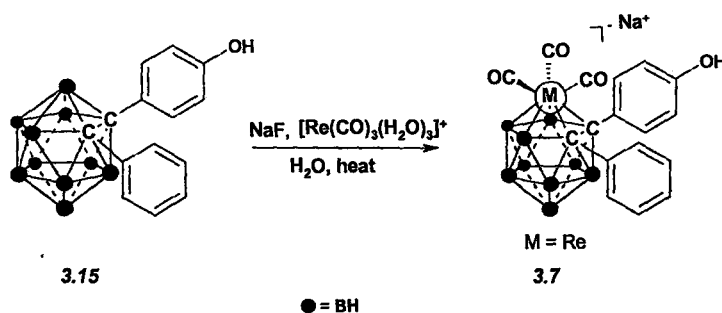
Figure 3.9: ^{11}B NMR (CD_3OD , 500 MHz), for *nido*-carborane **3.11**.

Fourier transformed infrared spectroscopy (FTIR) of *nido*-carborane **3.11** exhibited the hydroxyl O-H stretch at 3584 cm^{-1} , the B-H stretch of the cage at 2545 cm^{-1} , and the C=C aromatic stretches at 1610 , 1512 , and 1481 cm^{-1} . The aliphatic stretches of the counter ion were present at 2969 , 2880 , and 2840 cm^{-1} . The electrospray mass spectrum of **3.11** showed a molecular ion peak in the negative ion mode with a mass to charge ratio of 302.1. The positive mode displayed a peak at 242.1 m/z corresponding to the tetrabutylammonium cation.

In light of the advances made in preparation of Re-metallocarboranes using fluoride at the time of synthesis, and in attempts to avoid deprotonating the phenol group, the first attempt to prepare **3.7** was by reaction of compound **3.11** with 1.0

equivalents of **2.22a** in aqueous 0.1 M NaF. This reaction produced poor yields of the desired product, even when reaction durations were extended in excess of a week.

At that time, our group had discovered that the fluoride method could be used to prepare Re-complexes directly from the corresponding *closo*-carboranes. The reaction was carried out over 2 days using one equivalent of **3.15** and 2 equivalents of **2.22a** in 0.5 M aqueous sodium fluoride at oil bath temperatures of 150 °C (Scheme 3.7). Following the reaction by HPLC analysis showed complete consumption of the ligand **3.15** with the target compound being the major product. The TLC of the crude reaction mixture (1:5 methanol/chloroform) possessed only two spots that absorbed UV light but only one turned black when sprayed with the acidic PdCl₂ solution. Compound **3.7** was purified for with silica gel chromatography using an eluent of 10% methanol in chloroform. The complex was obtained as a yellow oil in 52 % yield.



Scheme 3.7: Preparation of complex **3.7**.

The ¹H NMR spectrum for **3.7** presents a complex series of signals in the aromatic region (Figure 3.10). COSY experiments (Figure 3.11a), along with HSQC and HMBC experiments, allowed for the assignment of two sets of aromatic signals for each ring system. This indicates that the steric bulk of the two phenyl rings compounded with the added bulk of the tripodal carbonyl system results in at least

two conformations relative to the pentagonal face binding the metal center (**Figure 3.11b**) (*vide infra*).^{8,9}

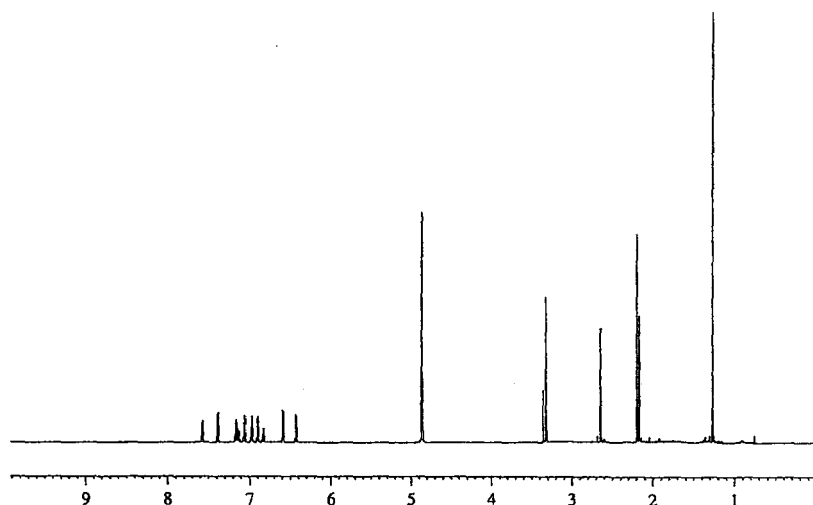


Figure 3.10: ^1H NMR spectrum (600 MHz, in CD_3OD), of sodium 1-(4-hydroxyphenyl)-2-phenyl-3,3,3-tricarbonyl-3- η^5 -Re-1,2-dicarbocloso-dodecaborate (**3.7**).

There are a number of possible orientations of the phenyl rings in the diaryl carboranes in solution which are feasible. Welch *et al.* showed from orbital overlap perspective that the most favourable conformation of the aryl rings is parallel to the binding face of the carborane.⁹ In diaryl carboranes interaction between the rings constitutes an energetically unfavourable conformation. As such, the rings lie at θ values from 5–40° where θ is defined as angle between the plane made by the ring and the plane defined by the two carbon vertices and the substituent bond. The rings can be rotated in a conrotatory or disrotatory manner.

For the purpose of the initial NMR assignments the conformer (and its atropomer) in **Figure 3.11b** was considered as the most likely structure. It should also be noted that upon degradation of compound **3.11**, two enantiomers are formed

(Figure 3.12). This is the result of the fact that the B3/B6 boron atoms are both equally reactive and accessible towards degradation. If atropisomers are present in solution then it is possible that the product exists as the two diastereomers, which may be observable in the ^1H or ^{13}C NMR spectra.

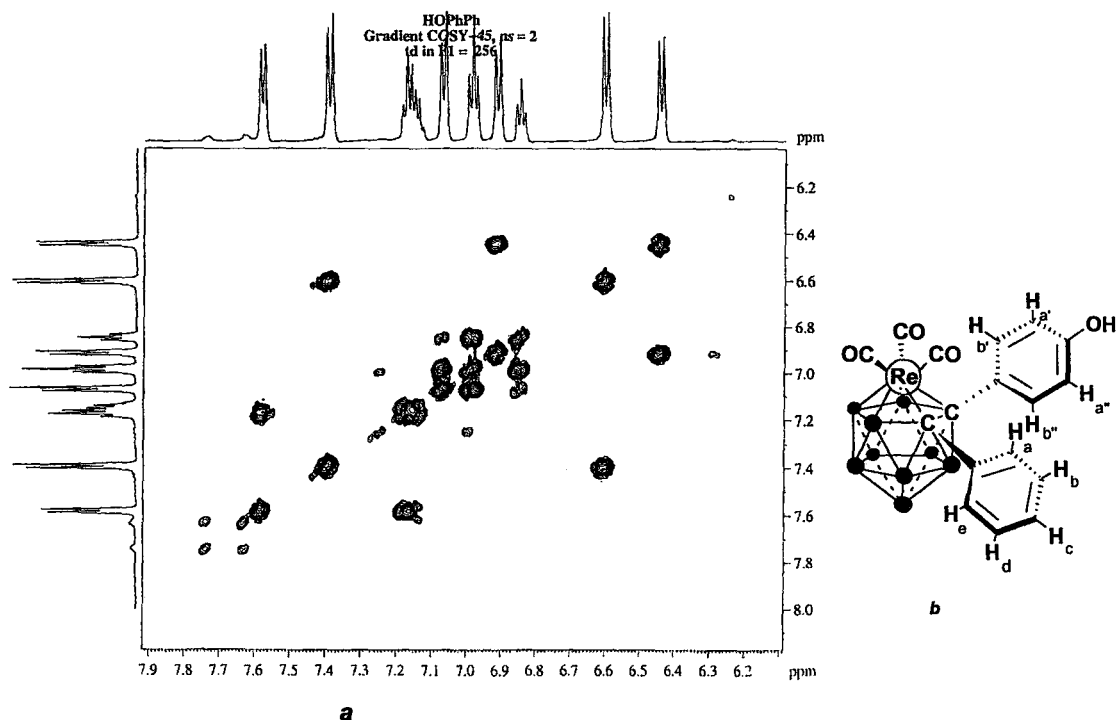


Figure 3.11: a) ^1H - ^1H COSY spectrum (600 MHz, in CD_3OD), of the aromatic region of (3.7). b) One atropisomer of 3.7.

There are four signals associated with the phenol ring which indicates that all protons are magnetically non-equivalent. The doublets associated with $\text{H}_a/\text{H}_{a'}$ appear at 7.90 and 6.91 ppm which are coupled to $\text{H}_b/\text{H}_{b'}$ at 6.59 and 6.43 ppm. There are five signals associated with the unsubstituted ring indicating that all five hydrogen atoms exist in unique environments. The protons of the phenyl substituent appear as follows: a doublet at 7.58 ppm, a multiplet from 7.18 to 7.12 ppm, a doublet at 7.07 ppm, a triplet at 6.99 ppm and a doublet at 6.83 ppm.

The presence of two atropisomers was apparent in the ^{13}C NMR spectrum of **3.7**, which contained 16 signals attributed to the four ring systems (**Figure 3.12**). The aromatic signals appeared at 156.85, 154.73, 149.24, 144.42, 140.88, 135.56, 132.36, 129.71, 128.20, 127.81, 127.22, 126.58, 125.71, 124.88, 114.57, and 114.07 ppm. Of particular significance was the observation of four carborane carbon signals, which were identified by HMBC experiments at 58.54, 58.38, 57.11, and 56.85 ppm. The ^{11}B NMR spectrum contained 6 signals at -9.04, -1.61, -15.80, -19.57, -20.46, and -21.93 ppm.

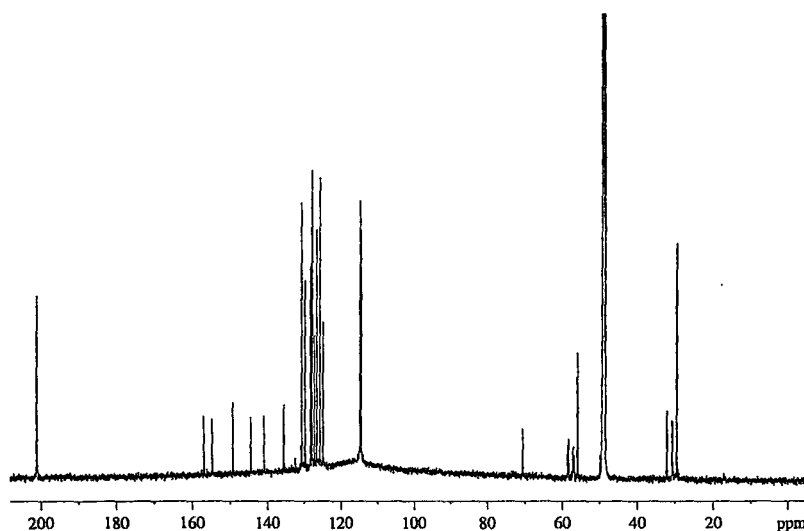


Figure 3.12: ^{13}C NMR spectrum (600 MHz, in CD_3OD), of sodium 1-(4-hydroxyphenyl)-2-phenyl-3,3,3-tricarbonyl-3- η^5 -Re-1,2-dicarba-closo-dodecaborate, (**3.7**).

The infrared spectrum of **3.7** contained a hydroxyl stretch at 3440 cm^{-1} , the B-H stretch at 2557 cm^{-1} , the two carbonyl stretches at 2001 and 1900 cm^{-1} , and the aromatic C=C stretches at 1615 and 1513 cm^{-1} (**Figure 3.13**). Complex **3.7** had an m/z value of 570.2 by electrospray mass spectroscopy, with the same isotopic distributions predicted by simulation.

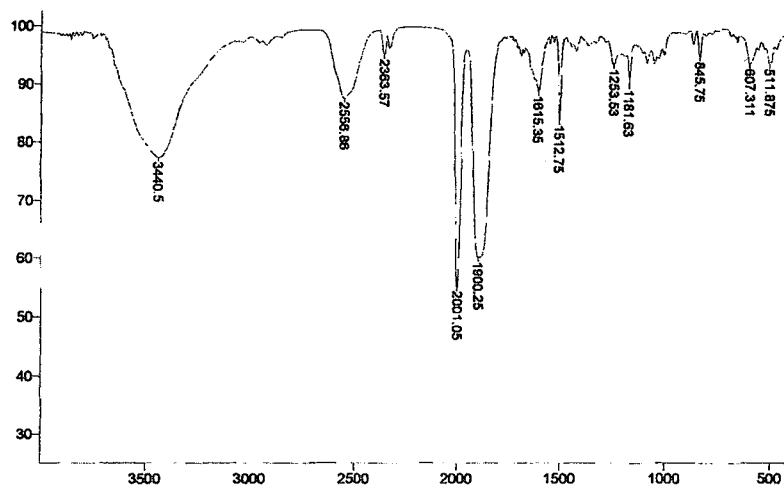
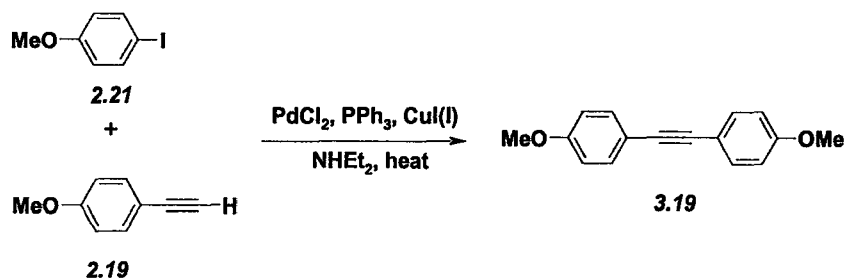


Figure 3.13: The FTIR (in KBr) of Re-metallocarborane 3.7.

3.7 Synthesis of 1,2-Bis(4-Hydroxyphenyl)-Re-Metallocarborane (3.8)

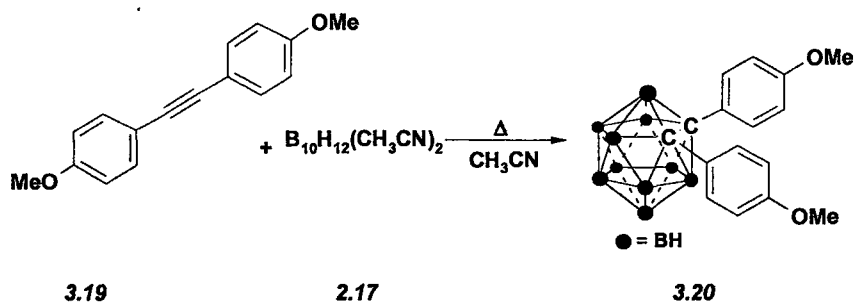
The 1,2-bis(4-hydroxyphenyl)-*closo*-carborane (3.16) was prepared by Endo *et al.* but no characterization data was provided.¹ To prepare 3.16, the synthetic approach reported in the literature was employed using the diaryl substituted alkyne, 1,2-bis(4-methoxyphenyl) acetylene, 3.19 (Scheme 3.8). The preparation of compound 3.19 took advantage of a Sonogashira coupling strategy, which called for equimolar amounts of *para*-iodoanisole (2.21) and *para*-ethynylanisole (2.19) in diethylamine with catalytic amounts of triphenylphosphine, palladium chloride and copper (I) iodide. The reaction was heated to reflux over night producing the target, which was purified using silica gel chromatography. Compound 3.19 was isolated as a white solid in 52% yield.



Scheme 3.8: Preparation of diarylalkyne 3.19.

In the aromatic region of the ^1H NMR spectrum of **3.19** a pair of doublets at 7.46 and 6.87 ppm ($J = 4.4$ Hz) were detected, while the methoxy singlet was observed at 3.82 ppm. The ^{13}C NMR spectrum contained four aromatic signals due to the symmetry of the compound at 159.34, 132.84, 115.65, and 113.92 ppm. The substituted acetylene carbon atom was observed at 87.91 ppm while the methoxy resonance was apparent at 55.25 ppm. Analysis of the IR spectrum for **3.19** found the carbon-carbon triple bond stretch at 2283 cm^{-1} with aromatic $\text{C}=\text{C}$ stretches at 1610 and 1519 cm^{-1} . The molecular ion peak in the electron impact mass spectrum was found to be 238.1 m/z .

Compound **3.20** was generated by heating a 1:1 mole ratio of **2.17** and **3.19** in acetonitrile (Scheme 3.9). The reaction mixture was a dark red solution that upon concentration generated an orange-red residue. The target was visualized on TLC, $R_f = 0.20$ (3% ethyl acetate/ hexanes), using palladium chloride spray and UV light (254 nm). Unwanted by-products were removed by precipitation in 30% ethyl acetate/hexanes. The final product, **3.20** was obtained via silica gel chromatography with a mobile phase of 5% ethyl acetate in hexanes, as a white solid in 8% yield.



Scheme 3.9: Preparation of 1,2-bis(4-methoxyphenyl)-1,2-dicarba-closo-dodecaborane (**3.20**).

The FTIR spectrum of **3.20** contained aliphatic C-H stretches at 3012, 2966, 2940, and 2843 cm^{-1} , with the BH stretch occurring at 2597 cm^{-1} . Aromatic C=C stretches were observed at 1609 and 1515 cm^{-1} . The electron impact mass spectrum confirmed the target mass at an m/z value of 356.3 possessing the expected $^{11}\text{B}/^{10}\text{B}$ isotopic distribution.

The ^1H NMR spectrum of **3.20** showed a pair of doublets at 7.34 and 6.64 ppm ($J = 4.5$ Hz), and a singlet at 3.72 ppm associated with the methoxy group. In the ^{13}C NMR spectrum, the aromatic signals were observed at 160.74, 132.08, 123.10, and 113.45 ppm. The carbon vertex signals occurred at 85.90 ppm while the methoxy signal was at 55.24 ppm. The ^{11}B NMR spectrum displayed the expected number of signals for a homo-disubstituted *closo*-carborane at -2.06, -8.40, and -10.03 ppm (Figure 3.14).

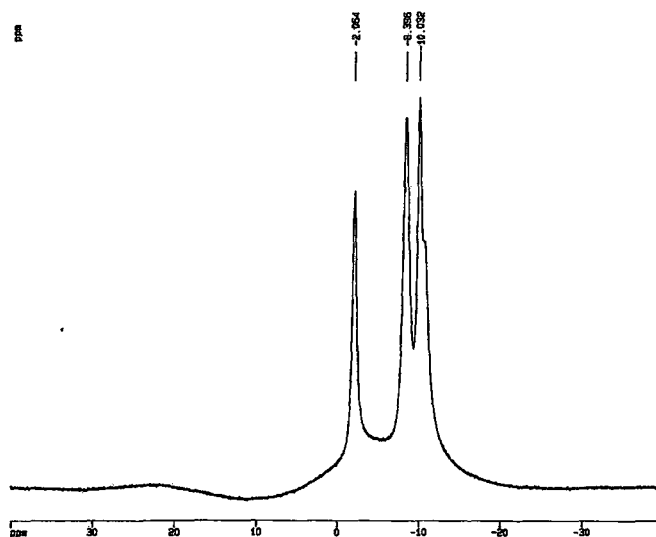
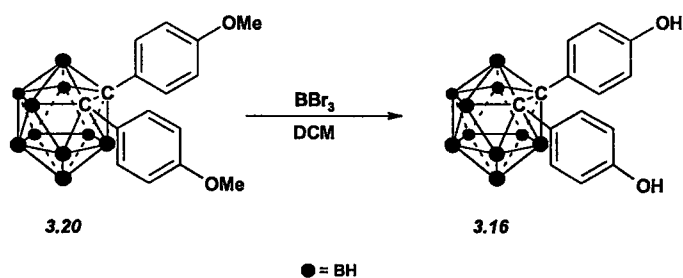


Figure 3.14: $^{11}\text{B}\{^1\text{H}\}$ NMR (500 MHz in CDCl_3) of compound **3.20**.

Preparation of the bis-hydroxyphenyl *o*-carborane, **3.16**, involved the reaction of one equivalent of **3.20** with 10 equivalents of boron tribromide, with analogy to the methods used to synthesize **3.15** (Scheme 3.10). The reaction mixture was allowed to

evaporate under a stream of nitrogen gas yielding an orange-brown solid. The addition of methanol at 0 °C was required to work up the reaction. TLC of the mixture produced one component which was both palladium active and which showed UV absorbance, having an R_f value lower than the starting material. Compound **3.16** was obtained by silica gel chromatography using 5% ethyl acetate in hexanes as the eluent. The product, **3.16**, was isolated as an off white-solid in 89 % yield.



Scheme 3.10: Demethylation of compound **3.20**.

The ^1H NMR spectrum for compound **3.16** contained two doublets in the aromatic region appearing at 7.13 and 6.38 ppm ($J = 3.4$ Hz). In the ^{13}C NMR spectrum there were four aromatic signals at 160.59, 133.49, 122.93, and 115.90 ppm (**Figure 3.15**). The carborane cage carbon signals appeared at 88.20 ppm. The ^{11}B NMR spectrum for **3.16** contained three signals at -2.52, -8.54, and -10.46 ppm. These results indicate that the phenyl rings adopt multiple conformations that are not individually observable by NMR.

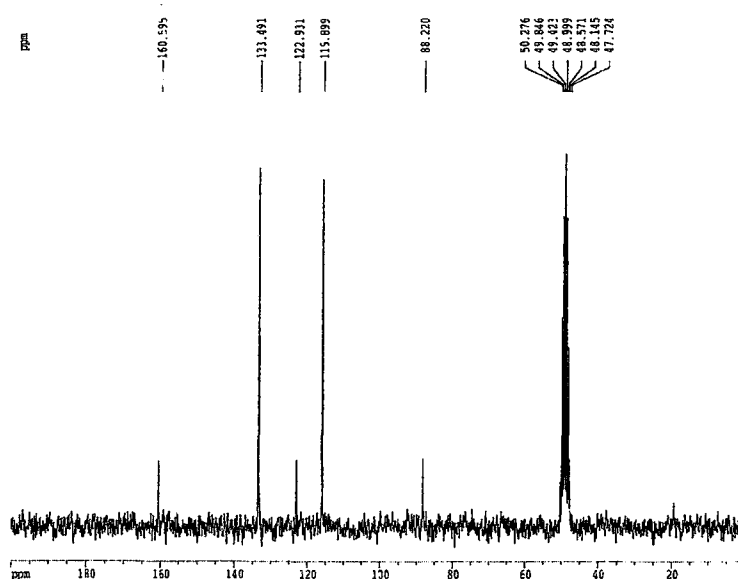
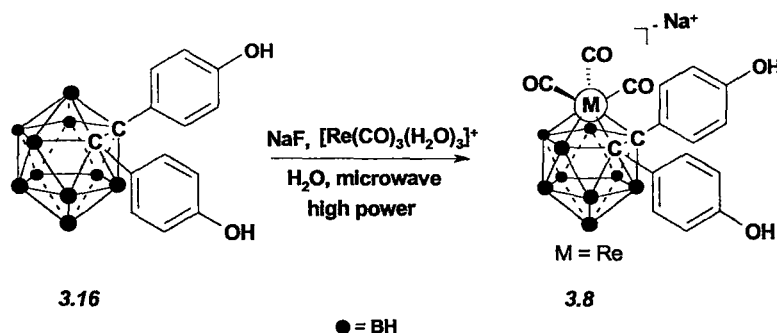


Figure 3.15: $^{13}\text{C} \{^1\text{H}\}$ NMR (200 MHz, in CD_3OD) of 1,2-bis(4-hydroxyphenyl)-1,2-dicarbido-closo-dodecaborane, (3.16).

Infrared analysis of compound 3.16 contained an alcohol stretch at 3340 cm^{-1} , a BH stretch at 2602 cm^{-1} and aromatic C=C stretches at 1613 , 1599 , and 1515 cm^{-1} . The time of flight electron impact mass spectrum contained the target mass to charge value of 328.2 with the expected boron isotope distribution.

The rhenium tricarbonyl carborane complex 3.8 was prepared directly from the *closo*-carborane 3.16 using microwave heating. Three equivalents of 2.22a in 0.5 M aqueous sodium fluoride solution and one equivalent of 3.16 were microwaved in the Parr bomb for 2 minutes (Scheme 3.11). After cooling, a small sample was analyzed by HPLC, which showed that there was only one major compound in the crude reaction mixture, which had a significantly different retention time than the *nido*-ligand (3.12). TLC analysis (20% methanol/chloroform) revealed two UV active components but only one showed palladium activity thus facilitating the identification of the metallocarboranes. The only other products were rhenium clusters.

The crude reaction mixture was acidified with 10 M HCl then diluted with acetonitrile. This mixture was cooled to $-10\text{ }^{\circ}\text{C}$ until a biphasic mixture was apparent. The top layer was removed by pipet and concentrated under reduced pressures yielding a dark brown residue. The target compound was isolated as a dark brown oil (10% yield) using multiple silica gel columns and an eluent of 10% methanol in chloroform.



Scheme 3.11: Preparation of sodium 1,2-bis(4-hydroxyphenyl)-3,3,3-tricarbonyl-3- η^5 -Re-1,2-dicarba-closo-dodecaborate, 3.8.

The aromatic region of ^1H NMR spectrum showed four sets of signals indicating that the two rings likely exist in two complementary conformations, based on 2-D NMR experiments (Figure 3.17), which render the complimentary protons in equivalent magnetic environments (Figure 3.16). The integration data in the ^1H NMR spectrum suggests that both conformers are equally populated.

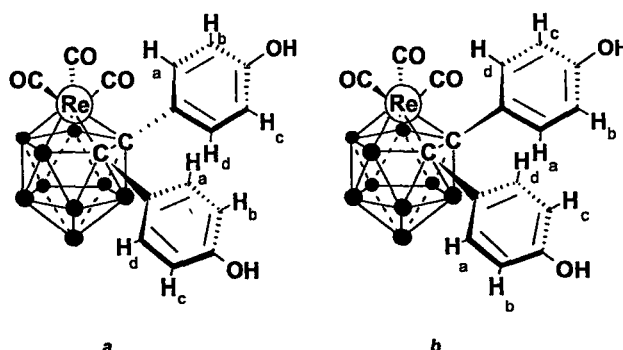


Figure 3.16: Two possible conformations for compound 3.8.

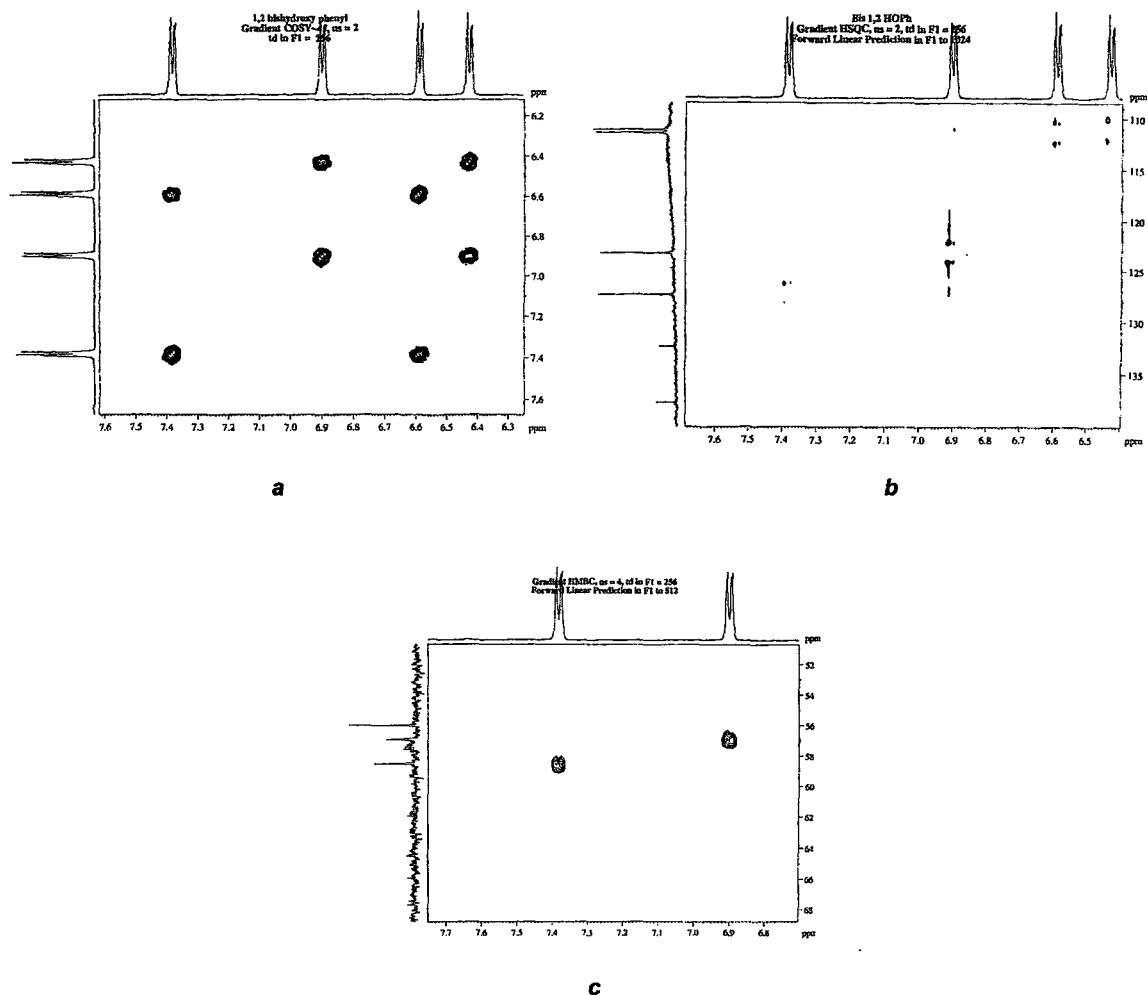


Figure 3.17: Two dimensional NMR data in the aromatic region (600 MHz, in CD_3OD) for complex 3.8. a) ^1H - ^1H COSY, b) ^1H - ^{13}C HSQC, and c) ^1H - ^{13}C HMBC.

In the ^1H NMR spectrum, there are two sets of spin coupled doublets. The resonance furthest downfield occurs at a 7.38 ppm and is coupled to a doublet at 6.59 ppm ($J = 1.5$ Hz). The second aromatic system occurs at 6.90 and 6.43 ppm ($J = 1.4$ Hz). The ^{13}C NMR spectrum show 8 aromatic resonances at 156.87, 154.73, 141.06, 135.71, 129.79, 126.63, 114.85, and 114.57 ppm, while the signal for the CO ligands of the metal were observed at 201.27 ppm. The signals for the carbon vertices of the cage, assigned using the HSQC and HMBC experiments, were observed at 58.55,

56.96, and 56.03 ppm. The ^{11}B NMR spectrum of compound **3.8** revealed a complex display of signals at -5.14, -12.13, -16.00, -20.54, and -22.11 ppm.

In the infrared spectrum the carbonyl stretches were observed at 2001 and 1884 cm^{-1} , while the B-H stretch mode was at 2559 cm^{-1} . The C=C aromatic stretching frequencies were observed at 1612 and 1510 cm^{-1} , while a peak associated with the O-H stretch at 3441 cm^{-1} . The negative ion electrospray mass spectrum showed a peak at 587.3 m/z which is consistent with the mass to charge ratio for **3.8** (Figure 3.18).

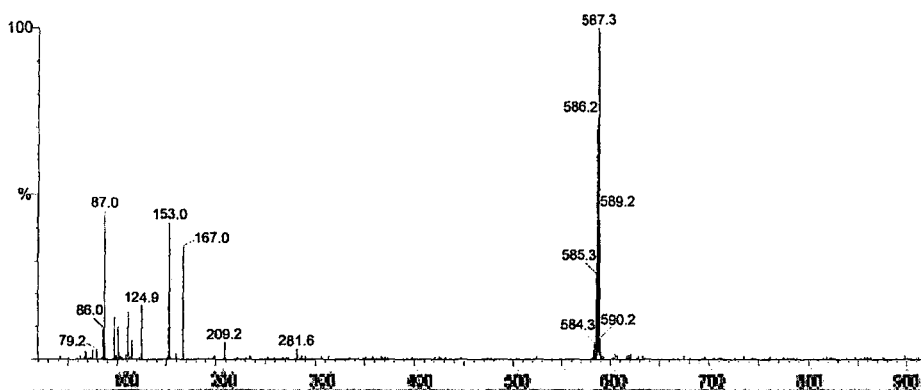
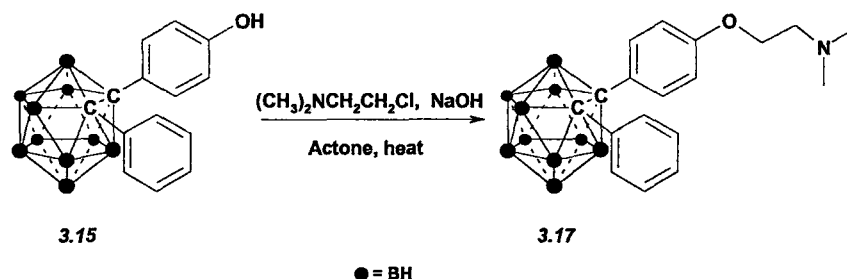


Figure 3.18: The negative ion ESMS of complex **3.8**.

3.8 Synthesis of 1-(4-(N,N-dimethylamino)ethoxyphenyl)-2-Phenyl-Re-Metallocarborane (**3.9**)

The last of the disubstituted carborane metal complexes **3.9** to be prepared was based on the carborane derivative prepared by Endo and coworkers,¹ which showed the highest receptor binding affinity for the ER. To prepare **3.9** it was first necessary to alkylate the *closo*-carborane **3.15** with the corresponding dimethylamino appendage to generate **3.17** (Scheme 3.12). This was accomplished with use of equimolar amounts of **3.15** and the hydrochloric salt of N,N-dimethylaminoethyl

chloride (3.22), in acetone with ten equivalents of sodium hydroxide. After heating to reflux for 3 hours, the mixture was analyzed by TLC (20% methanol/dichloromethane), which showed two carborane containing products. The faster running component was the starting material 3.15. The slower running compound was isolated by silica gel chromatography using a mobile phase of 10% methanol in dichloromethane in 50 % yield.



Scheme 3.12: Preparation of closo-carborane derivative 3.17.

The ^1H NMR spectrum of 3.26 contains a pair of doublets at 7.42 and 6.30 ppm ($J=1.5$ Hz), along with a pair of multiplets at 7.28 and 7.15 ppm (Figure 3.19). Signals arising from the protons on the ethylene spacer appeared as triplets at 3.94 and 2.66 ppm ($J = 2.8$ Hz). The N-methyl singlet appears at 2.29 ppm. In the ^{13}C NMR spectrum, eight aromatic signals are present at 160.00, 155.00, 131.96, 130.59, 130.04, 128.21, 122.96, and 113.97 ppm (Figure 3.20). The aliphatic region contains the two methylene carbons at 65.85 and 58.01 ppm as well as the methyl carbon signals at 45.80 ppm. The carborane carbon vertices were present at 85.64 and 85.34 ppm. Similar to the previous diaryl substituted closo-carboranes, the ^{11}B NMR spectrum consists of 4 peaks at -1.62, -8.28, and -9.76 ppm, which is a consequence of the pseudo symmetry of the molecule.

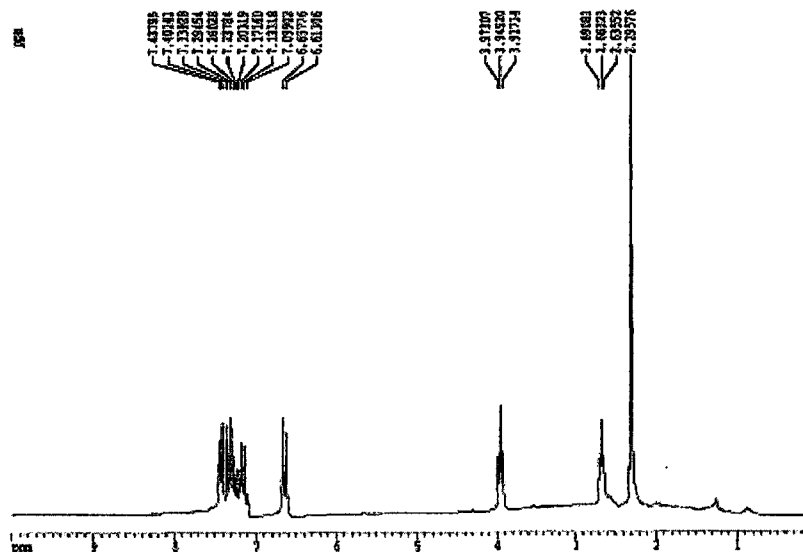


Figure 3.19: ^1H NMR (200 MHz, in CDCl_3) of closo-carborane 3.17.

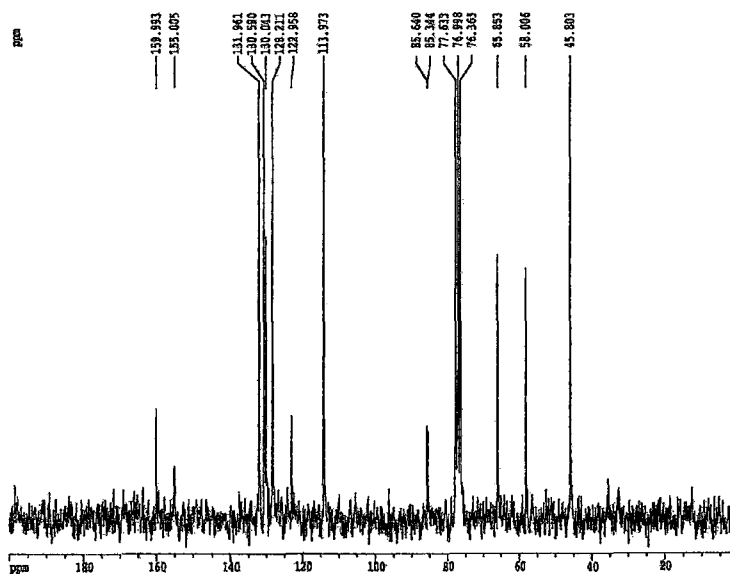
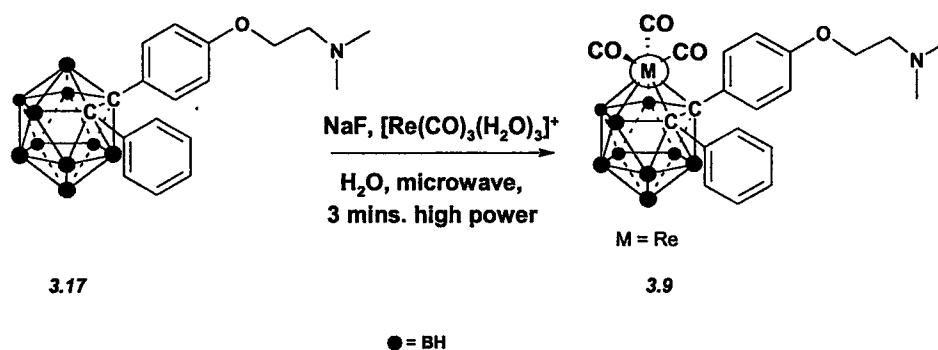


Figure 3.20: The ^{13}C NMR (200 MHz, in CDCl_3) spectrum of 3.17.

In the FTIR spectrum, the B-H stretch is apparent at 2598 cm^{-1} , with the aromatic C=C stretches occurring at 1608 and 1511 cm^{-1} . There is a peak at 3395 cm^{-1} which is attributed to a N-H stretch, as it is believed that amino group may be protonated, and finally the aliphatic peaks occur at 2962 and 2889 cm^{-1} . The target

was observed in the positive mode of the electrospray mass spectrometry at a mass to charge ratio of 384.1.

The preparation of the rhenium complex **3.9** was accomplished via microwave irradiation of the *closo*-carborane **3.17** with two equivalents of **2.22a** in 0.5 M aqueous sodium fluoride solution (Scheme 3.13). Observation of the reaction progress suggested that only one major carborane species existed in the solution. The reaction was not acidified but was diluted with acetonitrile. Upon cooling the sample the acetonitrile layer separated and was removed by pipet. TLC of the crude organic layer showed only one component with simultaneous UV and Pd activity. Electrospray mass spectrometry in contrast, showed both complex **3.9** and unlabelled *nido*-carborane (**3.13**) of the respective compound. Fortunately this complex showed retention times on the C-18 column that were adequate for preparative HPLC purification. Employing preparatory HPLC methods **3.9** was isolated in 8 mg (7% yield) as an off-white solid. The low yield of **3.9** is not indicative of the reaction and is likely a consequence insufficient time in the microwave.



Scheme 3.13: Preparation of complex **3.9** using microwave method.

The ^1H NMR spectrum of **3.9**, showed a similar pattern in the aromatic region as seen in comparison to **3.8** (Figure 3.21). There are three sets of doublets at 7.50,

6.78, and 6.64 ppm, and two sets of multiplets at 7.11 and 6.99 ppm. At 4.21 and 3.48 ppm there are two multiplets corresponding to the two methylene spacers in the aliphatic component. At 2.90 ppm there is a large singlet representing the dimethyl protons of the **3.9**. ^{13}C NMR and ^{11}B NMR spectra were unattainable given the small amount of sample available after purification.

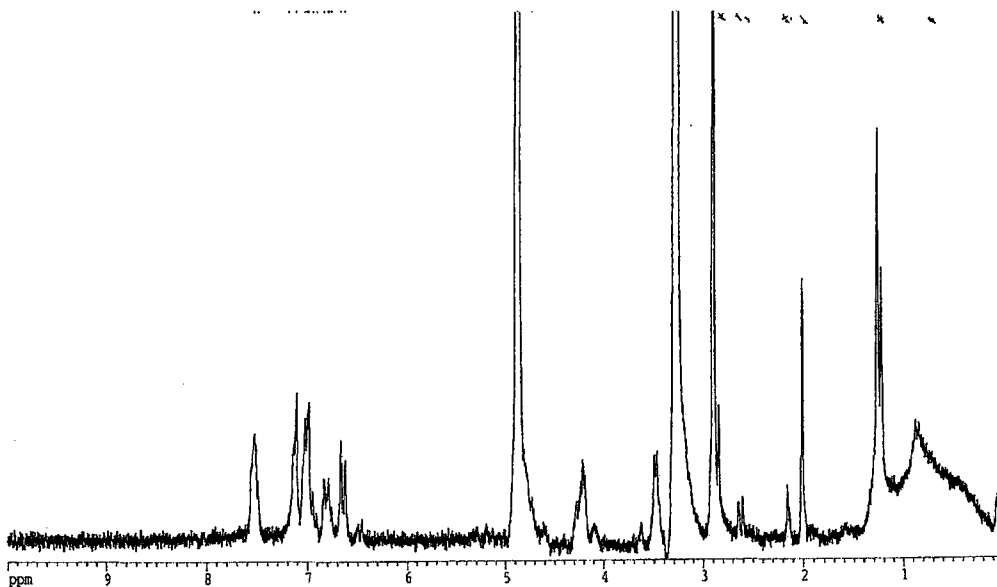


Figure 3.21: ^1H NMR (200 MHz, in CD_3OD) spectrum of complex **3.9**.

The infrared spectrum contained the B-H stretch at 2529 cm^{-1} and the expected carbonyl stretches at 2000 and 1907 cm^{-1} . Stretches attributed to aromatic C=C bonds were observed at 1728 , 1602 , and 1510 cm^{-1} (**Figure 3.22**). The negative mode electrospray mass spectra exhibited a mass to charge ratio of 642.3 which is consistent with the mass of **3.9** (**Figure 3.23**).

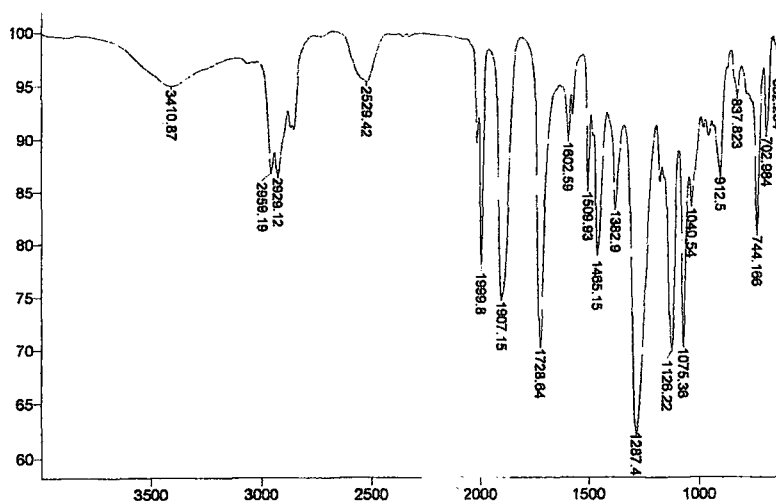


Figure 3.22: The FTIR (in KBr) of complex 3.9.

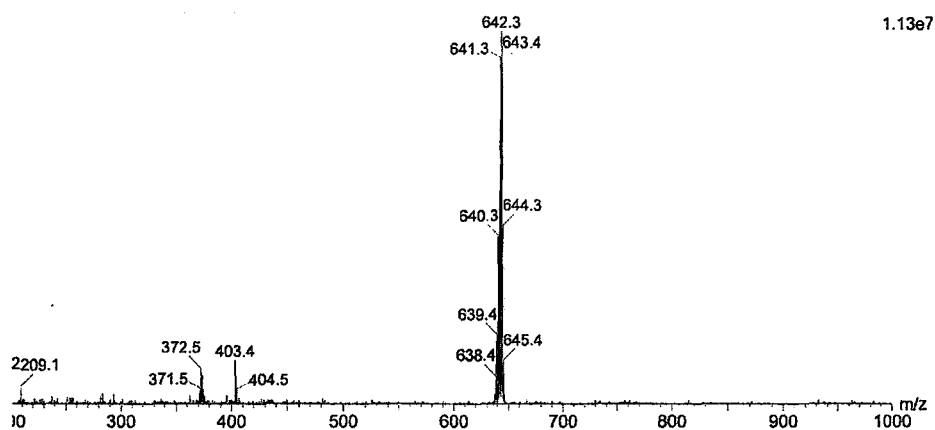


Figure 3.23: The negative ion mode electrospray mass spectrum of complex 3.9.

3.9 Conclusion

The synthesis and characterization of 2 di-substituted *nido*-carboranes and three novel diarylated Re (I) carborane complexes was successfully accomplished. The methods used to prepare the metal complexes have been greatly optimized over previously reported methods. The fourth complex, which contains a dimethylamino

substituent like that found in Tamoxifen, was successfully prepared, albeit in small quantities and must be synthesized on a larger scale for a complete characterization to be conducted.

3.10 Experimental

Synthesis of 1-(4-methoxyphenyl)-2-phenyl-acetylene, 3.18. Diethylamine (20 mL) was added to palladium (II) chloride (42 mg, 0.24 mmol) and triphenylphosphine (180 mg, 0.67 mmol) and the mixture stirred at room temperature for 30 minutes. *Para*-iodoanisole, **2.21** (2.03 g, 8.65 mmol) was added followed by addition of phenylacetylene, **2.18** (1.0 mL, 8.66 mmol) and copper (I) iodide (55 mg, 0.26 mmol), and the mixture was heated to reflux for 36 h. Upon cooling to room temperature, the mixture was diluted with diethyl ether, which in turn was washed consecutively with saturated aqueous solution of NH₄Cl (50 mL) and saturated aqueous solution of NaHCO₃ (50 mL). All organic fractions were combined, dried over MgSO₄, filtered, and the solvent removed by rotary evaporation. The product, a fluffy colorless solid, was isolated by silica gel chromatography (hexane/EtOAc, 95:5), giving pure **3.18** (1.20 g, 67%). MP: 54-56 °C. TLC: *R_f* 0.65 (10% EtOAc in Hex). FTIR (CH₂Cl₂, cm⁻¹): ν 3081, 3038, 3012, 2966, 2941, 2916, 2842, 2218, 1604, 1599, 1571, 1511. ¹H NMR (CDCl₃, 200 MHz): δ 7.55 (m, 2H, CH), 7.50 (d, *J* = 4.3 Hz, 2H, CH), 7.36 (m, 1H, CH), 7.34 (m, 2H, CH), 6.89 (d, 2H, *J* = 4.4), 3.83 (s, 3H, OCH₃). ¹³C{¹H} NMR (CDCl₃, 200 MHz): δ 159.56, 133.99, 131.39, 128.26, 127.88, 123.54, 115.30, 113.94, 89.34, 88.02, 55.21. HRMS (TOF, +): found *m/z* 208.0875.

Synthesis of 1-(4-methoxyphenyl)-2-phenyl-1,2-dicarba-closo-dodecaborane, 3.14. Acetonitrile (50 mL) was added to decaborane, **2.17** (600 mg, 4.92 mmol) and the mixture was stirred at room temperature overnight. 1-(4-Methoxyphenyl)-2-phenyl-acetylene **3.18** (1.13 g, 5.41 mmol) was subsequently added and the mixture heated to reflux for 48 h. Upon cooling to room temperature the solvent was removed by rotary evaporation. The product, a light yellow solid, was isolated by silica gel chromatography (hexane/EtOAc, 97:3), giving pure **3.14** (300 mg, 20%). MP: 81-84 °C. TLC: R_f 0.22 (10% EtOAc in Hex). FTIR (CH_2Cl_2 , cm^{-1}): ν 3013, 2965, 2939, 2915, 2844, 2598, 1725, 1609, 1515, 1464. ^1H NMR (CDCl_3 , 200 MHz): δ 7.44 (d, $J = 3.5$ Hz, 2H, CH), 7.35 (d, $J = 4.5$ Hz, 2H, CH), 7.22 (m, 1H, CH), 7.15 (m, 2H, CH), 6.63 (d, 2H, CH), 3.85-0.80 (br m, BH), 3.71 (s, 3H, OCH_3). $^{13}\text{C}\{^1\text{H}\}$ NMR (CDCl_3 , 200 MHz): δ 160.76, 132.01, 130.60, 130.10, 128.22, 122.87, 113.42, 85.67, 85.36, 55.21. $^{11}\text{B}\{^1\text{H}\}$ NMR (CDCl_3 , 500 MHz): δ -1.66, -8.367, -9.814, -10.663. CIMS (TOF, +): found m/z 326.3.

Synthesis of tetrabutylammonium 7-(4-methoxyphenyl)-8-phenyl-7,8-dicarba-nido-undecaborate, 3.10. Tetrahydrofuran (20 mL) was added to 1-(4-methoxyphenyl)-2-phenyl-1,2-dicarba-closo-dodecaborane **3.14** (70 mg, 0.214 mmol) and tetrabutylammonium fluoride hydrate (281 mg, 1.07 mmol). The mixture was heated to reflux overnight and then the solvent removed by rotary evaporation. The product was isolated by silica gel chromatography (hexane/ CH_2Cl_2 , 5:95), giving a pure colorless solid **3.10** (102 mg, 85%). MP: 142-144 °C. TLC: R_f 0.20 (100% dichloromethane). FTIR (CH_2Cl_2 , cm^{-1}): ν 3056, 2967, 2880, 2526, 1607, 1511. ^1H NMR (CDCl_3 , 200 MHz): δ 7.12 (d, $J = 1.4$ Hz, 2H, CH), 7.04 (d, $J = 1.7$ Hz, 2H,

CH), 6.87 (m, 2H, CH), 6.83 (m, 1H, CH), 6.41 (d, 2H, CH), 3.60 (s, 3H, OCH₃), 3.04 (t, $J = 1.7$ Hz, 2H, NCH₂CH₂CH₂CH₃), 1.51 (m, 2H, NCH₂CH₂CH₂CH₃), 1.36 (m, 2H, NCH₂CH₂CH₂CH₃), 0.96 (t, $J = 1.5$ Hz, 3H, NCH₂CH₂CH₂CH₃). ¹³C{¹H} NMR (CDCl₃, 500 MHz): δ 157.27, 142.06, 134.36, 132.74, 131.87, 126.65, 125.21, 112.06, 59.02, 55.13, 24.18, 19.76, 13.73. ¹¹B{¹H} NMR (CDCl₃, 500 MHz): δ -7.60, -13.55, -16.16, -18.04, -32.72, -35.05. ESMS (- ion): found m/z 315.2.

Synthesis of tetrabutylammonium 1-(4-methoxyphenyl)-2-phenyl-1-closo-3,3,3-(CO)₃-3- η^5 -1,2-ReC₂B₉H₉, 3.6. Tetrabutylammonium 7-(4-methoxyphenyl)-8-phenyl-7,8-dicarba-*nido*-undecaborate, **3.10** (50 mg, 0.09 mmol) was dissolved in tetrahydrofuran (10 mL) and cooled to -30 °C. *n*-Butyllithium (0.06 mL, 0.14 mmol) was then added dropwise and the reaction stirred at -30 °C for 20 minutes. The mixture was warmed to room temperature for 5 minutes followed by the addition of bis(tetraethylammonium)-[tricarboxyltribromorhenate(I)] **2.22** (107 mg, 0.14 mmol). The mixture was heated to reflux overnight. Upon cooling to room temperature, the mixture was diluted with dichloromethane (20 mL), filtered, and the solvent was removed by rotary evaporation. The product was isolated by silica gel chromatography (hexane/CH₂Cl₂, 5:95), giving pure **3.6** (30 mg, 40%), as a lightly yellow oil: TLC: R_f 0.20 (100% dichloromethane). FTIR (CH₂Cl₂, cm⁻¹): ν 3054, 2969, 2940, 2880, 2560, 2001, 1903, 1609, 1512, 1495. ¹H NMR (CDCl₃, 200 MHz): δ 7.76 (m, 2H, CH), 7.55 (d, $J = 4.3$ Hz, 2H, CH), 7.15 (m, 2H, CH), 7.03 (m, 2H, CH) 6.88 (m, 2H, CH), 6.86 (m, 1H, CH), 6.71 (d, $J = 4.4$ Hz, 2H, CH), 6.58 (d, $J = 4.5$ Hz, 2H, CH), 3.76 (s, 3H, OCH₃), 3.71 (s, 3H, OCH₃), 3.09 (t, $J = 4.3$ Hz, 2H, NCH₂CH₂CH₂CH₃), 1.53 (m, 2H, NCH₂CH₂CH₂CH₃), 1.33 (m, 2H,

NCH₂CH₂CH₂CH₃), 1.02 (t, $J = 3.5$ Hz, 3H, NCH₂CH₂CH₂CH₃). ¹³C{¹H} NMR (CDCl₃, 200 MHz): δ 200.12, 129.74, 128.75, 127.51, 126.5, 127.12, 125.40, 124.54, 124.12 112.71, 112.55, 59.00, 55.26, 23.96, 19.71, 13.65. ¹¹B{¹H} NMR (CDCl₃, 500 MHz): δ -7.04, -18.41. ESMS (- ion): found m/z 585.2. HRMS found m/z 585.1891.

Synthesis of 1,2-bis(4-methoxyphenyl)-acetylene, 3.19. Diethylamine (20 mL) was added to palladium (II) chloride (21 mg, 0.13 mmol) and triphenylphosphine (80 mg, 0.30 mmol) and the mixture stirred at room temperature for 30 minutes. *Para*-iodoanisole, **2.21** (980 mg, 4.18 mmol) was added followed by addition of 4-ethynylanisole, **2.19** (0.37 mL, 4.18 mmol) and copper (I) iodide (55 mg, 0.26 mmol). The mixture was heated to reflux for 36 h. Upon cooling to room temperature, the mixture was diluted with diethyl ether, which in turn was washed consecutively with saturated aqueous solution of NH₄Cl (50 mL) and saturated aqueous solution of NaHCO₃ (50 mL). All organic fractions were combined, dried over MgSO₄, filtered, and the solvent removed by rotary evaporation. The product, a fluffy colourless solid, was isolated by silica gel chromatography (hexane/EtOAc, 95:5), giving pure **3.19** (520 mg, 152%). MP: 144-146 °C (Lit. 145-147 °C). TLC: R_f 0.50 (10% EtOAc in Hex). FTIR (CH₂Cl₂, cm⁻¹): ν 3009, 2965, 2915, 2841, 2537, 2047, 1610, 1519. ¹H NMR (CDCl₃, 200 MHz): δ 7.46 (d, $J = 4.4$ Hz, 2H, CH), 6.87 (d, 2H, CH), 3.82 (s, 3H, OCH₃). ¹³C{¹H} NMR (CDCl₃, 200 MHz): δ 159.34, 132.84, 115.65, 113.92, 87.91, 55.25. EIMS (TOF, +): found m/z 238.1.

Synthesis of 1,2-bis(4-methoxyphenyl)-1,2-dicarbocloso-dodecaborane, 3.20. Acetonitrile (30 mL) was added to decaborane, **2.17** (300 mg, 2.46 mmol) and the mixture stirred at room temperature overnight. 1,2-Bis(4-methoxyphenyl)-

acetylene **3.19** (250 mg, 1.05 mmol) was subsequently added and the mixture heated to reflux for 48 h. Upon cooling to room temperature, the solvent was removed by rotary evaporation. The product, a light yellow solid, was isolated by first precipitating out the hydrophilic byproducts in 20% hexanes/EtOAc, followed by silica gel chromatography (hexane/EtOAc, 97:3), giving pure **3.20** (25 mg, 8%). MP: 141-143 °C. TLC: R_f 0.20 (10% EtOAc in hexanes). FTIR (CH_2Cl_2 , cm^{-1}): ν 3055, 2964, 2939, 2915, 2843, 2597, 1726, 1609, 1515, 1465. ^1H NMR (CDCl_3 , 200 MHz): δ 7.34 (d, $J = 4.5$ Hz, 2H, CH), 6.64 (d, 2H, CH), 3.72 (s, 3H, OCH_3). $^{13}\text{C}\{^1\text{H}\}$ NMR (CDCl_3 , 200 MHz): δ 160.74, 132.08, 123.10, 113.45, 85.90, 55.24. $^{11}\text{B}\{^1\text{H}\}$ NMR (CDCl_3 , 500 MHz): δ -2.06, -8.40, -10.03. EIMS (TOF, +): found m/z 356.3.

Synthesis of tetrabutylammonium 7,8-bis(4-methoxyphenyl)-7,8-dicarbonyl-undecaborate 3.24. Tetrahydrofuran (40 mL) was added to 1,2-bis(4-methoxyphenyl)-1,2-dicarbonyl-dodecaborane **3.20** (40 mg, 0.112 mmol) and tetrabutylammonium fluoride hydrate (147 mg, 0.56 mmol). The mixture heated to reflux overnight, followed by rotary evaporation of the solvent. The product was isolated by silica gel chromatography (CH_2Cl_2), giving a pure colourless solid **3.24**, (55 mg, 84%). MP: 104-106 °C. TLC: R_f 0.16 (100% dichloromethane). FTIR (CH_2Cl_2 , cm^{-1}): ν 2999, 2969, 2532, 1511. ^1H NMR (CDCl_3 , 200 MHz): δ 7.04 (d, $J = 4.4$ Hz, 2H, CH), 6.43 (d, 2H, CH), 3.62 (s, 3H, OCH_3), 3.05 (t, $J = 3.8$ Hz, 2H, $\text{NCH}_2\text{CH}_2\text{CH}_2\text{CH}_3$), 1.52 (m, 2H, $\text{NCH}_2\text{CH}_2\text{CH}_2\text{CH}_3$), 1.34 (m, 2H, $\text{NCH}_2\text{CH}_2\text{CH}_2\text{CH}_3$), 0.96 (t, $J = 3.6$ Hz, 3H, $\text{NCH}_2\text{CH}_2\text{CH}_2\text{CH}_3$). $^{13}\text{C}\{^1\text{H}\}$ NMR (CDCl_3 , 200 MHz): δ 156.98, 134.31, 132.54, 111.87, 58.76, 54.95, 23.87, 19.59,

13.62. $^{11}\text{B}\{^1\text{H}\}$ NMR (CDCl_3 , 500 MHz): δ -7.215, -16.052, -18.023, -32.827, -35.086. ESMS (- ion): found m/z 346.1.

Synthesis of 1-(4-hydroxyphenyl)-2-phenyl-1,2-dicarba-closo-dodecaborane, 3.15. Dichloromethane (10 mL) was added to 1-(4-methoxyphenyl)-2-phenyl-1,2-dicarba-closo-dodecaborane, **3.14** (0.60 mg, 0.18 mmol). The temperature was reduced to $-30\text{ }^\circ\text{C}$ and borontribromide (0.92 mL, 0.92 mmol) was added dropwise and the mixture stirred at this temperature for 30 minutes. The mixture was then allowed to warm to room temperature and evaporate overnight. The following morning the temperature was reduced to $-10\text{ }^\circ\text{C}$ and tetrahydrofuran (10 mL) was added slowly. The mixture was allowed to warm to room temperature and evaporate overnight. The next morning the temperature was dropped to $0\text{ }^\circ\text{C}$ and methanol (10 mL) was slowly added. This was stirred for 1 hour before allowing to warm to room temperature. The solvent was then removed under reduced pressures and the product was isolated by silica gel column chromatography (1:10 EtOAc/hexane) to yield an off-white solid, **3.15** (50 mg, 89%). MP: $130\text{-}131\text{ }^\circ\text{C}$. TLC: R_f 0.15 (10% ethyl acetate/hexane). FTIR (CH_2Cl_2 , cm^{-1}): ν 3574, 3054, 3000, 2966, 2940, 2642, 2599, 2580, 1612, 1515. ^1H NMR (CDCl_3 , 200 MHz): δ 7.44 (d, $J = 3.6\text{ Hz}$, 2H, CH), 7.31 (d, $J = 3.8\text{ Hz}$, 2H, CH), 7.19(m, 3H, CH), 6.56(d, 2H, CH), 5.13 (s, 1H, OH) 4.00-0.90 (br m, BH). $^{13}\text{C}\{^1\text{H}\}$ NMR (CDCl_3 , 200 MHz): δ 157.09, 132.27, 130.62, 130.08, 128.23, 123.10, 115.01, 85.34. $^{11}\text{B}\{^1\text{H}\}$ NMR (CDCl_3 , 500 MHz): δ -1.60, -8.23, -9.71, -10.52. EIMS (TOF, +): found m/z 312.2.

Synthesis of tetrabutylammonium 7-(4-hydroxyphenyl)-7-phenyl-7,8-dicarba-*nido*-undecaborate, 3.11. Tetrahydrofuran (50 mL) was added to 1-(4-hydroxyphenyl)-2-phenyl-1,2-dicarba-*closo*-dodecaborane, 3.15 (50 mg, 0.16 mmol) and tetrabutylammonium fluoride hydrate (260 mg, 0.8 mmol), whereupon the mixture turned bright orange instantaneously. The mixture was heated to reflux overnight and then the solvent removed by rotary evaporation. The product, a colourless solid, was isolated by silica gel chromatography (1:20 methanol/ CH₂Cl₂), giving pure 3.11 (45 mg, 52%). MP: 92-94 °C. TLC: *R_f* 0.30 (10% methanol/ dichloromethane). FTIR (CH₂Cl₂, cm⁻¹): ν 3584, 3033, 2969, 2880, 2840, 2524, 1610, 1512, 1481. ¹H NMR (CD₃OD, 200 MHz): δ 6.94 (d, *J* = 3.2 Hz, 2H, CH), 6.73 (m, 5H, CH), 6.14(d, *J* = 4.0 Hz, 2H, CH), 3.09 (t, *J* = 4.1 Hz, 2H, NCH₂CH₂CH₂CH₃), 1.51 (m, 2H, NCH₂CH₂CH₂CH₃), 1.30 (m, 2H, NCH₂CH₂CH₂CH₃), 0.90 (t, *J* = 3.6 Hz, 3H, NCH₂CH₂CH₂CH₃). ¹³C{¹H} NMR (CD₃OD, 200 MHz): δ 155.47, 143.78, 134.86, 133.88, 133.00, 127.30, 125.84, 114.11, 59.55, 24.83, 20.72, 14.00. ¹¹B{¹H} NMR (CD₃OD, 500 MHz): δ -7.18, -12.95, -15.72, -17.73, -32.23, -34.52. ESMS (- ion): found *m/z* 302.1.

Synthesis of sodium 1-(4-hydroxyphenyl)-2-phenyl-3,3,3-tricarbonyl-3- η^5 -Re-1,2-dicarba-*closo*-dodecaborate, 3.7. Aqueous sodium fluoride (0.5 M, 5 mL) was added to 3.15 (50 mg, 0.21 mmol) in a 15 mL 2-neck round bottom flask along with 3 equivalents of 2.22a (258 mg, 0.64 mmol) and the mixture heated in an oil bath warmed to 150 °C for two days. After allowing the reaction to cool the sample was acidified with 5 ml of 10 M HCl. The mixture was diluted with acetonitrile (10 mL) and cooled at -10 °C until the organic layer separated. The acetonitrile layer was

removed by pipet and concentrated under reduced pressures. The product (**3.7**), was isolated by silica gel chromatography (5% methanol/chloroform) (70 mg, 52%) as a dark brown oil. TLC: R_f 0.15 (10% methanol/chloroform). FTIR (KBr, cm^{-1}): ν 3440, 2557, 2001, 1900, 1615, 1513. ^1H NMR (CD_3OD , 600 MHz): δ 7.90 (d, $J = 1.5$ Hz, 2H, CH), 7.58 (d, $J = 1.3$ Hz, 2H, CH), 7.07 (d, 2H, CH), 6.91 (d, $J = 1.5$ Hz, 2H, CH), 6.83 (d, 2H, CH), 6.59 (d, 2H, CH), 6.43 (d, 2H, CH), 7.18-7.12 (m, 2H, CH). $^{13}\text{C}\{^1\text{H}\}$ NMR (CD_3OD , 600 MHz): δ 206.01, 156.85, 154.73, 149.24, 144.42, 140.88, 135.56, 132.36, 129.71, 128.20, 127.81, 127.22, 126.58, 125.71, 124.88, 114.57, 114.07, 58.54, 58.38, 57.11, 56.85. $^{11}\text{B}\{^1\text{H}\}$ NMR (CD_3OD , 500 MHz): δ -9.04, -11.61, -15.80, -19.57, -20.46, -21.93. ESMS (- ion): found m/z 570.2. HRMS found m/z 570.1725.

Synthesis of 1,2-bis(4-hydroxyphenyl)-1,2-dicarba-closo-dodecaborane, 3.16. Dichloromethane (10 mL) was added to 1,2-bis(4-methoxyphenyl)-1,2-dicarba-closo-dodecaborane, **3.20** (0.70 mg, 0.17 mmol). The temperature was reduced to -30 °C and borontribromide (1.84 mL, 1.84 mmol) was added dropwise and the mixture stirred at this temperature for 30 minutes. The mixture was then allowed to warm to room temperature and evaporate overnight. The following morning the temperature was reduced to -10 °C and tetrahydrofuran (10 mL) added slowly. This solution was allowed to warm to room temperature and evaporate overnight. The next morning the temperature was reduced to 0 °C and methanol (10 mL) added slowly. This was stirred for 1 hour before allowing to warm to room temperature. The solvent was then removed under reduced pressures and the product isolated by silica gel column chromatography (1:10 EtOAc/hexane) to yield an off white solid, **3.16** (43 mg, 89%). MP.: 120-123 °C. TLC: R_f 0.15 (10% ethyl acetate/hexane).

FTIR (KBr, cm^{-1}): ν 3344, 2602, 1613, 1515. ^1H NMR (CDCl_3 , 200 MHz): δ 7.13 (d, $J = 3.6$ Hz, 4H, CH), 6.38 (d, 2H, CH), 4.00-0.90 (br m, BH). $^{13}\text{C}\{^1\text{H}\}$ NMR (CDCl_3 , 200 MHz): δ 160.59, 133.49, 122.93, 115.90, 88.20. $^{11}\text{B}\{^1\text{H}\}$ NMR (CDCl_3 , 500 MHz): δ -2.52, -8.54, -10.46. MSEI (TOF, +): found m/z 328.2.

Synthesis of sodium 1,2-bis(4-hydroxyphenyl)-3,3,3-tricarbonyl-3- η^5 -Re-1,2-dicarbocloso-dodecaborate, 3.8. Aqueous sodium fluoride (0.5 M, 10 mL) was added to **3.16** (50 mg, 0.17 mmol) in a Parr Microwave Digestion Bomb (Model # 4781) along with 3 equivalents of **2.22a** (250 mg, 0.58 mmol) and the mixture irradiated in a conventional microwave for two 1-minute intervals at high power. After allowing the reaction to cool the sample was acidified with 5 ml of 10 M HCl. The mixture was diluted with acetonitrile (10 mL) and cooled at -10 °C until the organic layer separated. The acetonitrile layer was removed by pipet and concentrated under reduced pressures. The product (**3.8**) was isolated by silica gel chromatography (5% methanol/chloroform) as a dark brown oil (15 mg, 10%). TLC: R_f 0.15 (10% methanol/chloroform). FTIR (KBr, cm^{-1}): ν 3438, 2559, 2001, 1884, 1612, 1511. ^1H NMR (CD_3OD , 600 MHz): δ 7.38 (d, $J = 1.5$ Hz, 2H, CH), 6.59 (d, 2H, CH), 6.90 (d, $J = 1.4$ Hz, 2H, CH), 6.43 (d, 2H, CH). $^{13}\text{C}\{^1\text{H}\}$ NMR (CD_3OD , 600 MHz): δ 201.27, 156.87, 154.73, 141.06, 135.71, 129.79, 126.63, 114.85, 114.57, 58.55, 56.96, 56.03. $^{11}\text{B}\{^1\text{H}\}$ NMR (CD_3OD , 500 MHz): δ -5.14, -12.13, -16.00, -20.54, -22.11. ESMS (-ion): found m/z 587.3. HRMS found m/z 587.1686.

Synthesis of 1-(4-(N,N-dimethylamino)ethoxyphenyl)-2-phenyl-1,2-dicarbocloso-dodecaborane, 3.17. Acetone (20 mL) was added to 1-(4-

hydroxyphenyl)-2-phenyl-1,2-dicarba-*closo*-dodecaborane, **3.15** (0.75 mg, 0.19 mmol), along with 10 equivalents of sodium hydroxide and one equivalent of dimethylaminoethylchloride hydrochloride salt (**3.22**) and the mixture heated to reflux for 3 hours. The solvent was then removed under reduced pressures and the product (**3.17**) was isolated by silica gel column chromatography (10% methanol/dichloromethane) (45 mg, 50%). as yellow oil. TLC: R_f 0.10 (20% methanol/chloroform). FTIR (KBr, cm^{-1}): ν 3395, 2962, 2889, 2598, 1608, 1511. ^1H NMR (CD_3OD , 200 MHz): δ 7.42 (d, $J = 1.5$ Hz, 2H, CH), 6.30 (d, 2H, CH), 7.28 (m, 3H, CH), 7.15 (m, 2H, CH), 3.94 (t, $J = 2.8$ Hz, 2H, $\text{OCH}_2\text{CH}_2\text{N}$), 2.66 (t, 2H, $\text{OCH}_2\text{CH}_2\text{N}$), 2.29 (s, 6H, $\text{N}(\text{CH}_3)_2$). $^{13}\text{C}\{^1\text{H}\}$ NMR (CD_3OD , 200 MHz): δ 160.00, 155.00, 131.96, 130.59, 130.04, 128.21, 122.96, 113.97, 85.64, 85.34, 65.85, 58.01, 45.80. $^{11}\text{B}\{^1\text{H}\}$ NMR (CD_3OD , 500 MHz): δ -1.62, -8.28, -9.76. ESMS (+ ion): found m/z 384.1.

Synthesis of sodium 1-(4-(N,N-dimethylamino)ethoxyphenyl)-3,3,3-tricarbonyl-3- η^5 -Re-1,2-dicarba-*closo*-dodecaborate, 3.9. Aqueous sodium fluoride (0.5 M, 10 mL) was added to **3.17** (20 mg, 0.15 mmol) in a Parr Microwave Digestion Bomb (Model # 4781) along with 3 equivalents of **2.22a** (155 mg, 0.44 mmol) and the mixture irradiated in a conventional microwave for three 1-minute intervals at high power. After allowing the water to cool (20 min.) the mixture was diluted with acetonitrile (10 mL) and cooled at -10 °C until the organic layer separated. The acetonitrile layer was removed by pipet and concentrated under reduced pressures. The product (**3.9**) was isolated by silica gel chromatography (5% methanol/chloroform) but required semi-preparative HPLC purification to be isolated

as a clear film (8 mg, 7%). TLC: R_f 0.10 (20% methanol/chloroform). FTIR (KBr, cm^{-1}): ν 3411, 2529, 2000, 1907, 1728, 1602, 1510. ^1H NMR (CD_3OD , 200 MHz): δ 7.50 (d, 2H, CH), 6.78 (d, 2H, CH), 6.64 (d, 2H, CH), 7.11 (m, 2H, CH), 6.99 (m, 2H, CH), 4.21 (m, 2H, $\text{OCH}_2\text{CH}_2\text{N}$), 3.48 (m, 2H, $\text{OCH}_2\text{CH}_2\text{N}$), 2.90 (s, 6H, $\text{N}(\text{CH}_3)_2$)
ESMS (- ion): found m/z 642.3.

3.11 References

- ¹ Endo, Y.; Yoshimi, T.; Iijima, T.; Yamakoshi, I.; *Bioorg. Med. Chem. Lett.* **1999**, *9*, 3387.
- ² Mull, E.S.; Sattigeri, V.J.; Rodriguez, A.L.; Katzenellenbogen, J.A.; *Bioorg. Med. Chem.* **2002**, *10*, 1381.
- ³ Katzenellenbogen, J.A.; Muthyalal, R. S.; Sheng, S.; Carlson, K.E.; Katzenellenbogen, B.S.; *J. Med. Chem.* **2003**, *46*, 1589.
- ⁴ Fox, M.A.; MacBride, J.A.H.; Peace, R.J.; Wade, K.; *J. Chem. Soc. Trans.* **1998**, 401.
- ⁵ Ph.D. Thesis, J.F. Valliant, **1997**, McMaster University.
- ⁶ Suarez, A.; Méndez-Rojas, M. A.; Pizzano, A.; *Organomet.* **2002**, *21*, 4611.
- ⁷ Fox, M.A.; MacBride, J.A.; Wade, K.; *Polyhedron.* **1996**, *16*, 2499.
- ⁸ Brain, P.T.; Cowie, J.; Donohoe, D.J.; Hnyk, D.; Rankin, D.W.H.; Reed, D.; Reid, B.D.; Robertson, H.E.; Welch, A.J.; *Inorg. Chem.* **1996**, *35*, 1701.
- ⁹ Robertson, S.; Ellis, D.; McGrath, T.D.; Rosair, G.M.; Welch, A.J.; *Polyhedron.* **2003**, *22*, 1293.

Summary and Future Work

This work utilized three methods to prepare arylated Re-metallocarboranes, specifically two monoaryl Re-carborane complexes and three diaryl Re-carborane complexes. During the course of this work, three target complexes were unobtainable because of difficulties associated with purification. As such, future work should entail preparing these complexes using methods which ensure complete consumption of the starting carborane ligand and the use of a single counter ion.

With Re-carboranes **2.10**, **3.7**, **3.8**, and **3.9** in hand, ER binding studies should be performed to validate the use of metallocarborane as anti-estrogens. These studies should also be done using the *closo*- and *nido*-carborane precursors to compare the impact of the Re(I)CO₃ core on RBA values. For compounds showing high binding affinity, the corresponding ^{99m}Tc complexes should be prepared and biodistribution studies performed.

Another important idea for future work is a detailed low temperature NMR study of the bis-aryl Re-carborane complexes. These compounds could exhibit unique dynamic processes including correlated rotation. Detailed assignments of spectra acquired at various temperatures are therefore needed.

Appendix I Supplementary Data

Chapter 2: Mono-Arylated Carboranes

- Figure 1-A.** ^1H NMR of **2.14**, 200 MHz, in CDCl_3
Figure 1-B. $^{13}\text{C}\{\text{H}\}$ NMR of **2.14**, 200 MHz, in CDCl_3
Figure 1-C. $^{11}\text{B}\{\text{H}\}$ NMR of **2.14**, 500 MHz, in CDCl_3
Figure 1-D. FTIR of **2.14**, in CH_2Cl_2
Figure 1-E. EI-MS of **2.14**
Figure 1-F. Analytical HPLC chromatogram of **2.14**
- Figure 2-A.** ^1H NMR of **2.11**, 200 MHz, in CDCl_3
Figure 2-B. $^{13}\text{C}\{\text{H}\}$ NMR of **2.11**, 200 MHz, in CDCl_3
Figure 2-C. $^{11}\text{B}\{\text{H}\}$ NMR of **2.11**, 500 MHz, in CDCl_3
Figure 2-D. FTIR of **2.11**, in CH_2Cl_2
Figure 2-E. Negative Ion Mode ESI-MS of **2.11**
Figure 2-F. Analytical HPLC chromatogram of **2.11**
- Figure 3-A.** ^1H NMR of **2.8**, 200 MHz, in CDCl_3
Figure 3-B. $^{13}\text{C}\{\text{H}\}$ NMR of **2.8**, 200 MHz, in CDCl_3
Figure 3-C. $^{11}\text{B}\{\text{H}\}$ NMR of **2.8**, 500 MHz, in CDCl_3
Figure 3-D. FTIR of **2.8**, in CH_2Cl_2
Figure 3-E. Negative Ion Mode ESI-MS of **2.8**
Figure 3-F. Analytical HPLC chromatogram of **2.8**
Figure 3-G. X-ray structure and data for **2.8**
- Figure 4-A.** ^1H NMR of **2.15**, 200 MHz, in CDCl_3
Figure 4-B. $^{13}\text{C}\{\text{H}\}$ NMR of **2.15**, 200 MHz, in CDCl_3
Figure 4-C. $^{11}\text{B}\{\text{H}\}$ NMR of **2.15**, 500 MHz, in CDCl_3
Figure 4-D. FTIR of **2.15**, in CH_2Cl_2
Figure 4-E. EI-MS of **2.15**
Figure 4-F. Analytical HPLC chromatogram of **2.15**
- Figure 5-A.** ^1H NMR of **2.12**, 200 MHz, in CDCl_3
Figure 5-B. $^{13}\text{C}\{\text{H}\}$ NMR of **2.12**, 200 MHz, in CDCl_3
Figure 5-C. $^{11}\text{B}\{\text{H}\}$ NMR of **2.12**, 500 MHz, in CDCl_3
Figure 5-D. FTIR of **2.12**, in CH_2Cl_2
Figure 5-E. Negative Ion Mode ESI-MS of **2.12**
Figure 5-F. Analytical HPLC chromatogram of **2.12**
- Figure 7-A.** ^1H NMR of **2.16**, 200 MHz, in CDCl_3
Figure 7-B. $^{13}\text{C}\{\text{H}\}$ NMR of **2.16**, 200 MHz, in CDCl_3
Figure 7-C. $^{11}\text{B}\{\text{H}\}$ NMR of **2.16**, 500 MHz, in CDCl_3
Figure 7-D. FTIR of **2.16**, in CH_2Cl_2
Figure 7-E. EI-MS of **2.16**
Figure 7-F. Analytical HPLC chromatogram of **2.16**

- Figure 8-A. ^1H NMR of **2.13**, 200 MHz, in CDCl_3
- Figure 8-B. $^{13}\text{C}\{\text{H}\}$ NMR of **2.13**, 200 MHz, in CDCl_3
- Figure 8-C. $^{11}\text{B}\{\text{H}\}$ NMR of **2.13**, 200 MHz, in CDCl_3
- Figure 8-D. FTIR of **2.13**, in CH_2Cl_2
- Figure 8-E. Negative Ion Mode ESI-MS of **2.13**
- Figure 8-F. Analytical HPLC chromatogram of **2.13**

- Figure 9-A. ^1H NMR of **2.10**, 600 MHz, in CD_3OD
- Figure 9-B. $^{13}\text{C}\{\text{H}\}$ NMR of **2.10**, 600 MHz, in CD_3OD
- Figure 9-C. $^{11}\text{B}\{\text{H}\}$ NMR of **2.10**, 500 MHz, in CD_3OD
- Figure 9-D. FTIR of **2.10**, in CH_2Cl_2
- Figure 9-E. Negative Ion Mode ESI-MS of **2.10**

Chapter 3: Di-Arylated Carboranes

- Figure 10-A. ^1H NMR of **3.18**, 200 MHz, in CDCl_3
- Figure 10-B. $^{13}\text{C}\{\text{H}\}$ NMR of **3.18**, 200 MHz, in CDCl_3
- Figure 10-C. FTIR of **3.18**, in CH_2Cl_2
- Figure 10-D. EI-MS of **3.18**

- Figure 11-A. ^1H NMR of **3.14**, 200 MHz, in CDCl_3
- Figure 11-B. $^{13}\text{C}\{\text{H}\}$ NMR of **3.14**, 200 MHz, in CDCl_3
- Figure 11-C. $^{11}\text{B}\{\text{H}\}$ NMR of **3.14**, 500 MHz, in CDCl_3
- Figure 11-D. FTIR of **3.14**, in CH_2Cl_2
- Figure 11-E. EI-MS of **3.14**

- Figure 12-A. ^1H NMR of **3.10**, 200 MHz, in CDCl_3
- Figure 12-B. $^{13}\text{C}\{\text{H}\}$ NMR of **3.10**, 200 MHz, in CDCl_3
- Figure 12-C. $^{11}\text{B}\{\text{H}\}$ NMR of **3.10**, 500 MHz, in CDCl_3
- Figure 12-D. FTIR of **3.10**, in CH_2Cl_2
- Figure 12-E. Negative Ion Mode ESI-MS of **3.10**
- Figure 12-F. Analytical HPLC chromatogram of **3.10**

- Figure 13-A. ^1H NMR of **3.6**, 200 MHz, in CDCl_3
- Figure 13-B. $^{13}\text{C}\{\text{H}\}$ NMR of **3.6**, 200 MHz, in CDCl_3
- Figure 13-C. FTIR of **3.6**, in CH_2Cl_2
- Figure 13-D. Negative Ion Mode ESI-MS of **3.6**
- Figure 13-E. Analytical HPLC chromatogram of **3.6**

- Figure 14-A. ^1H NMR of **3.19**, 200 MHz, in CDCl_3
- Figure 14-B. $^{13}\text{C}\{\text{H}\}$ NMR of **3.19**, 200 MHz, in CDCl_3
- Figure 14-C. FTIR of **3.19**, in CH_2Cl_2 .
- Figure 14-D. EI-MS of **3.19**

- Figure 15-A.** ^1H NMR of **3.20**, 200 MHz, in CDCl_3
- Figure 15-B.** $^{13}\text{C}\{\text{H}\}$ NMR of **3.20**, 200 MHz, in CDCl_3
- Figure 15-C.** $^{11}\text{B}\{\text{H}\}$ NMR of **3.20**, 500 MHz, in CDCl_3
- Figure 15-D.** FTIR of **3.20**, in CH_2Cl_2
- Figure 15-E.** EI-MS of **3.20**
- Figure 15-F.** Analytical HPLC chromatogram of **3.20**

- Figure 16-A.** ^1H NMR of **3.15**, 200 MHz, in CDCl_3
- Figure 16-B.** $^{13}\text{C}\{\text{H}\}$ NMR of **3.15**, 200 MHz, in CDCl_3
- Figure 16-C.** $^{11}\text{B}\{\text{H}\}$ NMR of **3.15**, 500 MHz, in CDCl_3
- Figure 16-D.** FTIR of **3.15**, in CH_2Cl_2
- Figure 16-E.** EI-MS of **3.15**
- Figure 16-F.** Analytical HPLC chromatogram of **3.15**

- Figure 17-A.** ^1H NMR of **3.11**, 200 MHz, in CDCl_3
- Figure 17-B.** $^{13}\text{C}\{\text{H}\}$ NMR of **3.11**, 200 MHz, in CDCl_3
- Figure 17-C.** $^{11}\text{B}\{\text{H}\}$ NMR of **3.11**, 500 MHz, in CDCl_3
- Figure 17-D.** FTIR of **3.11**, in CH_2Cl_2
- Figure 17-E.** Negative Ion Mode ESI-MS of **3.11**
- Figure 17-F.** Analytical HPLC chromatogram of **3.11**

- Figure 18-A.** ^1H NMR of **3.7**, 200 MHz, in CD_3OD
- Figure 18-B.** $^{13}\text{C}\{\text{H}\}$ NMR of **3.7**, 200 MHz, in CD_3OD
- Figure 18-C.** $^{11}\text{B}\{\text{H}\}$ NMR of **3.7**, 500 MHz, in CD_3OD
- Figure 18-D.** FTIR of **3.7**, in KBr
- Figure 18-E.** Negative Ion Mode ESI-MS of **3.7**

- Figure 19-A.** ^1H NMR of **3.16**, 200 MHz, in CD_3OD
- Figure 19-B.** $^{13}\text{C}\{\text{H}\}$ NMR of **3.16**, 200 MHz, in CD_3OD
- Figure 19-C.** $^{11}\text{B}\{\text{H}\}$ NMR of **3.16**, 500 MHz, in CD_3OD
- Figure 19-D.** FTIR of **3.16**, in KBr
- Figure 19-E.** EI-MS of **3.16**

- Figure 20-A.** ^1H NMR of **3.8**, 200 MHz, in CD_3OD
- Figure 20-B.** $^{13}\text{C}\{\text{H}\}$ NMR of **3.8**, 200 MHz, in CD_3OD
- Figure 20-C.** $^{11}\text{B}\{\text{H}\}$ NMR of **3.8**, 500 MHz, in CD_3OD
- Figure 20-D.** FTIR of **3.8**, in CH_2Cl_2
- Figure 20-E.** Negative Ion Mode ESI-MS of **3.8**

- Figure 21-A.** ^1H NMR of **3.17**, 200 MHz, in CDCl_3
- Figure 21-B.** $^{13}\text{C}\{\text{H}\}$ NMR of **3.17**, 200 MHz, in CDCl_3
- Figure 21-C.** $^{11}\text{B}\{\text{H}\}$ NMR of **3.17**, 500 MHz, in CDCl_3
- Figure 21-D.** FTIR of **3.17**, in CH_2Cl_2
- Figure 21-E.** Negative Ion Mode ESI-MS of **3.17**

Figure 22-A. ^1H NMR of 3.9, 200 MHz, in CD_3OD

Figure 22-B. FTIR of 3.9, in KBr

Figure 22-C. Negative Ion Mode ESI-MS of 3.9

Chapter 2: Mono-Arylated Carboranes-2.14

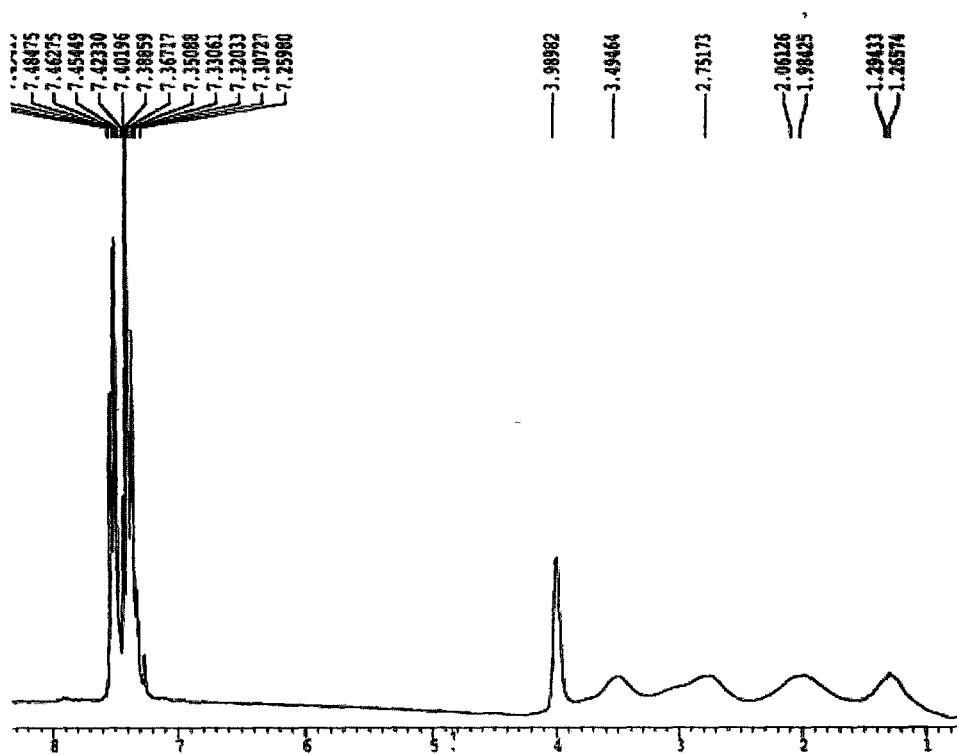


Figure 1-A. ^1H NMR of 2.14, 200 MHz, CDCl_3 .

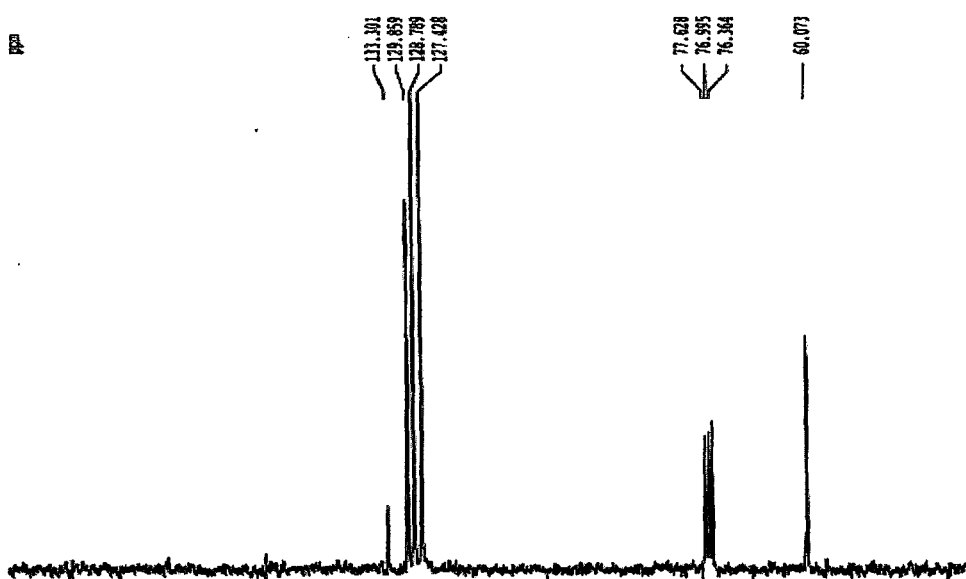


Figure 1-B. $^{13}\text{C}\{\text{H}\}$ NMR of 2.14, 200 MHz, in CDCl_3 .

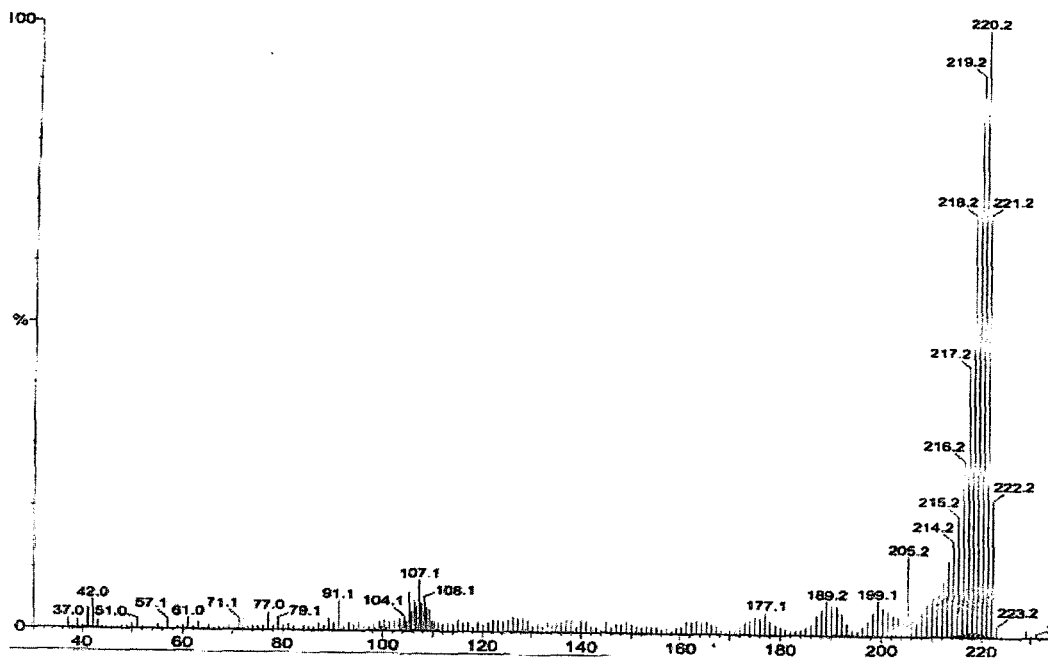


Figure 1-E. EI-MS of 2.14

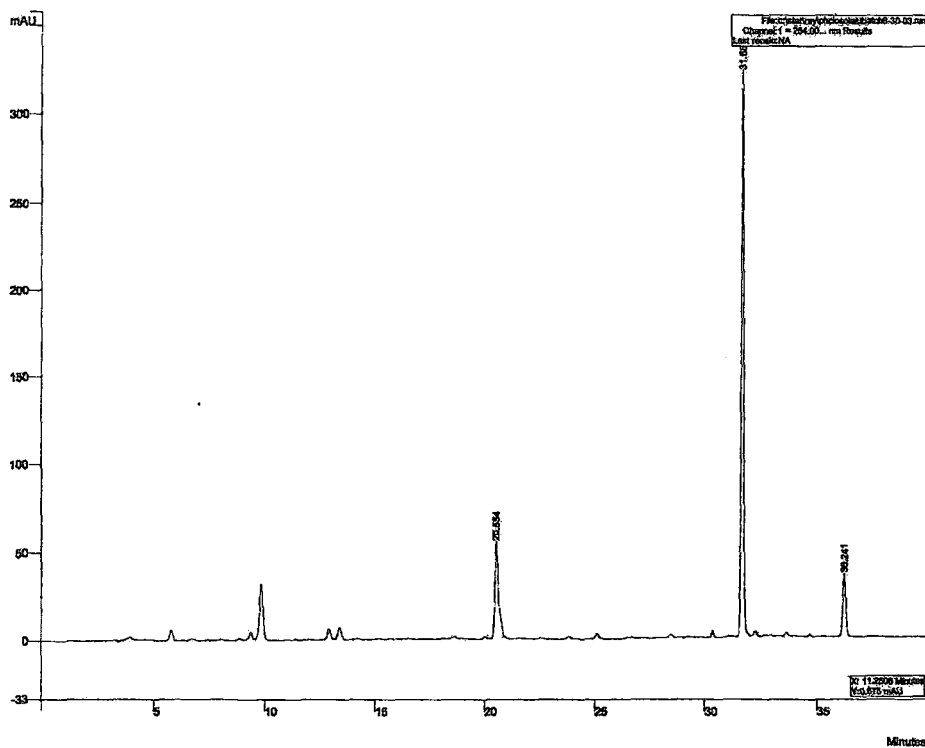


Figure 1-F Analytical HPLC of 2.14

Chapter 2: Mono-Arylated Carboranes-2.11

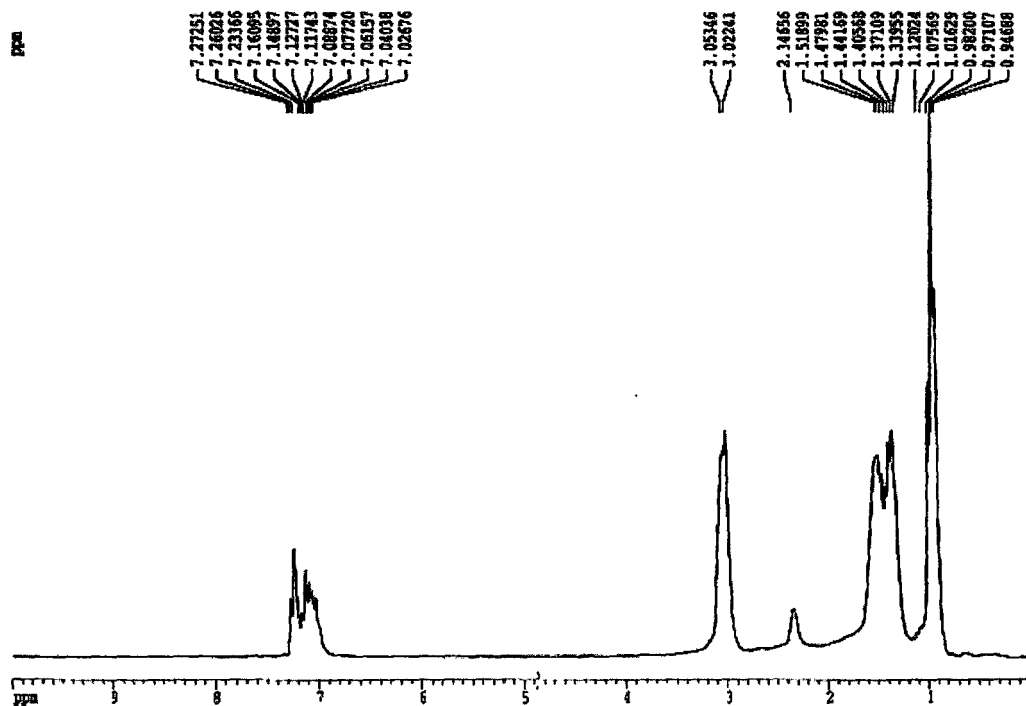


Figure 2-A. ^1H NMR of 2.11, 200 MHz, in CDCl_3 .

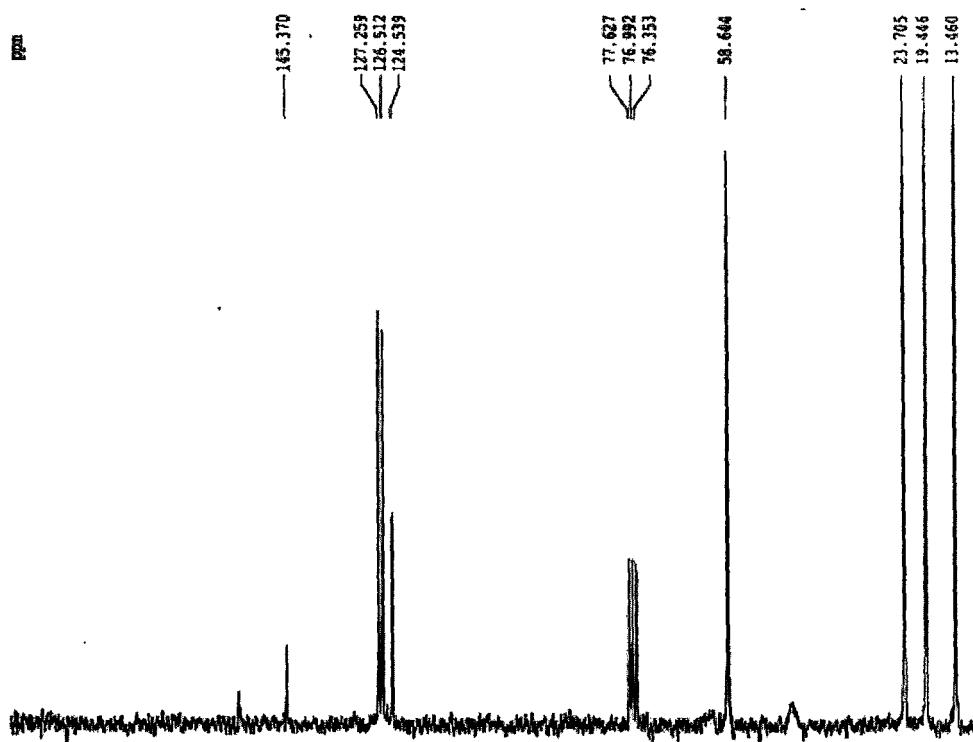


Figure 2-B. $^{13}\text{C}\{^1\text{H}\}$ NMR of 2.11, 200 MHz, in CDCl_3 .

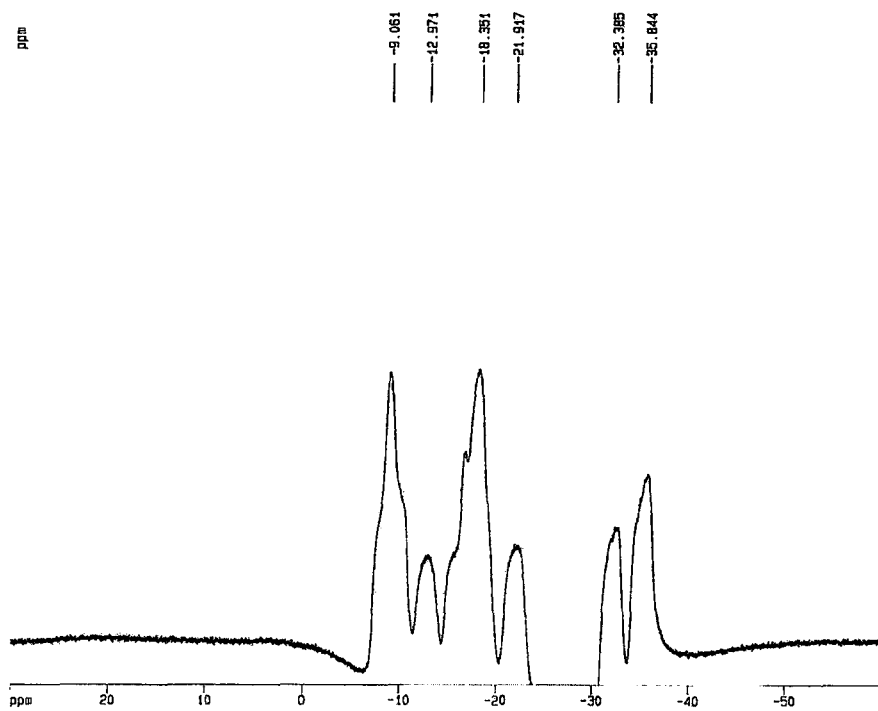


Figure 2-C. $^{11}\text{B}\{\text{H}\}$ NMR of 2.11, 500 MHz, in CDCl_3 .

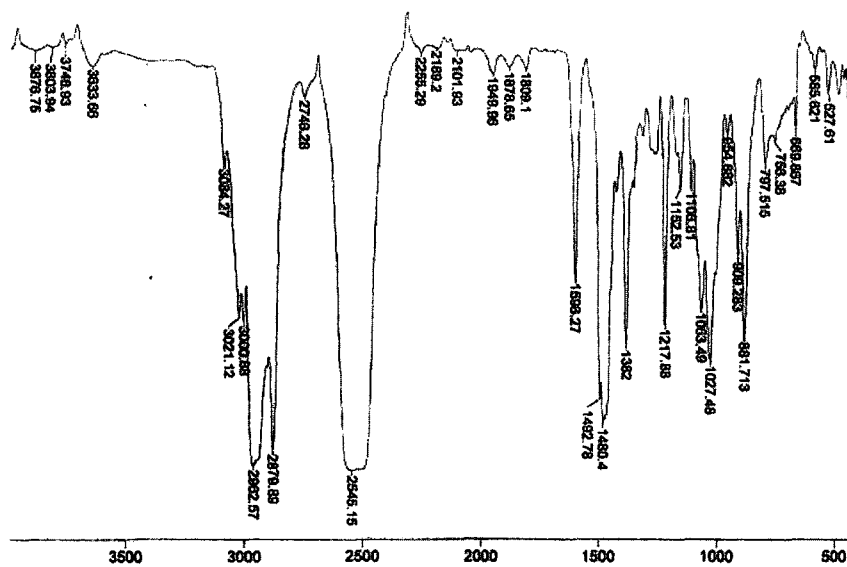


Figure 2-D. FTIR of 2.11 in CH_2Cl_2 .

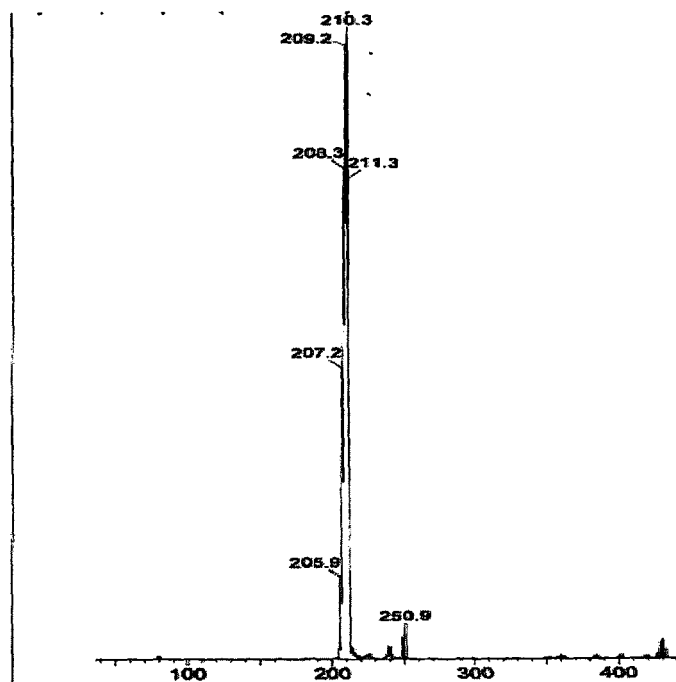


Figure 2-E. Negative Ion Mode ESI-MS of 2.11.

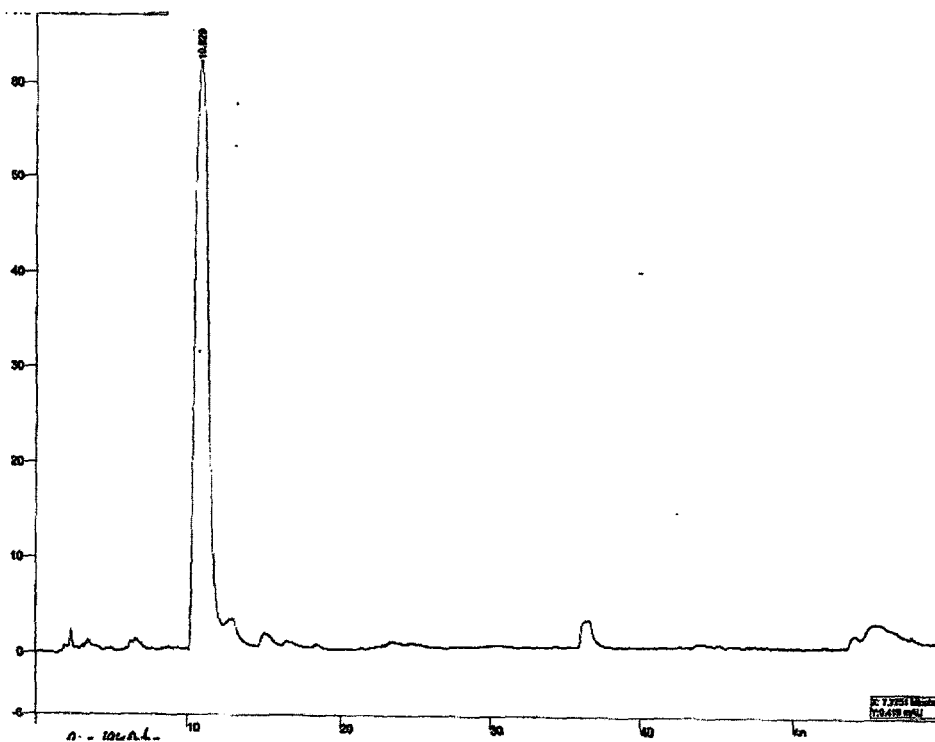


Figure 2-F. Analytical HPLC chromatogram of 2.11.

Chapter 2: Monoarylated Carboranes –2.8

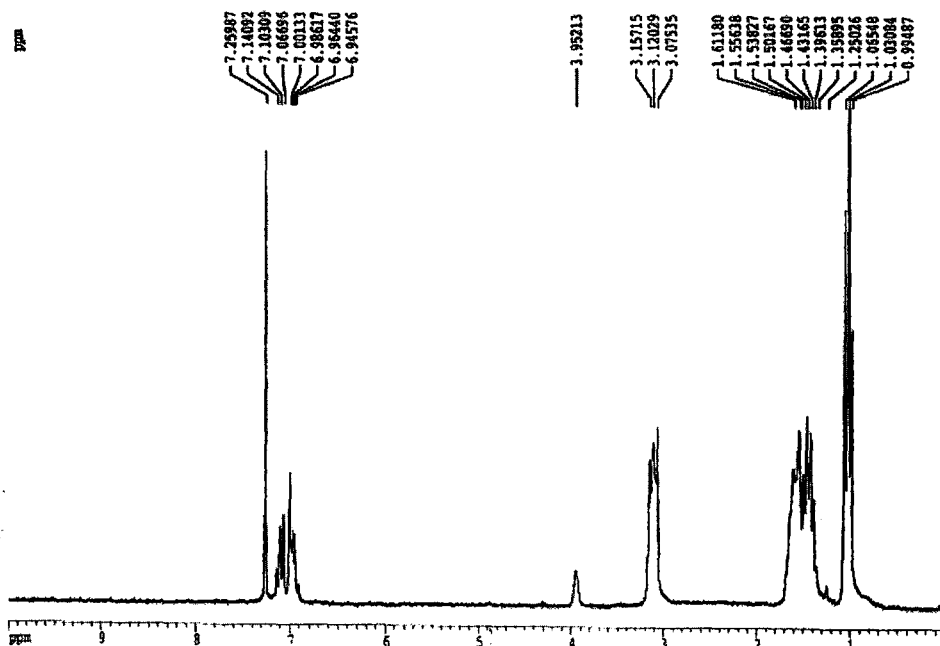


Figure 3-A. ^1H NMR of 2.8 200 MHz, in CDCl_3 .

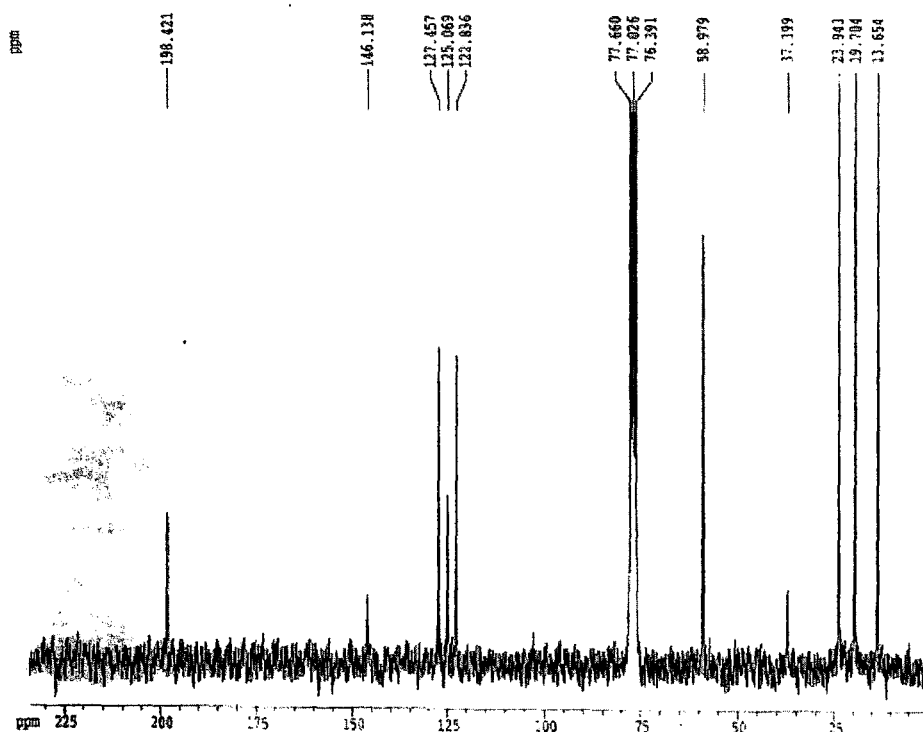


Figure 3-B. $^{13}\text{C}\{\text{H}\}$ NMR of 2.8, 200 MHz in CDCl_3 .

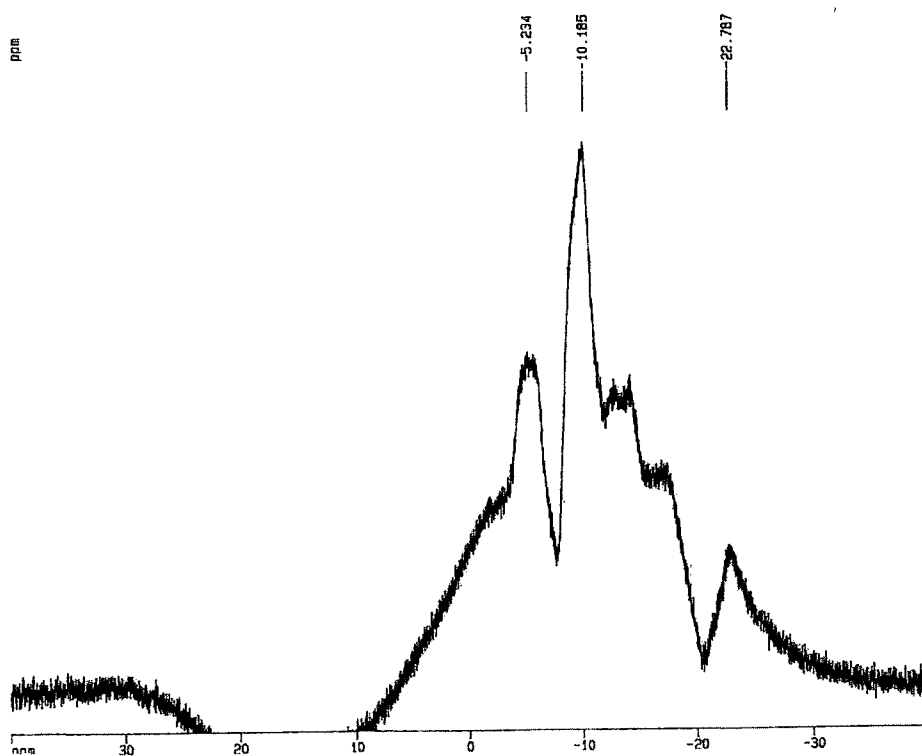


Figure 3-C. $^{11}\text{B}\{\text{H}\}$ NMR of 2.8, 500 MHz in CDCl_3 .

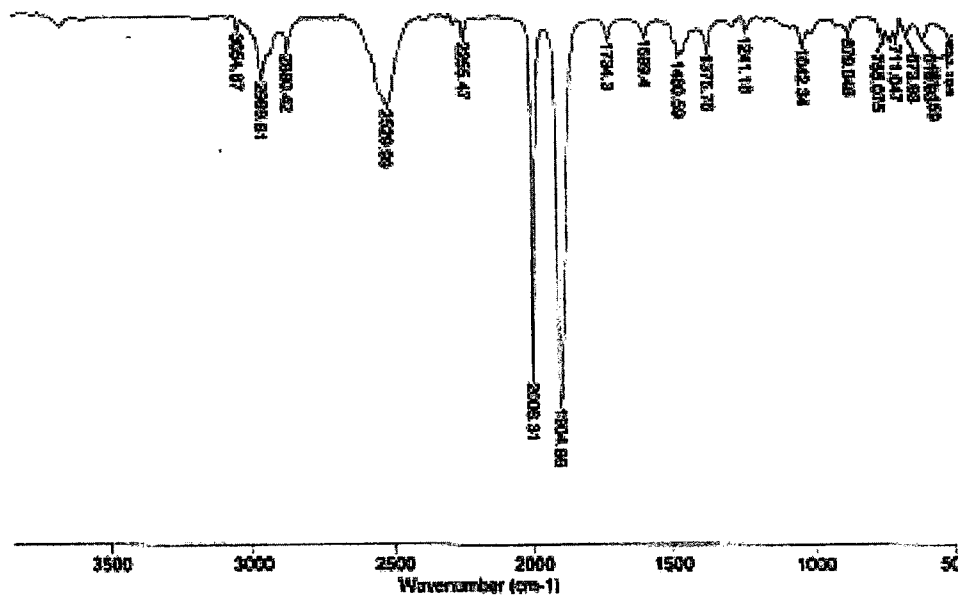


Figure 3-D. FTIR of 2.8 in CH_2Cl_2 .

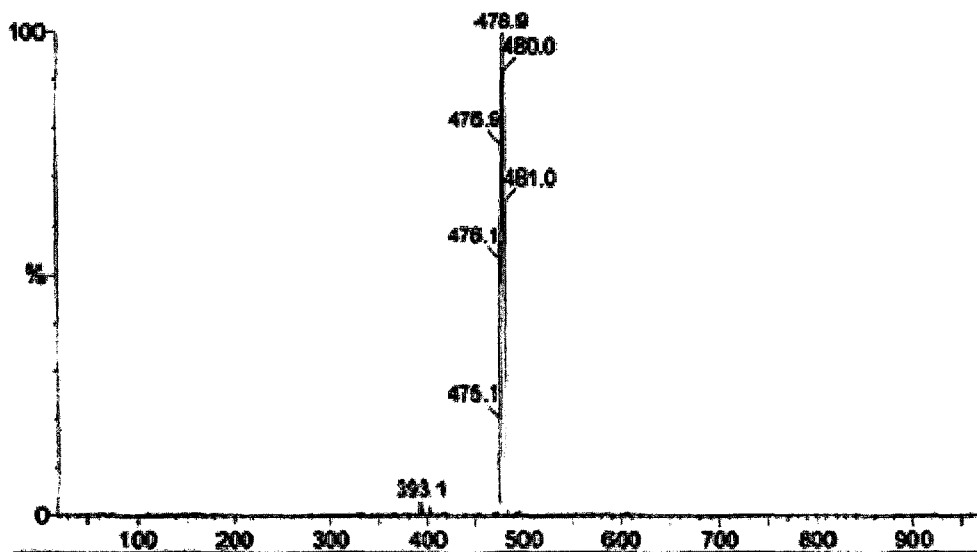


Figure 3-E. Negative Ion Mode ES-MS of 2.8.

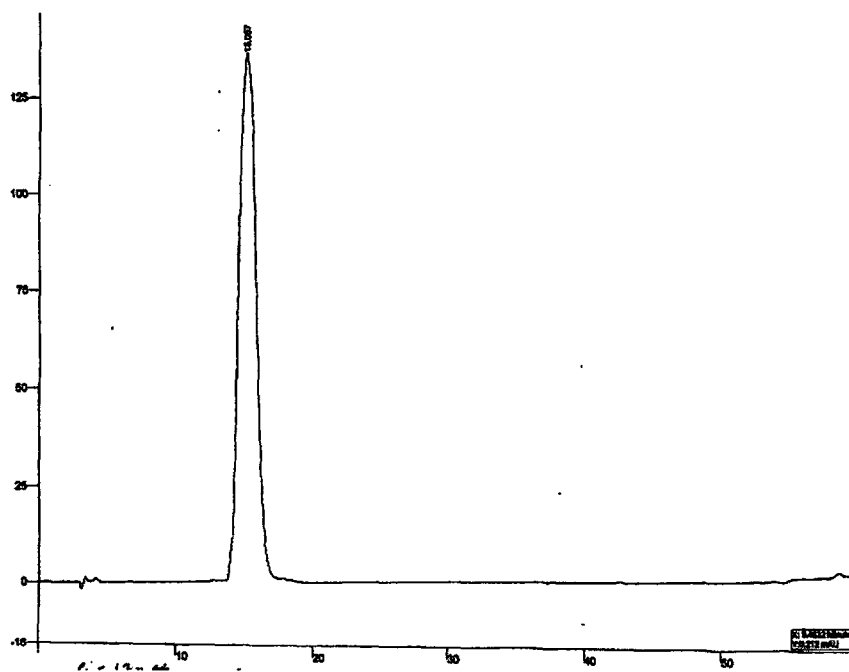


Figure 3-F. Analytical HPLC chromatogram of 2.8

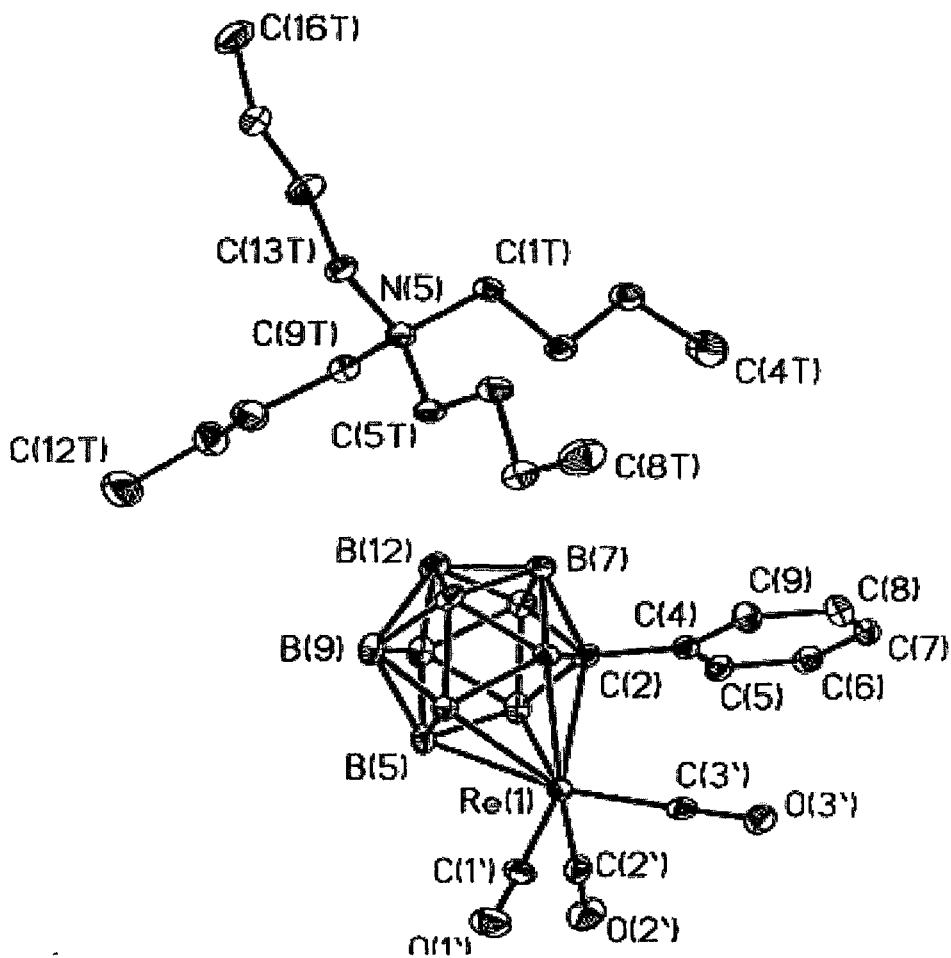


Figure 3-G. X-ray Structure of 2.8. Crystallographic Data Below.

Table 1. Crystal data and structure refinement for XXX.

Empirical formula	C ₂₇ H ₅₁ B ₉ N O ₃ Re	
Formula weight	721.18	
Temperature	173(2) K	
Wavelength	0.71073 Å	
Crystal system	Triclinic	
Space group	P-1	
Unit cell dimensions	a = 10.300(5) Å	α = 76.226(8)°.
	b = 12.125(5) Å	β = 70.644(7)°.
	c = 14.693(7) Å	γ = 80.864(7)°.
Volume	1675.0(13) Å ³	
Z	2	
Density (calculated)	1.430 Mg/m ³	
Absorption coefficient	3.656 mm ⁻¹	
F(000)	728	
Crystal size	0.210 x 0.10 x 0.03 mm ³	
θ range for data collection	1.50 to 27.50°.	
Index ranges	-13 ≤ h ≤ 13, -15 ≤ k ≤ 15, -17 ≤ l ≤ 18	
Reflections collected	15103	
Independent reflections	7532 [R(int) = 0.0379]	
Completeness to θ = 27.50°	97.6 %	
Absorption correction	Semi-empirical from equivalents	
Max. and min. transmission	1.000000 and 0.821260	
Refinement method	Full-matrix least-squares on F ²	
Data / restraints / parameters	7532 / 0 / 427	
Goodness-of-fit on F ²	0.946	
Final R indices [I > 2σ(I)]	R1 = 0.0382, wR2 = 0.0749	
R indices (all data)	R1 = 0.0559, wR2 = 0.0807	
Extinction coefficient	0.0004(2)	
Largest diff. peak and hole	1.367 and -0.872 e.Å ⁻³	

Table 2. Atomic coordinates ($\times 10^4$) and equivalent isotropic displacement parameters ($\text{\AA}^2 \times 10^3$) for XXX. $U(\text{eq})$ is defined as one third of the trace of the orthogonalized U_{ij} tensor.

	x	y	z	U(eq)
Re(1)	5639(1)	7206(1)	1060(1)	26(1)
C(1')	7315(5)	6869(4)	91(4)	37(1)
O(1')	8381(4)	6693(4)	-477(3)	57(1)
C(2')	5020(5)	5813(4)	1055(4)	37(1)
O(2')	4614(4)	4955(3)	1095(3)	55(1)
C(3')	4871(4)	7903(4)	17(4)	29(1)
O(3')	4390(3)	8338(3)	-608(3)	39(1)
C(4)	2896(4)	8726(4)	1855(3)	26(1)
C(5)	1767(5)	8076(4)	2165(4)	32(1)
C(6)	606(5)	8495(5)	1862(4)	36(1)
C(7)	552(5)	9538(5)	1250(4)	37(1)
C(8)	1659(5)	10193(5)	937(4)	40(1)
C(9)	2817(5)	9785(4)	1244(4)	36(1)
C(2)	4155(4)	8264(4)	2186(3)	25(1)
C(3)	5633(4)	8840(4)	1616(4)	25(1)
B(4)	7014(5)	7900(4)	1742(4)	26(1)
B(5)	6312(5)	6616(5)	2514(5)	32(1)
B(6)	4468(5)	6874(5)	2747(4)	34(1)
B(7)	4596(5)	9249(5)	2714(4)	32(1)
B(8)	6414(5)	9003(5)	2436(4)	30(1)
B(9)	6818(5)	7600(5)	3029(4)	35(1)
B(10)	5230(6)	6966(5)	3647(4)	35(1)
B(11)	3871(5)	7976(5)	3443(4)	32(1)
B(12)	5307(5)	8434(5)	3616(4)	36(1)
N(5)	7419(4)	12600(3)	2874(3)	28(1)
C(1T)	5961(4)	13194(4)	3047(4)	28(1)
C(2T)	4976(4)	12635(4)	2748(4)	32(1)
C(3T)	3498(4)	13124(4)	3174(4)	39(1)
C(4T)	2517(5)	12739(5)	2753(5)	62(2)
C(5T)	8016(4)	12357(4)	1838(3)	29(1)

C(6T)	8110(5)	13374(4)	998(3)	32(1)
C(7T)	8708(5)	13002(4)	10(4)	34(1)
C(8T)	8962(6)	14003(5)	-851(4)	53(2)
C(9T)	7322(5)	11492(4)	3627(4)	34(1)
C(10T)	8639(5)	10736(4)	3638(4)	44(1)
C(11T)	8269(6)	9665(5)	4466(5)	53(2)
C(12T)	9486(7)	8811(6)	4509(5)	68(2)
C(13T)	8345(4)	13389(4)	2989(4)	30(1)
C(14T)	7924(5)	13736(4)	3976(4)	39(1)
C(15T)	8819(5)	14623(4)	3967(4)	37(1)
C(16T)	8283(6)	15102(5)	4902(4)	49(1)

Table 3. Bond lengths [\AA] and angles [$^\circ$] for XXX.

Re(1)-C(1')	1.897(5)	B(7)-B(8)	1.771(7)
Re(1)-C(2')	1.900(5)	B(7)-B(11)	1.771(8)
Re(1)-C(3')	1.914(5)	B(8)-B(9)	1.771(8)
Re(1)-C(3)	2.314(4)	B(8)-B(12)	1.775(8)
Re(1)-C(2)	2.330(4)	B(9)-B(10)	1.781(7)
Re(1)-B(4)	2.332(4)	B(9)-B(12)	1.793(8)
Re(1)-B(6)	2.336(6)	B(10)-B(11)	1.762(8)
Re(1)-B(5)	2.378(6)	B(10)-B(12)	1.783(8)
C(1')-O(1')	1.162(6)	B(11)-B(12)	1.772(7)
C(2')-O(2')	1.164(5)	N(5)-C(9T)	1.517(6)
C(3')-O(3')	1.163(6)	N(5)-C(5T)	1.523(6)
C(4)-C(9)	1.388(7)	N(5)-C(13T)	1.526(5)
C(4)-C(5)	1.397(6)	N(5)-C(1T)	1.527(5)
C(4)-C(2)	1.512(6)	C(1T)-C(2T)	1.528(5)
C(5)-C(6)	1.392(6)	C(2T)-C(3T)	1.522(6)
C(6)-C(7)	1.371(7)	C(3T)-C(4T)	1.524(6)
C(7)-C(8)	1.381(7)	C(5T)-C(6T)	1.512(7)
C(8)-C(9)	1.390(7)	C(6T)-C(7T)	1.524(6)
C(2)-C(3)	1.650(6)	C(7T)-C(8T)	1.513(7)
C(2)-B(6)	1.722(7)	C(9T)-C(10T)	1.514(7)
C(2)-B(11)	1.729(7)	C(10T)-C(11T)	1.552(8)
C(2)-B(7)	1.757(6)	C(11T)-C(12T)	1.502(8)
-C(3)-B(4)	1.708(7)	C(13T)-C(14T)	1.511(6)
C(3)-B(8)	1.717(6)	C(14T)-C(15T)	1.519(6)
C(3)-B(7)	1.749(7)	C(15T)-C(16T)	1.518(7)
B(4)-B(8)	1.784(7)		
B(4)-B(9)	1.786(8)	C(1')-Re(1)-C(2')	89.2(2)
B(4)-B(5)	1.790(8)	C(1')-Re(1)-C(3')	88.2(2)
B(5)-B(10)	1.775(8)	C(2')-Re(1)-C(3')	87.54(19)
B(5)-B(9)	1.776(7)	C(1')-Re(1)-C(3)	113.07(17)
B(5)-B(6)	1.804(7)	C(2')-Re(1)-C(3)	157.2(2)
B(6)-B(10)	1.779(8)	C(3')-Re(1)-C(3)	97.69(17)
B(6)-B(11)	1.784(8)	C(1')-Re(1)-C(2)	154.69(16)
B(7)-B(12)	1.749(8)	C(2')-Re(1)-C(2)	115.95(19)

C(3')-Re(1)-C(2)	95.16(17)	B(6)-C(2)-B(11)	62.2(3)
C(3)-Re(1)-C(2)	41.63(14)	C(4)-C(2)-B(7)	110.8(3)
C(1')-Re(1)-B(4)	85.63(18)	C(3)-C(2)-B(7)	61.7(3)
C(2')-Re(1)-B(4)	140.42(19)	B(6)-C(2)-B(7)	112.5(4)
C(3')-Re(1)-B(4)	131.36(18)	B(11)-C(2)-B(7)	61.1(3)
C(3)-Re(1)-B(4)	43.13(16)	C(4)-C(2)-Re(1)	108.3(3)
C(2)-Re(1)-B(4)	73.32(16)	C(3)-C(2)-Re(1)	68.7(2)
C(1')-Re(1)-B(6)	144.2(2)	B(6)-C(2)-Re(1)	68.5(3)
C(2')-Re(1)-B(6)	86.4(2)	B(11)-C(2)-Re(1)	126.8(3)
C(3')-Re(1)-B(6)	126.97(19)	B(7)-C(2)-Re(1)	127.4(3)
C(3)-Re(1)-B(6)	72.64(18)	C(2)-C(3)-B(4)	111.9(3)
C(2)-Re(1)-B(6)	43.33(17)	C(2)-C(3)-B(8)	111.5(4)
B(4)-Re(1)-B(6)	75.66(18)	B(4)-C(3)-B(8)	62.8(3)
C(1')-Re(1)-B(5)	101.0(2)	C(2)-C(3)-B(7)	62.1(3)
C(2')-Re(1)-B(5)	98.59(19)	B(4)-C(3)-B(7)	113.7(4)
C(3')-Re(1)-B(5)	168.92(18)	B(8)-C(3)-B(7)	61.4(3)
C(3)-Re(1)-B(5)	73.16(17)	C(2)-C(3)-Re(1)	69.7(2)
C(2)-Re(1)-B(5)	73.87(18)	B(4)-C(3)-Re(1)	69.0(2)
B(4)-Re(1)-B(5)	44.66(18)	B(8)-C(3)-Re(1)	128.0(3)
B(6)-Re(1)-B(5)	44.98(18)	B(7)-C(3)-Re(1)	128.8(3)
O(1')-C(1')-Re(1)	176.0(4)	C(3)-B(4)-B(8)	58.9(3)
O(2')-C(2')-Re(1)	177.0(5)	C(3)-B(4)-B(9)	104.9(4)
O(3')-C(3')-Re(1)	178.9(4)	B(8)-B(4)-B(9)	59.5(3)
C(9)-C(4)-C(5)	118.0(4)	C(3)-B(4)-B(5)	106.1(3)
C(9)-C(4)-C(2)	122.3(4)	B(8)-B(4)-B(5)	107.7(4)
C(5)-C(4)-C(2)	119.7(4)	B(9)-B(4)-B(5)	59.6(3)
C(6)-C(5)-C(4)	120.0(5)	C(3)-B(4)-Re(1)	67.9(2)
C(7)-C(6)-C(5)	121.1(4)	B(8)-B(4)-Re(1)	123.4(3)
C(6)-C(7)-C(8)	119.6(5)	B(9)-B(4)-Re(1)	123.6(3)
C(7)-C(8)-C(9)	119.6(5)	B(5)-B(4)-Re(1)	69.0(2)
C(4)-C(9)-C(8)	121.6(5)	B(10)-B(5)-B(9)	60.2(3)
C(4)-C(2)-C(3)	120.3(4)	B(10)-B(5)-B(4)	107.2(4)
C(4)-C(2)-B(6)	124.9(3)	B(9)-B(5)-B(4)	60.1(3)
C(3)-C(2)-B(6)	109.5(3)	B(10)-B(5)-B(6)	59.6(3)
C(4)-C(2)-B(11)	115.6(4)	B(9)-B(5)-B(6)	107.4(4)
C(3)-C(2)-B(11)	109.7(3)	B(4)-B(5)-B(6)	105.6(4)

B(10)-B(5)-Re(1)	121.1(3)	B(5)-B(9)-B(10)	59.9(3)
B(9)-B(5)-Re(1)	121.6(3)	B(8)-B(9)-B(4)	60.2(3)
B(4)-B(5)-Re(1)	66.3(2)	B(5)-B(9)-B(4)	60.4(3)
B(6)-B(5)-Re(1)	66.3(2)	B(10)-B(9)-B(4)	107.1(3)
C(2)-B(6)-B(10)	105.1(4)	B(8)-B(9)-B(12)	59.8(3)
C(2)-B(6)-B(11)	59.0(3)	B(5)-B(9)-B(12)	108.7(4)
B(10)-B(6)-B(11)	59.3(3)	B(10)-B(9)-B(12)	59.8(3)
C(2)-B(6)-B(5)	106.7(4)	B(4)-B(9)-B(12)	107.9(4)
B(10)-B(6)-B(5)	59.4(3)	B(11)-B(10)-B(5)	109.8(4)
B(11)-B(6)-B(5)	107.6(3)	B(11)-B(10)-B(6)	60.5(3)
C(2)-B(6)-Re(1)	68.1(2)	B(5)-B(10)-B(6)	61.0(3)
B(10)-B(6)-Re(1)	123.1(3)	B(11)-B(10)-B(9)	108.4(4)
B(11)-B(6)-Re(1)	123.5(3)	B(5)-B(10)-B(9)	59.9(3)
B(5)-B(6)-Re(1)	68.7(3)	B(6)-B(10)-B(9)	108.2(4)
B(12)-B(7)-C(3)	105.0(4)	B(11)-B(10)-B(12)	60.0(3)
B(12)-B(7)-C(2)	105.7(4)	B(5)-B(10)-B(12)	109.2(4)
C(3)-B(7)-C(2)	56.2(2)	B(6)-B(10)-B(12)	108.5(4)
B(12)-B(7)-B(8)	60.6(3)	B(9)-B(10)-B(12)	60.4(3)
C(3)-B(7)-B(8)	58.4(3)	C(2)-B(11)-B(10)	105.6(4)
C(2)-B(7)-B(8)	104.2(3)	C(2)-B(11)-B(7)	60.2(3)
B(12)-B(7)-B(11)	60.4(3)	B(10)-B(11)-B(7)	108.1(4)
C(3)-B(7)-B(11)	103.4(3)	C(2)-B(11)-B(12)	105.9(4)
C(2)-B(7)-B(11)	58.7(3)	B(10)-B(11)-B(12)	60.6(3)
B(8)-B(7)-B(11)	107.8(4)	B(7)-B(11)-B(12)	59.2(3)
C(3)-B(8)-B(9)	105.1(3)	C(2)-B(11)-B(6)	58.7(3)
C(3)-B(8)-B(7)	60.2(3)	B(10)-B(11)-B(6)	60.2(3)
B(9)-B(8)-B(7)	108.4(4)	B(7)-B(11)-B(6)	108.9(4)
C(3)-B(8)-B(12)	105.2(3)	B(12)-B(11)-B(6)	108.8(4)
B(9)-B(8)-B(12)	60.7(3)	B(7)-B(12)-B(11)	60.4(3)
B(7)-B(8)-B(12)	59.1(3)	B(7)-B(12)-B(8)	60.3(3)
C(3)-B(8)-B(4)	58.4(3)	B(11)-B(12)-B(8)	107.6(4)
B(9)-B(8)-B(4)	60.3(3)	B(7)-B(12)-B(10)	108.1(4)
B(7)-B(8)-B(4)	109.0(3)	B(11)-B(12)-B(10)	59.4(3)
B(12)-B(8)-B(4)	108.8(4)	B(8)-B(12)-B(10)	107.0(4)
B(8)-B(9)-B(5)	109.0(4)	B(7)-B(12)-B(9)	108.4(4)
B(8)-B(9)-B(10)	107.3(4)	B(11)-B(12)-B(9)	107.4(4)

B(8)-B(12)-B(9)	59.5(3)	C(2T)-C(3T)-C(4T)	111.2(4)
B(10)-B(12)-B(9)	59.7(3)	C(6T)-C(5T)-N(5)	116.6(3)
C(9T)-N(5)-C(5T)	110.1(3)	C(5T)-C(6T)-C(7T)	110.8(4)
C(9T)-N(5)-C(13T)	112.1(3)	C(8T)-C(7T)-C(6T)	112.5(4)
C(5T)-N(5)-C(13T)	107.8(3)	C(10T)-C(9T)-N(5)	118.3(4)
C(9T)-N(5)-C(1T)	107.0(3)	C(9T)-C(10T)-C(11T)	108.5(4)
C(5T)-N(5)-C(1T)	111.4(3)	C(12T)-C(11T)-C(10T)	113.4(5)
C(13T)-N(5)-C(1T)	108.5(3)	C(14T)-C(13T)-N(5)	116.1(4)
N(5)-C(1T)-C(2T)	115.0(3)	C(13T)-C(14T)-C(15T)	111.3(4)
C(3T)-C(2T)-C(1T)	109.7(4)	C(16T)-C(15T)-C(14T)	111.9(4)

Table 4. Anisotropic displacement parameters ($\text{\AA}^2 \times 10^3$) for XXX. The anisotropic displacement factor exponent takes the form: $-2\pi^2[h^2a^2U^{11} + \dots + 2hka^*b^*U^{12}]$

	U ¹¹	U ²²	U ³³	U ²³	U ¹³	U ¹²
Re(1)	24(1)	23(1)	34(1)	-9(1)	-11(1)	-2(1)
C(1')	28(2)	40(3)	50(3)	-22(3)	-15(2)	4(2)
O(1')	33(2)	72(3)	77(3)	-46(2)	-13(2)	4(2)
C(2')	47(3)	29(3)	42(3)	-8(2)	-25(3)	1(2)
O(2')	79(3)	34(2)	67(3)	-8(2)	-36(2)	-17(2)
C(3')	26(2)	29(2)	32(3)	-15(2)	-4(2)	-3(2)
O(3')	42(2)	41(2)	39(2)	-10(2)	-18(2)	-5(2)
C(4)	24(2)	28(2)	26(3)	-8(2)	-5(2)	-3(2)
C(5)	30(2)	36(3)	32(3)	-8(2)	-11(2)	-5(2)
C(6)	21(2)	50(3)	42(3)	-17(3)	-7(2)	-9(2)
C(7)	28(2)	50(3)	37(3)	-19(3)	-15(2)	7(2)
C(8)	36(3)	38(3)	43(3)	-3(3)	-15(2)	5(2)
C(9)	27(2)	36(3)	40(3)	-1(2)	-8(2)	-6(2)
C(2)	23(2)	29(2)	25(2)	-7(2)	-5(2)	-7(2)
C(3)	23(2)	20(2)	33(3)	-5(2)	-10(2)	-3(2)
B(4)	21(2)	30(3)	29(3)	-9(2)	-8(2)	-3(2)
B(5)	27(3)	28(3)	45(4)	-4(2)	-20(3)	-3(2)
B(6)	30(3)	32(3)	40(3)	3(2)	-16(3)	-9(2)
B(7)	27(3)	34(3)	36(3)	-16(3)	-9(2)	-2(2)
B(8)	31(3)	37(3)	28(3)	-11(2)	-8(2)	-10(2)
B(9)	28(3)	44(3)	36(3)	-4(3)	-14(3)	-8(2)
B(10)	32(3)	40(3)	32(3)	1(3)	-12(3)	-8(2)
B(11)	26(3)	42(3)	25(3)	-5(2)	-5(2)	-6(2)
B(12)	29(3)	51(4)	31(3)	-17(3)	-8(2)	-4(2)
N(5)	26(2)	27(2)	31(2)	-11(2)	-8(2)	-1(2)
C(1T)	22(2)	28(2)	33(3)	-14(2)	-2(2)	0(2)
C(2T)	27(2)	35(3)	40(3)	-17(2)	-11(2)	-1(2)
C(3T)	26(2)	41(3)	50(3)	-20(3)	-7(2)	-1(2)
C(4T)	32(3)	70(4)	99(6)	-40(4)	-27(3)	5(3)
C(5T)	24(2)	32(2)	33(3)	-18(2)	-6(2)	0(2)
C(6T)	29(2)	34(3)	32(3)	-14(2)	-2(2)	-3(2)

C(7T)	35(2)	37(3)	33(3)	-13(2)	-6(2)	-7(2)
C(8T)	70(4)	53(4)	36(3)	-9(3)	-13(3)	-13(3)
C(9T)	40(3)	34(3)	33(3)	-12(2)	-14(2)	-3(2)
C(10T)	52(3)	47(3)	32(3)	-11(3)	-17(3)	7(3)
C(11T)	60(4)	38(3)	68(4)	-6(3)	-34(3)	2(3)
C(12T)	79(5)	66(4)	60(4)	-20(4)	-33(4)	20(4)
C(13T)	28(2)	35(3)	35(3)	-16(2)	-10(2)	-4(2)
C(14T)	48(3)	45(3)	26(3)	-9(2)	-10(2)	-13(2)
C(15T)	37(3)	43(3)	39(3)	-18(2)	-19(2)	2(2)
C(16T)	53(3)	64(4)	45(4)	-28(3)	-20(3)	-8(3)

Table 5. Hydrogen coordinates ($\times 10^4$) and isotropic displacement parameters ($\text{\AA}^2 \times 10^3$) for XXX.

	x	y	z	U(eq)
H(6)	3780	6165	2882	40
H(1TA)	6023	13991	2675	33
H(1TB)	5560	13221	3755	33
H(2TA)	5226	12777	2022	39
H(2TB)	5054	11801	2996	39
H(3TA)	3460	13967	3021	46
H(3TB)	3201	12872	3899	46
H(4TA)	1574	13059	3044	94
H(4TB)	2550	11905	2908	94
H(4TC)	2796	13006	2038	94
H(5TA)	8955	11970	1767	35
H(5TB)	7444	11817	1769	35
H(6TA)	8704	13915	1040	39
H(6TB)	7179	13771	1051	39
H(7TA)	9591	12530	-9	41
H(7TB)	8062	12524	-56	41
H(8TA)	9351	13723	-1467	79
H(8TB)	9612	14474	-794	79
H(8TC)	8087	14462	-847	79
H(9TA)	6893	11681	4288	41
H(9TB)	6680	11038	3528	41
H(10A)	9295	11155	3761	52
H(10B)	9080	10507	2994	52
H(11A)	7869	9907	5107	64
H(11B)	7555	9293	4362	64
H(12A)	9188	8159	5045	101
H(12B)	10191	9167	4625	101
H(12C)	9873	8549	3883	101
H(13A)	9294	13008	2865	36
H(13B)	8377	14089	2475	36
H(14A)	8007	13056	4490	46

H(14B)	6945	14049	4144	46
H(15A)	9775	14274	3894	44
H(15B)	8843	15253	3393	44
H(16A)	8875	15681	4862	74
H(16B)	8293	14486	5470	74
H(16C)	7336	15448	4977	74
H(4)	7970(40)	8040(40)	1270(30)	22(11)
H(6A)	-110(40)	8110(30)	2050(30)	12(10)
H(11)	2850(40)	8090(30)	3860(30)	14(10)
H(3)	5670(40)	9460(40)	1080(30)	22(11)
H(7)	3980(40)	10090(40)	2700(30)	27(12)
H(8)	7030(40)	9760(40)	2220(30)	27(12)
H(5)	6850(50)	5830(40)	2560(30)	29(12)
H(5A)	1860(50)	7380(40)	2550(40)	41(15)
H(12)	5230(50)	8700(40)	4250(40)	33(12)
H(9)	7660(50)	7390(40)	3350(40)	38(13)
H(8A)	1620(60)	10950(50)	500(40)	65(19)
H(7A)	-200(60)	9790(50)	1030(40)	65(18)
H(10)	5060(50)	6360(40)	4320(40)	36(13)
H(9A)	3500(50)	10210(40)	1030(40)	36(13)

Chapter 2: Mono-Arylated Carboranes-2.15

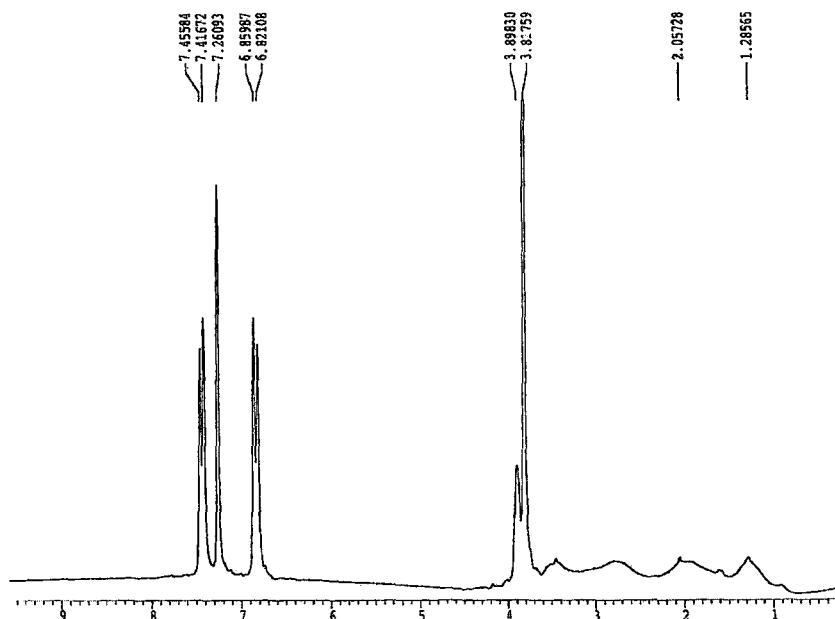


Figure 4-A. ^1H NMR of 2.15, 200 MHz, in CDCl_3 .

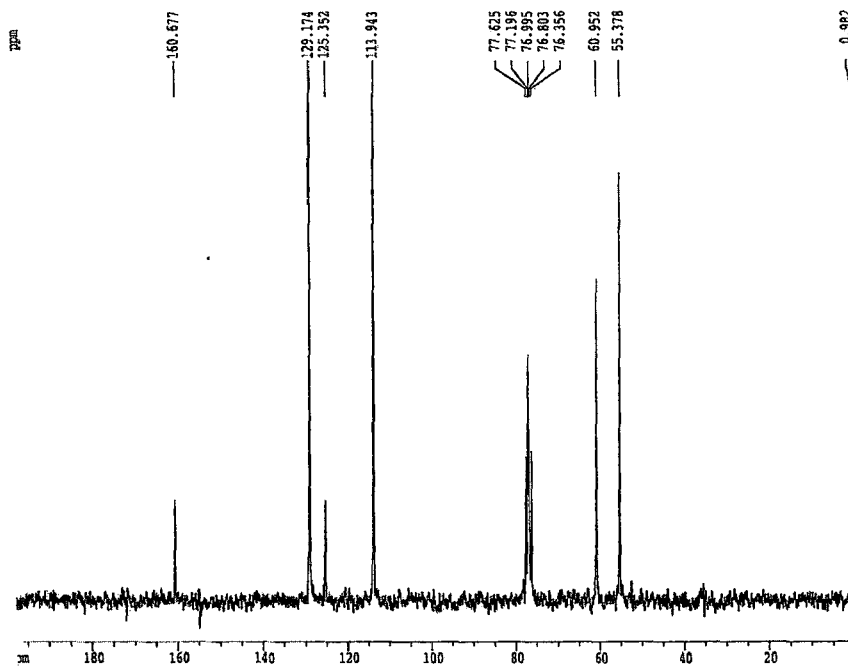


Figure 4-B. $^{13}\text{C}\{\text{H}\}$ NMR of 2.15, 200 MHz, in CDCl_3 .

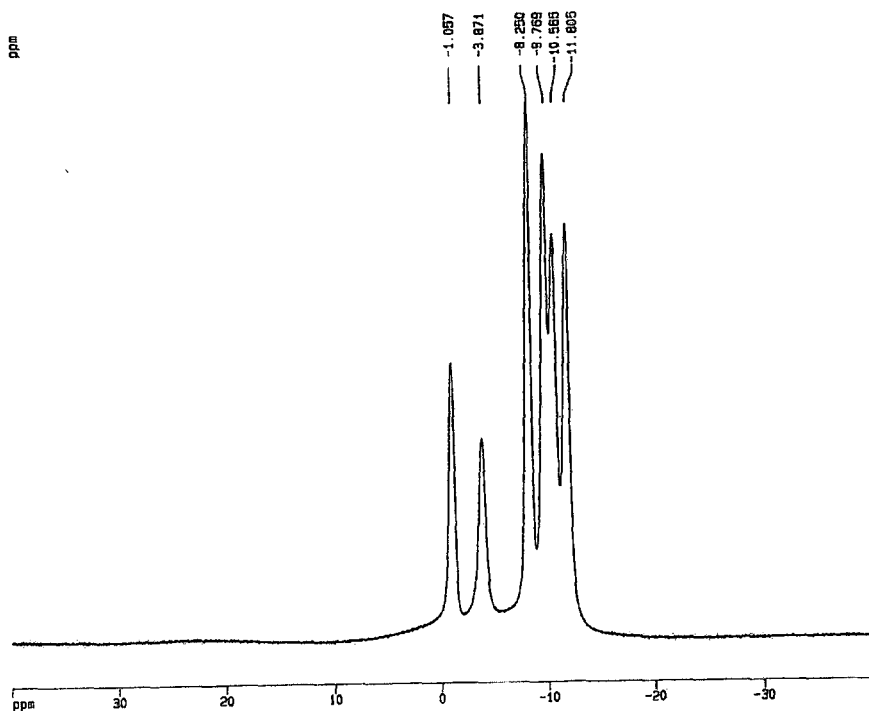


Figure 4-C. $^{11}\text{B}\{\text{H}\}$ NMR of 2.15, 500 MHz, in CDCl_3 .

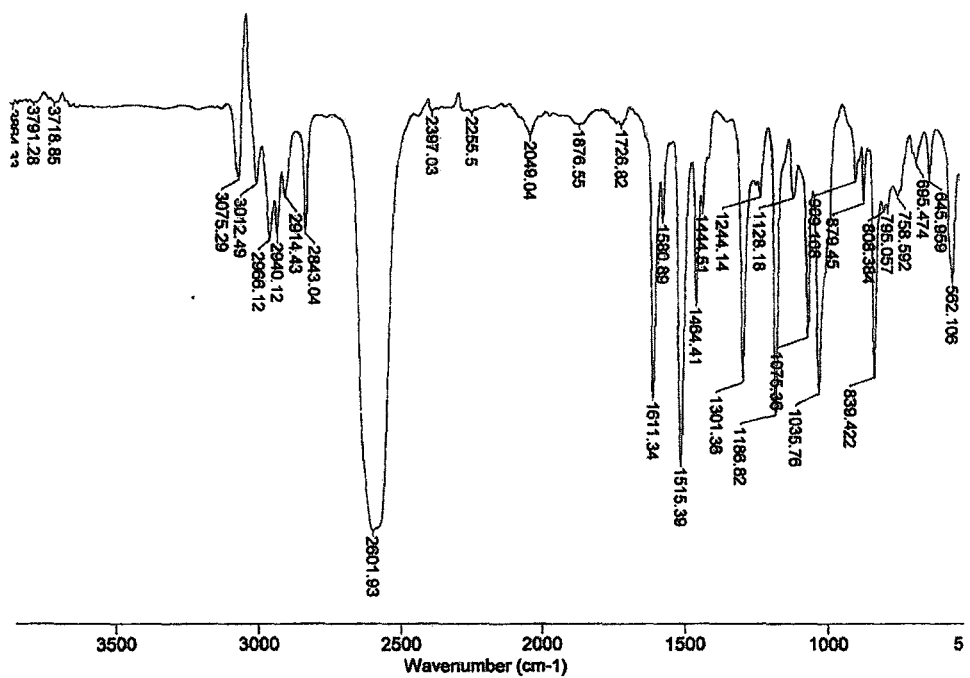


Figure 4-D. FTIR of 2.15, in CH_2Cl_2 .

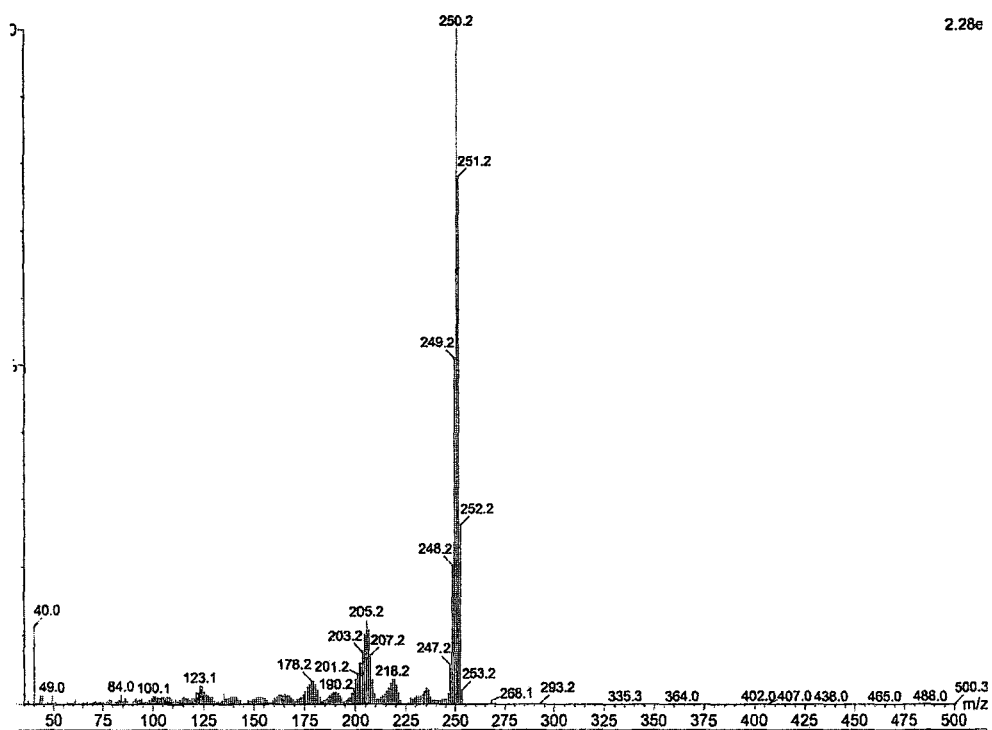


Figure 4-E. EI-MS of 2.15.

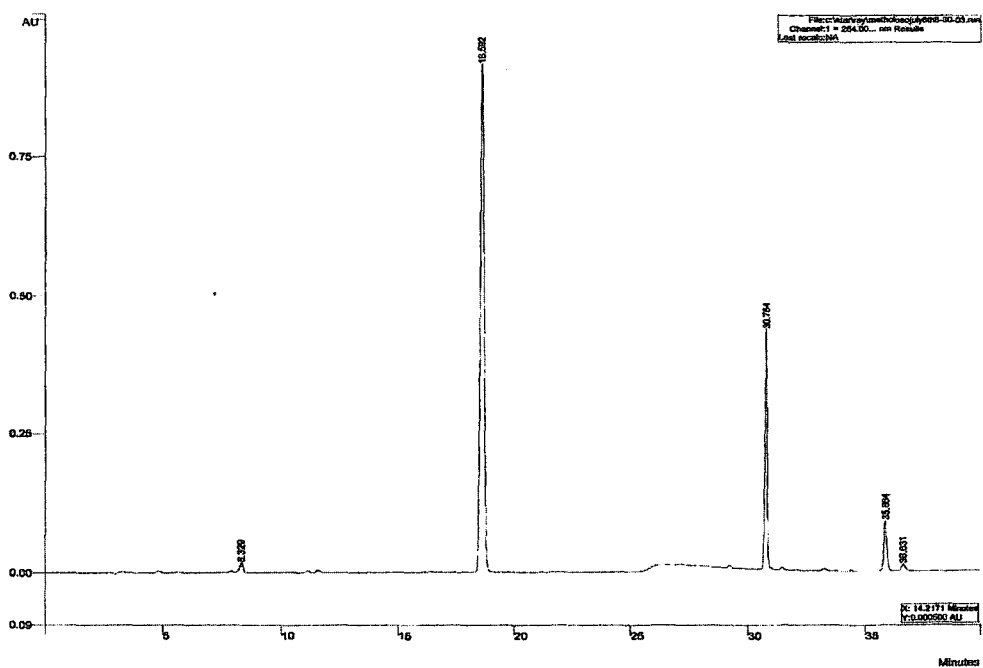


Figure 4-F. Analytical HPLC chromatogram of 2.15.

Chapter 2: Mono-Arylated Carboranes-2.12

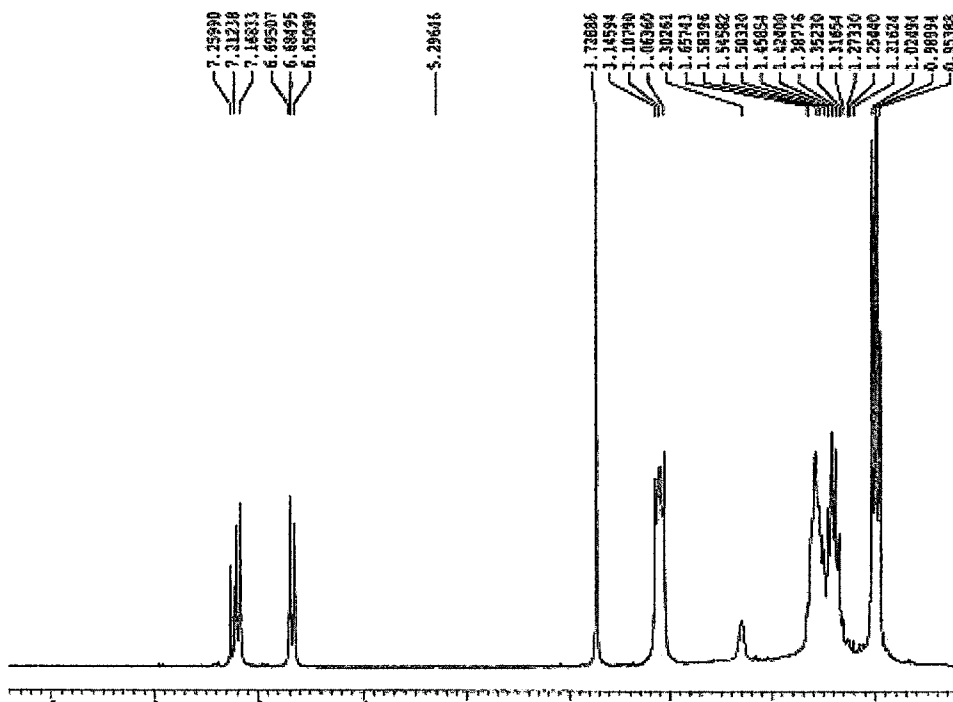


Figure 5-A. ^1H NMR of 2.12, 200 MHz, in CDCl_3 .

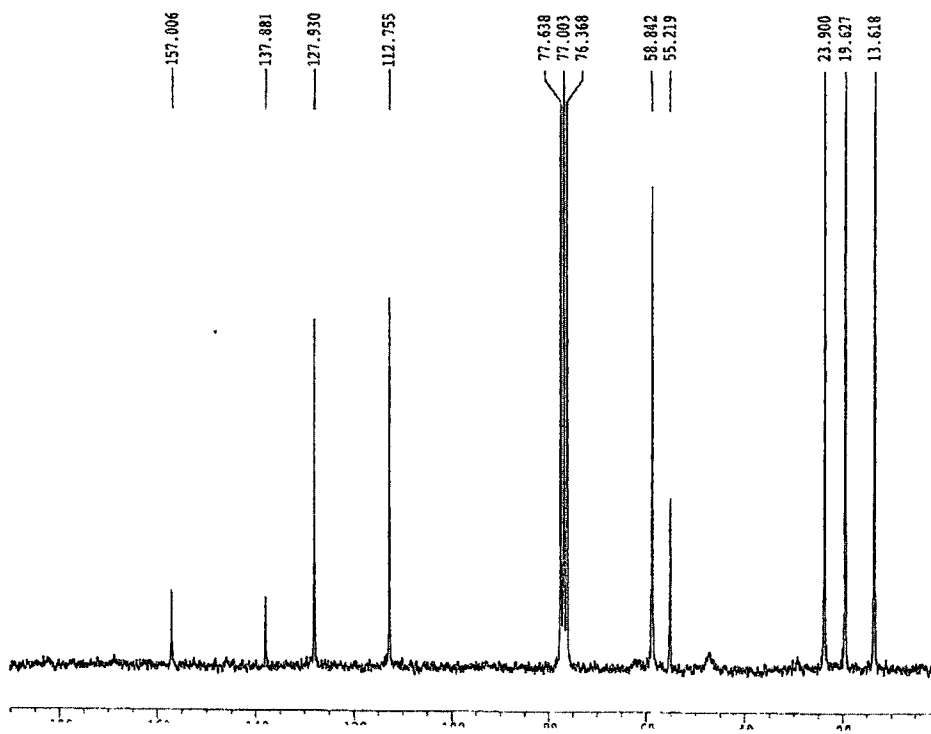


Figure 5-B. $^{13}\text{C}\{^1\text{H}\}$ NMR of 2.12, 200 MHz, in CDCl_3 .

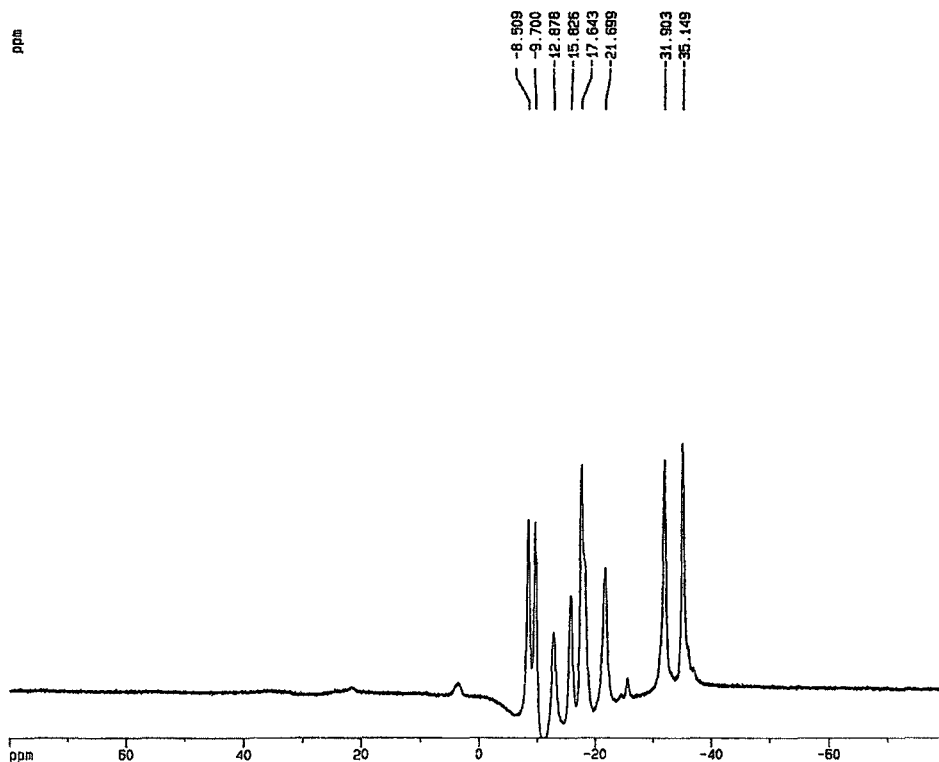


Figure 5-C. $^{11}\text{B}\{\text{H}\}$ NMR of 2.12, 500 MHz, in CDCl_3 .

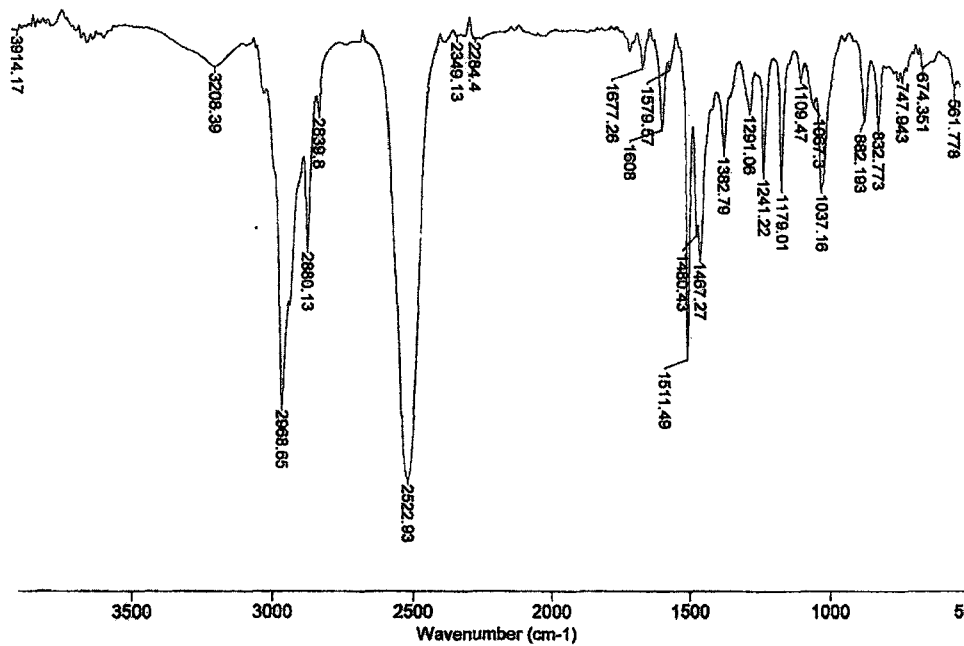


Figure 5-D. FTIR of 2.12, in CH_2Cl_2 .

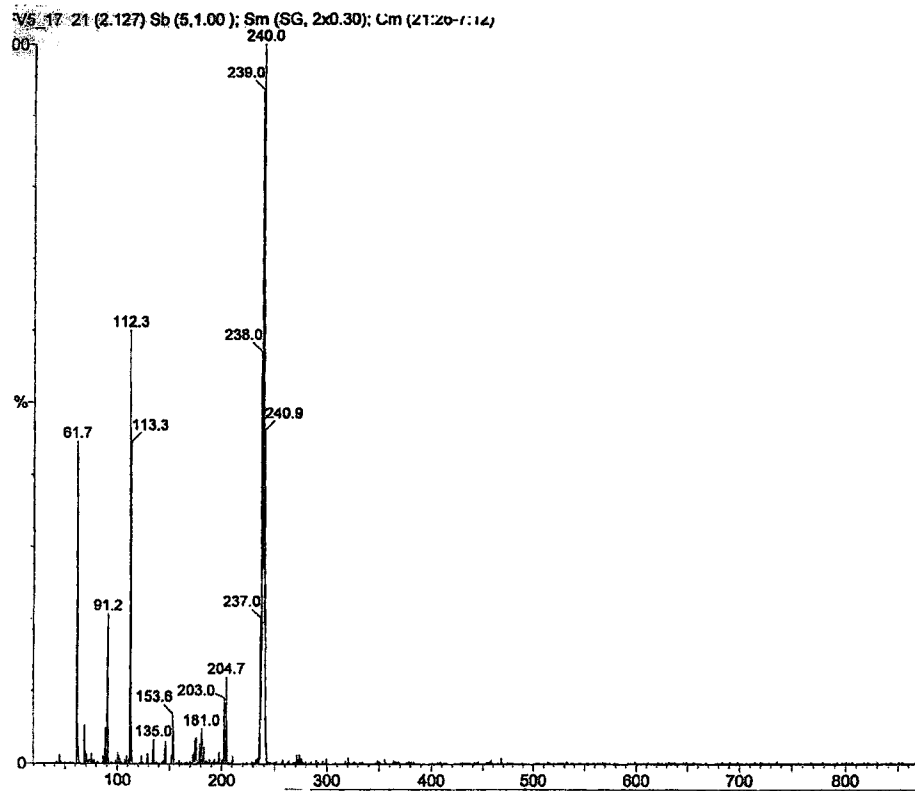


Figure 5-E. Negative Ion Mode ESI-MS of 2.12.

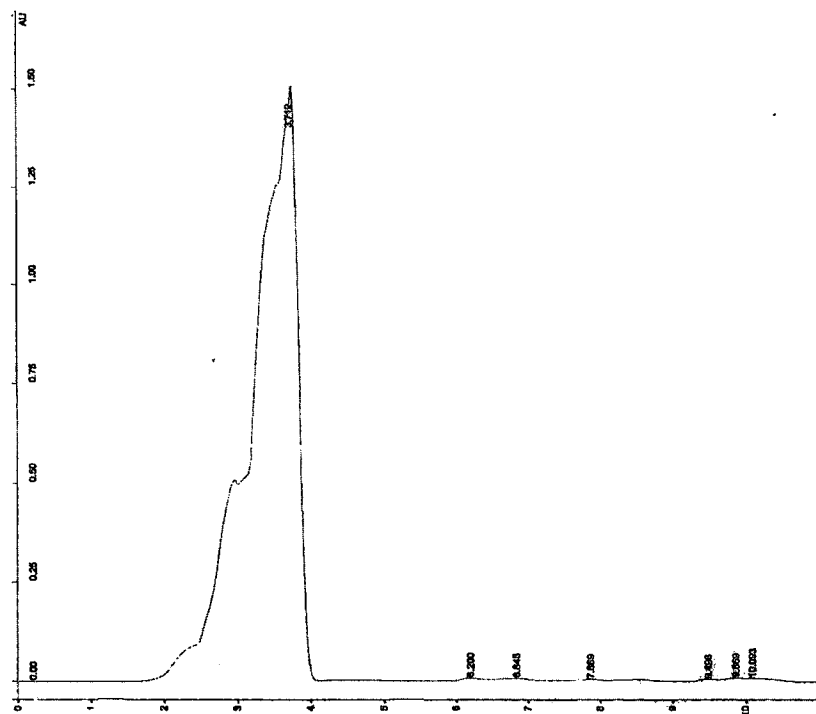


Figure 5-F. Analytical HPLC chromatogram of 2.12.

Chapter 2: Mono-Arylated Carboranes-2.16

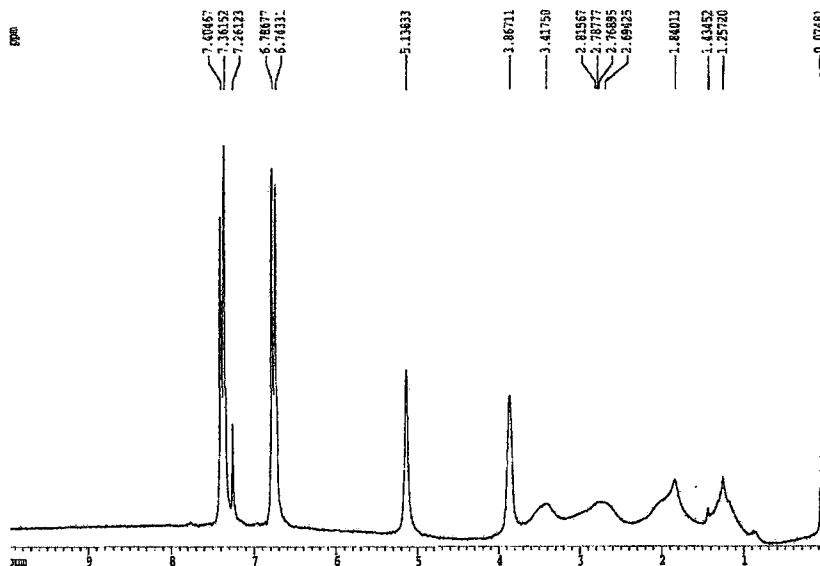


Figure 7-A. ^1H NMR of 2.16, 200 MHz, in CDCl_3 ...

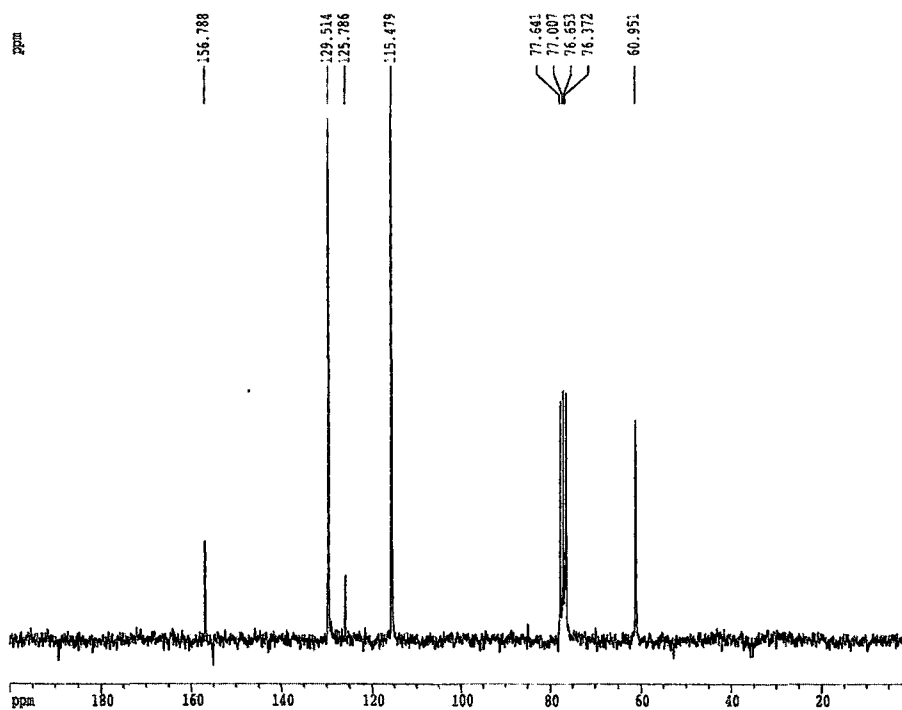


Figure 7-B. $^{13}\text{C}\{\text{H}\}$ NMR of 2.16, 200 MHz, in CDCl_3 .

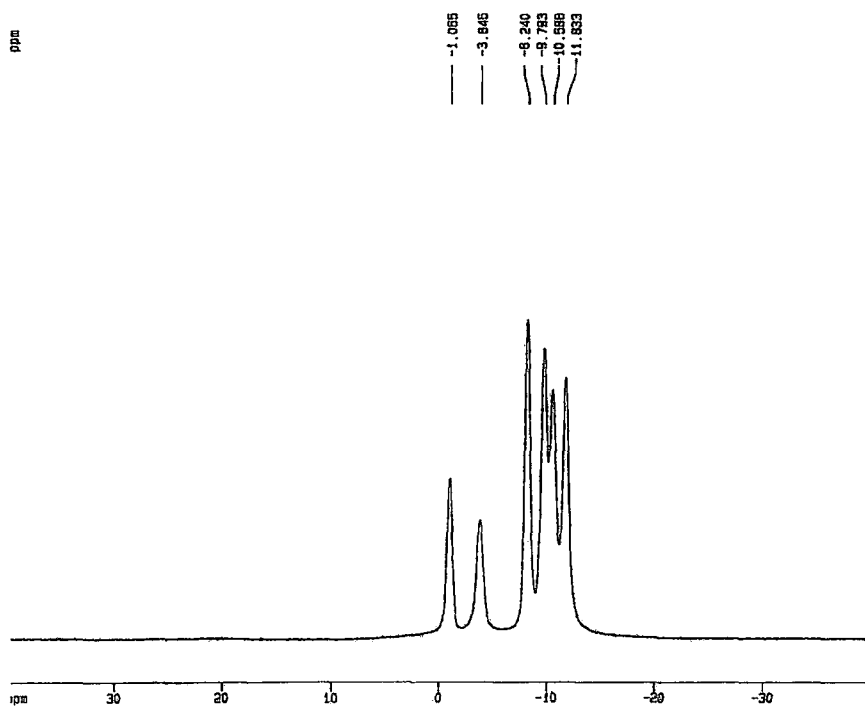


Figure 7-C. $^{11}\text{B}\{\text{H}\}$ NMR of 2.16, 500 MHz, in CDCl_3 .

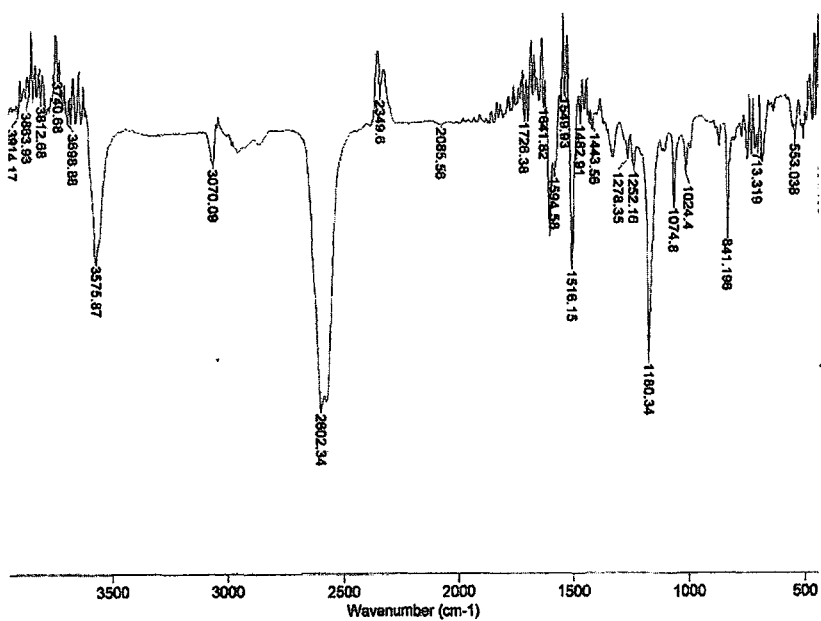


Figure 7-D. FTIR of 2.16, in CH_2Cl_2 .

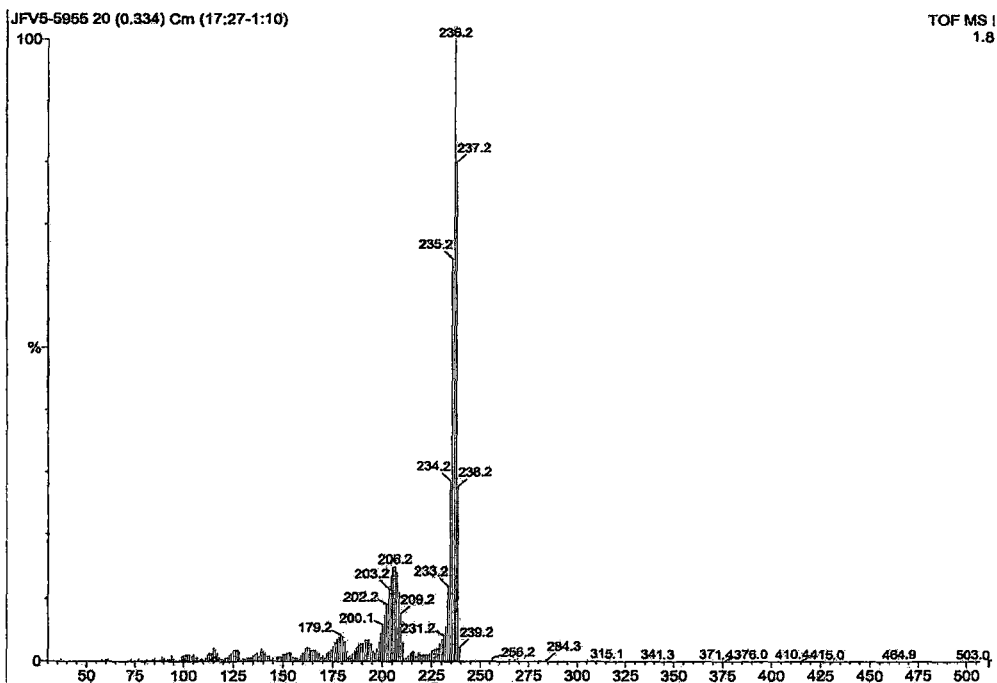


Figure 7-E EI-MS of 2.16.

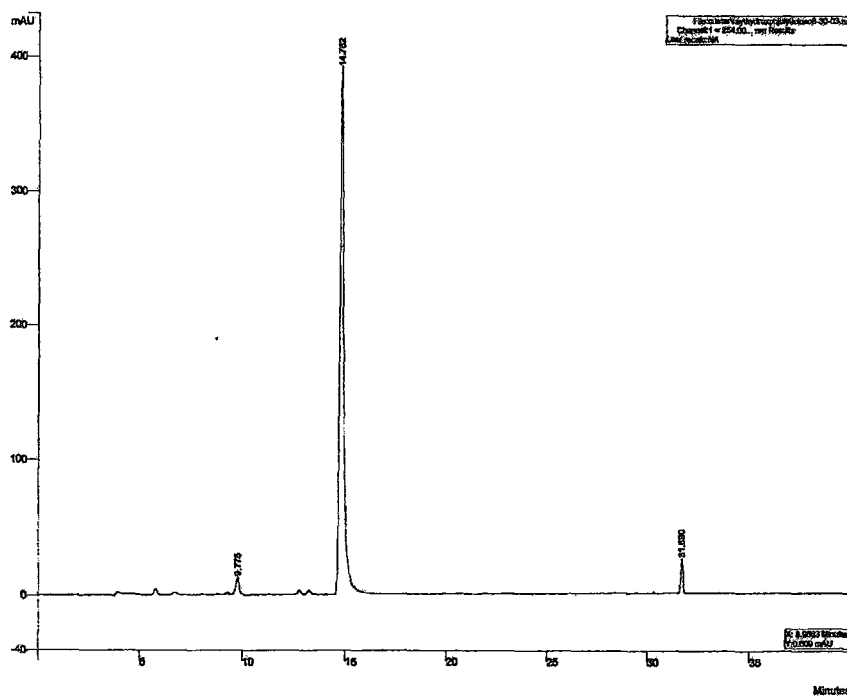


Figure 7-F. Analytical HPLC chromatogram of 2.16.

Chapter 2: Mono-Arylated Carboranes-2.13

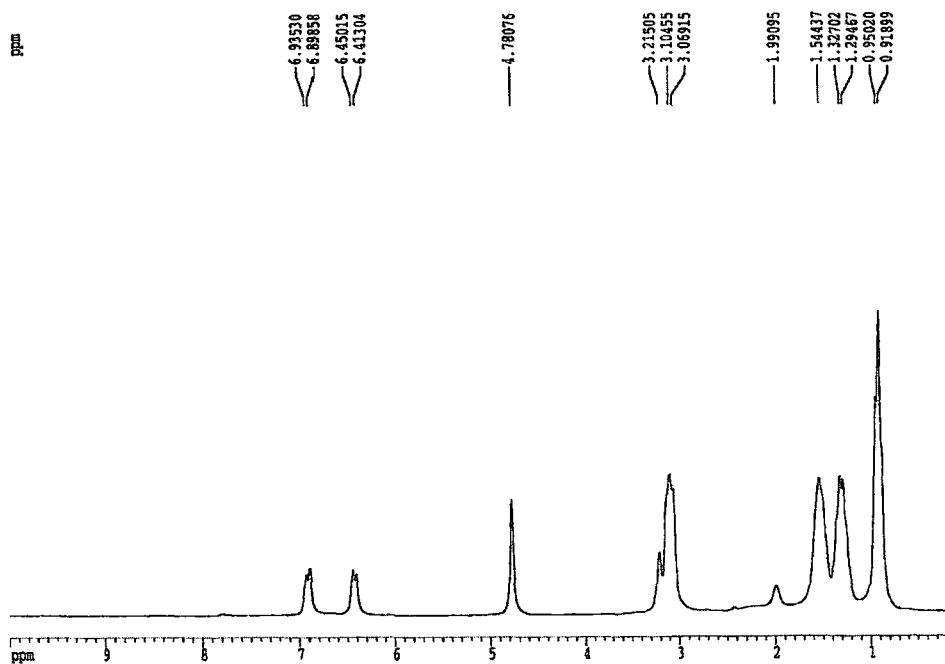


Figure 8-A. ^1H NMR of 2.13, 200 MHz, in CDCl_3 .

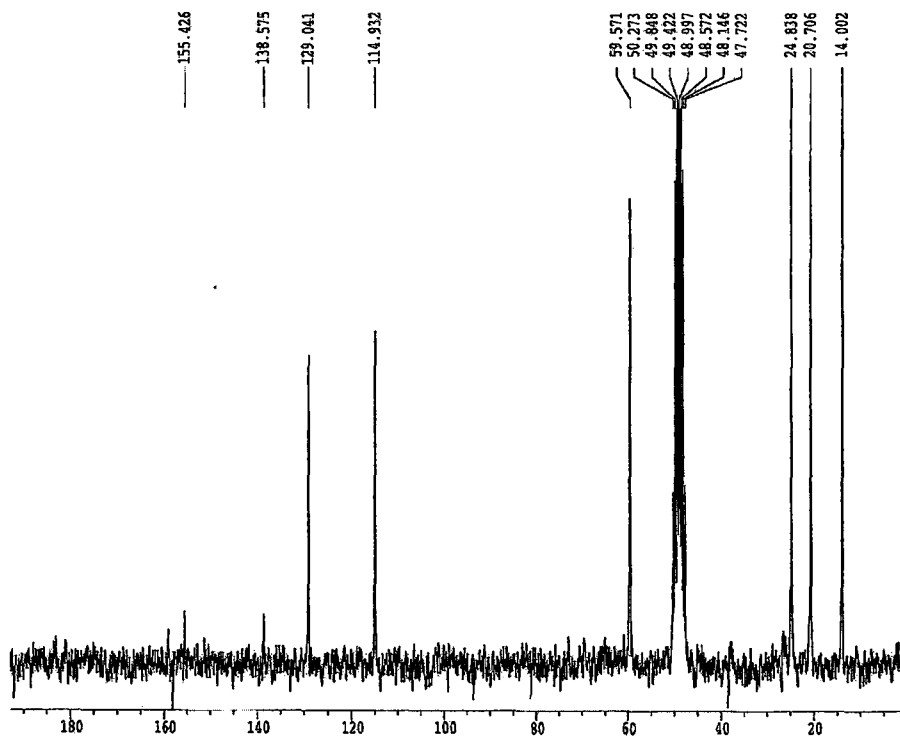


Figure 8-B. $^{13}\text{C}\{^1\text{H}\}$ NMR of 2.13, 200 MHz, in CDCl_3 .

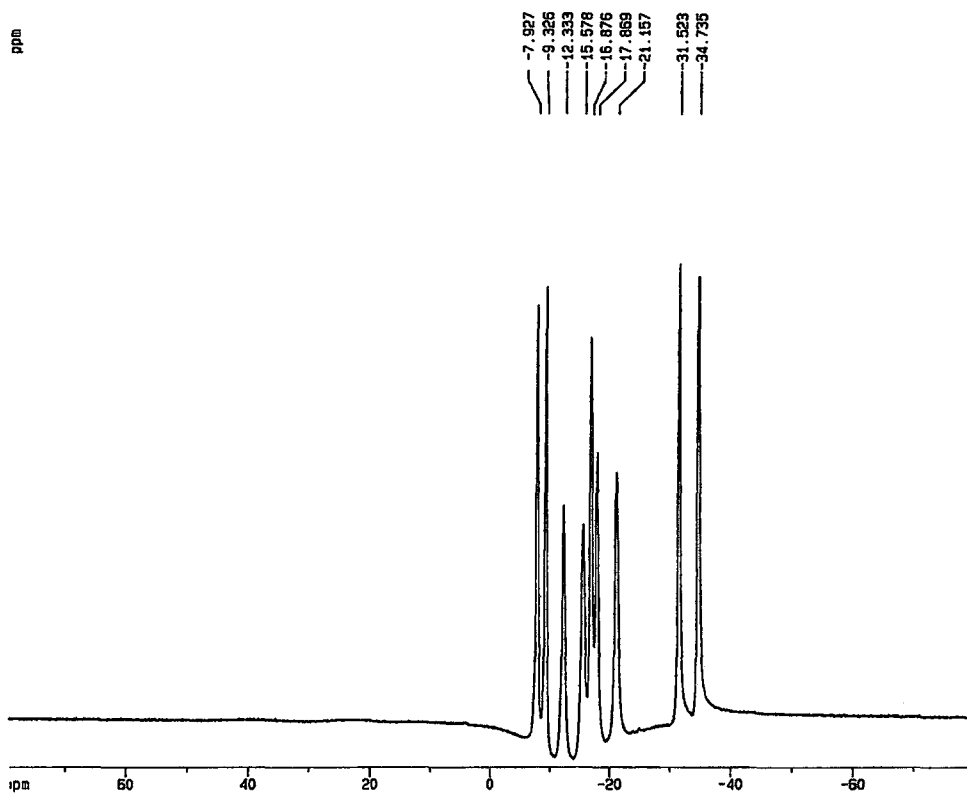


Figure 8-C. $^{11}\text{B}\{\text{H}\}$ NMR of 2.13, 500 MHz, in CDCl_3 .

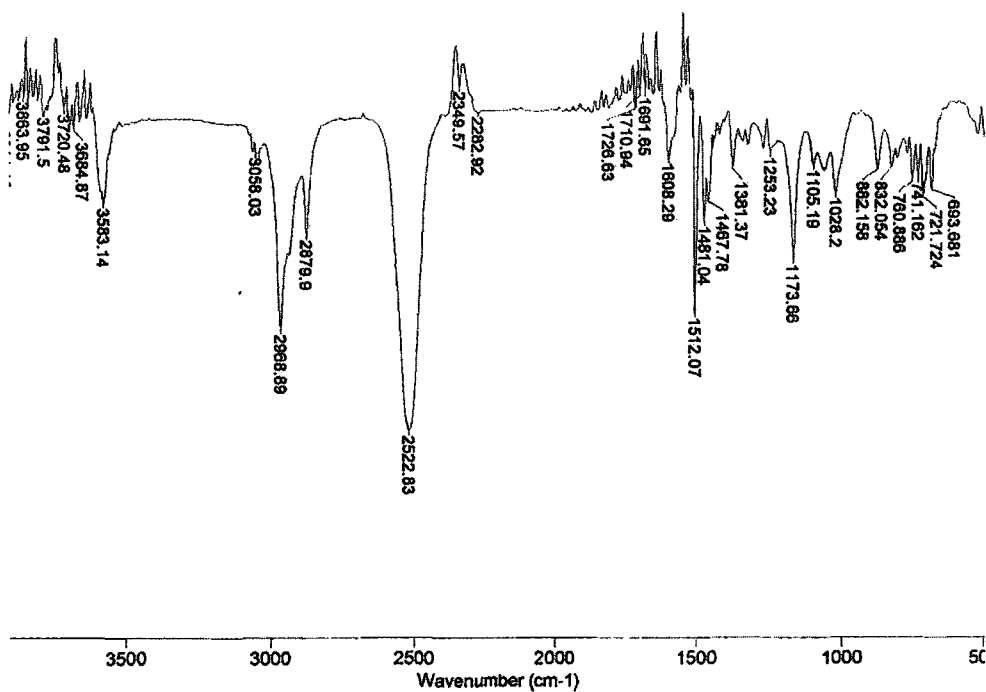


Figure 8-D. FTIR of 2.13, in CH_2Cl_2 .

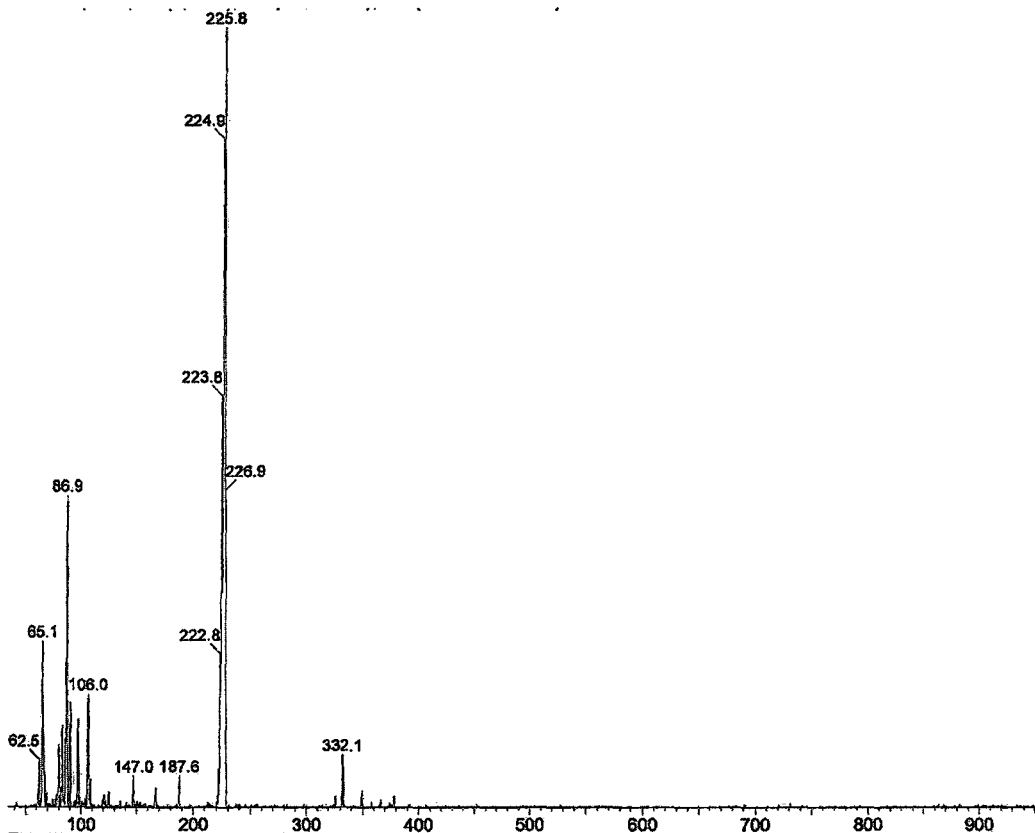


Figure 8-E. Negative Ion Mode ESI-MS of 2.13.

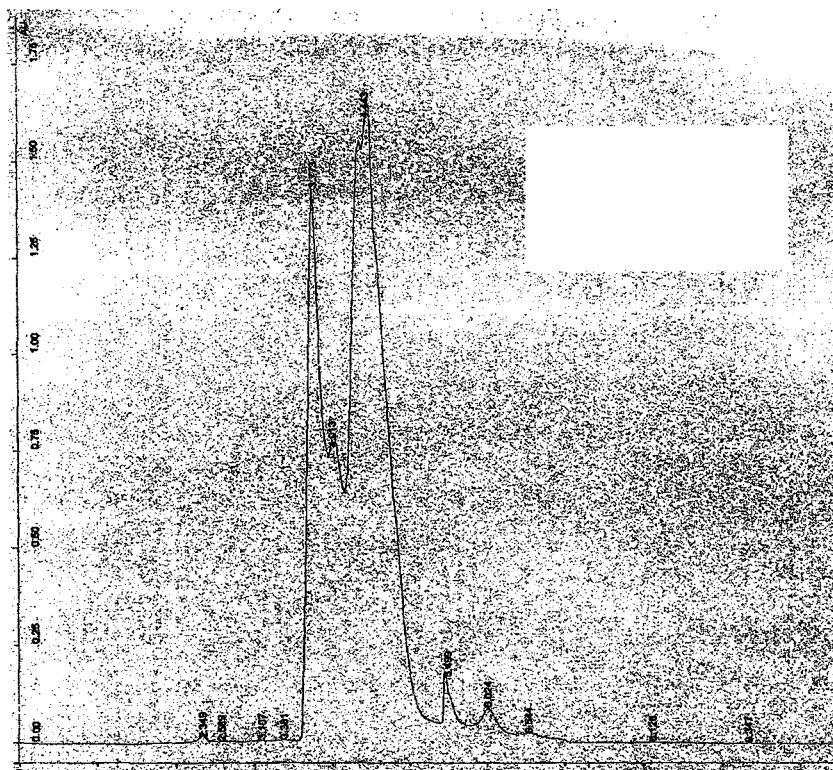


Figure 8-F. Analytical HPLC chromatogram of 2.13

Chapter 2: Mono-Arylated Carboranes-2.10

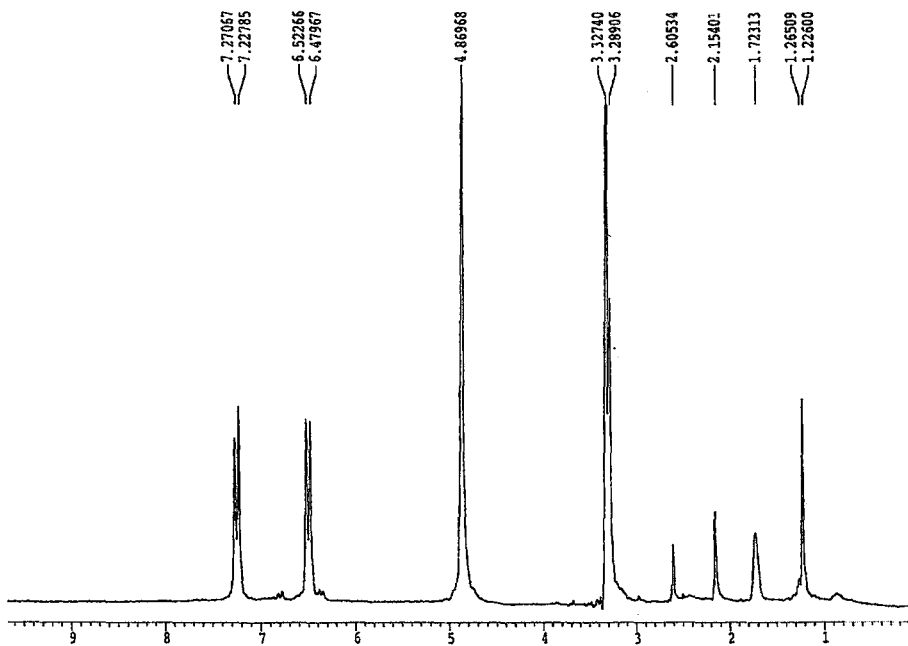


Figure 9-A. ^1H NMR of 2.10, 200 MHz, in CD_3OD .

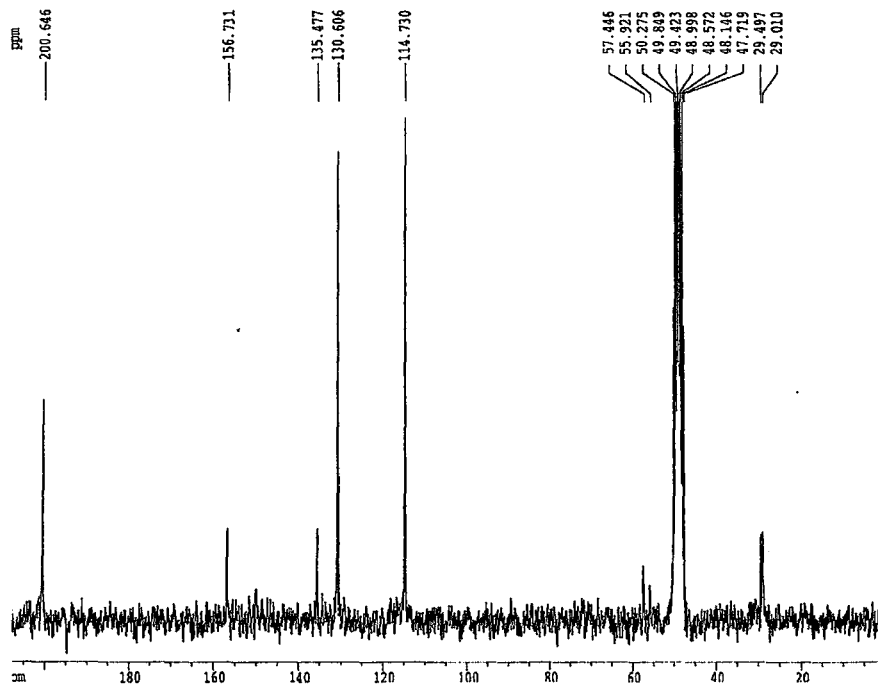


Figure 9-B. $^{13}\text{C}\{\text{H}\}$ NMR of 2.10, 200 MHz, in CD_3OD

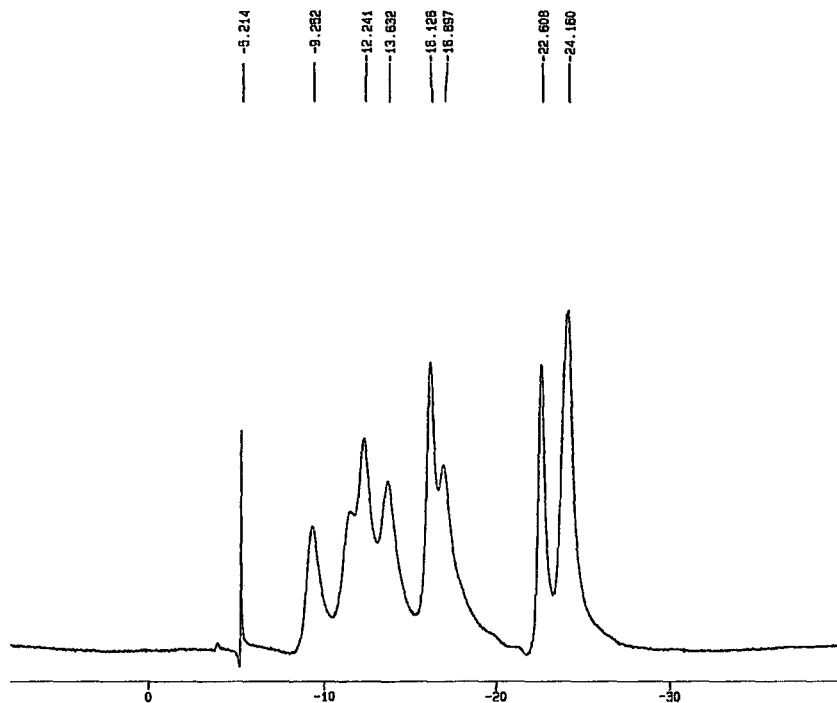


Figure 9-C. $^{11}\text{B}\{\text{H}\}$ NMR of 2.10, 500 MHz, in CD_3OD

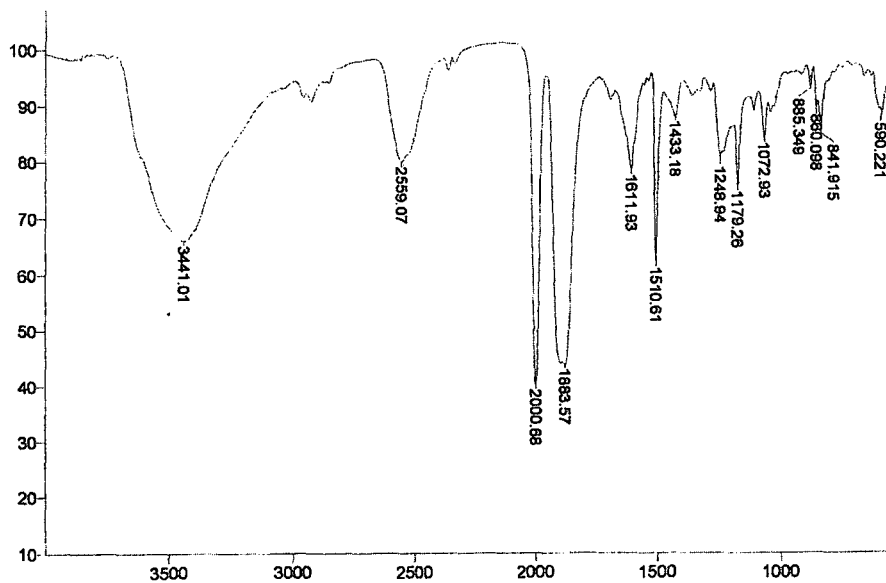


Figure 9-D. FTIR of 2.10, in KBr

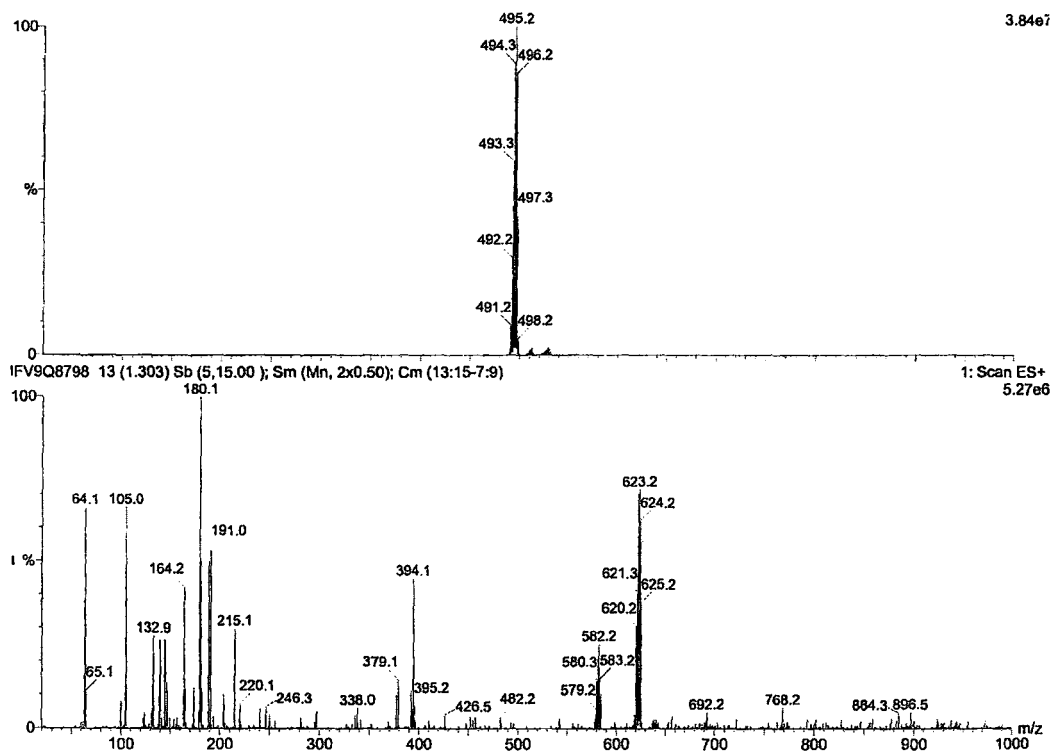


Figure 9-E. Negative Ion Mode ESI-MS of 2.10

Chapter 3: Di-Arylated Carboranes-3.18

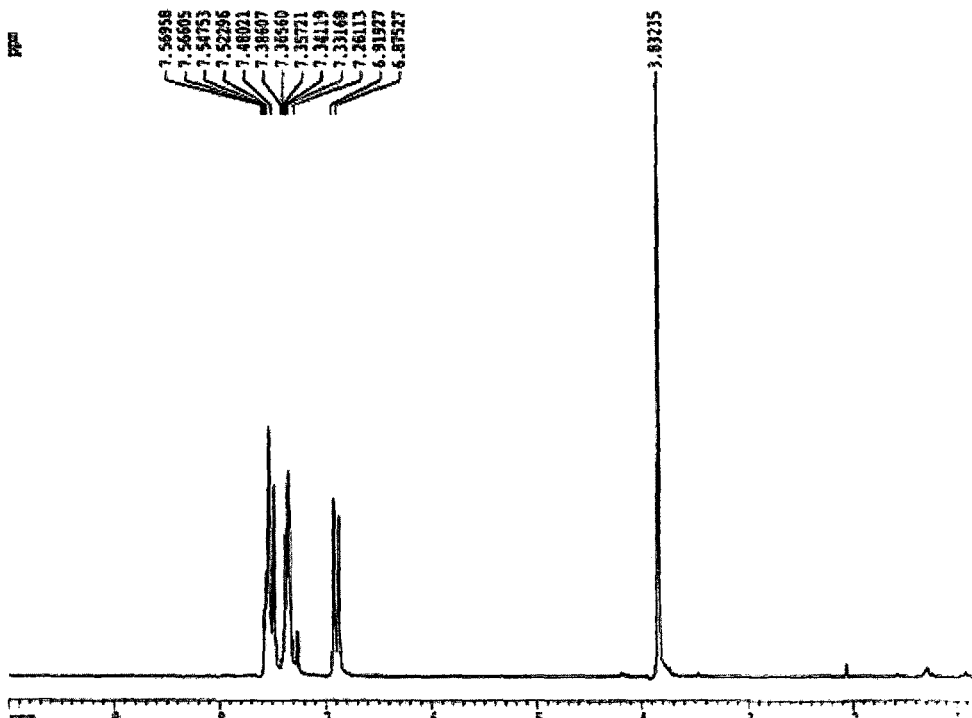


Figure 10-A. ^1H NMR of 3.18, 200 MHz, in CDCl_3 .

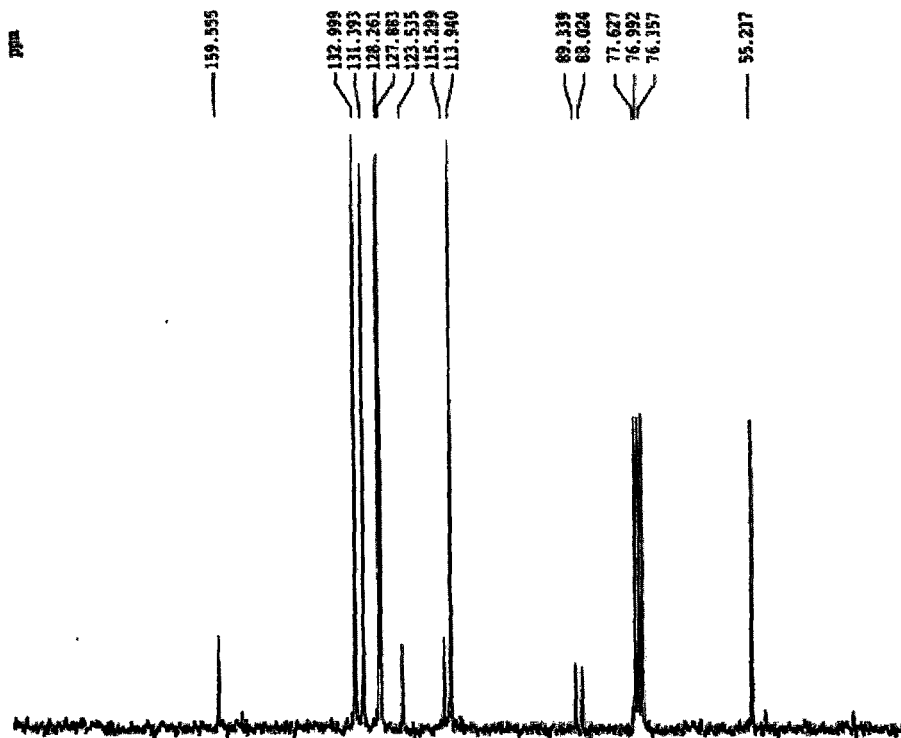


Figure 10-B. $^{13}\text{C}\{^1\text{H}\}$ NMR of 3.18, 200 MHz, in CDCl_3 .

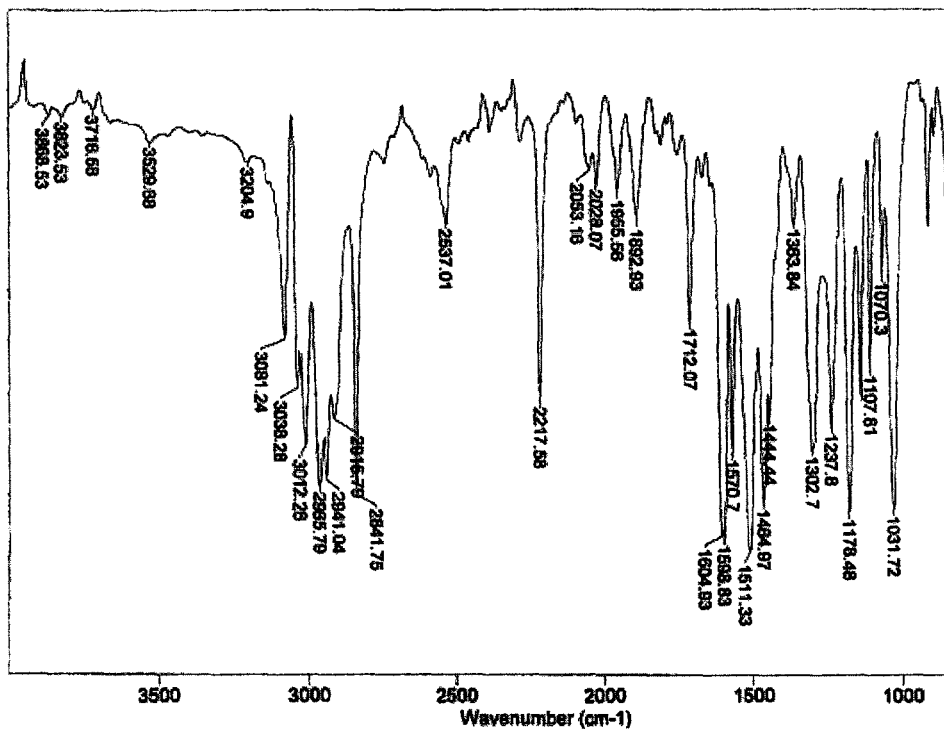


Figure 10-C. FTIR of 3.18, in CH₂Cl₂.

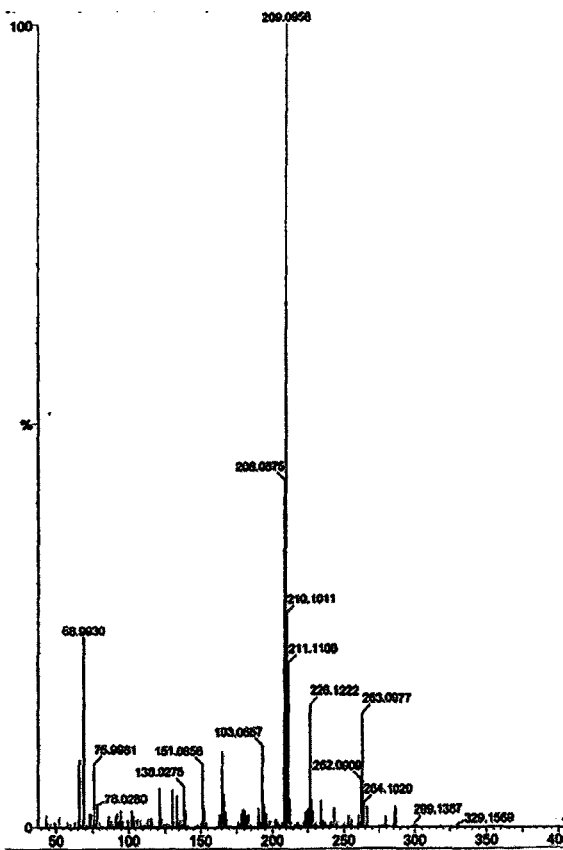


Figure 10-D. EI-MS of 3.18.

Chapter 3: Di-Arylated Carboranes-3.14

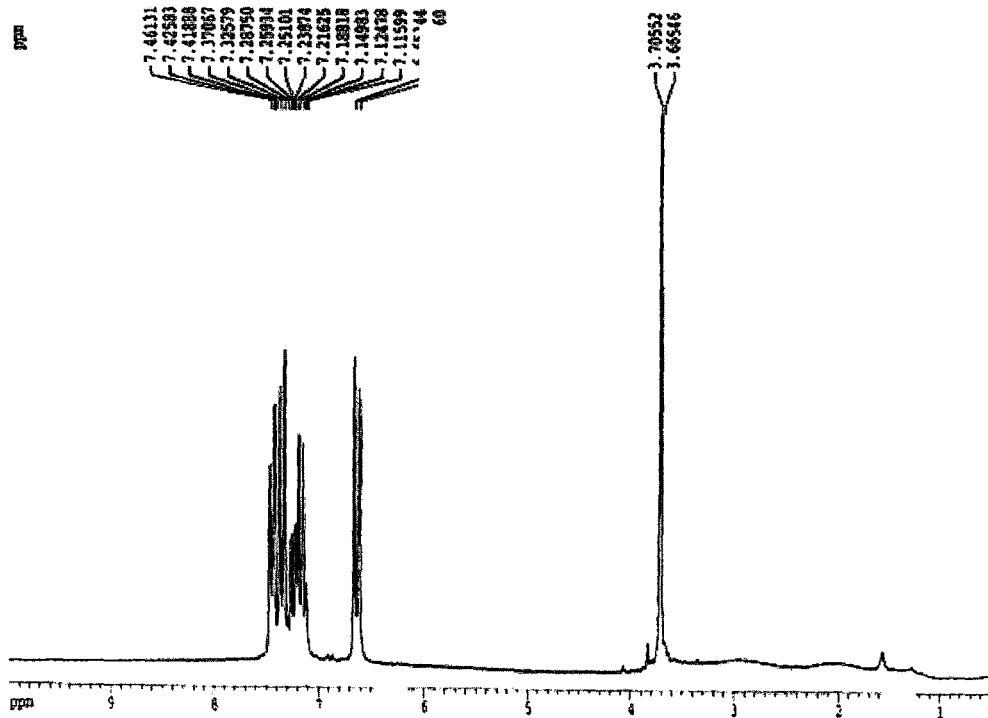


Figure 11-A. ^1H NMR of 3.14, 200 MHz, in CDCl_3 .

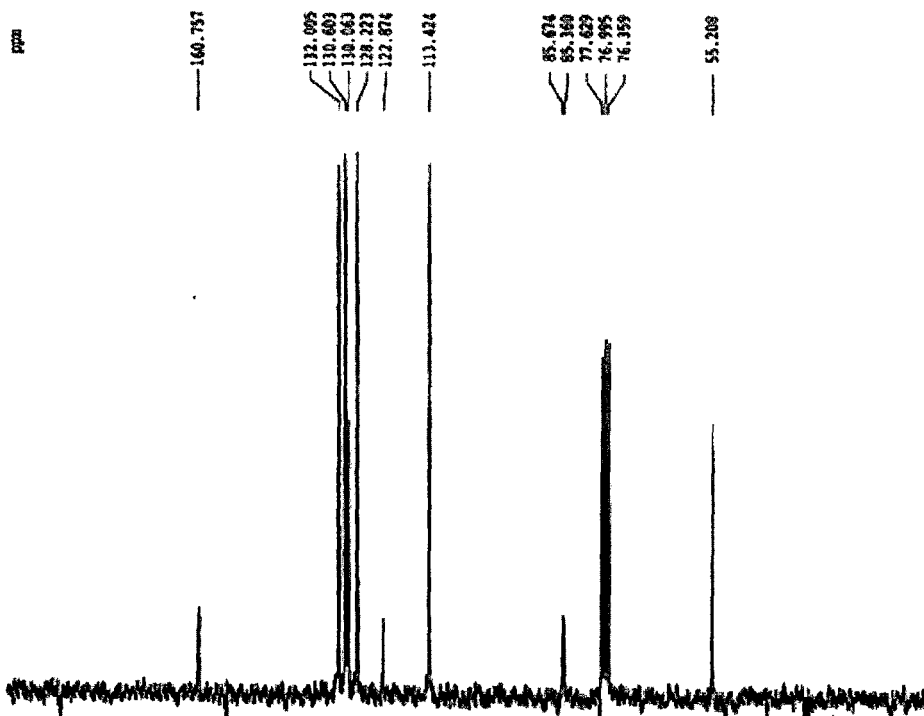


Figure 11-B. $^{13}\text{C}\{^1\text{H}\}$ NMR of 3.14, 200 MHz, in CDCl_3 .

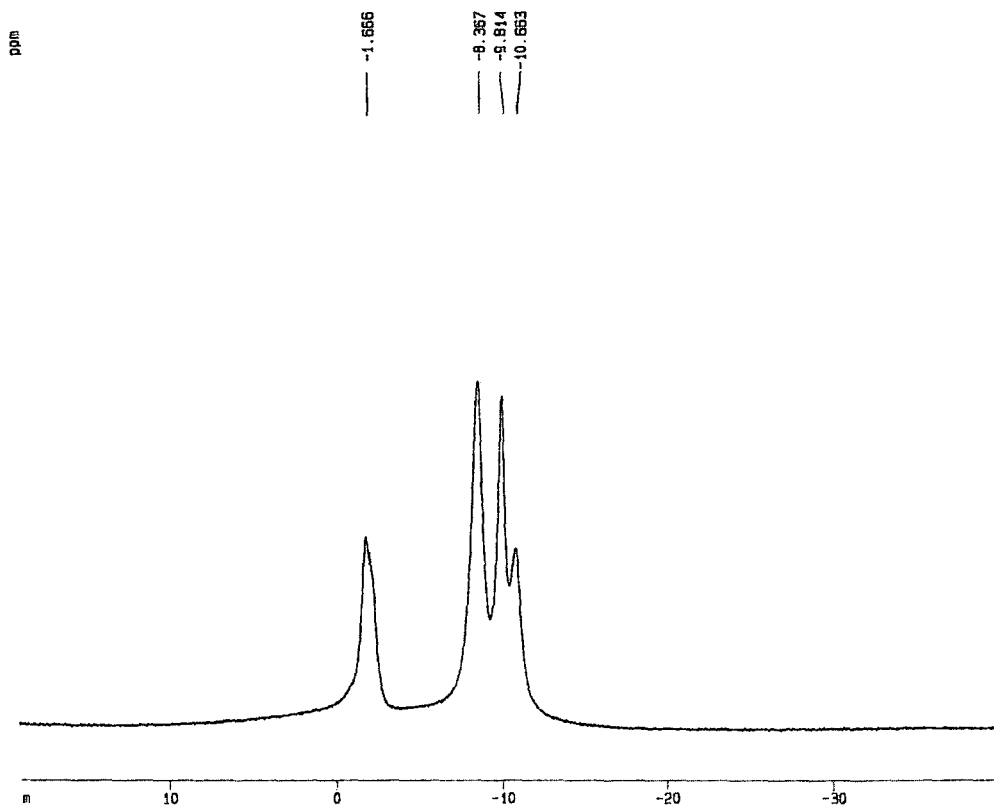


Figure 11-C. $^{11}\text{B}\{\text{H}\}$ NMR of 3.14, 500 MHz, in CDCl_3 .

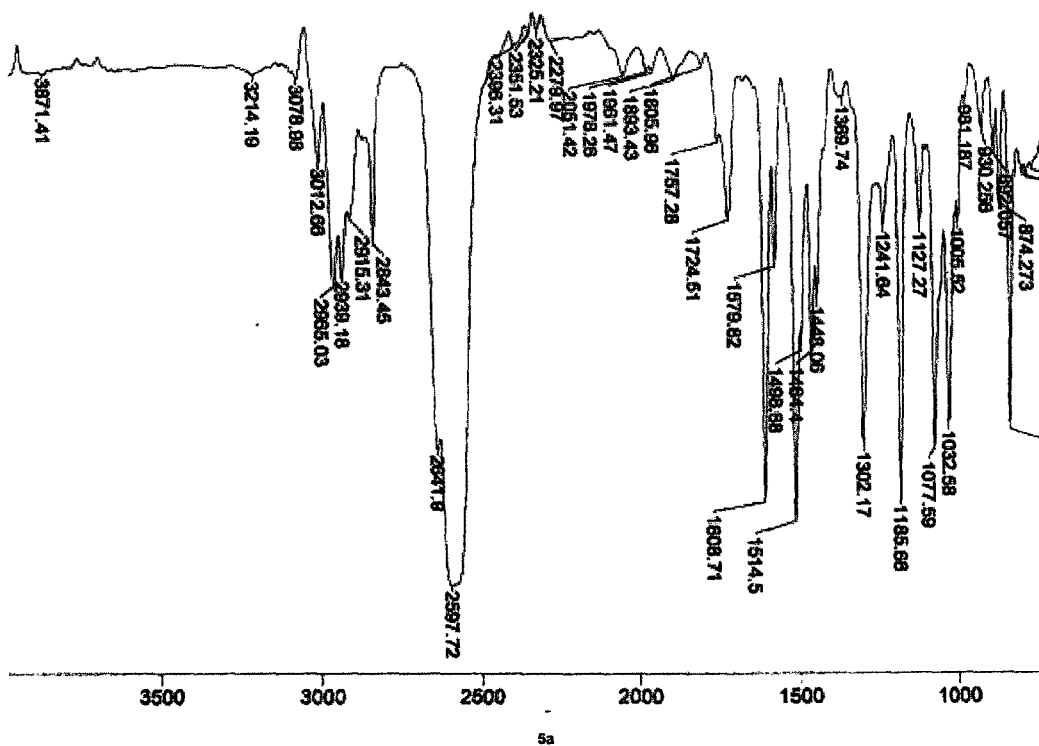


Figure 11-D. FTIR of 3.14, in CH_2Cl_2

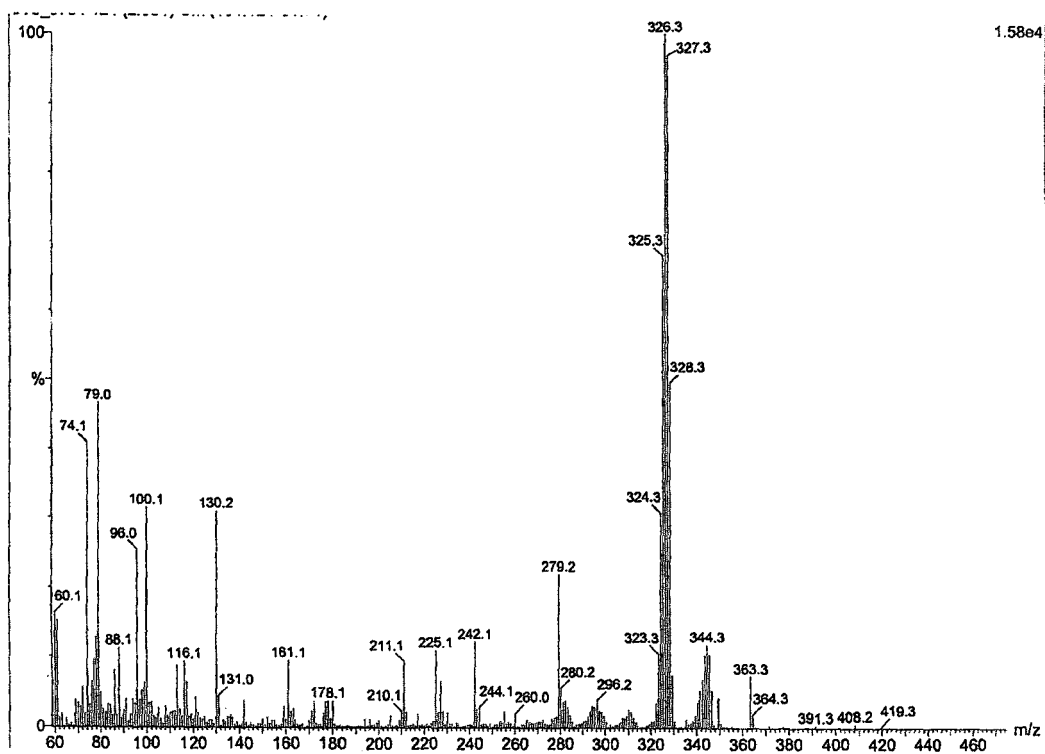


Figure 11-E. EI-MS of 3.14.

Chapter 3: Di-Arylated Carboranes-3.10

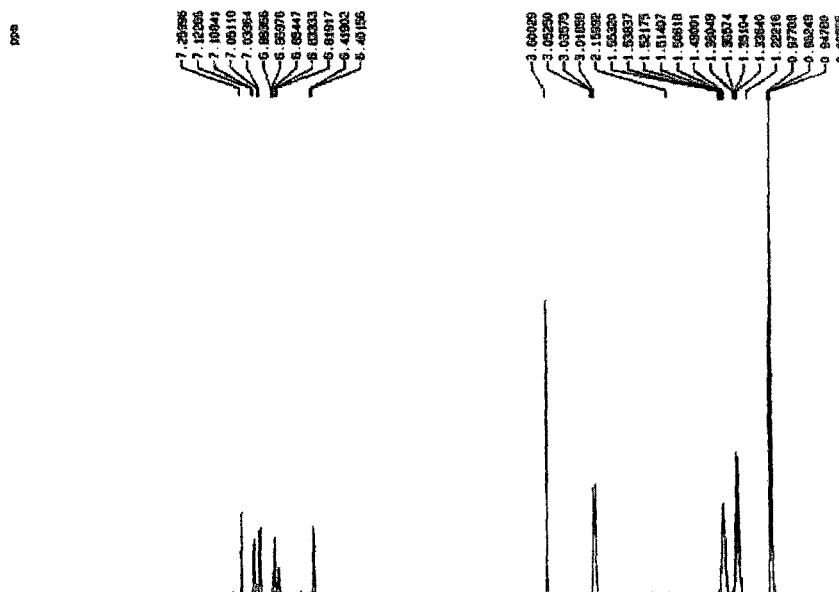


Figure 12-A. ^1H NMR of 3.10, 500 MHz, in CDCl_3

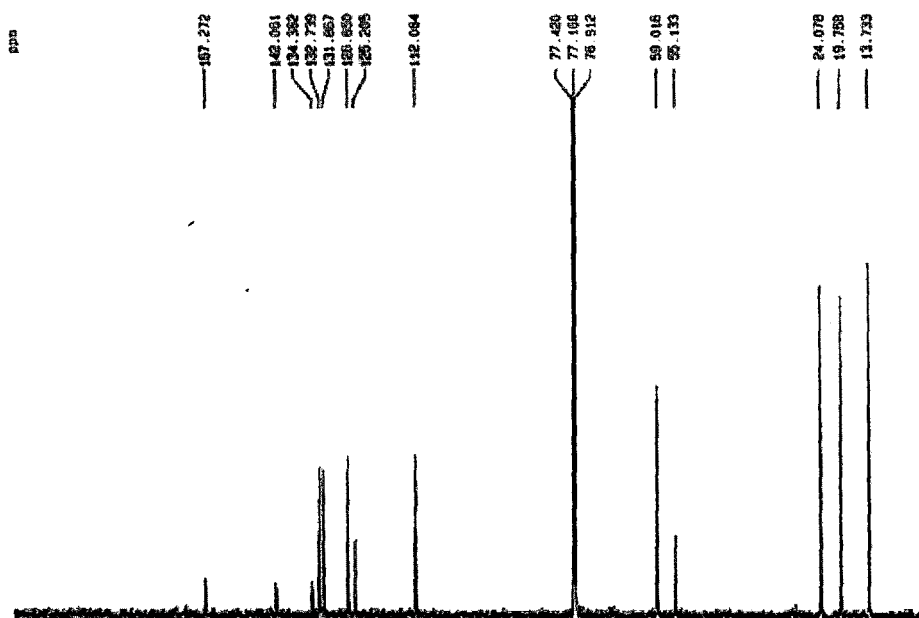


Figure 12-B. $^{13}\text{C}\{^1\text{H}\}$ NMR of 3.10, 500 MHz, in CDCl_3 .

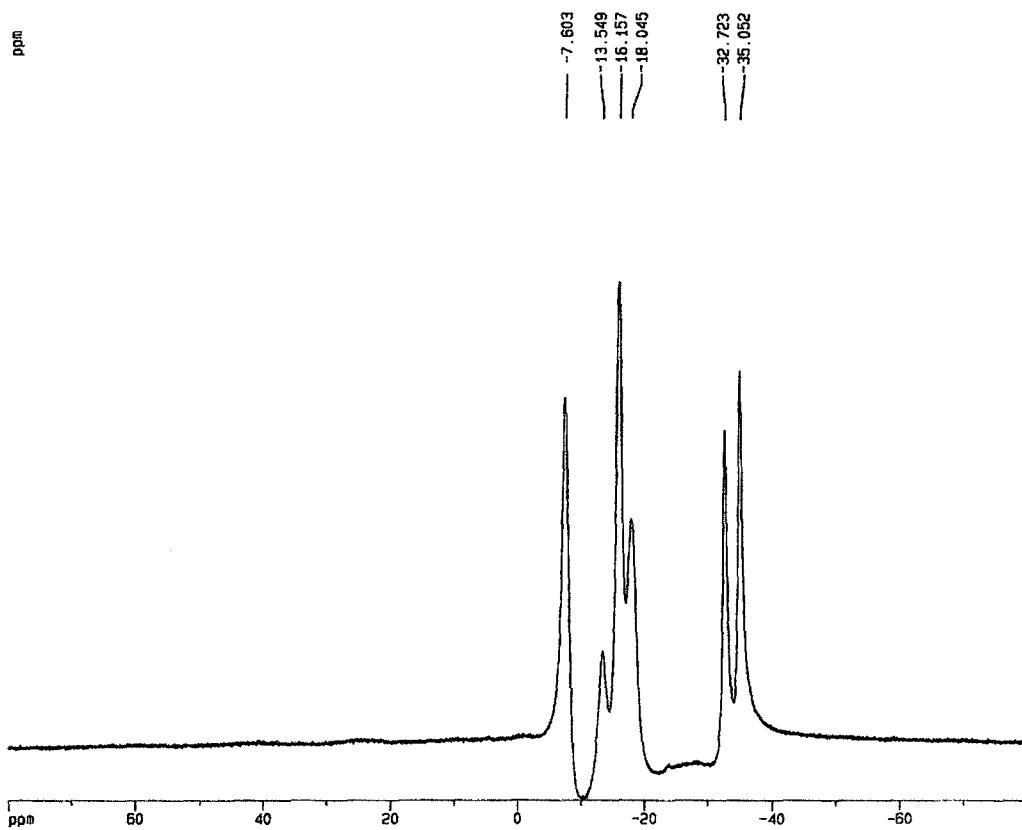


Figure 12-C. $^{11}\text{B}\{\text{H}\}$ NMR of 3.10, 500 MHz, in CDCl_3 .

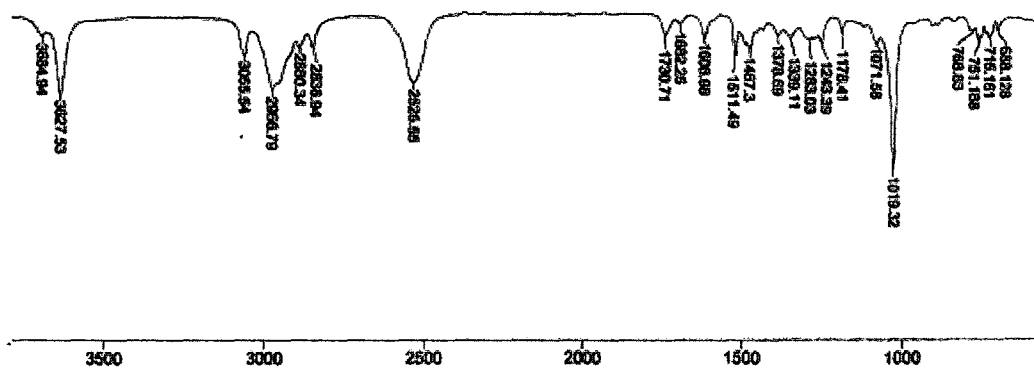


Figure 12-D. FTIR of 3.10, in CH_2Cl_2 .

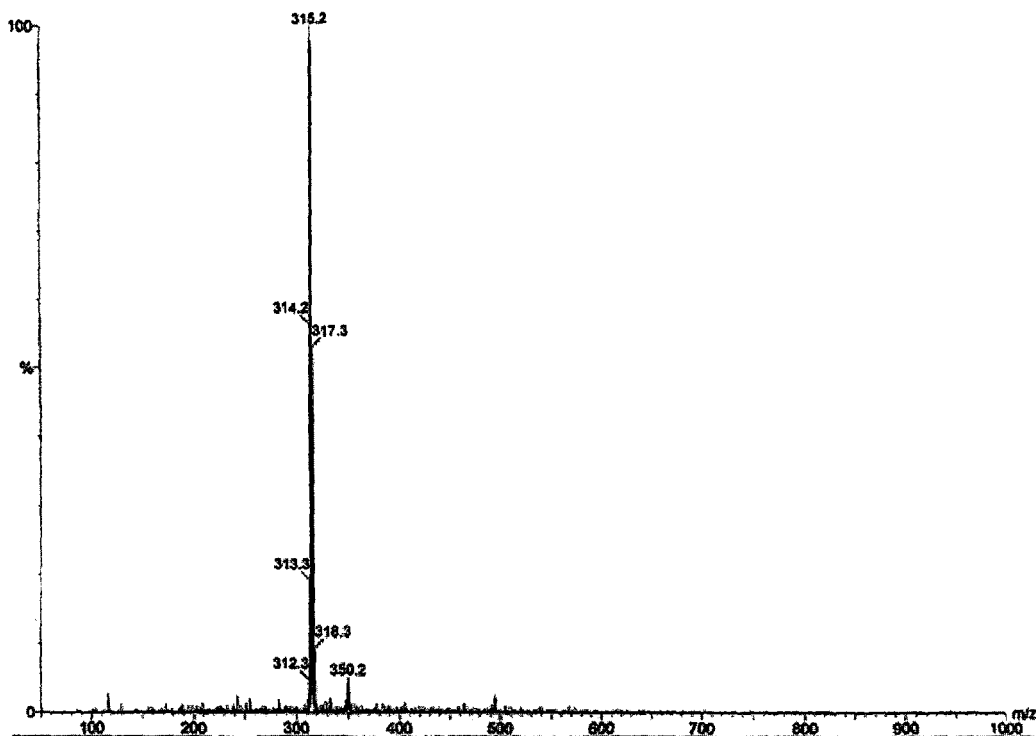


Figure 12-E. Negative Ion Mode ESI-MS of 3.10.

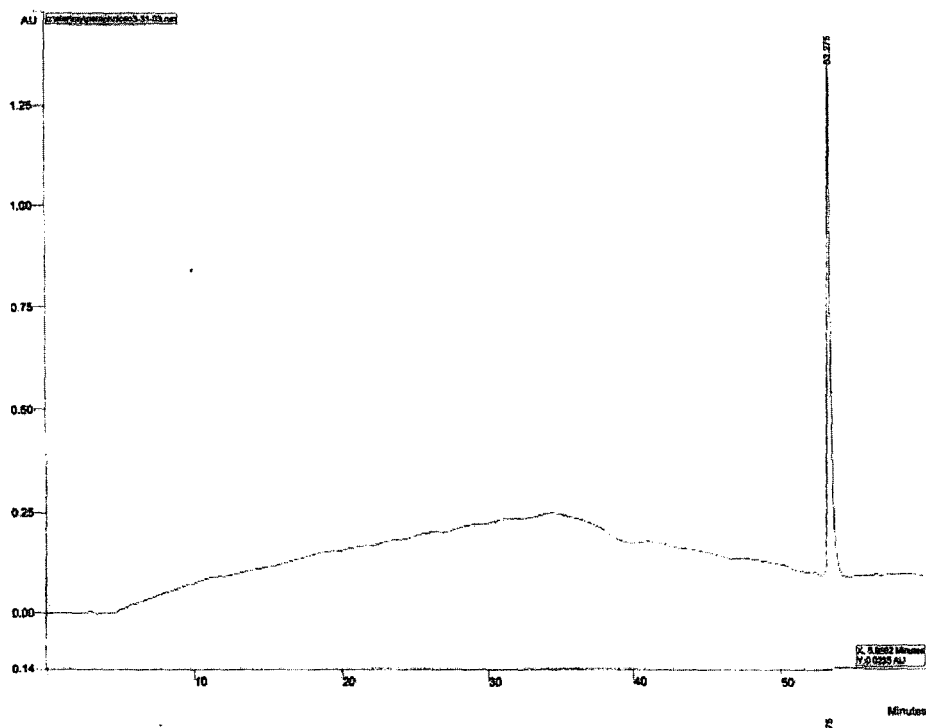


Figure 12-F. Analytical HPLC chromatogram of 3.10

Chapter 3: Di-Arylated Carboranes-3.6

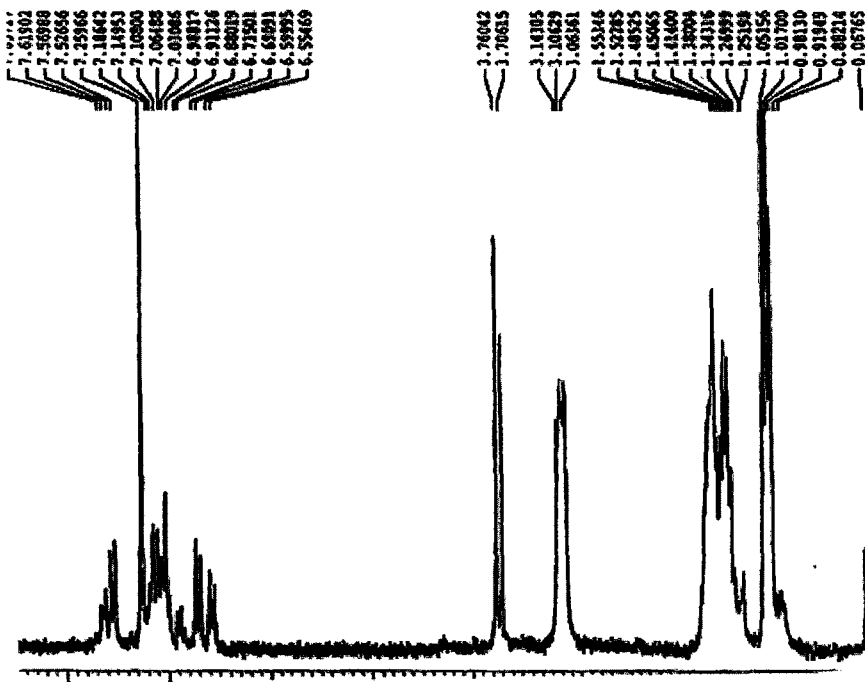


Figure 13-A. ^1H NMR of 3.6, 200 MHz, in CDCl_3 .

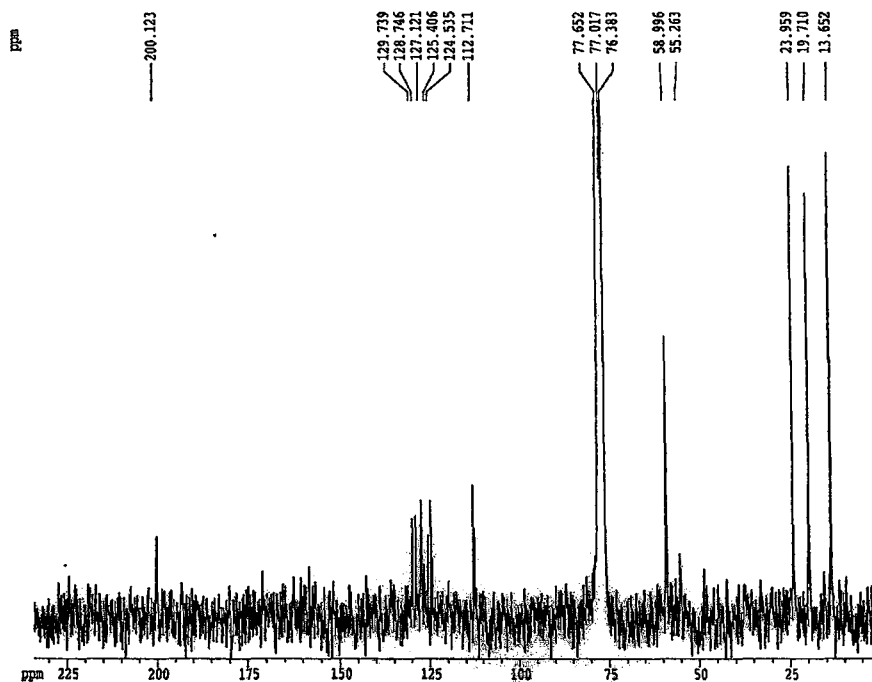


Figure 13-B. $^{13}\text{C}\{^1\text{H}\}$ NMR of 3.6, 200 MHz, in CDCl_3 .

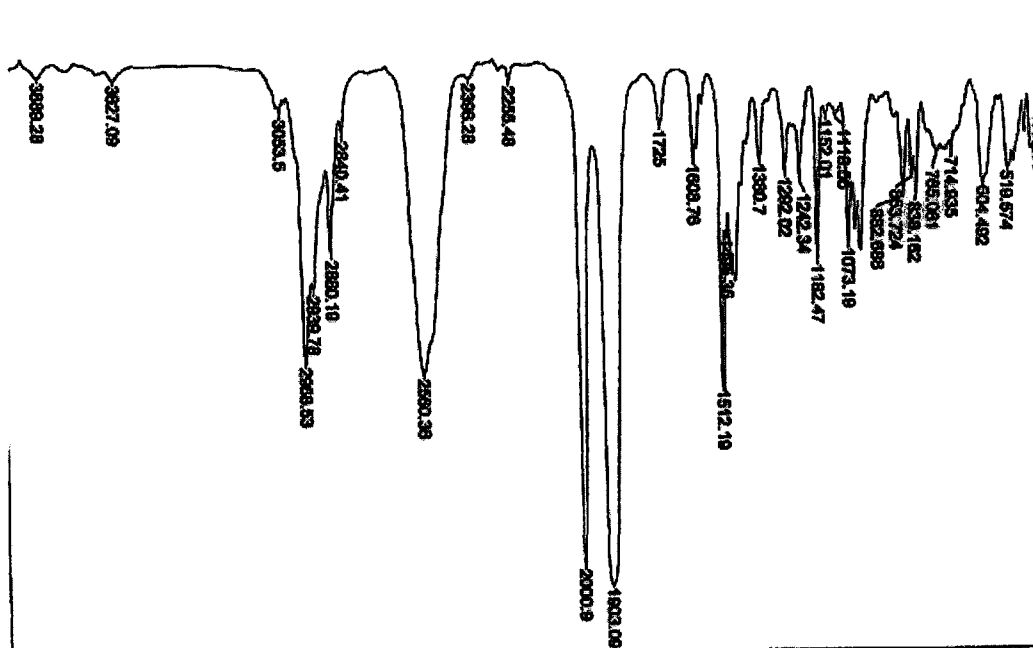


Figure 13-C. FTIR of 3.6, in CH₂Cl₂.

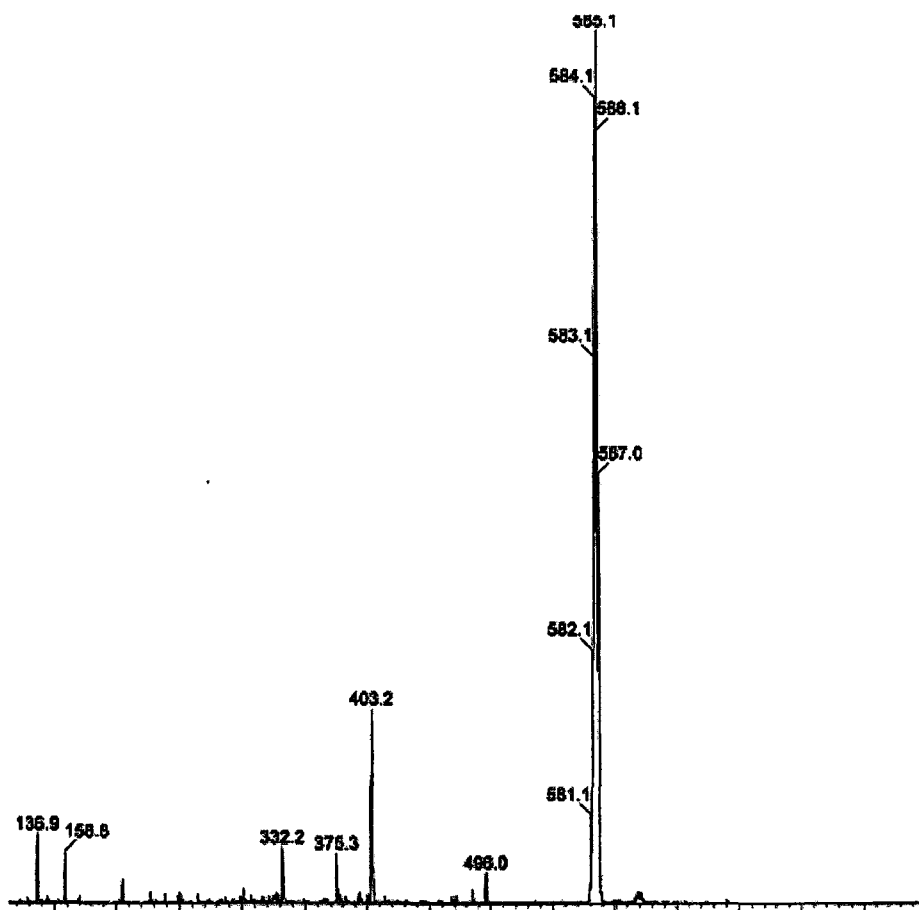


Figure 13-D. Negative Ion Mode ESI-MS of 3.6.

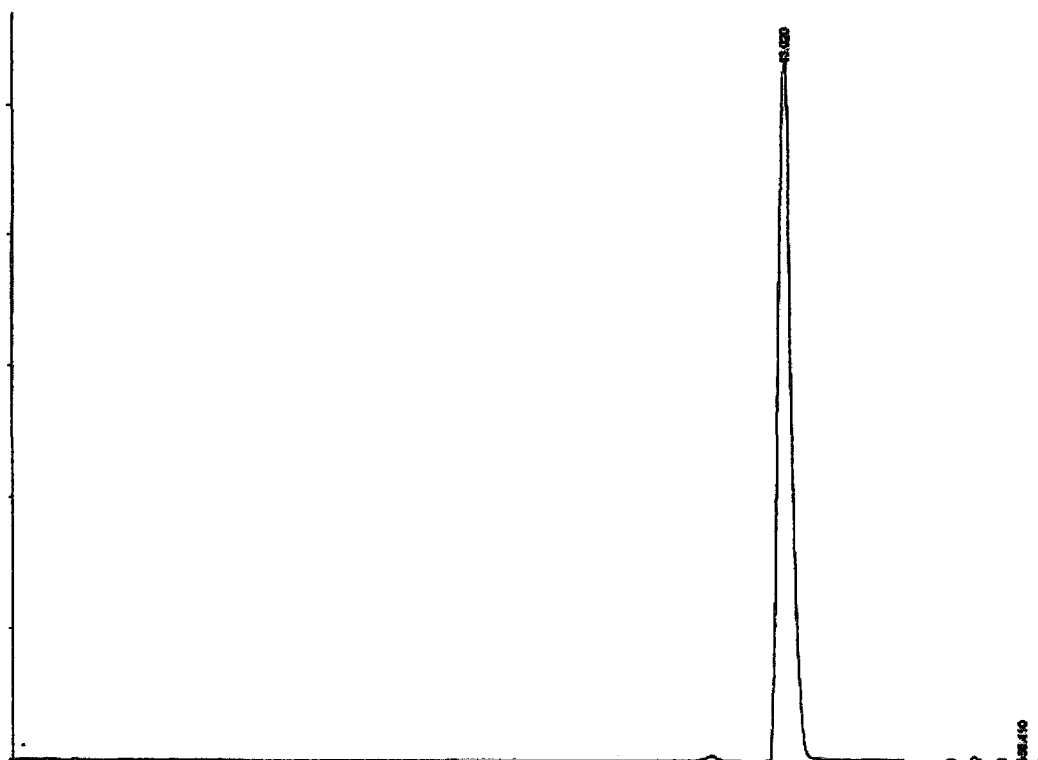


Figure 13-E. Analytical HPLC chromatogram of 3.6

Chapter 3: Di-Arylated Carboranes-3.19

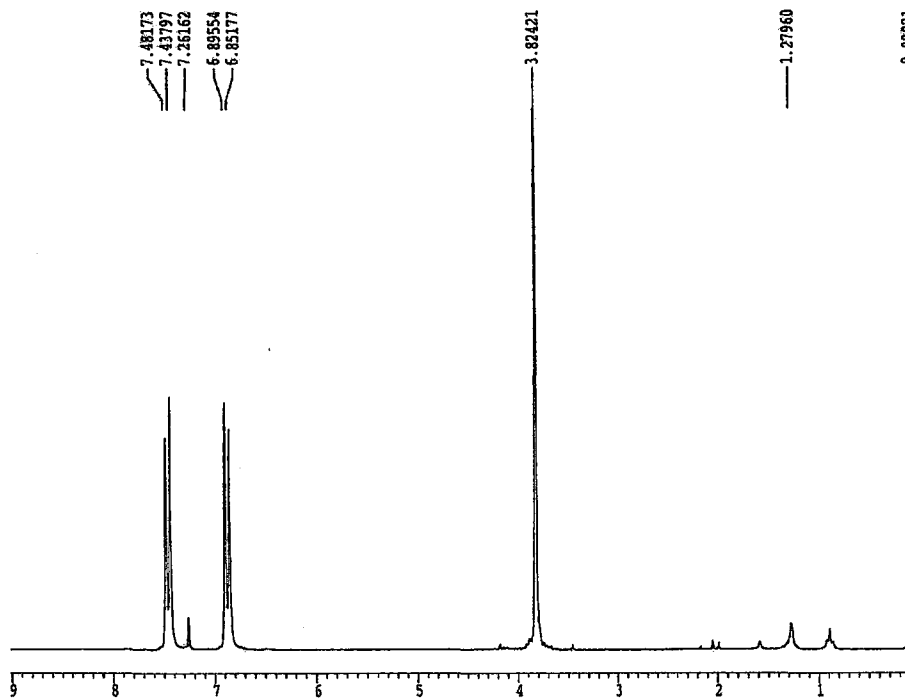


Figure 14-A. ^1H NMR of 3.19, 200 MHz, in CDCl_3 .

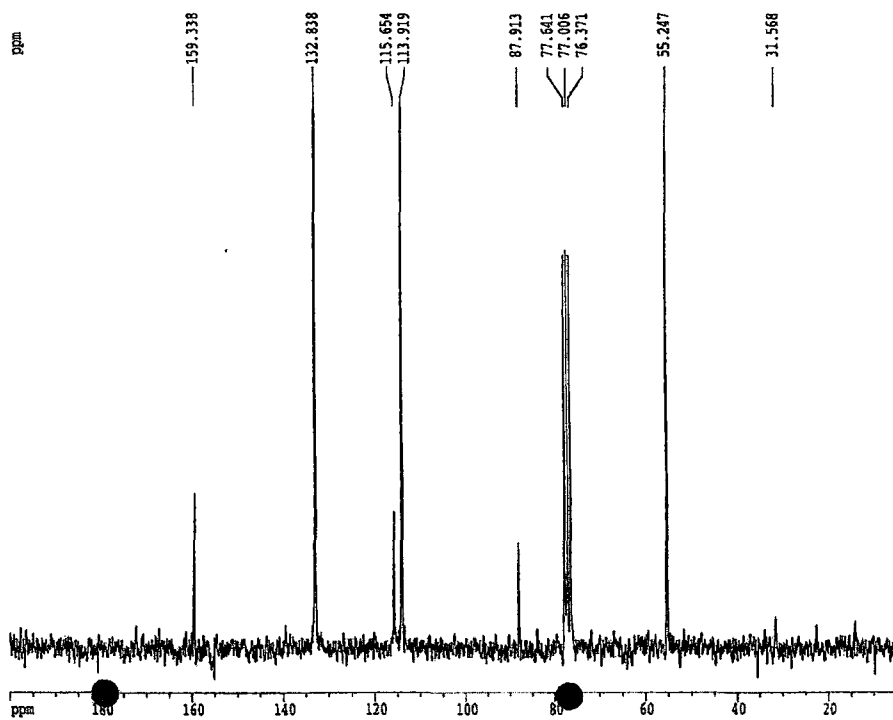


Figure 14-B. $^{13}\text{C}\{^1\text{H}\}$ NMR of 3.19, 200 MHz, in CDCl_3 .

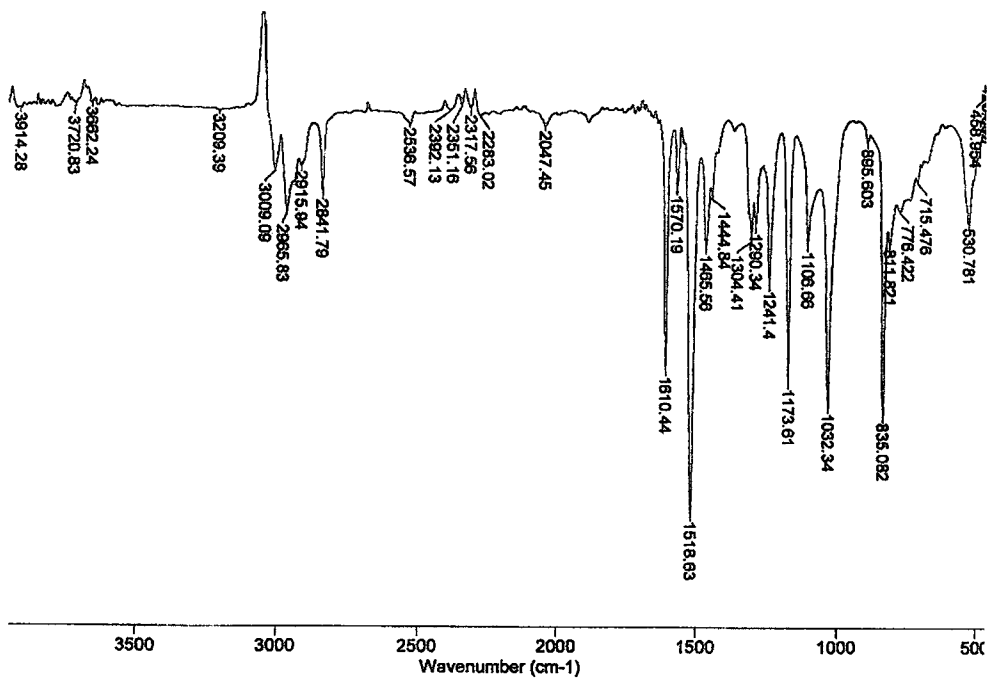


Figure 14-C. FTIR of 3.19, in CH₂Cl₂.

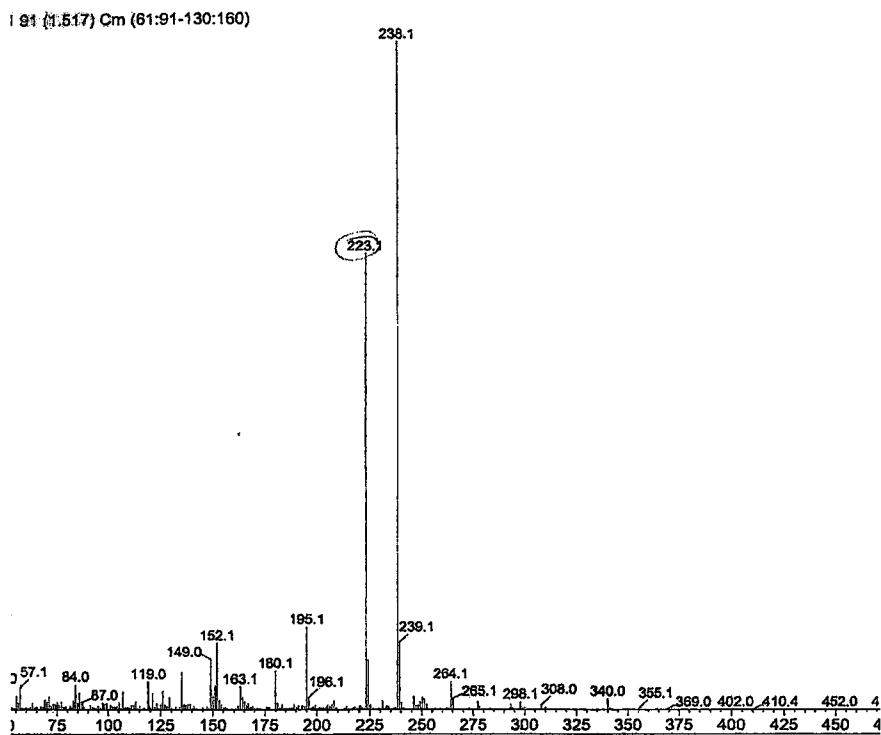


Figure 14-D. EI-MS of 3.19.

Chapter 3: Di-Arylated Carboranes-3.20

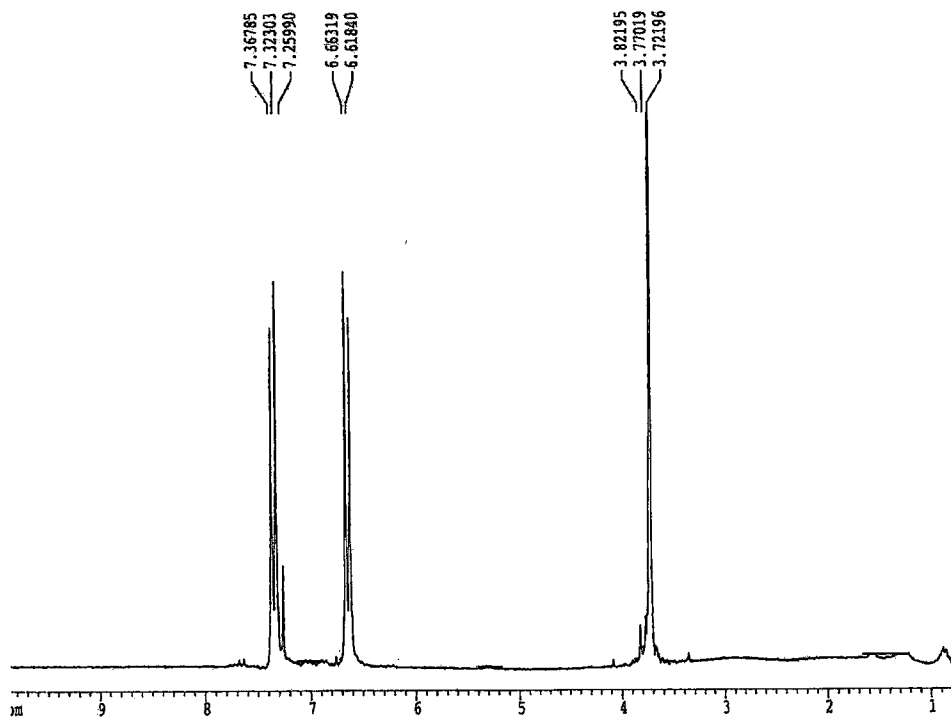


Figure 15-A. ^1H NMR of 3.20, 200 MHz, in CDCl_3 .

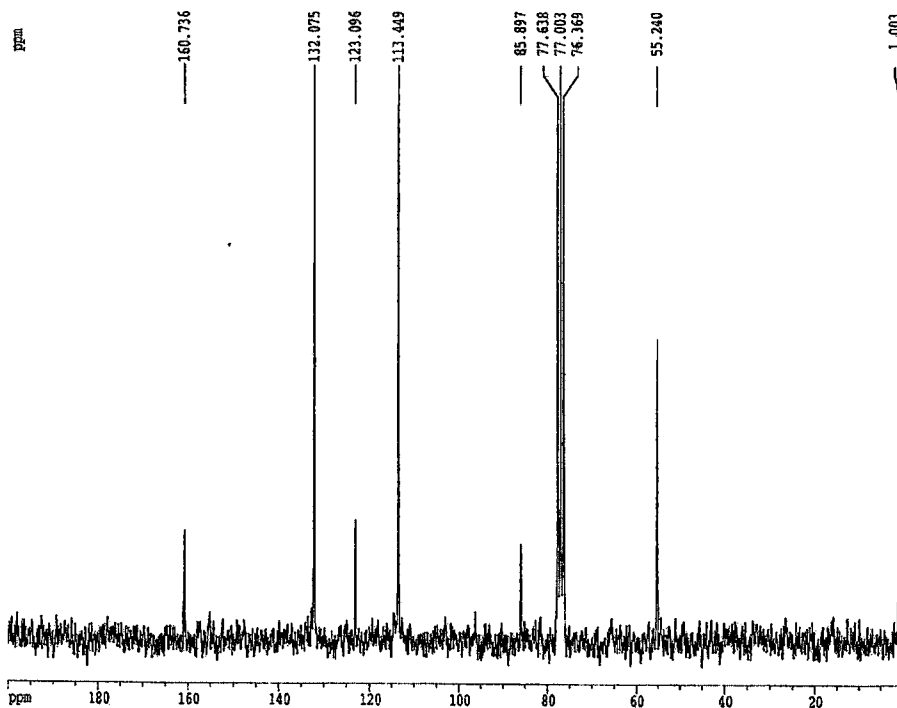


Figure 15-B. $^{13}\text{C}\{\text{H}\}$ NMR of 3.20, 200 MHz, in CDCl_3 .

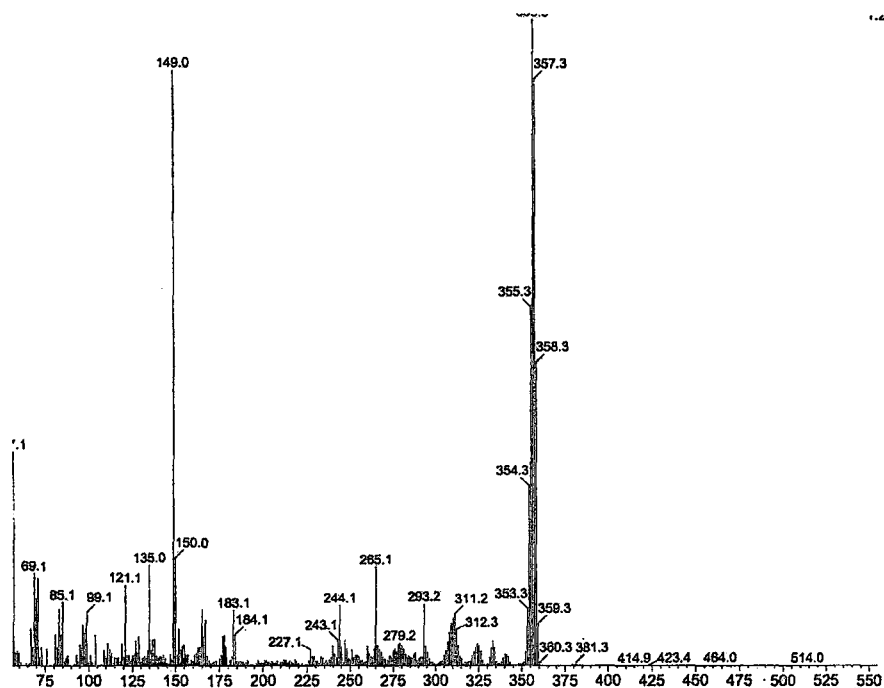


Figure 15-E. EI-MS of 3.20.

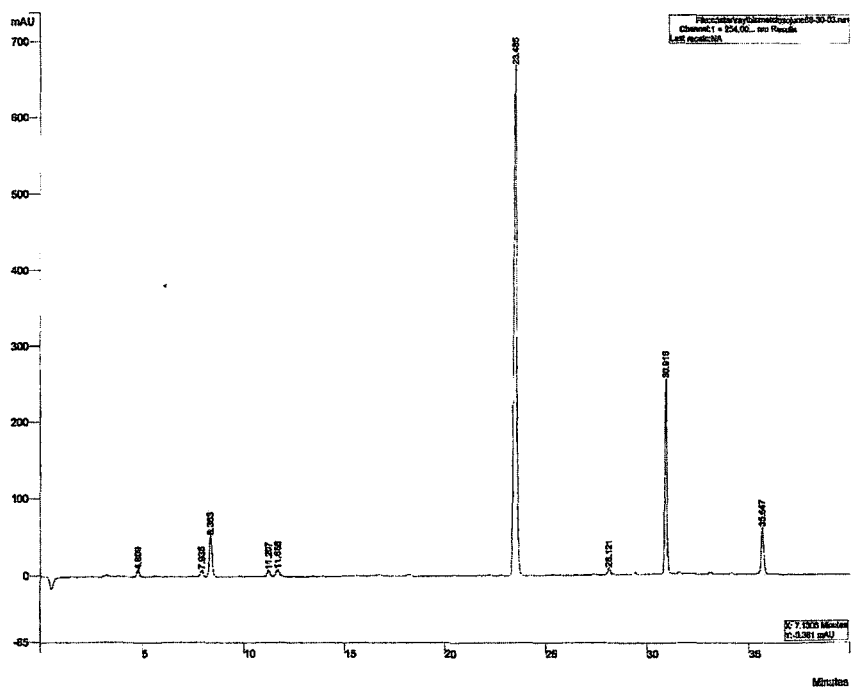


Figure 15-F. Analytical HPLC chromatogram of 3.20.

Chapter 3: Di-Arylated Carboranes-3.15

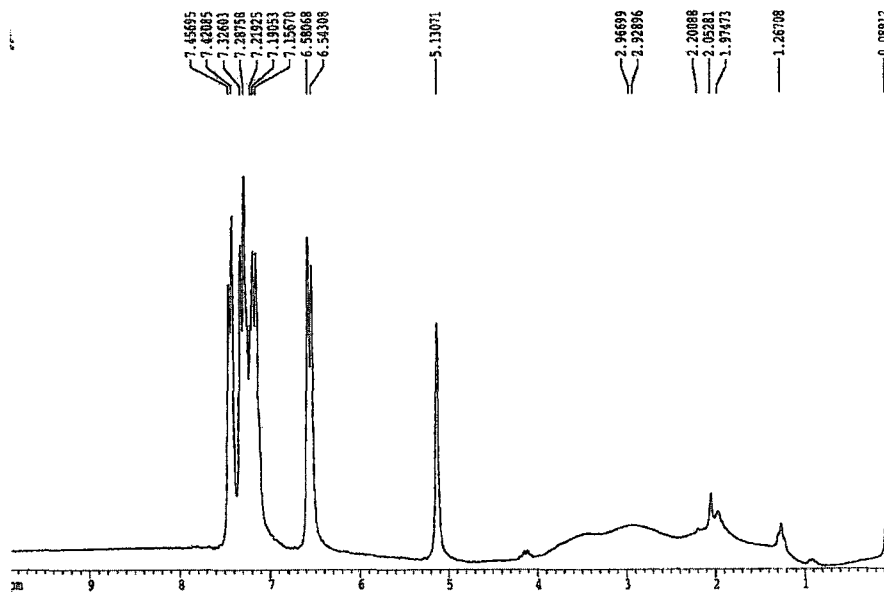


Figure 16-A. ^1H NMR of 3.15, 200 MHz, in CDCl_3 .

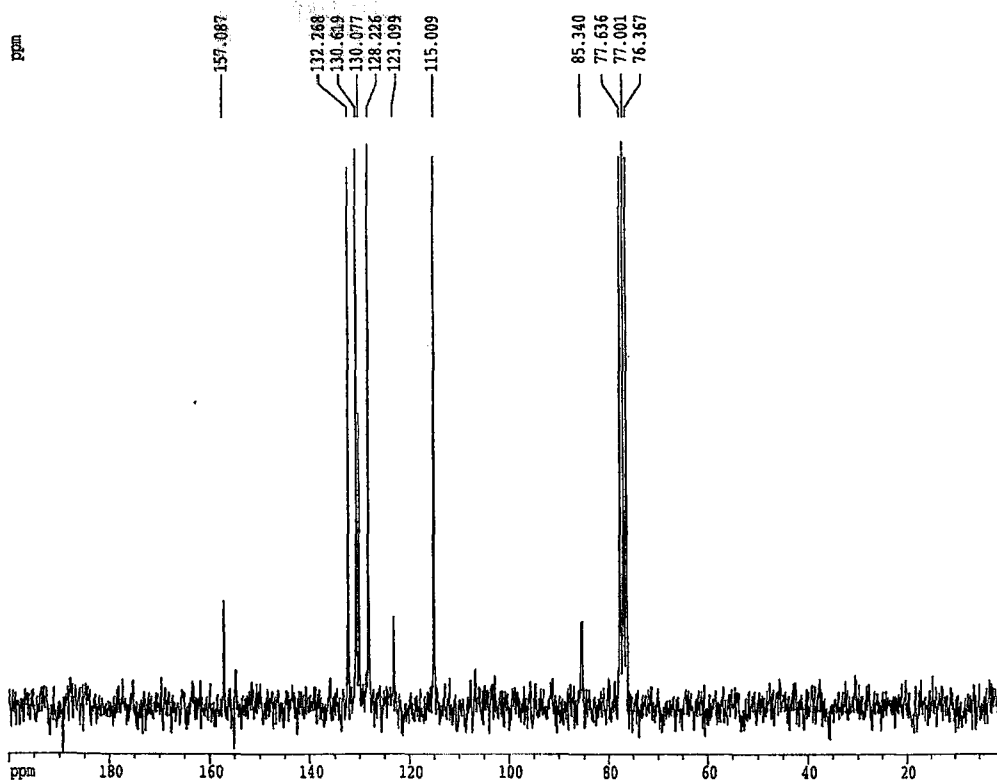


Figure 16-B. $^{13}\text{C}\{^1\text{H}\}$ NMR of 3.15, 200 MHz, in CDCl_3 .

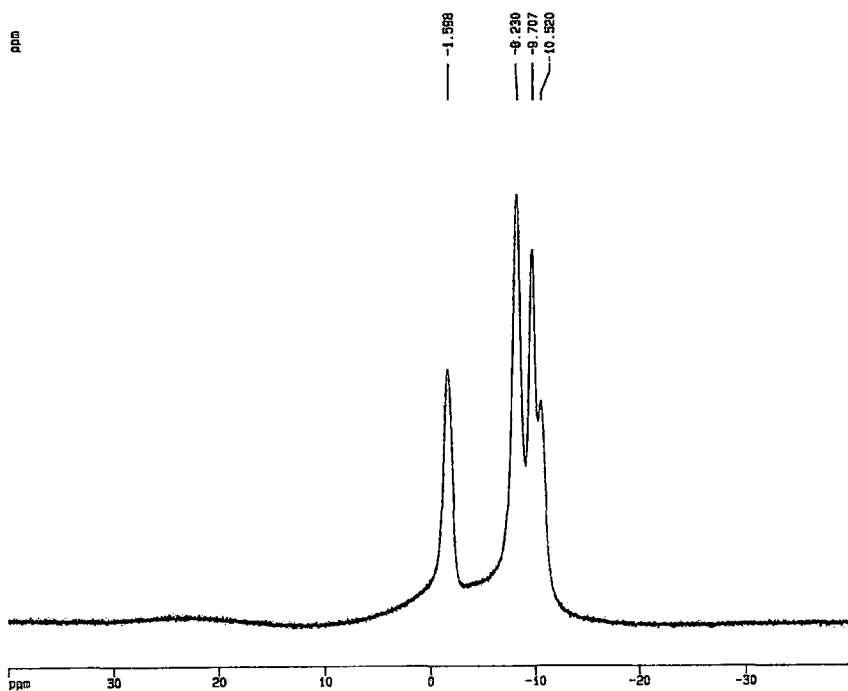


Figure 16-C. $^{11}\text{B}\{\text{H}\}$ NMR of 3.15, 500 MHz, in CDCl_3 .

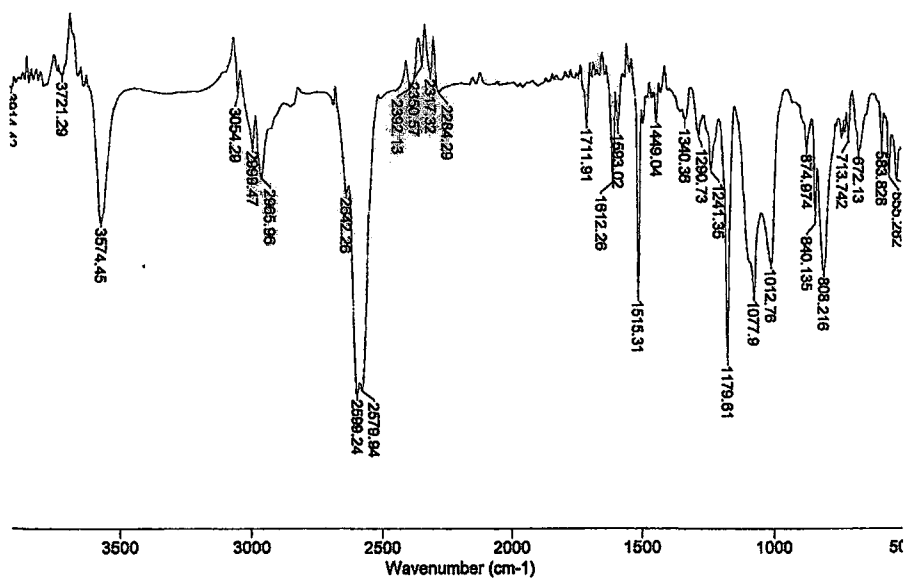


Figure 16-D. FTIR of 3.15, in CH_2Cl_2 .

Chapter 3: Di-Arylated Carboranes-3.11

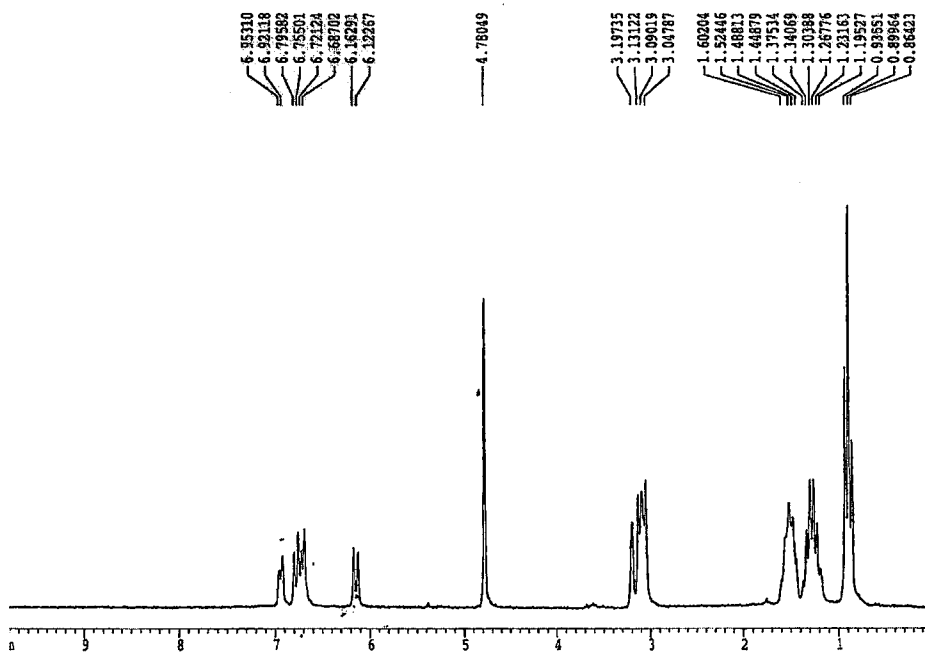


Figure 17-A. ^1H NMR of 3.11, 200 MHz, in CD_3OD .

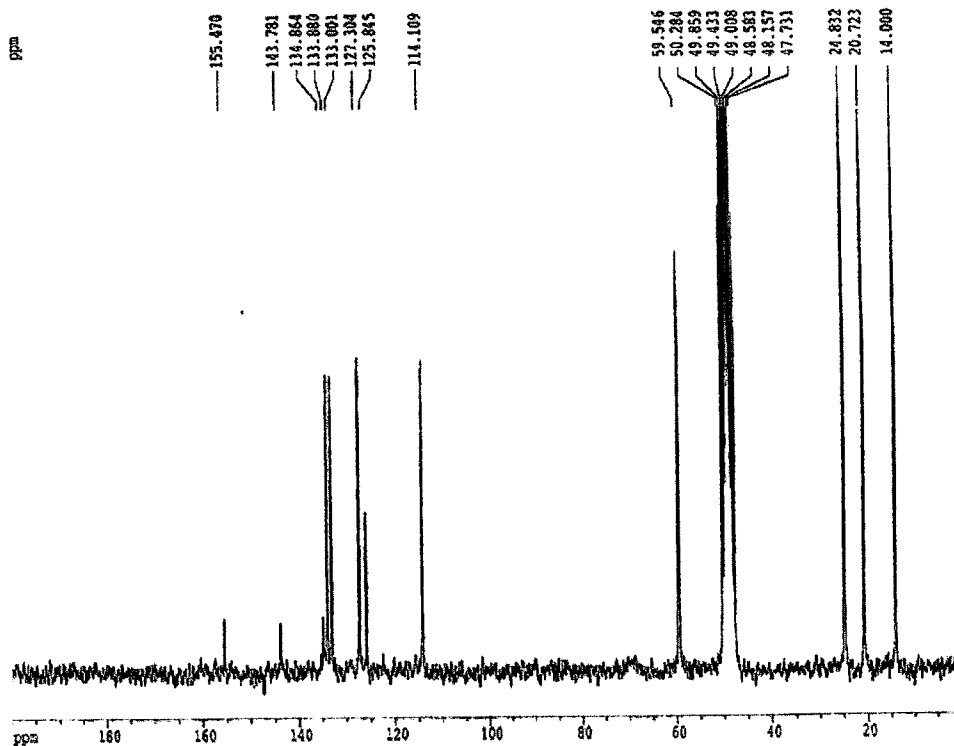


Figure 17-B. $^{13}\text{C}\{^1\text{H}\}$ NMR of 3.11, 200 MHz, in CD_3OD .

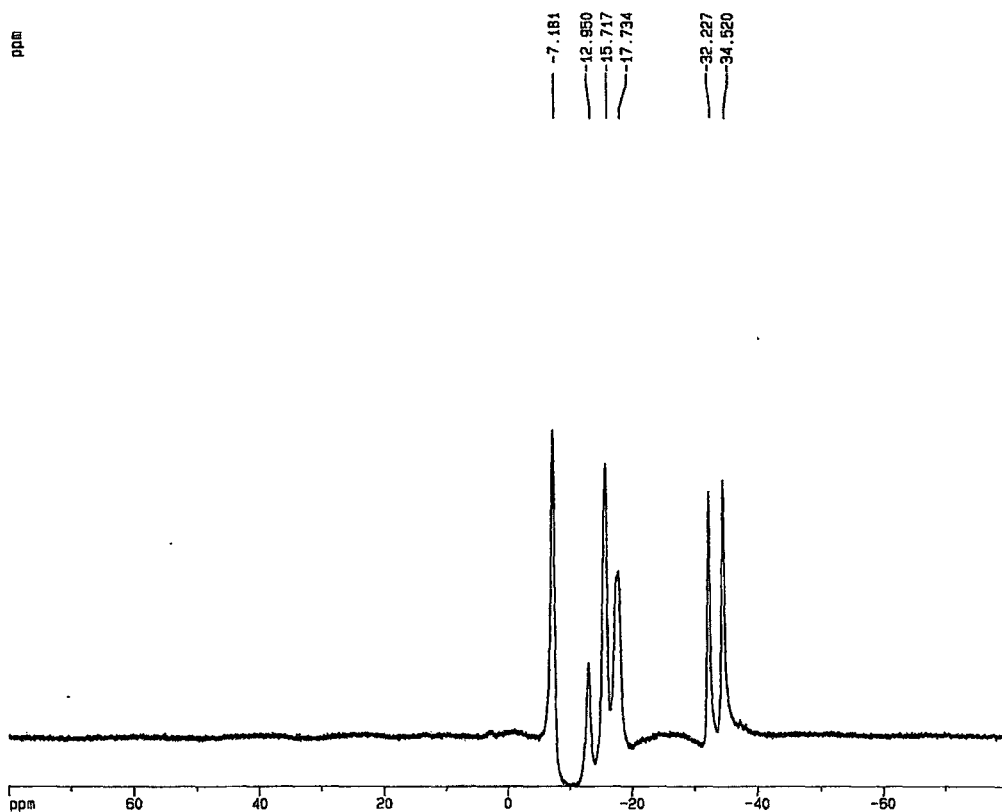


Figure 17-C. $^{11}\text{B}\{\text{H}\}$ NMR of 3.11, 500 MHz, in CD_3OD .

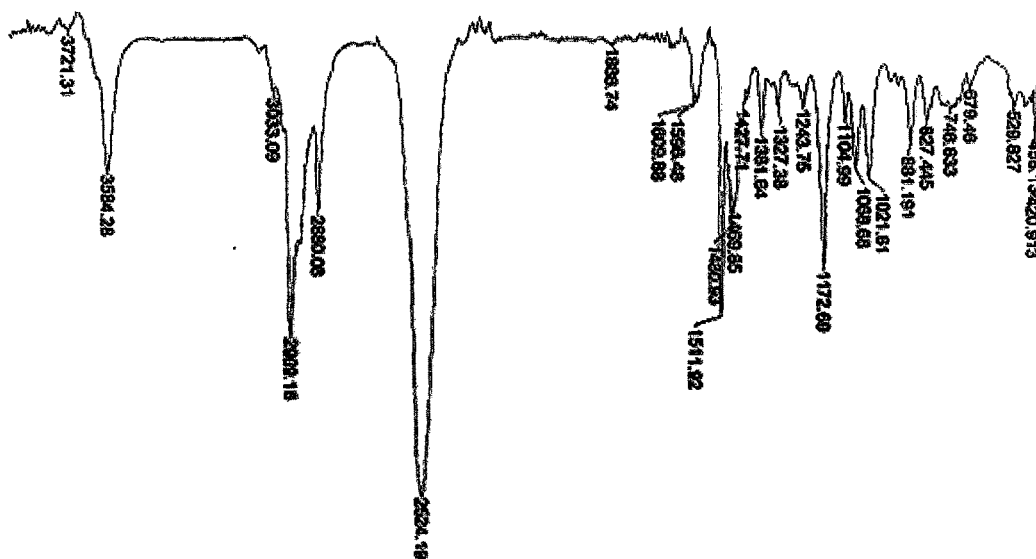


Figure 17-D. FTIR of 3.11, in CH_2Cl_2 .

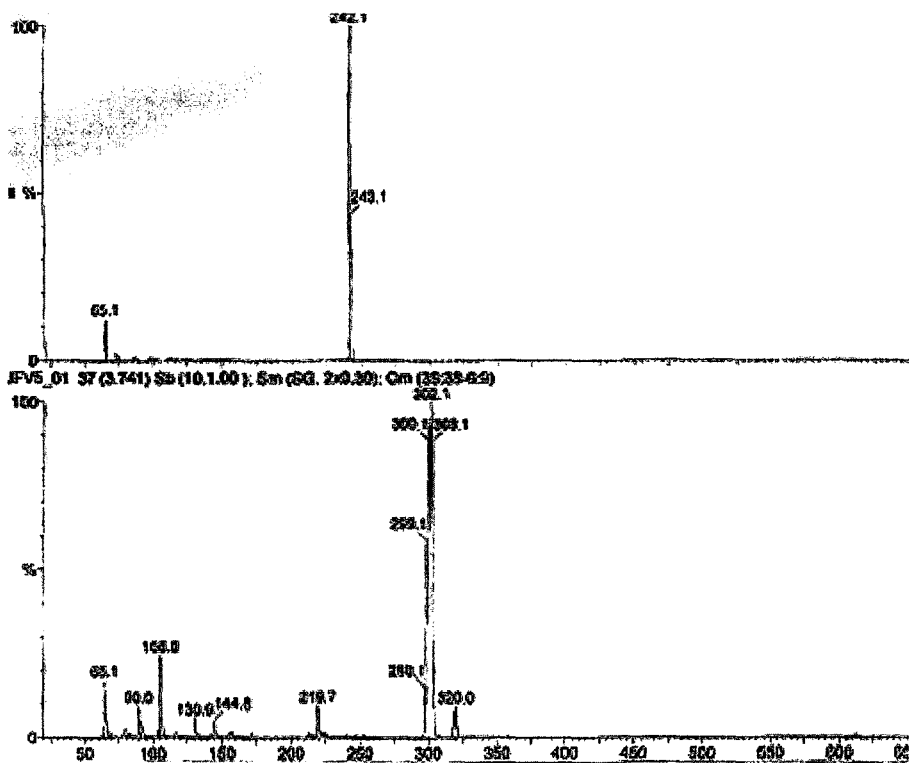


Figure 17-E. Negative Ion Mode ESI-MS of 3.11.

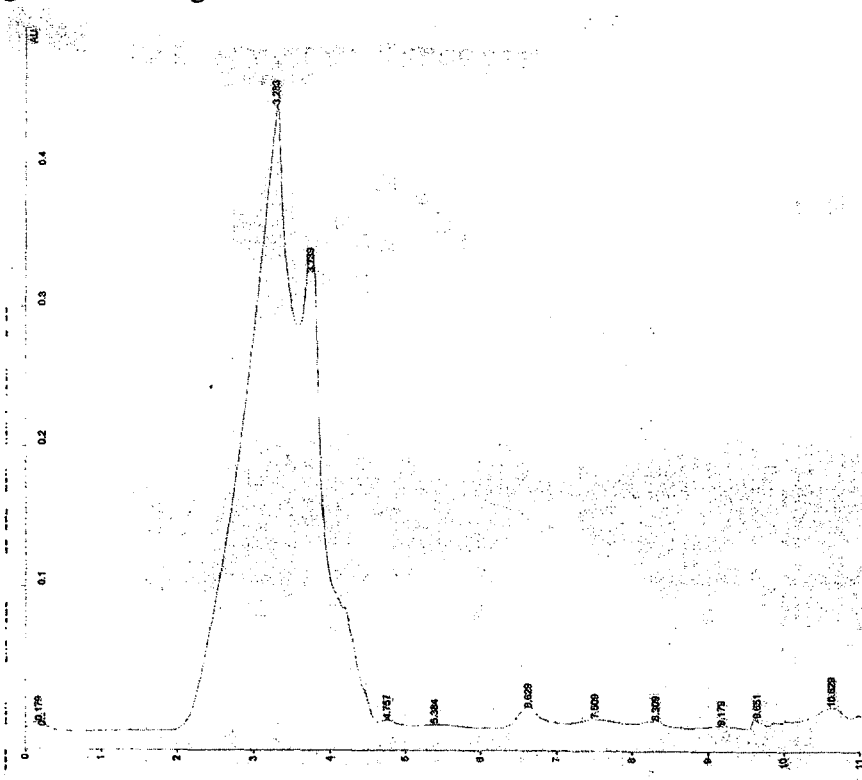


Figure 16-F. Analytical HPLC chromatogram of 3.11.

Chapter 2: Mono-Arylated Carboranes-3.7

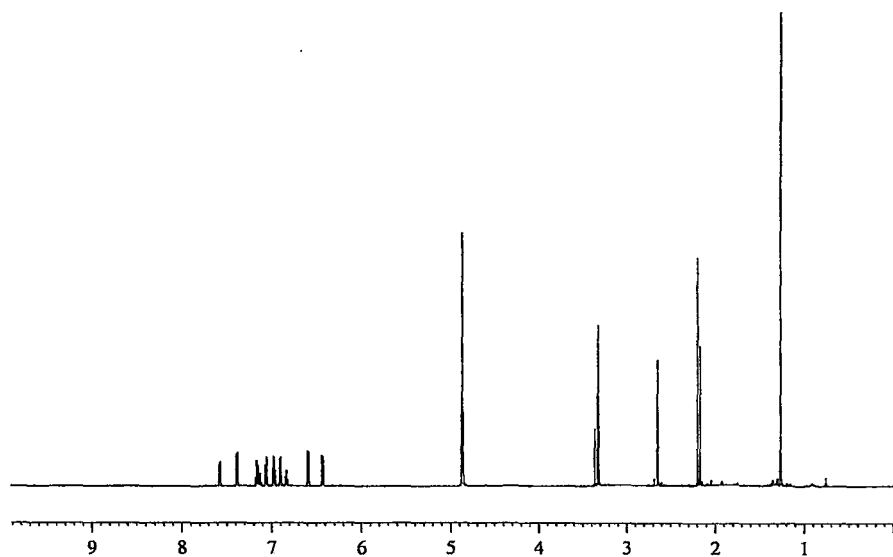


Figure 18-B. ^1H NMR of 3.7, 600 MHz, in CD_3OD

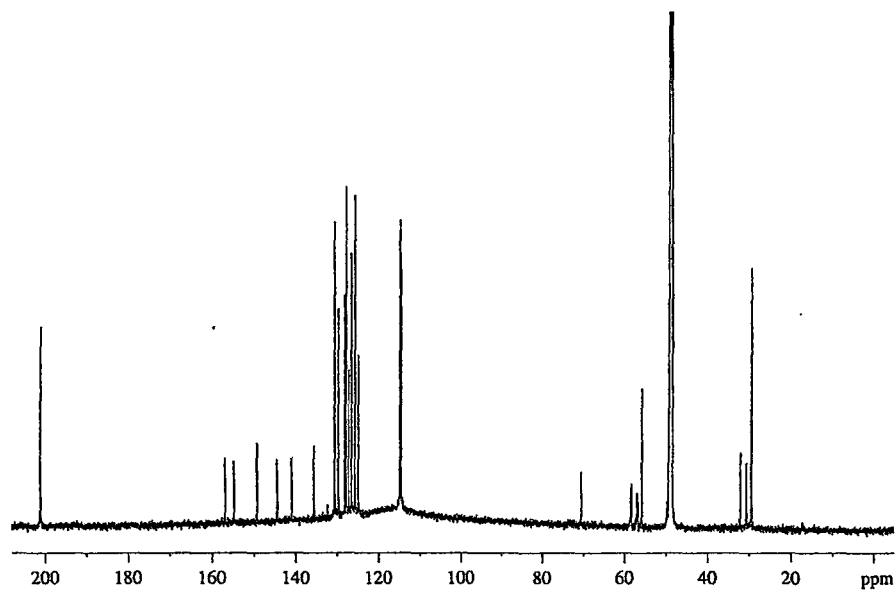


Figure 18-B. $^{13}\text{C}\{\text{H}\}$ NMR of 3.7, 600 MHz, in CD_3OD

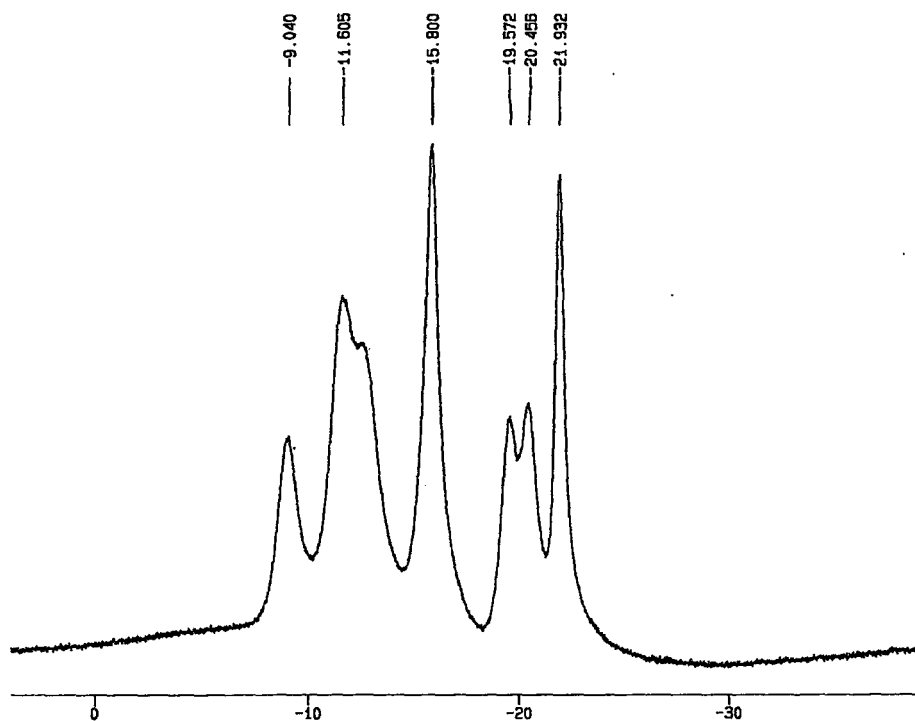


Figure 18-C. $^{11}\text{B}\{\text{H}\}$ NMR of 3.7, 500 MHz, in CD_3OD

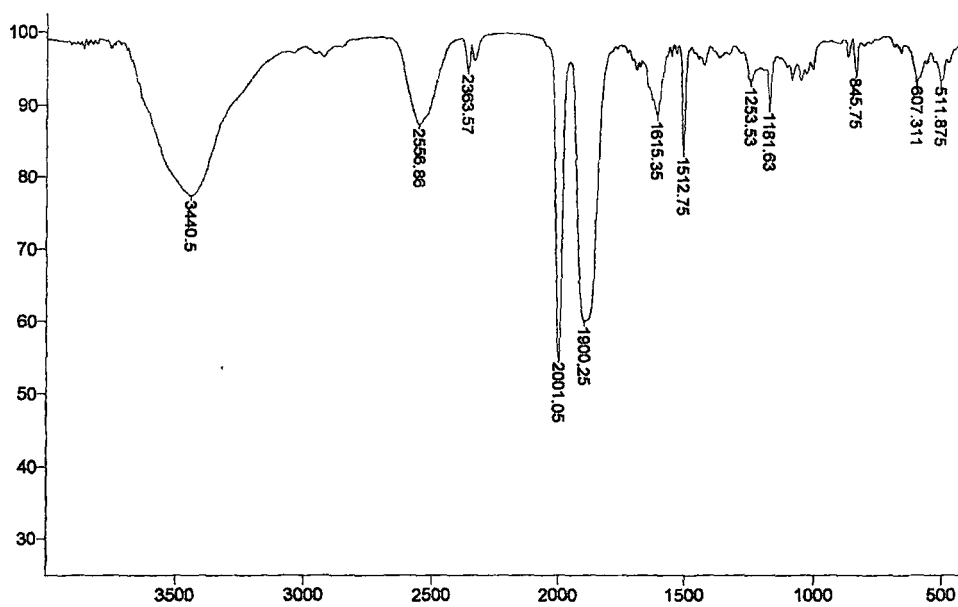


Figure 9-D. FTIR of 3.7, in KBr.

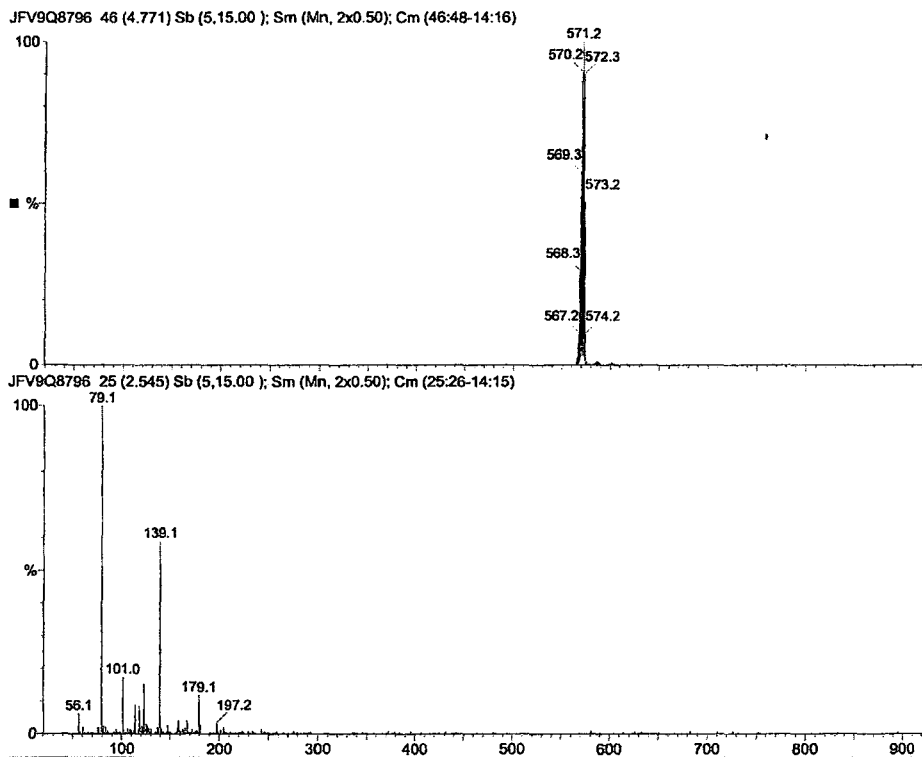


Figure 9-E. Negative Ion Mode ESI-MS of 3.7

Chapter 3: Di-Arylated Carboranes-3.16

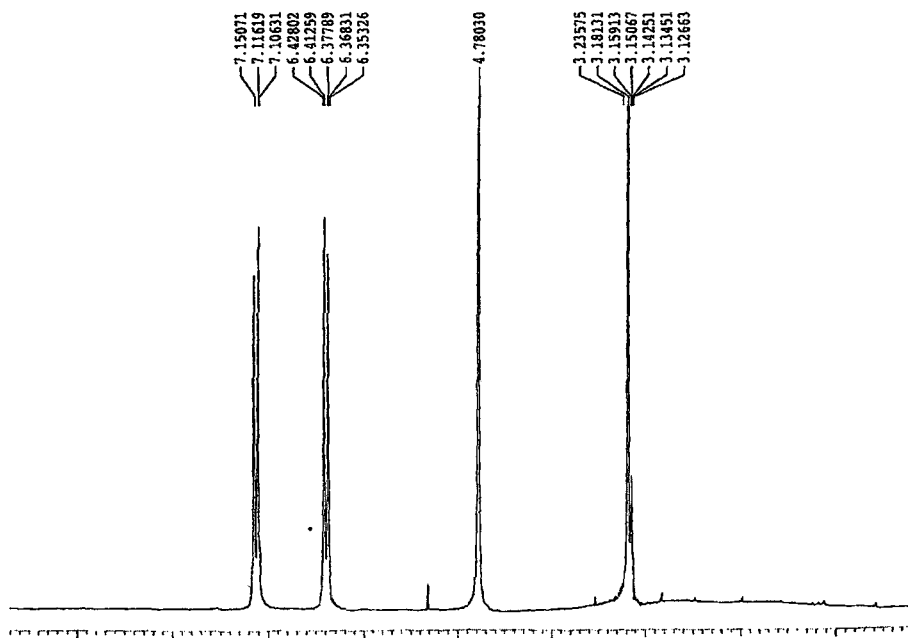


Figure 19-A. ^1H NMR of 3.16, 200 MHz, in CD_3OD

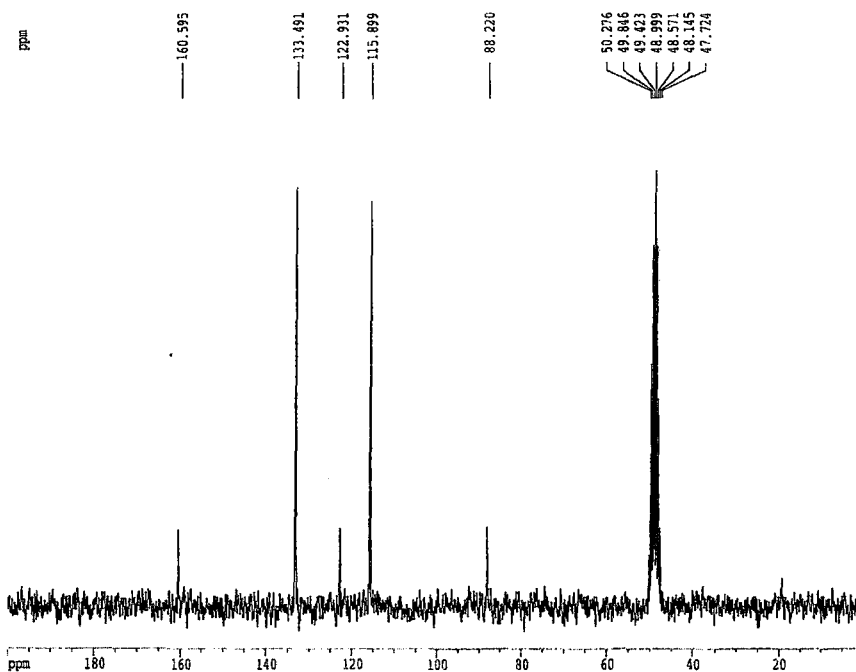


Figure 19-B. $^{13}\text{C}\{\text{H}\}$ NMR of 3.16, 200 MHz, in CD_3OD .

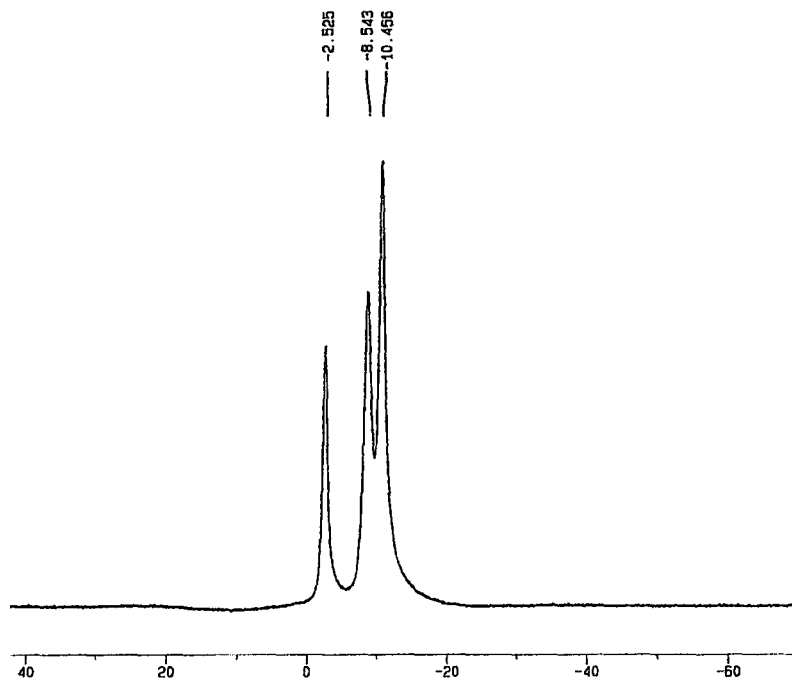


Figure 19-C. $^{11}\text{B}\{\text{H}\}$ NMR of 3.16, 500 MHz, in CD_3OD .

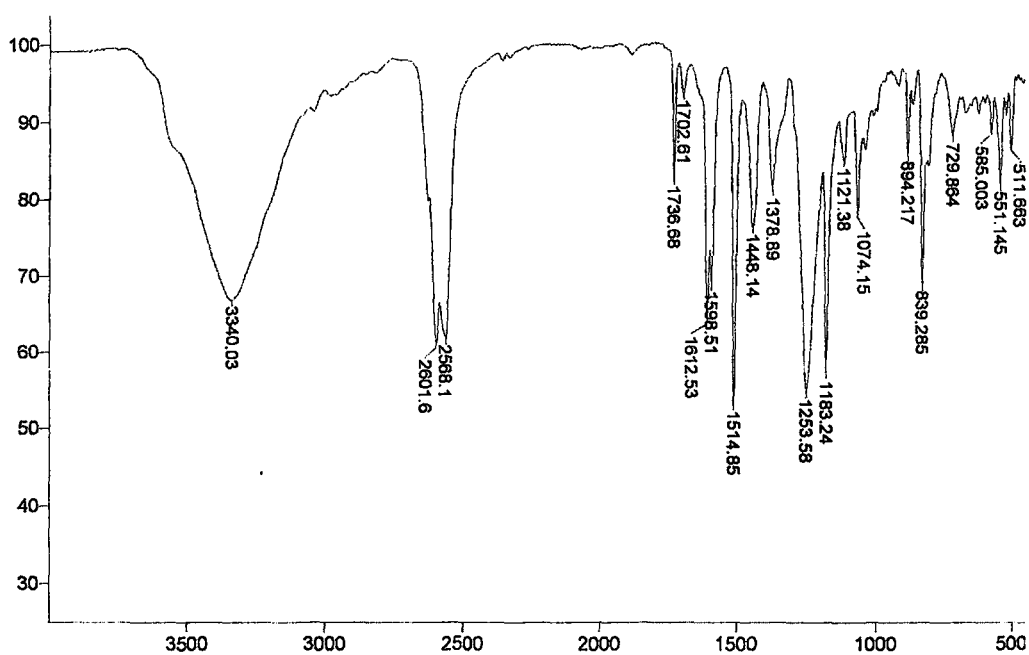


Figure 19-D. FTIR of 3.16, in KBr.

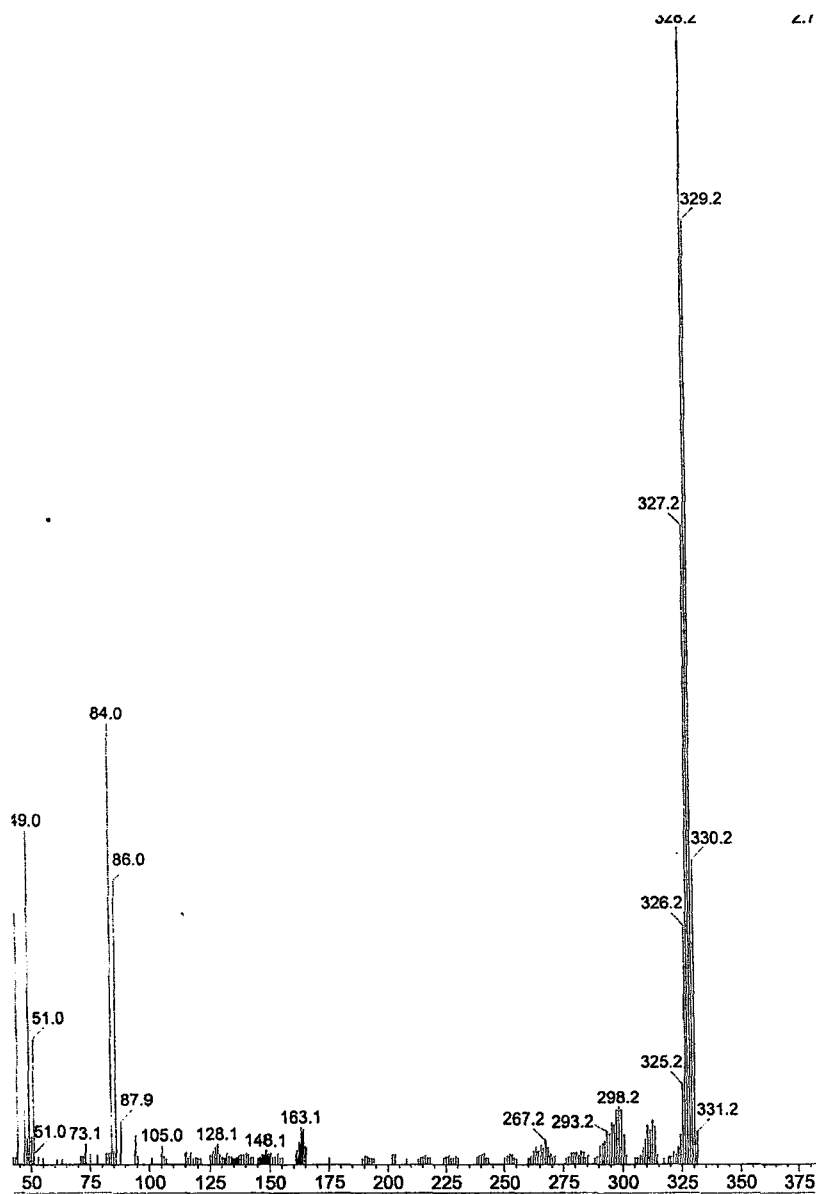


Figure 19-E. EI-MS of 3.16.

Chapter 3: Di-Arylated Carboranes-3.8

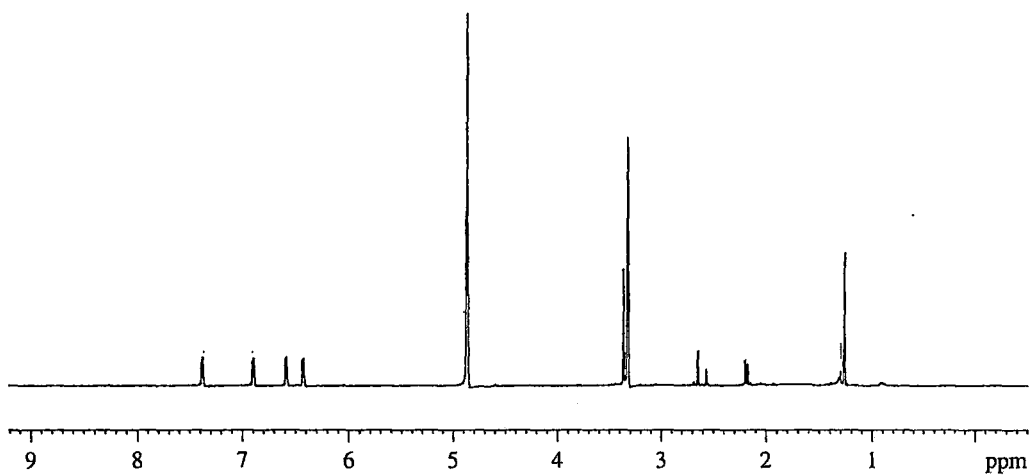


Figure 20-B. ^1H NMR of 3.8, 600 MHz, in CD_3OD

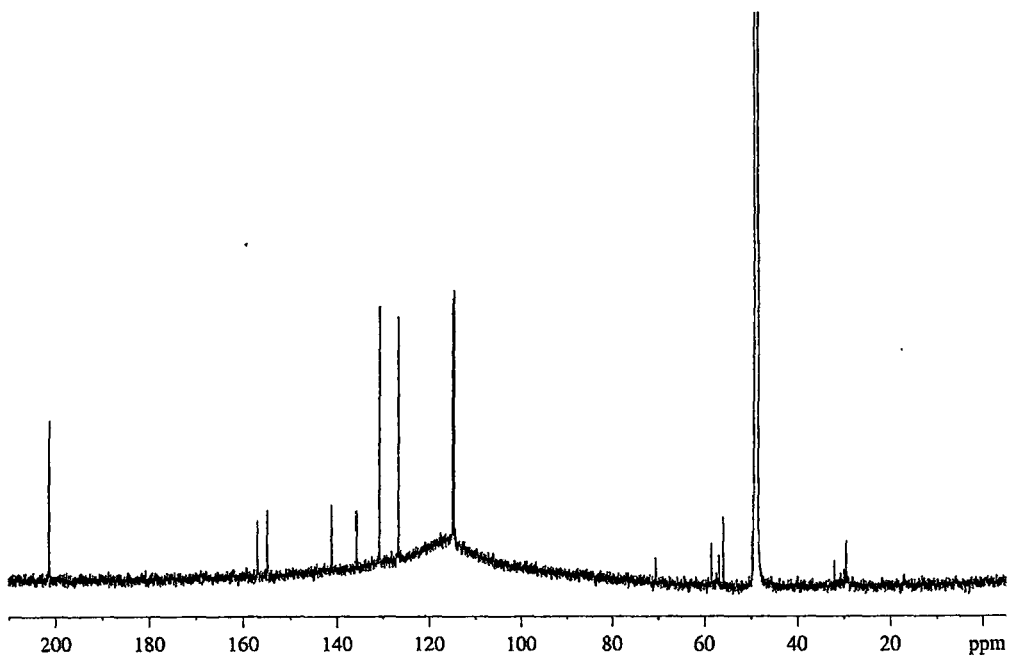


Figure 20-B. $^{13}\text{C}\{\text{H}\}$ NMR of 3.8, 600 MHz, in CD_3OD

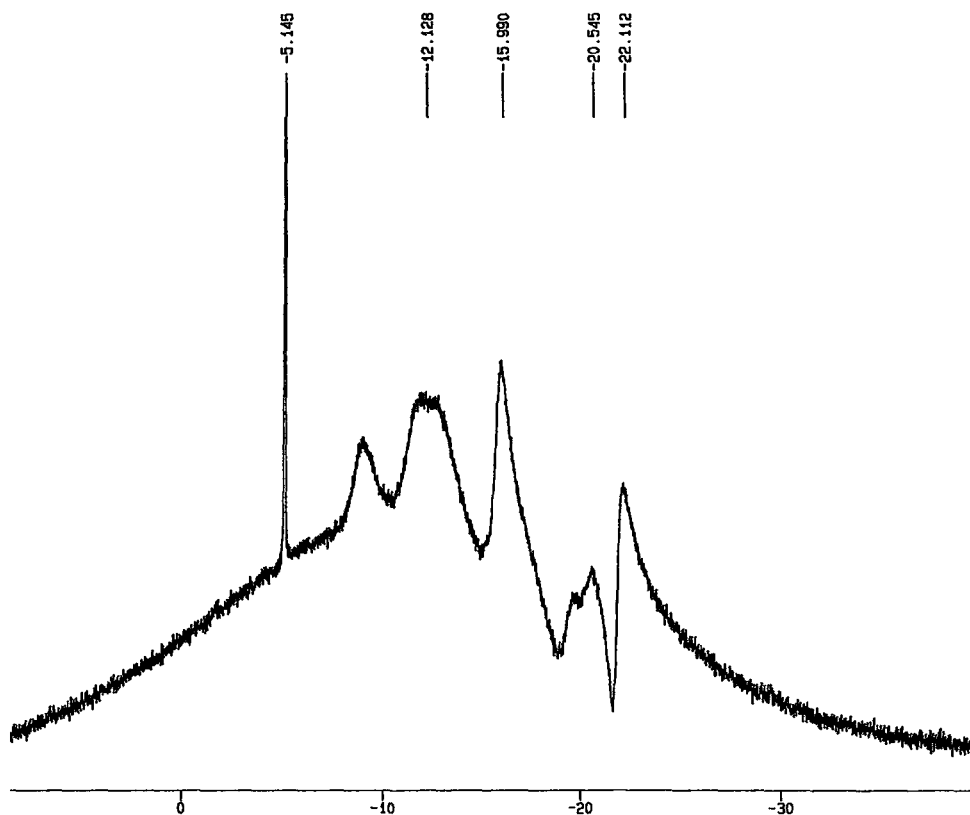


Figure 20-C. $^{11}\text{B}\{\text{H}\}$ NMR of 3.8, 500 MHz, in CD_3OD

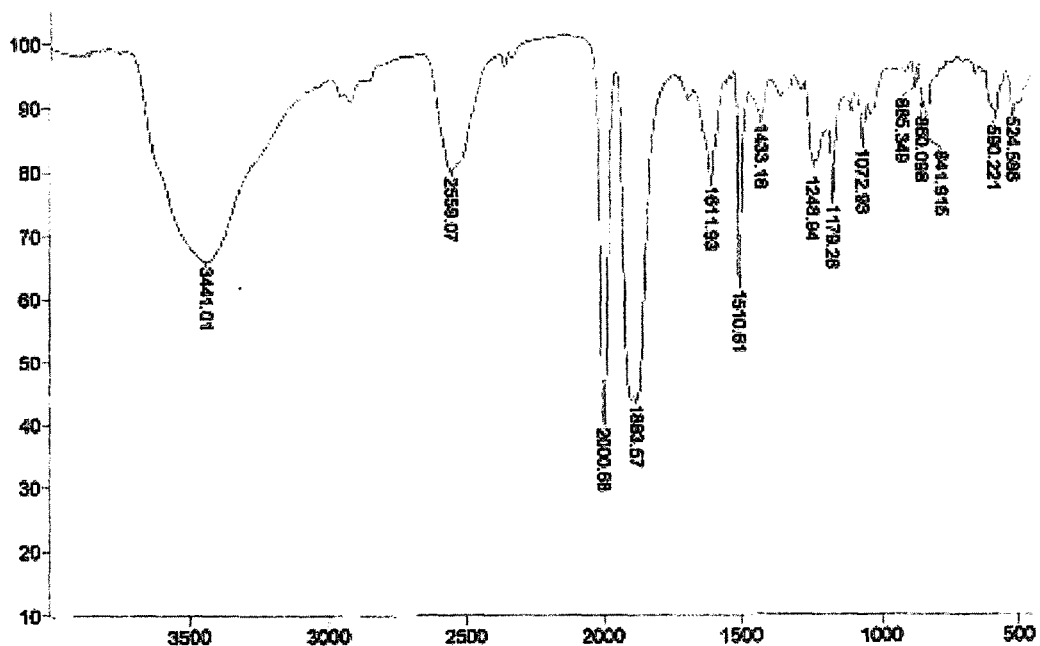


Figure 20-D. FTIR of 3.8, in KBr.

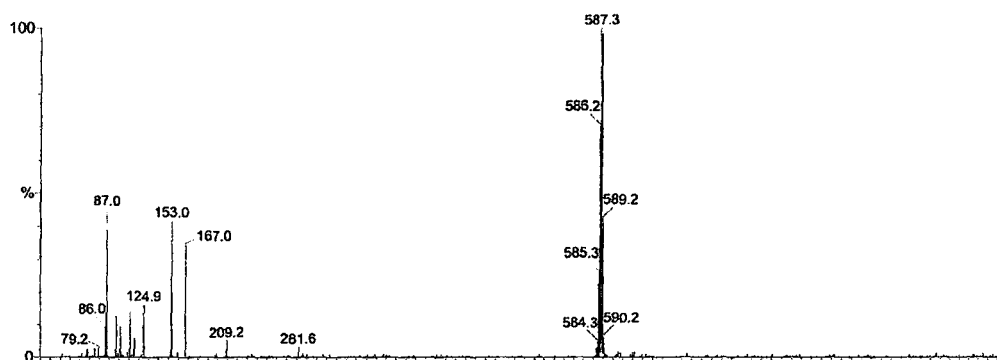


Figure 20-E. Negative Ion Mode ESI-MS of 3.8

Chapter 3: Di-Arylated Carboranes-3.17

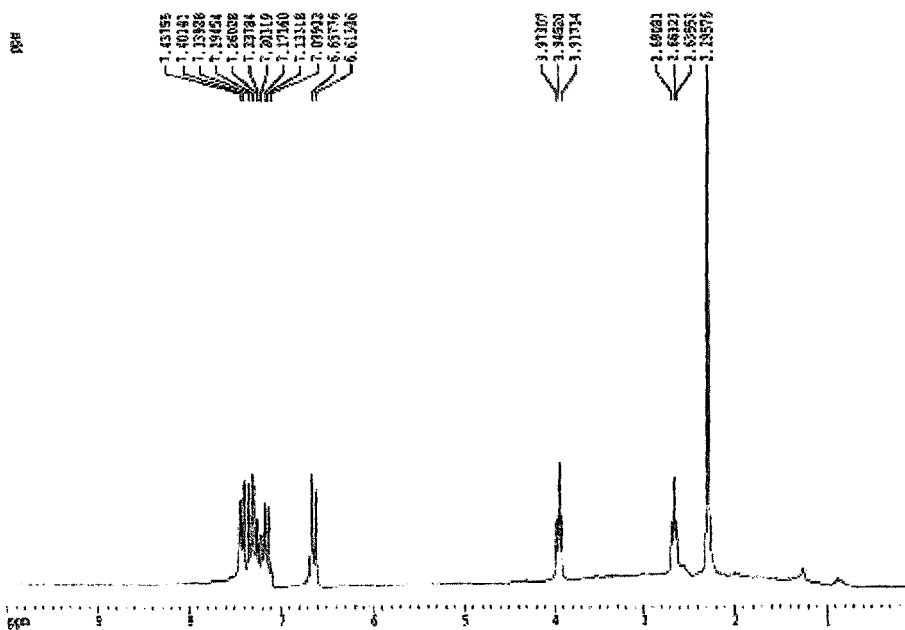


Figure 21-A. ^1H NMR of 3.17, 200 MHz, in CDCl_3

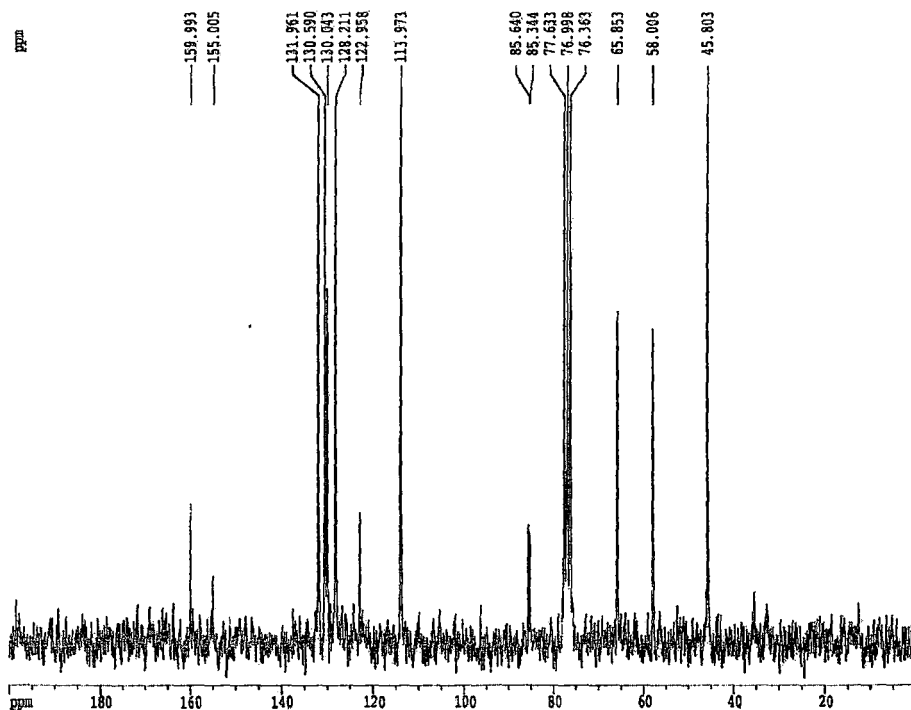


Figure 21-B. $^{13}\text{C}\{^1\text{H}\}$ NMR of 3.17, 200 MHz, in CDCl_3

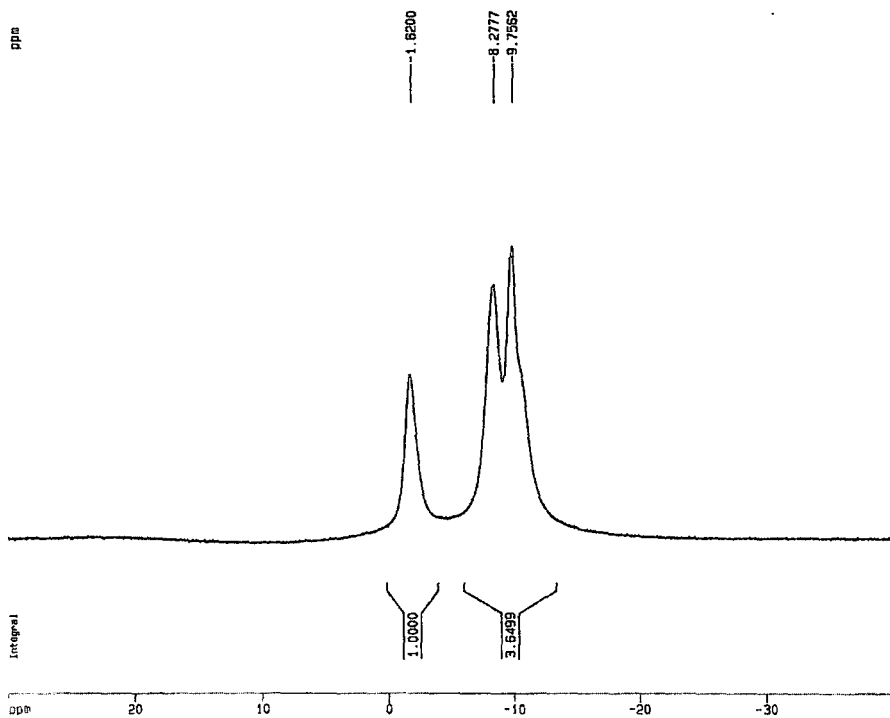


Figure 21-C. $^{11}\text{B}\{^1\text{H}\}$ NMR of 3.17, 500 MHz, in CDCl_3

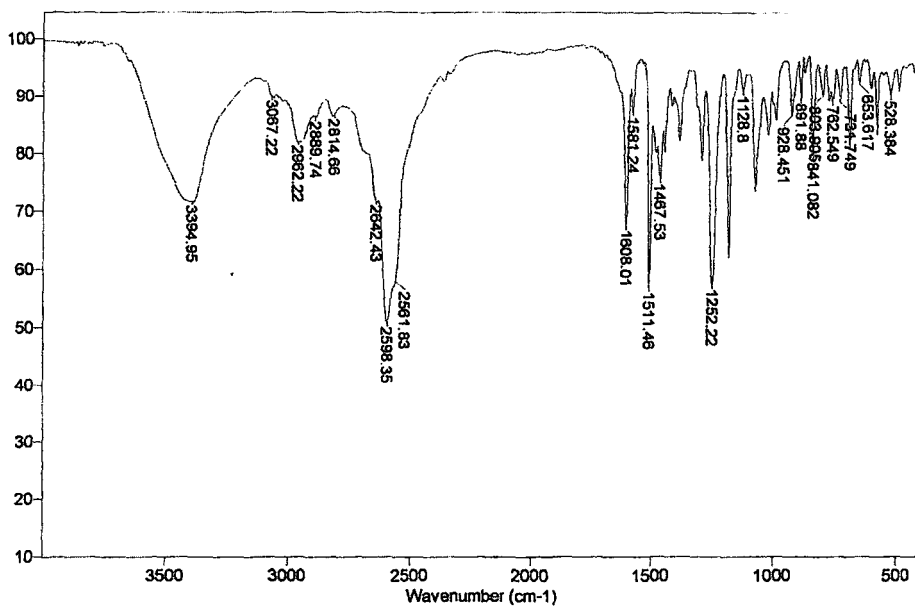


Figure 21-D. FTIR of 3.17, in KBr

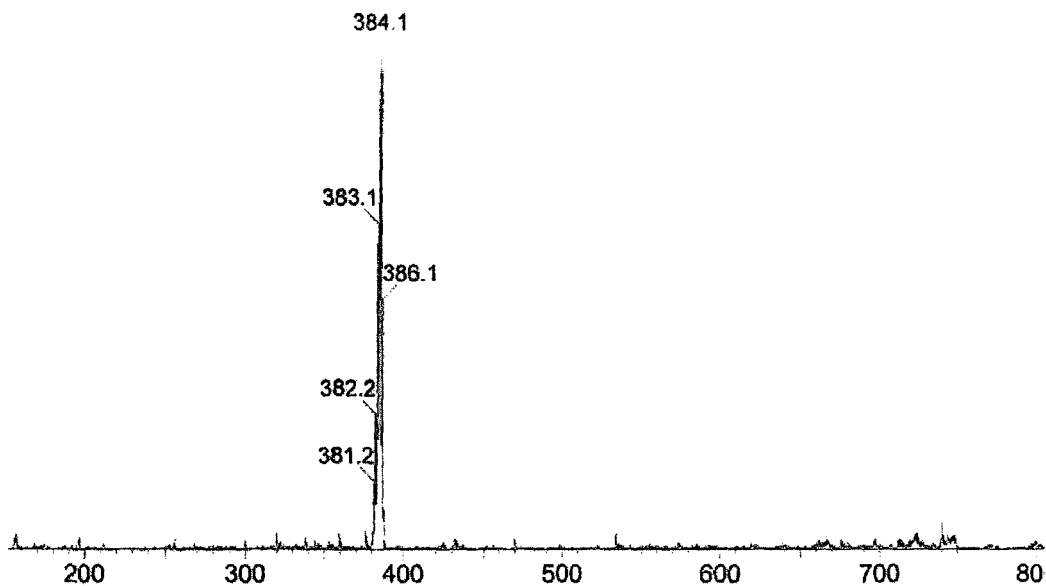


Figure 21-E. ESMS of 3.17

Chapter 2: Mono-Arylated Carboranes-3.9

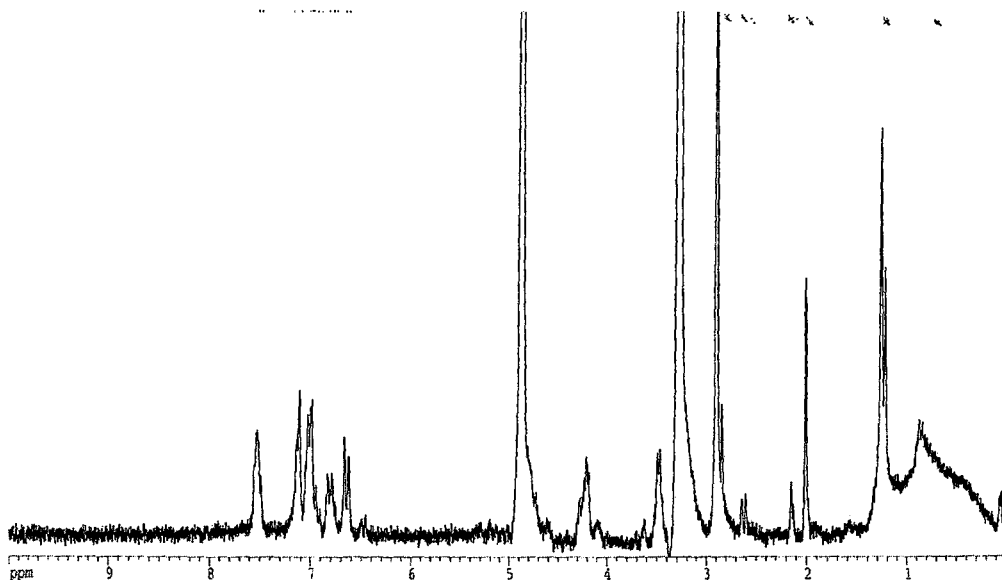


Figure 22-B. ^1H NMR of 3.9, 200 MHz, in CD_3OD .

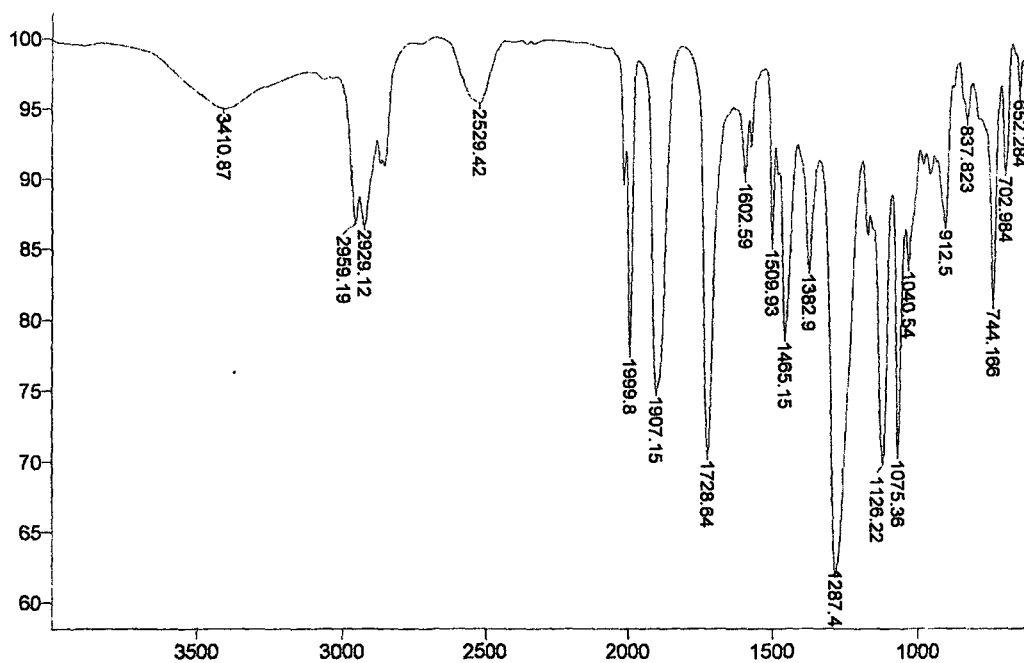


Figure 22-B. FTIR of 3.9, in KBr.

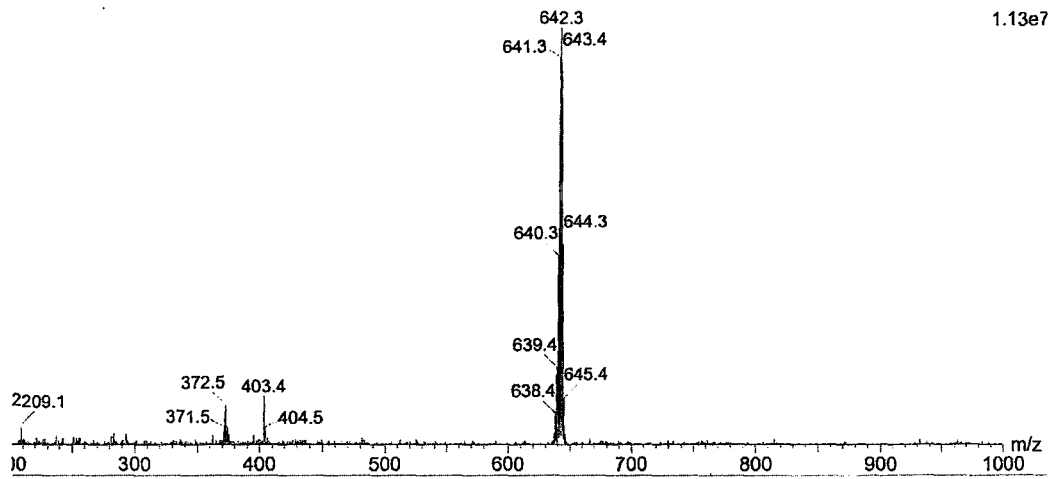


Figure 22-C. Negative Ion Mode ESI-MS of 3.9